Polish Journal of Microbiology

CONTENTS

INSTRUCTIONS FOR AUTHORS
Instructions for authors: https://www.exeley.com/journal/polish_journal_of_microbiology

Emerging Applications of Bacteriocins as Antimicrobials, Anticancer Drugs, and Modulators of the Gastrointestinal Microbiota

CATHERINE CESA-LUNA[1], JULIA-MARÍA ALATORRE-CRUZ[2], RICARDO CARREÑO-LÓPEZ[1],
VERÓNICA QUINTERO-HERNÁNDEZ[3] and ANTONINO BAEZ[1]*

[1] Centro de Investigaciones en Ciencias Microbiológicas (CICM), Instituto de Ciencias (IC),
Benemérita Universidad Autónoma de Puebla (BUAP), Puebla, México
[2] Laboratorio de Biología Celular y Molecular, Universidad Autónoma de Querétaro, Querétaro, México
[3] CONACYT – CICM, IC, BUAP, Puebla, México

A b s t r a c t

The use of bacteriocins holds great promise in different areas such as health, food, nutrition, veterinary, nanotechnology, among others. Many research groups worldwide continue to advance the knowledge to unravel a novel range of therapeutic agents and food preservatives. This review addresses the advances of bacteriocins and their producer organisms as biocontrol agents for applications in the medical industry and agriculture. Furthermore, the bacteriocin mechanism of action and structural characteristics will be reviewed. Finally, the potential role of bacteriocins to modulate the signaling in host-associated microbial communities will be discussed.

K e y w o r d s: bacteriocin, bio-preservatives, agriculture, biomedical, microbial communities

Introduction

Bacteria living in microbial communities use several functions and strategies to survive or coexist with other microorganisms, competing to obtain nutrients and colonize space in their habitat (Hibbing et al. 2010). One of the strategies used by bacteria to guarantee their growth in communities is antagonism, which effectively limits the growth of other microorganisms (Russel et al. 2017). To accomplish antagonism, bacteria must produce inhibitory substances such as antibiotics, organic acids, siderophores, volatile organic compounds, antifungals, and bacteriocins (Riley 2009). In addition to inhibiting the growth of other microorganisms, bacteriocins have different traits that make them attractive for biotechnological applications. For example, while resistance against nisin exists, in general, the bacteriocin mechanism of action less often induces resistance as it happens with conventional antibiotics (Behrens et al. 2017). Furthermore, some bacteriocins are compounds produced by the natural host-associated microbiome; therefore, they are harmless to the host. Bacteriocins also show selective cytotoxicity toward cancer cells compared to normal cells (Kaur and Kaur 2015).

Classification, mechanism of action, and structural characteristics

Bacteriocins are antimicrobial peptides synthesized by the ribosome representing the most abundant and diverse group of bacterial defense systems (Silva et al. 2018). Bacteriocins were considered to have a narrow antimicrobial spectrum that could only inhibit bacterial strains closely related to produced bacteria; however, several studies have shown that there are bacteriocins able to kill different genera of bacteria and even certain yeasts, parasites, and cancer cells (Kaur and Kaur 2015; Baindara et al. 2018).

The success of bacteriocins in eliminating multi-drug resistant pathogens (MDR) has led to medical applications to treat bacterial infections. *In vivo* tests
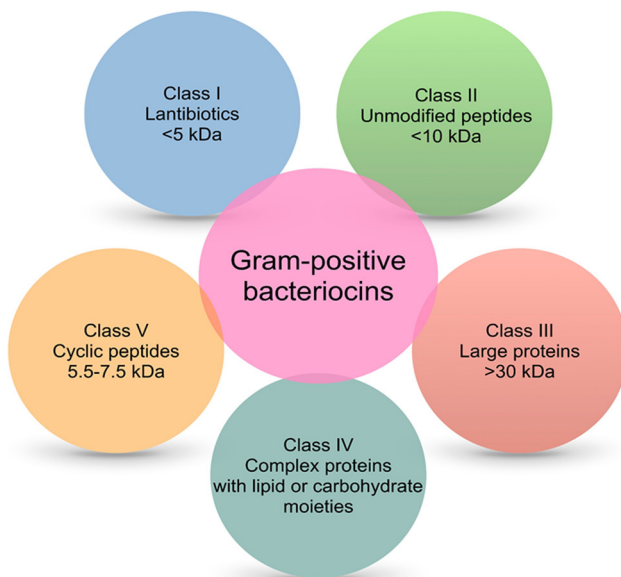
Fig. 1. Structure-based classification of Gram-positive bacteriocins.

have demonstrated the effectiveness of bacteriocins to treat infections in animal models, too (McCaughey et al. 2016; Van Staden et al. 2016). Lactic acid bacteria (LAB) produce bacteriocins, being nisin from *Lactococcus lactis*, the most well-known example (Silva et al. 2018). Nisin was approved for use as a food preservative for preventing the growth of *Listeria monocytogenes* and other Gram-positive pathogens (Price et al. 2018). The *Bacillus* genus also produces bacteriocins with attractive characteristics (Salazar-Marroquín et al. 2016), including subtilin (produced by *Bacillus subtilis*) and coagulin (produced by *Bacillus coagulans*). *Bacillus thuringiensis* produces bacteriocins with broad-spectrum activity, inhibiting various pathogens such as *L. monocytogenes*, *Staphylococcus aureus*, *Klebsiella pneumoniae*, *Pseudomonas aeruginosa*, and *Vibrio cholerae*, in addition to the *Aspergillus* fungus (Salazar-Marroquín et al. 2016).

Bacteriocins of Gram-positive bacteria are cationic and amphiphilic molecules whose mass varies from < 5 to more than 30 kDa (Balciunas et al. 2013) (Fig. 1). Many classifications of bacteriocins are available, but their diverse chemical structures and inhibitory activities make their classification into a specific group quite difficult. Class I bacteriocins, also known as lantibiotics, contain in their primary structure uncommon amino acids like lanthionine, β-methyl lanthionine, and dehydroalanine. These unique amino acids formed by post-translational modifications can provide antimicrobial activity and peptide stability. For example, they can create covalent bridges that result in internal rings that give stability to the peptide structure. In addition, internal rings contribute to the formation of a secondary structure in water that favors antimicrobial activity (Almeida and Pokorni 2012). Around 30%

of lantibiotics already identified have been purified from lactic acid bacteria, including the well-known nisin, mersacidin, and lacticin 3147 (Stoyanova et al. 2012). The class II bacteriocins are membrane-active and heat-stable peptides known as non-lantibiotics or pediocin-like antibiotics (Balandin et al. 2019). They do not harbor modified amino acids, and their molecular weights are lower than 10 kDa. Prototype bacteriocins of this group are pediocin PA-1, pentocin 31–1, enterocin P, sakacin G, enterocin A, two-peptide components (enterocin DD14, plantaracin E/F), sec-dependent secreted (acidocin B), and other not yet subclassified (bactofencin A peptides) (Liu et al. 2008; Balandin et al. 2019; Ladjouzi et al. 2020). The class III bacteriocins are large (> 30 kDa) heat-labile peptides composed of an N-terminal endopeptidase domain and a C-terminal substrate recognition domain. Bacteriocins of this group can lyse the cell wall of sensitive bacteria, although there are non-lytic bacteriocins in this group too, like helveticin J. Some examples of Class III bacteriocins are helveticin M, zoocin A and enterolysin A (bacteriolysins), and millericin B (murein hydrolase) (Alvarez-Sieiro et al. 2016; Sun et al. 2018). Class IV are complex peptide structures associated with lipid and carbohydrate moiety forming glycoproteins and lipoproteins. These structural characteristics make them sensitive to the action of glycolytic or lipolytic enzymes. Lactocin 27 and leuconocin S are prototype bacteriocins of this group and are recognized to disrupt bacterial cell membranes (Simons et al. 2020). Class V includes cyclic peptide structures like enterocin AS-48, pumilarin, lactocyclicin Q, and plantaricyclin A (Perez et al. 2018; Sánchez-Hidalgo et al. 2011). The circular nature of their structures provides Class V with superior stability against several stresses compared to most linear bacteriocins. Biosynthesis of circular bacteriocins involves cleavage of the leader peptide, circularization, and export to the extracellular space.

Gram-negative bacteria produce both high molecular weight (> 30 kDa) and low molecular weight (< 10 kDa) bacteriocins (Rebuffat 2016). The first bacteriocin identified from a Gram-negative bacterium was colicin, produced by *Escherichia coli* (Riley 2009). Bacteriocins of Gram-negative bacteria are classified into two main groups, colicins, and microcins (Fig. 2). Genes encoding colicins are found on plasmids whose products vary between 20 and 80 kDa. Colicins from *E. coli* inhibits closely related strains of the genus *Salmonella* and other *E. coli* strains. Colicins are organized in three different domains: the translocation domain (T) N-terminally located, the receptor binding (R) located in the central region, and the cytotoxic domain (C) located at C-terminus (Helbig and Braun 2011). Microcins are pH and heat-stable antimicrobial peptides ribosomally synthesized, hydrophobic, and low
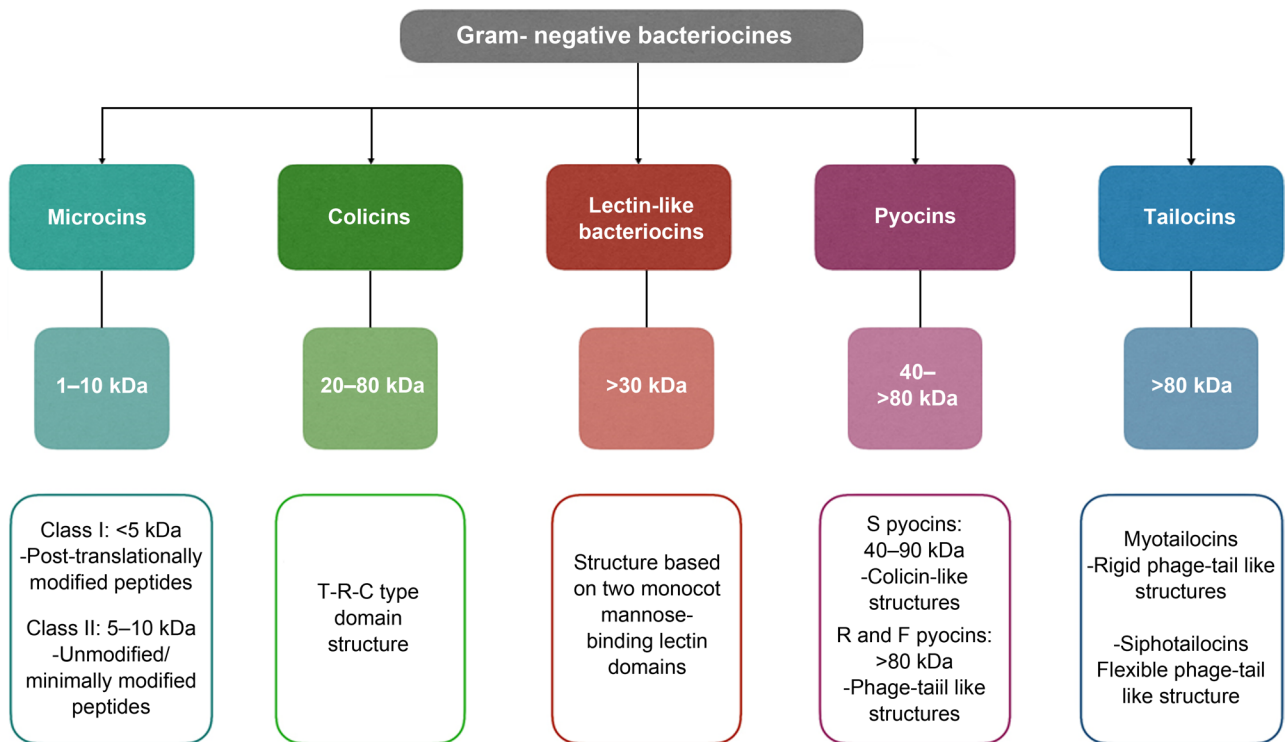
Fig. 2. Structural-based classification of Gram-negative bacteriocins.

molecular weight. In some cases, microcins require post-translational modifications to be active, and they do not require a lysis process to be secreted (Baquero et al. 2019). Microcin production has been reported in several Enterobacteriaceae and some cyanobacteria (Rebuffat 2016; Parnasa et al. 2019).

Microcin mJ25 produced by *E. coli* was initially described as a circular peptide; now it is known that there is no union between the terminal residues, but a union through the lactamic link between the amino group (Gly1) and the carboxyl group (Glu8). These structures are known as "lasso-peptides" and are also described in organisms of the genus *Streptomyces* (Hegemann et al. 2015). Other types of high molecular weight bacteriocins of Gram-negative bacteria are pyocins (type R, F, and S), tailocins, and lectin-like bacteriocins. Genes encoding for pyocins are located on the bacterial chromosome, and their expression is induced by agents that damage DNA by activating the SOS response. R-type and F-type pyocins are non-flexible and flexible phage tail-like bacteriocins, respectively. The S-type pyocin is like the colicins and is formed by two proteins (a big one and a small one) that remain associated even during its purification process. The large protein is responsible for the antimicrobial activity, and the small one has an immune function for the producing bacteria (Michel-Briand and Baysse 2002; Atanaskovic and Kleanthous 2019; Oluyombo et al. 2019).

Tailocins are bacteriocins like phage tails and display a rigid or flexible structure, similar to R-type and F-type pyocins. Tailocins with contractile and flexible tail morphologies are designated as myotailocins and siphotailocins, respectively (Yao et al. 2017). These bacteriocins have been described in plant-associated *Pseudomonas* and *Burkholderia* strains, although similar bacteriocins are also produced by *Clostridium difficile*, *Serratia plymithicum*, and *Serratia proteamaculans* (Gebhart et al. 2015; Ghequire and De Mot 2015; Hurst et al. 2018).

Lectin-like bacteriocins (LlpAs) represent another type of antimicrobial protein secreted by members of the genus *Pseudomonas*. LlpAs are ~30 kDa proteins that resemble monocot mannose-binding lectins (MMBL) consisting of two B-lectin domains followed by a short carboxy-terminal extension and do not contain an immunity protein. They also include a preserved consensus sequence QxDxNxVx necessary for the activity of the bacteriocin. The best examples of LlpAs include LlpABW11M1 of *Pseudomonas mosselii*, LlpA1Pf-5 of *Pseudomonas protegens* Pf-5, and pyocin L1 of *P. aeruginosa* (Ghequire et al. 2018a). The production of LlpAs has also been reported in *Burkholderia cepacia* strains.

Bacteriocins exert several mechanisms of action towards Gram-positive and Gram-negative bacteria (Fig. 3). Class I bacteriocins produced by Gram-positive bacteria permeabilize bacterial membranes through pore-formation, leading to ion leakage and cell death. These include bacteriocins produced by *Bacillus*, *Lactococcus*, and *Pediococcus* genera. They cause
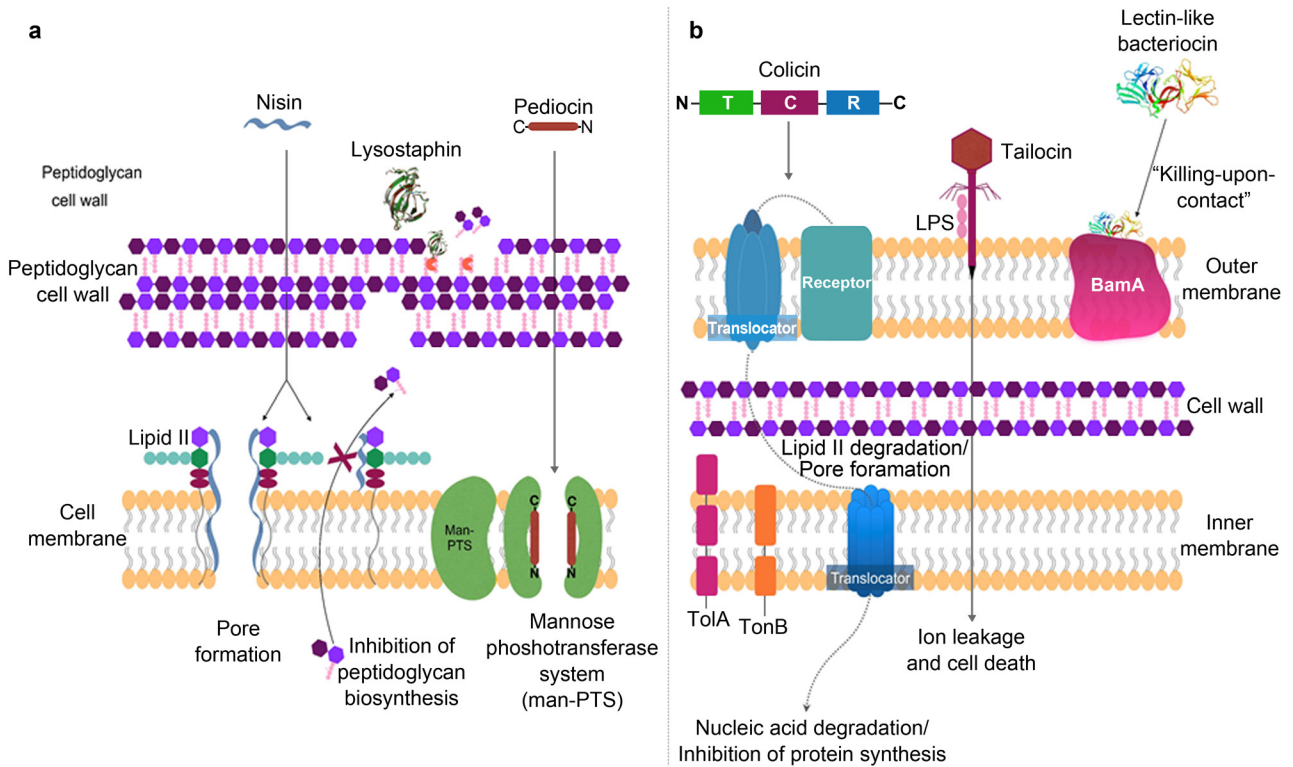
Fig. 3. Bacteriocin mechanism of action on a) Gram-positive and b) Gram-negative bacteria.

pore-formation by recognizing lipid II or the mannose phosphotransferase system (Paiva et al. 2011). Class I bacteriocins of Gram-positive bacteria also inhibit cell wall synthesis (Abriouel et al. 2011; Sun et al. 2018) (Fig. 3a). Class II bacteriocins make pores as described by the barrel stave or carpet model. Some class III bacteriocins produced by *Bacillus* inhibit the activity of the phospholipase A2, responsible for membrane repair (Abriouel et al. 2011). Class III bacteriocins, like lysostaphin, act directly on the cell wall inhibiting peptidoglycan synthesis without permeabilizing the membrane (Mitkowski et al. 2019). The mannose phosphotransferase system is involved in recognition of some Gram-positive bacteriocins, such as lactococcin A and pediocin, leading to pore-formation and membrane permeabilization (Zhou et al. 2016).

The mechanism of action of Gram-negative bacteriocins, such as colicins, is through recognizing cell surface receptors of a target cell, through the Tol or TonB machinery, as shown in Fig. 3b. Colicins C domain (cytotoxicity domain) is responsible for eliminating other microorganisms through various mechanisms such as membrane permeabilization, nuclease activity, and inhibition of peptidoglycan or lipopolysaccharide O-antigen synthesis (Budič et al. 2011). *Salmonella* colicins (salmocins) display three mechanisms of action: SalE1a and SalE1b cause pore-formation in the membrane, SalE2 and SalE7 have DNase activity, and SalE3 have RNase activity (Schneider et al.

2018). Microcins are also membrane-pore formers, have DNase or RNase activity, and may inhibit protein synthesis (Yang et al. 2014).

The genus *Pseudomonas* produces high molecular weight bacteriocins such as R, F, and S type pyocins (Oluyombo et al. 2018). Besides the type B microcins (Ghequire et al. 2018a), tailocins (Ghequire and De Mot 2015), and LlpAs (Ghequire et al. 2018b). Pyocins and tailocins are characterized by having a complex structure that resembles phage tails (Ghequire and De Mot 2015; Patz et al. 2019), and the mechanism of action is based on the recognition of specific receptors on the cell surface causing pore formation, nonspecific degradation of nucleic acids or lipid II-degradation (Ghequire and De Mot 2018; Patz et al. 2019) (Fig. 3b).

Pyocins have a limited antimicrobial spectrum, mainly inhibiting competitors highly related to the producer strain (Redero et al. 2018). However, some R-type pyocins can inhibit other species such as *Campylobacter* sp., *Neisseria gonorrhea*, *Neisseria meningitides*, and *Haemophilus ducreyi* (Naz et al. 2015). Since the mechanism of action of pyocins depends on a cellular receptor, its use has been proposed to replace broad-spectrum antibiotics, to reduce the damage that antibiotics usually cause to the human microbiome (McCaughey et al. 2014).

LlpAs have a selective mechanism of action, different from other bacteriocins produced by *Pseudomonas* species. Probably because their structure does not

consist of the classic three-domain model present in bacteriocins of similar size (T, R, and C). Instead, they contain two monocotyledonous mannose-binding lectin (MMBL) domains associate with the recognition of BamA (Ghequire et al. 2018a). This protein of the outer membrane of Gram-negative bacteria facilitates the insertion of other proteins into the cell membrane (Noinaj et al. 2014). Although the mechanism of action of LlpAs remains unknown, a "killing upon contact" mechanism has been suggested (Ghequire et al. 2018a).

Bacteriocins and natural DNA transformation

Bacteria can take up exogenous DNA and incorporate it into their genome through a process termed competence. Competent bacteria can use absorbed DNA as a source of nutrients, DNA reparation, or recombination with the genome. Natural DNA transformation happens when absorbed DNA is integrated into the genome (Veening and Blokesh 2017). This process is considered the primary mode of horizontal gene transfer (HGT) in bacteria, along with conjugation (direct cell to cell transfer of DNA via a specialized conjugal pilus) and phage transduction (DNA transfer mediated by viruses). Naturally competent bacteria couple the DNA-uptake process with other physiological responses, such as growth arrest and synthesis of antimicrobial polypeptides (bacteriocins) (Mignolet et al. 2018). Bacteria secrete bacteriocins upon entry into the competence state to kill surrounding competitors.

The competence pathway in *Streptococcus pneumoniae* is regulated by a secreted peptide pheromone, the competence-stimulating peptide (CSP). The precursor peptide of CSP, ComC, is processed by an ABC transporter/protease, ComAB, immediately after the double-glycine motif to yield the active CSP (Shanker and Federle 2017). Extracellular CSP activates the ComCDE two-component signal-transduction pathway, which turns on the sigma factor gene *sig*X/*com*X, to activate the expression of over 100 genes upon entering the competent state (reviewed by Shanker and Federle 2017). At least six CSP-responsive genes are involved in fratricide (killing/lytic factors directed against non-competent siblings). Among them, *cib*ABC encodes a two-peptide bacteriocin responsible for lysis of cells lacking the corresponding immunity factor, CibC. The *cbp*D gene encodes a murein hydrolase containing a cytosine, histidine-dependent amidohydrolase peptidase. *lyt*A encodes an effector of autolysis in *S. pneumoniae*. Interestingly, this predation mechanism appears to be restricted to isogenic or closely related strains, suggesting that competent cells target corresponding cells to acquire homologous DNA sequences to maintain genome integrity or acquire new

gene alleles from siblings. This ability to tackle closely related strains would be discussed in the section "Bacteriocins as modulators of gastrointestinal microbiota and population diversity". *Streptococcus salivarius*, on the other hand, modules competence and bacteriocin production through the ComRS complex, which serves as the connector that directly regulates both *com*X and bacteriocin genes (Mignolet et al. 2018). *S. salivarius* bacteriocins have a broad spectrum of bacterial prey including the closely related *Streptococcus vestibularis*, more distant streptococci (*Streptococcus mutans* and *Streptococcus pyogenes*), and opportunistic pathogens such as *Enterococcus faecalis*, *L. monocytogenes*, and *S. aureus* (Mignolet et al. 2018).

Bacteriocins as food antimicrobial and anticancer agents

Bacteriocin applications have been focused primarily on food preservation, either alone or in combination with other compounds. The long shelf life of food products relies on adding chemicals, sugars, salts, and other preservatives allowed by the regulation. The addition of these substances reduces water activity, inhibiting the growth of undesirable pathogenic microorganisms that can spoil food. However, the addition of these chemicals benefits the industry but not the consumer since the continuous consumption of chemical preservatives through packaged foods can affect consumers' health. There is an association of these additives with chronic degenerative diseases, and the intake of these additives can prompt the development of some types of cancer (Monteiro et al. 2010; Moubarac et al. 2013). A more friendly strategy to preserve food products is the use of bacteriocins beneficial for both the food industry and consumers, helping to reduce the use of chemical preservatives in food (Sarika et al. 2019). The growth of pathogens in food can be controlled by the inoculation of bacteriocin-producing lactic acid bacteria or by the addition of purified bacteriocins (Silva et al. 2018). Bacteriocins have also been added to the coating of food packaging to reduce food spoilage (Salgado et al. 2015; Castellano et al. 2017).

The use of bacteriocins as food preservatives does not affect the organoleptic properties of foods. There are safe bacteriocins for human consumption, such as Enterocin AS-48 (Sánchez-Hidalgo et al. 2011), lacticin 3147 (Mills et al. 2017), and salmocins (Schneider et al. 2018) but only nisin (Nisaplin™, Biosafe™), pediocin PA-1 (Microgard™, Alta 2431), sakacin (Bactoferm™ B-2, Bactoferm™ B-FM) and leucocin A (Bactoferm™ B-SF-43) are commercially used to improve shelf-life of food (Vijay Simha et al. 2012; Daba and Elkhateeb 2020).

The Food and Agriculture Organization (FAO) support the use of probiotics in food systems, since probiotics offer health benefits, especially for the gastrointestinal tract. Probiotics play an important role in modifying some metabolic pathways that, in turn, regulate cell proliferation, apoptosis, differentiation, angiogenesis, inflammation, and metastasis, which are relevant aspects to prevent the development of cancer (Bermudez-Brito et al. 2012).

Bacteriocins have shown cytotoxic activity against cancer cells, and therefore they could be considered tools to develop new anticancer drugs (Baindara et al. 2018). The charge of normal cell membranes is neutral, while cancer cells have a negative charge due to the high content of anionic phosphatidylserine, o-glycosylated mucins, sialylated gangliosides, and heparin sulfates. Bacteriocins, being cationic peptides, can preferentially bind to the negatively charged membrane of cancer cells compared to normal cells. Some bacteriocins with anticancer activities are colicins, which have shown cytotoxic activity against various human tumor cell lines such as breast cancer, colon cancer, and bone cancer (Kaur and Kaur 2015). Some examples of the potential applications of bacteriocins are shown in Table I.

The potential therapeutic uses of bacteriocins produced by lactic acid bacteria have increased over time. López-Cuellar et al. (2016) found that 37% of the investigations on bacteriocins were focused on medical applications including cancer, systemic infections, stomatology, skincare, and contraceptives. 29% of studies focused on food preservation, 25% on bio-nanomaterials, and 9% within veterinary. The number of patents on bacteriocins has also increased. From 2004 to 2015, 245 bacteriocin patents were issued, 31% related to the biomedical field, 29% to food preservation, 5% to veterinary medicine, 13% to production and purification process, and 16% to molecular modifications in producer strains. The smallest proportion concerns bio-nanomaterials and industrial applications.

Bacteriocins in agriculture

The indiscriminate use of agrochemicals has caused severe damage to human health and the environment. This problem aims to find alternatives to fight pests and diseases in a more environmentally friendly way. Bacteria that produce inhibitory substances have been used as inoculants to indirectly stimulate the growth of crops, fighting the phytopathogens. Plant growth-promoting rhizobacteria (PGPR) are generally marketed in the form of mono or multi-inoculants that include bacteria such as *Streptomyces venezuelae*, *Gluconacetobacter diazotrophicus*, *Burkholderia* sp., *Azospirillum*

brasilense, *P. protegens*, *Pseudomonas putida*, among others. Most of these formulations have been traded to promote plant growth and not fight plant pathogens (Cesa-Luna et al. 2020). Therefore, little efforts have been focused on applying of bacteriocins for plant disease biocontrol, and hence their production by PGPR is poorly understood.

Some examples of bacteriocins applied to agriculture are agrocin 84 and thuricin 17. Agrocin 84 is produced by *Agrobacterium radiobacter* K84 and is useful to kill *Agrobacterium tumefaciens*, the causal agent of crown gall disease in plants (Kim et al. 2006). Thuricin 17 is produced by *B. thuringiensis* NEB17, this bacteriocin is a plant biostimulant with no harmful effects on nodulating rhizobia or other PGPR (Nazari and Smith 2020). *Pseudomonas syringae* pv. ciccaronei strain NCPPB2355 produces an inhibitory bacteriocin against *P. syringae* subsp. *savastanoi*, the causal agent of olive knot disease. Other important bacteriocins are those produced by the genus of *Pseudomonas* and *Bacillus* (Table II). These bacteriocins inhibit one of the primary phytopathogenic fungi, *Fusarium*, which can infect different types of plants, including celery, onion, cabbage, banana, cucumber, tomato, eggplant, cantaloupe, watermelon, spinach, among others. Direct application of bacteriocin induces a resistance mechanism in plants against pathogens and abiotic stresses. Application of thuricin 17 on plants enhanced production of phenolics, phenylalanine ammonia-lyase activity, and antioxidant defense (Nazari and Smith 2020).

Bacteriocins as modulators of gastrointestinal microbiota and population diversity

The autochthonous bacteria that colonize the entire human gastrointestinal tract, from the mouth to the colon, confer various physiologic benefits to the host. The prokaryotic symbiont population in humans ranges from 10^3–10^5 CFU/ml in the jejunal lumen) of healthy individuals to 10^{11}–10^{12} CFU/ml in the colon, gut microbiota, prevents pathogen growth in the gastrointestinal tract (Sundin et al. 2017). This regulation is given through various microbial mechanisms, one of them is the release of bacteriocins, which prevent dysbiosis and consolidate the homeostasis of the gastrointestinal microbiota. The homeostatic balance in the human gut microbiota has become a significant public health problem due to changes in eating habits, type of diet, and administration of broad-spectrum antibiotics (Cotter et al. 2013). Ultra-processed food intake has increased saturated fats, omega-6 fatty acids, transfatty acids, and simple carbohydrates in the human diet while it has decreased the intake of omega-3 fatty acids, fiber, and complex carbohydrates. This diet high in fat

Table I
Bacteriocins with potential application as therapeutic and food preservatives.

Bacteriocin	Producer bacteria	Target microorganism	Use	Reference
1. Food preservation				
AMA-K, Leucocin K7	*L. plantarum* AMA-K	*Enterococcus* spp., *E. coli*, *K. pneumoniae*, *Listeria* spp.	Amasi, fermented milk product	(Todorov 2008)
Aureocin A70	*S. aureus* A70	*L. monocytogenes*	Dairy product	(Carlin Fagundes et al. 2016)
Bacteriocin 32Y	*L. curvatus*	*L. monocytogenes*	Pork and beef	(Gálvez et al. 2007)
Bacteriocin GP1	*L. rhamnosus* GP1	*Staphylococcus* sp., *Aeromonas* sp., *Lactobacillus* sp., *Pseudomonas* sp., *Vibrio* sp.	Fish	(Sarika et al. 2019)
Bovicin HC5 + Nisin	*Streptococcus bovis* HC5	*L. monocytogenes*, *S. aureus*	Fresh cheese	(Pimentel-Filho et al. 2014)
Divergicin M35	*Carnobacterium divergens* M35	*L. monocytogenes*	Smoked fish	(Benabbou et al. 2020)
Enterocin	*E. faecium* FAIR-E 198	*Listeria* spp.	Feta cheese	(Sarantinopoulos et al. 2002)
Enterocin 416K1	*E. casseliflavus* IM 416K1	*L. monocytogenes* NCTC 10888	Cottage cheese	(Iseppi et al. 2008)
Enterocin AS-48	*Enterococcus* sp.	*L. monocytogenes*, *B. cereus*	Cheese, vegetable, purees, and soups	(Gálvez et al. 2007)
H1, H2, H3, H4	*Bacillus* sp.	*V. alginolyticus*, *Aeromonas hydrophilla*, *P. stutzeri*	Antimicrobial used in fish	(Feliatra et al. 2018)
Lacticin 3147	*L. lactis*	*L. monocytogenes*	Matured and cottage cheese	(Mills et al. 2017)
Lacticin NK24	*L. lactis*	*Leuconostoc mesenteroides* KCCM 11324	Seafood	(Lee and Paik 2001)
Leucocin K7	L. mesenteroides K7	*L. monocytogenes*	Dairy product	(Shi et al. 2016)
Mecedocin	*S. macedonicus* ACA-DC 198	*C. tyrobutyricum* LMG 1285T	Kasseri cheese	(Anastasiou et al. 2009)
NE	*L. gasseri* K7 (Rifr), *L. gasseri* LF221(Rifr)	*C. tyrobutyricum*	Semi-mature cheese	(Bogovič Matijašić et al. 2007)
Nisin	*Lactococcus* spp., *Streptococcus* spp.	*L. monocytogenes*, *Clostridium botulinum*, *S. mutans*, *L. innocua*, *S. aureus*, *S. pneumoniae*, *B. cereus*	Dairy products, meat, seafood	(Juturu and Wu 2018)
Pediocin PA1	*P. acidilactici*	*L. monocytogenes*	Dairy products, meat	(Liu et al. 2008)
Plant-made salmocins	*Salmonella* spp.	*S. enterica*	Red meat	(Schneider et al. 2018)
Plant-made colicins (GRN 676, GRN 593)	*E. coli*	*E. coli*, *P. aeruginosa*, *Salmonella* spp.	Meat, fruits, or vegetables	(Hahn-Löbmann et al. 2019)
Psicolin 126, carnocyclin A	*C. maltoaromaticum*	*L. monocytogenes*	Ready-to-eat meat products	(Liu et al. 2014)
Reuterin	*L. reuteri*	*E. coli*, *S. aureus*, *Candida albicans*	Food preservation	(Helal et al. 2016)
Sakacin P	*L. sakei*	*L. monocytogenes*	Beef and Salmon	(Teneva-Angelova et al. 2018)
Thuricin *Bt*CspB	B. thuringiensis	*B. cereus*	Food preservation and disease associate to *B. cereus*	(Huang et al. 2016)
2. Bacterial infections				
ABP118	*L. salivarius* subsp. salivarius UCC118	*Bacteroides*	Antimicrobial agent	(Riboulet-Bisson et al. 2012)
Colicins Js and Z	*E. coli*	*Enteroinvasive*, *E. coli* (EIEC) and *Shigella*	Gastrointestinal infections	Bosák et al. 2021
Divercin V41	*C. divergens*	*L. monocytogenes*	Antimicrobial agent	(Rihakova et al. 2010)
Duramycin	*Streptomyces cinnamoneus*	*B. subtilis*	Antimicrobial, antiviral, immunomodulation, ion channel modulation, treatment of atherosclerosis and cystic fibrosis	(Huo et al. 2017)

Table I. Continued

Bacteriocin	Producer bacteria	Target microorganism	Use	Reference
Enterocin CRL35	*E. mundtii*	*L. monocytogenes*	Gastrointestinal infections	(Salvucci et al. 2012)
Epidermin and mers-acidin-like peptides	*S. epidermidis*	*P. acnes*	Acne, folliculitis.	(Gillor et al. 2008)
Gallidermin/ epidermin	*S. gallinarum*	*S. epidermidis*, S. aureus	Skin infections or associated with implants and prostheses	(Bengtsson et al. 2018; Bonelli et al. 2006)
Gassericin E	*L. gasseri* EV1461	Pathogens associated with vaginosis	Vaginal infections	(Maldonado-Barragán et al. 2016)
Haemocin type B	*Haemophilus haemolyticus*	*H. influenza*	Respiratory infections	(Latham et al. 2017)
Lactocin 160	*L. rhamnosus*	*G. vaginalis*	Urogenital tract infections, bacterial vaginosis	(Turovskiy et al. 2009)
Laterosporulin10	*Brevibacillus* sp. strain SKDU10	*S. aureus*, *Mycobacterium tuberculosis* (Mtb H37Rv), *M. smegmatis* MC2 155	Human microbial pathogens	(Baindara et al. 2016)
Mersacidin	*B. amyloliquefaciens*	Methicillin-resistant *S. aureus* (MRSA)	Skin infection	(Kruszewska et al. 2004)
Microcin J25 (lasso-peptide)	*E. coli*	*S. enterica, E. coli, S. flexnerii*	Gastrointestinal infections	(Dobson et al. 2012)
Nisin A, Nisin Z, Nisaplin	*L. lactis*	*S. mutans, S. aureus, E. faecalis, S. mastitis, C. albicans*	Gastrointestinal, respiratory, and skin infections, oral health	(Shin et al. 2016)
Oralpeace TM (encapsulated nisin)	*L. lactis*	*S. mutans, P. gingivalis*	Dental caries, gingivitis	(Perez et al. 2014)
Piscicolin 126	*Carnobacterium* spp.	*Listeria* spp.	Antimicrobial agent	(Miller and McMullen 2014)
Plantaricin 423	*L. plantarum*	*Listeria* spp.	Antimicrobial agent	(Guralp et al. 2013)
PLNC8 αβ	*L. plantarum*	*Staphylococcus* sp., *Porphyromonas gingivalis*	Antimicrobial agent	(Bengtsson et al. 2020)
R-pyocins	*P. aeruginosa*	*P. aeruginosa*	Antimicrobial agent	(Redero et al. 2018)
TOMM Streptolysin S (SLS)	*S. pyogenes*	*Clostridium* sp., *Listeria* sp.	Hemolytic and cytotoxic activity against macro-phages and neutrophils	(Molloy et al. 2015)
3. Anticancer drugs				
Cancer cell lines				
Azurin	*P. aeruginosa*	MCF-7, UISO-Mel-2, osteosarcoma (U2OS)		(Nguyen and Nguyen 2016)
Bovicin HC5	*S. bovis* HC5	MCF-7, HepG2		(Rodrigues et al. 2019)
Colicin E3	*E. coli*	P388, HeLa, HS913T		(Kohoutova et al. 2014
Duramycin	*S. cinnamoneus*	AsPC-1, Caco-2, Colo320, CT116, JJN3, Lovo, MCF-7, MDA-B-231, MIA PaCa-2		(Rodrigues et al. 2019)
Enterocin LNS18	*E. thailandicus*	HepG2		(Al-Madboly et al. 2020)
Laterosporulin LS10	*Brevibacillus latero-sporus* SKDU10	HeLa, MCF-7, H1299, HEK293T, HT1080		(Baindara et al. 2016)
M2163, M2386	*L. casei* ATCC 334	SW480		(Rodrigues et al. 2019)
Microcin E492	*K. pneumoniae*	HeLa, Burkitt lymphoma variant (RJ2.25)		(Kaur and Kaur 2015)
Nisin A	*L. lactis*	Head and neck squamous cell carcinoma (HNSCC)		(Shin et al. 2016)
Pediocin K2a2-3	*P. acidilactici* K2a2-3	HT2a, HeLa		(Villarante et al. 2011)
Pediocin CP2	*P. acidilactici* CP2 MTCC501	HeLa, MCF-7, HepG2, murine myeloma (Sp2/0-Ag 14)		(Kumar et al. 2012)

Table I. Continued

Bacteriocin	Producer bacteria	Cancer cell lines	Reference
Pep27anal2	*S. pneumoniae*	Jurkat, HL-60, AML-2, MCF-7, SNU-601	(Rodrigues et al. 2019)
Plantaricin A	*L. plantarum* C11	GH4, Reh, Jurkat, PC12, N2A	(Sand et al. 2013)
Plantaricin P1053	*L. plantarum* PBS067	E705	(De Giani et al. 2019)
Pyocin S2	*P. aeruginosa* 42A	HepG2, Im9, murine tumor (mKS-A TU-7), human fetal foreskin fibroblast (HFFF)	(Abdi-Ali et al. 2004)
Sungsanpin	*Streptomyces* spp.	A549	(Um et al. 2013)
Smegmatocin	*M. smegmatis* 14468	HeLa, AS-II, HGC-27, mKS-A TU-7	(Kaur and Kaur 2015)

NE – non specified

Table II
Biocontrol potential of bacteriocin-producing microorganisms in agriculture.

Bacteriocin	Producer bacterium	Phytopathogen	Reference
Amylocyclin	*B. amyloliquefaciens*	*Ralstonia solanacearum* and *X. campestris*	(Scholz et al. 2014)
Bacteriocin 32Y	*P. aeruginosa* RsB29	*Fusarium* sp.	(Sindhu et al. 2016)
Carocin D	*P. carotovorum* subsp. *carotovorum*	*P. carotovorum* subsp. *Carotovorum*	(Grinter et al. 2012; Roh et al. 2010)
Enterocin UNAD 046	*E. faecalis*	*B. theobromae*, *A. niger*, *P. expansum*, *P. ultimum.*	(David and Onifade, 2018)
Fluoricin BC8	*P. fluorescens* BC8	*P. solanacearum*	(Sindhu et al. 2016)
Gluconacin	*G. diazotrophicus* PAL5	*X. albilineans* and *X. vasicola* pv. *vasculorum.*	(Oliveira et al. 2018)
LlpA	*P. putida* BW11M1	*P. syringae*	(Parret et al. 2005)
Morricin 269, Kurstacin 287, Kenyacin 404, Entomocin 420, Tolworthcin 524	*B. thurigiensis*	*Trichoderma* spp., *A. nodulans*, *F. graminis*, *F. oxysporum*, *Rhizopus* sp., *Mucor rouxii*	(De La Fuente-Salcido et al. 2008; Salazar-Marroquín et al. 2016)
NE	*P. syringae* pv. *ciccaronei*	*P. syringae* subsp. *savastanoi*	(Lavermicocca et al. 2002)
BLIS RC-2	*B. amyloliquefaciens* RC-2	*R. necatrix*, *P. oryzae*, *A. tumefaciens*, *Xanthomonas campestris* pv. *campestris*, *C. dematium*	(Abriouel et al. 2011)
NE	*B. gladioli*	*Tatumella ptyseos*	(Marín-Cevada et al. 2012)
BL8	*B. thuringiensis* subsp. *tochigiensis* HD868	*A. niger*, *A. fumigatus*, *A. flavus*, *Cryphonectria parasitica*, *F. oxysporum*, *Penicillium digitatum.*	(Subramanian and Smith 2015)
Plantazolicin	*B. velezensis* FZB42 (*B. amyloliquefaciens* subsp. *plantarum*)	*B. anthracis* and nematodes.	(Chowdhury et al. 2015)
Putidacin L1	*P. protegens*, *P. putida*	*P. syringae*	(Rooney et al. 2020)
Rhizobiocin	*Rhizobium* spp.	*P. savastanoi*	(Kaur Maan and Garcha 2018)
SF4c tailocins	*P. fluorescens* SF4c	*X. vesicatoria*	(Príncipe et al. 2018)
Syringacin M	*P. syringae* pv. *tomato* DC3000	*P. syringae*	(Li et al. 2020)

NE – non specified

and carbohydrates and low in micronutrients can disturb the human microbiota with concomitant metabolic disorders (Miclotte and Van de Wiele 2020).

Probiotics can colonize, at least temporally, the human gastrointestinal tract due to the efficient competition mediate by bacteriocin production. Thus, the intake of *Lactobacillus* species in probiotherapy has shown health-promoting effects on treating inflammatory gastrointestinal diseases like constipation, diarrhea, irritable bowel syndrome, gastritis, gastroesophageal reflux, ulcerative colitis syndrome, Crohn's disease, among others (Kumar et al. 2016). Bacteriocins can play an essential role in the homeostasis of different subpopulations of microbial communities. For example, in the relationship of certain bacteriocin-producing, sensitive, and resistant bacterial populations bacteria

can interact with each other in a set of incessant battles without a clear winner (Kerr et al. 2002).

In some cases, the growth rate of a resistant population can be higher than that of the bacteriocin-producing population (P), which generally possess a plasmid with genes encoding the bacteriocin and bacteriocin-specific immunity protein that make the bacteriocin-producing population immune to its bacteriocin. Still, at the same time, the resistant population (R) has a slower growth rate than that of the sensitive population (S). The susceptible population has an advantage over the resistant population because sensitive bacteria have a higher growth rate. The resistant population has an advantage over the bacteriocin-producing population because of its higher growth rate. And the bacteriocin-producing population can displace susceptible populations because bacteriocin-producing bacteria can kill sensitive bacteria making the three types of bacterial populations coexist in a balance of subpopulations preserving the diversity of the community (Kerr et al. 2002).

The bioinformatic analysis of bacteriocins encoded within 317 microbial genomes found in the human intestine revealed 175 bacteriocins in Firmicutes (which includes LAB), 79 in Proteobacteria, 34 in Bacteroidetes, and 25 in Actinobacteria (Drissi et al. 2015). The analysis showed that bacteriocins produced by the intestinal bacteria display wide differences, in the size and amino acid composition, compared to other bacteriocins. These bacteriocins contain less aspartic acid, leucine, arginine, and glutamic acid but more lysine and methionine. Depending on their α-helical structure, charge, and hydrophobicity, they may have a broader spectrum of activity (Zelezetsky and Tossi 2006) but, in turn, lower antimicrobial activity and, therefore, they can better modulate microbial populations (Drissi et al. 2015). The microbial community that inhabits the human gut appears to impart specific functions to human metabolism and health by interconnecting signals from the brain, the immune system, the endocrine system, and the gut microbiota itself (Vivarelli et al. 2019). So, depending on the type of bacteria colonizing the gastrointestinal tract will determine the type of signaling molecules released and, therefore, the impact on host health and disease. That is why the microbial diversity of microbiota is tightly regulated. An example of this type of regulation exerted by bacteriocins is the effect of plantaricin P1053 produced by *Lactobacillus plantarum* strain PBS067; which exhibited a broad-spectrum of antimicrobial activity against Gram-positive and Gram-negative bacteria. Furthermore, plantaricin P1053 showed an improvement in the viability of healthy cells and a proliferation reduction of cancerogenic human intestinal cells. The mechanism involved in this case was through the epidermal growth factor receptor (EGFR) pathways (De Giani et al. 2019). *Bifidobacterium longum* subsp. *longum* NCC2705 produces the bacteriocin serpin, which is a protease inhibitor that interacts directly with the host factors. Serpin inhibits pancreatic and neutrophil elastases by mediating some gastrointestinal anti-inflammatory effects (Ivanov et al. 2006). The production of bacteriocins by the microbiota that inhabits the human gut affects the individual's metabolic processes, whether it improves health or causes dysbiosis and disease Therefore, bacteriocins production by the microbiota is tightly regulated. One way of exploiting the bacteriocin potential of prevailing bacterial commensals to cure multiresistant infections is to stimulate the endogenous bacteriocin producers at specific times and locations. *S. salivarius* population, for example, produces bacteriocins of high potency against infectious pathogens and is dominant and genetically diverse in the human digestive tract (Hols et al. 2019). Bacteriocin-related genes of *S. salivarius* can be activated upon addition of short ComS pheromone into the culture medium (Mignolet et al. 2018). Thus pheromone-based mobilization of bacteriocins in the commensal microbiota could be achieved *in vivo* by the addition of ComS pheromone which complexes with the ComR sensor activating the master regulator of competence (ComX), and coupling competence and predation response in *S. salivarius* (Hols et al. 2019). Nevertheless, oral administration of signaling pheromones remains elusive. To minimize environmental influences (i.e. resist most digestive proteases, the stomach barrier, and low solubility of signaling pheromones) and ensure the activating pheromone efficiency *in vivo*, more advanced enabling formulations to improve oral bioavailability is required.

A multidrug-resistant *E. faecalis* strain was actively killed by commensal enterococci. A heptapeptide pheromone, cOB1, produced by native *E. faecalis;* was involved in the killing of multidrug-resistant *E. faecalis* strain V583, the killing of V583, resulted from lethal cross-talk between accumulated mobile elements (Gilmore et al. 2015). Since multidrug-resistant *Enterococcus* possessed the limited ability to grow in the presence of commensal *Enterococcus* strains due to the production of peptide pheromones. We could hypothesize that infections caused by MDR strains can be fought by the same genera commensal strains using the suitable pheromone to activate the killing response. MDR enterococci colonize the patient after perturbating the native flora by antibiotic treatment when commensal enterococci strains are excluded. Therefore, a potential therapy could be the formulation of enterococci native strain along with the signaling pheromone. Currently, there is controversy over the adequate use of probiotherapy, more research must be done about whether probiotics are helpful and safe for various health condi-

tions. We still do not know the concentrations necessary to benefit healthy and sick individuals and the time of probiotics intake to improve individual health.

Bacteriocins commercially available: a patent perspective

According to the World Intellectual Property Organization (WIPO), over the last 30 years, more than 800 patent applications with the term "bacteriocin" in title or abstract were published, while Espacenet website reports more than 8900. Fig. 4 shows the patents published between January 1, 2000, and August 7, 2020, using the Patent Inspiration search engine with the term "bacteriocin". Over the last 20 years, China has published 234 patents, followed by the United States with 132, while Mexico only published 17 patents (Fig. 4). Among these patents, 312 (36.4%) are associated with nisin and lactic acid bacteria.

Bacteriocins have fascinating properties concerning their size, structure, mechanism of action, inhibitory spectrum, and immunity mechanisms that endorse them with market potential. However, just four bacteriocin formulations are commercially available: nisin (Nisaplin™, Biosafe™, Oralpeace™), pediocin PA-1 (Microgard™, Alta 2341), sakacin (Bactoferm™ B-2, Bactoferm™ B-FM) and leucocin A (Bactoferm™ B-SF-43) are mainly used as food preservatives in the United States and Canada (Daba and Elkhateeb 2020; Radaic

et al. 2020). Other FDA-approved bacteriocins, with the intended use as an antibacterial for food, are colicins, salmocins, and *Clostridium* phage lysins, but they are not in the market yet (Hahn-Löbmann et al. 2019). One limitation of using purified bacteriocins in the food industry could be the high cost of production and purification compared to the price of food additives. It is more feasible to produce formulations of whole bacteria with their metabolites and use them as "protective cultures" on foods. Thus, several bacteria that produce bacteriocin have obtained the GRAS status and are used commercially as a preservative in a wide range of food products or as probiotics. In the list is *Carnobacterium divergens* M35, *Bacillus coagulans* GBI-30, *Bacillus subtilis* strain SG 188, *Lactobacillus plantarum* Lp-115, *Lactobacillus fermentum* CECT5716, *Lactobacillus paracasei* strain F19, *Lactobacillus plantarum* strain 299v, *Bacillus coagulans* SNZ1969, *Lactobacillus acidophilus* DDS-1, *Bifidobacterium animalis* subsp. lactic UABla-12, *Bifidobacterium longum* BB536, *Bifidobacterium bifidum* Rosell®-71, *Bifidobacterium longum* ssp. infantis Rosell®-33, *Lactobacillus helveticus* Rosell®-52, *Lactobacillus rhamnosus* LGG®, *Lactobacillus curvatus* DSM 18775, and *Streptococcus salivarius* K12. An alternative to the costly fermentation production and purification of bacteriocins from a natural producer strain is chemical synthesis. Advances in solid-phase peptide chemical synthesis, lower price for reagents and building blocks, has made the chemical synthesis of bacteriocins more attractive and competitive. Furthermore, through
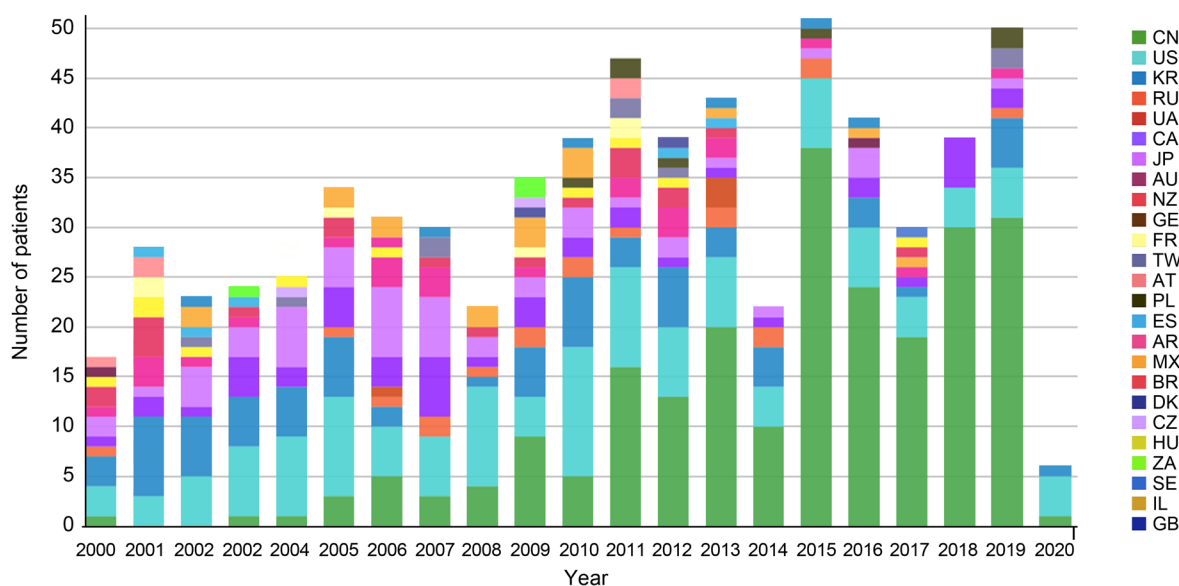
Fig. 4. Timeline of bacteriocin patents reported worldwide from January 1, 2000 to August 7, 2020. Countries with the highest number of reported patents per year are shown. The figure was generated with the Patent Inspiration search engine (https://www.patentinspiration.com).

CN – China, US – United States, KR – Korea, RU – Russian Federation, UA – Ukraine, CA – Canada, JP – Japan, AU – Australia, NZ – New Zealand, GE – Germany, FR – France, TW – Taiwan, AT – Austria, PL – Poland, ES – Spain, AR – Argentina, MX – Mexico, BR – Brazil, DK – Denmark, CZ – Czech Republic, HU – Hungary, ZA – South Africa, SE – Sweden, IL – Israel, GB – United Kingdom.

chemical approaches, it is possible to perform amino acid substitution, use non-natural or modified residues, and make backbone and side-chain modifications to improve potency or stability of bacteriocins (Bédard and Biron 2018). Those advanced chemical methods will surely enable the screening and identification of more potent or stable bacteriocins.

Bacteriocin formulations can be used as nutritional supplementation. Few *in vivo* experiments on bacteriocin dietary formulations have described the effects of bacteriocins on the gastrointestinal microbiota of mice, rats, rabbits, ruminants, fish, and poultry. A multispecies probiotic combination (*Lactobacillus reuteri*, *Enterococcus faecium*, *B. animalis*, *Pediococcus acidilactici*, and *Lactobacillus salivarius*) increased nutrient digestibility, digestive enzyme activities, and anti-inflammatory effect in broilers (Palamidi et al. 2016). The efficacy of *L. acidophilus*, *B. subtilis*, and *Clostridium butyricum* supplementation in broilers improved growth performance, ileal amino acids digestibility, and humoral immunity (Zhang and Kim 2014). The addition of nisin (alone or in combination with salinomycin or monensin) to broilers' diet was associated with an apparent nutrient digestibility (Kierończyk et al. 2017). Dietary supplementation with *Paenibacillus ehimensis* NPUST1 (bacteriocin-like activities against *Aeromonas hydrophila*) improved the growth performance, immunity, and disease resistance in Nile tilapia (Chen et al. 2019). Altogether, these reports indicate the potential of bacteriocins as nutritional supplementation.

Compared to the food industry, the medical field could represent a higher profit for the use of bacteriocins. However, to exploit the full potential of bacteriocins in the medical industry, they must overcome some drawbacks such as sensitivity to proteases, immunogenicity issues, and the development of bacteriocin resistance by pathogenic bacteria. In this regard, advanced chemical approaches can be used to make disulfide bridges, head-to-tail macrocyclization, N-terminus formylation, amino acid substitutions, and other modifications; to make bacteriocins more potent and stable, enabling them to surpass their current drawbacks (Bédard and Biron 2018). Another factor that prevents the commercial use of bacteriocins in medical applications might be attributed to the low approval of the regulatory process. Over the last decade, the number of *in vivo* trials has increased, but clinical application of bacteriocins requires more investigation to determine their efficacy, stability, and kinetic properties in/on the human body. For example, nisin ZP and nisin AP, significantly reduced the tumor volume in mouse-induced oral cancer. Lacticin 3147 reduced *S. aureus* Xen 29 growth and prevented dissemination of the pathogen in the spleen, liver, and kidney of a murine model. Salivaricin prevented *Candida albicans* coloni-

zation in the oral cavity of a mouse model. ESL5 has been applied as a lotion in a patient with inflammatory acne lesions caused by *Propionibacterium acnes* (López-Cuellar et al. 2016; Soltani et al. 2021). Lantibiotics such as nisin, clausin, and amyloliquecidin (AmyA) are effective in treating *S. aureus*-induced skin infection in mice (van Staden et al. 2016). AS-48 prevents and treats skin diseases, even with multi-drug resistant microorganisms, and has the potential as a leishmanicidal agent (Cebrian et al. 2019). Despite their therapeutic possibilities, bacteriocins have not yet entered into clinical use, and only a limited number have been selected for tests in clinical trials. NAI-107 (*Microbispora corallina*) and mutacin 1140 (*S. mutans* JH1000) are at the late preclinical phase; NVB302 and Moli1901 (Actinoplanes liguriae NCIMB41362) have completed phase I and phase II clinical trials (for clinical studies, see Ongey et al. 2017; Soltani et al. 2021). Finally, apart from those technical limitations mentioned, several factors not covered in this review preclude most patented products make it to market.

Conclusions

Bacteriocins have become an attractive tool to preserve food and improve human health. Bacteriocins can eliminate specific pathogen microorganisms while favoring the preservation of other populations. Since the impact of bacteriocins on each microbial community is not well understood yet, there are limitations to exploit all their potential. It is necessary to continue performing rigorous research focused on developing antimicrobials, anticancer agents, and microbiota modulators before bacteriocins can be available to consumers.

ⓘ ORCID

Catherine Cesa-Luna https://orcid.org/0000-0003-2482-1316
Julia-María Alatorre-Cruz https://orcid.org/0000-0003-4796-0829
Ricardo Carreño-López https://orcid.org/0000-0002-6477-297X
Verónica Quintero-Hernández
        https://orcid.org/0000-0002-1856-8134
Antonino Baez https://orcid.org/0000-0001-8453-3178

Conflict of interest

The authors do not report any financial or personal connections with other persons or organizations, which might negatively affect the contents of this publication and/or claim authorship rights to this publication.

Literature

Abdi-Ali A, Worobec EA, Deezagi A, Malekzadeh F. Cytotoxic effects of pyocin S2 produced by *Pseudomonas aeruginosa* on the growth of three human cell lines. Can J Microbiol. 2004 May 01;50(5):375–381. https://doi.org/10.1139/w04-019

Abriouel H, Franz CMAP, Omar NB, Gálvez A. Diversity and applications of *Bacillus* bacteriocins. FEMS Microbiol Rev. 2011 Jan;35(1):201–232.
https://doi.org/10.1111/j.1574-6976.2010.00244.x

Al-Madboly LA, El-Deeb NM, Kabbash A, Nael MA, Kenawy AM, Ragab AE. Purification, characterization, identification, and anti-cancer activity of a circular bacteriocin from *Enterococcus thailandicus*. Front Bioeng Biotechnol. 2020 Jun 23;8:450.
https://doi.org/10.3389/fbioe.2020.00450

Almeida PF, Pokorny A. Interactions of antimicrobial peptides with lipid bilayers. In: Egelman EH, editor. Comprehensive Biophysics. Amsterdam (Netherlands): Elsevier; 2012. p. 189–222.
https://doi.org/10.1016/B978-0-12-374920-8.00515-4

Alvarez-Sieiro P, Montalbán-López M, Mu D, Kuipers OP. Bacteriocins of lactic acid bacteria: extending the family. Appl Microbiol Biotechnol. 2016 Apr;100(7):2939–2951.
https://doi.org/10.1007/s00253-016-7343-9

Anastasiou R, Aktypis A, Georgalaki M, Papadelli M, De Vuyst L, Tsakalidou E. Inhibition of *Clostridium tyrobutyricum* by *Streptococcus macedonicus* ACA-DC 198 under conditions mimicking Kasseri cheese production and ripening. Int Dairy J. 2009 May;19(5):330–335. https://doi.org/10.1016/j.idairyj.2008.12.001

Atanaskovic I, Kleanthous C. Tools and approaches for dissecting protein bacteriocin import in Gram-Negative bacteria. Front Microbiol. 2019 Mar 28;10:646. https://doi.org/10.3389/fmicb.2019.00646

Baindara P, Korpole S, Grover V. Bacteriocins: perspective for the development of novel anticancer drugs. Appl Microbiol Biotechnol. 2018 Dec;102(24):10393–10408.
https://doi.org/10.1007/s00253-018-9420-8

Baindara P, Singh N, Ranjan M, Nallabelli N, Chaudhry V, Pathania GL, Sharma N, Kumar A, Patil PB, Korpole S. Laterosporulin10: a novel defensin like Class IId bacteriocin from *Brevibacillus* sp. strain SKDU10 with inhibitory activity against microbial pathogens. Microbiology. 2016 Aug 01;162(8):1286–1299.
https://doi.org/10.1099/mic.0.000316

Balandin SV, Sheremeteva EV, Ovchinnikova TV. Pediocin-like antimicrobial peptides of bacteria. Biochemistry (Mosc). 2019 May;84(5):464–478. https://doi.org/10.1134/S000629791905002X

Balciunas EM, Castillo Martinez FA, Todorov SD, Franco BDGM, Converti A, Oliveira RPS. Novel biotechnological applications of bacteriocins: a review. Food Control. 2013 Jul;32(1):134–142.
https://doi.org/10.1016/j.foodcont.2012.11.025

Baquero F, Lanza VF, Baquero MR, del Campo R, Bravo-Vázquez DA. Microcins in *Enterobacteriaceae*: peptide antimicrobials in the eco-active intestinal chemosphere. Front Microbiol. 2019 Oct 9;10:2261. https://doi.org/10.3389/fmicb.2019.02261

Bédard F, Biron E. Recent progress in the chemical synthesis of class II and S-glycosylated bacteriocins. Front Microbiol. 2018 May 23;9:1048. https://doi.org/10.3389/fmicb.2018.01048

Behrens HM, Six A, Walker D, Kleanthous C. The therapeutic potential of bacteriocins as protein antibiotics. Emerging Top Life Sci. 2017 Apr 21;1(1):65–74. https://doi.org/10.1042/ETLS20160016

Benabbou R, Subirade M, Desbiens M, Fliss I. Divergicin M35-chitosan film: development and characterization. Probiotics Antimicrob Proteins. 2020 Dec;12(4):1562–1570.
https://doi.org/10.1007/s12602-020-09660-9

Bengtsson T, Lönn J, Khalaf H, Palm E. The lantibiotic gallidermin acts bactericidal against *Staphylococcus epidermidis* and *Staphylococcus aureus* and antagonizes the bacteria-induced proinflamma-tory responses in dermal fibroblasts. MicrobiologyOpen. 2018 Dec; 7(6):e00606. https://doi.org/10.1002/mbo3.606

Bengtsson T, Selegård R, Musa A, Hultenby K, Utterström J, Sivlér P, Skog M, Nayeri F, Hellmark B, Söderquist B, et al. Plantaricin NC8 αβ exerts potent antimicrobial activity against *Staphylococcus* spp. and enhances the effects of antibiotics. Sci Rep. 2020 Dec; 10(1):3580. https://doi.org/10.1038/s41598-020-60570-w

Bermudez-Brito M, Plaza-Díaz J, Muñoz-Quezada S, Gómez-Llorente C, Gil A. Probiotic mechanisms of action. Ann Nutr Metab. 2012;61(2):160–174.
https://doi.org/10.1159/000342079

Bogovič Matijašić B, Koman Rajšp M, Perko B, Rogelj I. Inhibition of *Clostridium tyrobutyricum* in cheese by *Lactobacillus gasseri*. Int Dairy J. 2007 Feb;17(2):157–166.
https://doi.org/10.1016/j.idairyj.2006.01.011

Bonelli RR, Schneider T, Sahl HG, Wiedemann I. Insights into *in vivo* activities of lantibiotics from gallidermin and epidermin mode-of-action studies. Antimicrob Agents Chemother. 2006 Apr;50(4): 1449–1457. https://doi.org/10.1128/AAC.50.4.1449-1457.2006

Bosák J, Hrala M, Micenková L, Šmajs D. Non-antibiotic antibacte-rial peptides and proteins of *Escherichia coli*: efficacy and potency of bacteriocins. Expert Rev Anti Infect Ther. 2021 Mar;19(3):309–322.
https://doi.org/10.1080/14787210.2020.1816824

Budič M, Rijavec M, Petkovšek Ž, Žgur-Bertok D. *Escherichia coli* bacteriocins: antimicrobial efficacy and prevalence among isola-tes from patients with bacteraemia. PLoS One. 2011 Dec 19;6(12): e28769. https://doi.org/10.1371/journal.pone.0028769

Carlin Fagundes P, Miceli de Farias F, Cabral da Silva Santos O, Souza da Paz JA, Ceotto-Vigoder H, Sales Alviano D, Villela Romanos MT, de Freire Bastos MC. The four-component aureocin A70 as a promising agent for food biopreservation. Int J Food Microbiol. 2016 Nov;237:39–46.
https://doi.org/10.1016/j.ijfoodmicro.2016.08.017

Castellano P, Pérez Ibarreche M, Blanco Massani M, Fontana C, Vignolo G. Strategies for pathogen biocontrol using lactic acid bac-teria and their metabolites: A focus on meat ecosystems and indus-trial environments. Microorganisms. 2017 Jul 11;5(3):38.
https://doi.org/10.3390/microorganisms5030038

Cebrián R, Rodríguez-Cabezas ME, Martín-Escolano R, Rubiño S, Garrido-Barros M, Montalbán-López M, Rosales MJ, Sánchez-Moreno M, Valdivia E, Martínez-Bueno M, et al. Preclinical stud-ies of toxicity and safety of the AS-48 bacteriocin. J Adv Res. 2019 Nov;20:129–139. https://doi.org/10.1016/j.jare.2019.06.003

Cesa-Luna C, Baez A, Quintero-Hernández V, De la Cruz-Enríquez J, Castañeda-Antonio MD, Muñoz-Rojas J. The impor-tance of antimicrobial compounds produced by beneficial bacteria on the biocontrol of phytopathogens. Acta Biol Colomb. 2020 Jan 01;25(1):140–154. https://doi.org/10.15446/abc.v25n1.76867

Chen SW, Liu CH, Hu SY. Dietary administration of probiotic *Paenibacillus ehimensis* NPUST1 with bacteriocin-like activity improves growth performance and immunity against *Aeromonas hydrophila* and *Streptococcus iniae* in Nile tilapia (*Oreochromis niloti-cus*). Fish Shellfish Immunol. 2019 Jan;84:695–703.
https://doi.org/10.1016/j.fsi.2018.10.059

Chowdhury SP, Hartmann A, Gao X, Borriss R. Biocontrol mecha-nism by root-associated *Bacillus amyloliquefaciens* FZB42 – a review. Front Microbiol. 2015 Jul 28;6:780.
https://doi.org/10.3389/fmicb.2015.00780

Cotter PD, Ross RP, Hill C. Bacteriocins – a viable alternative to antibiotics? Nat Rev Microbiol. 2013 Feb;11(2):95–105.
https://doi.org/10.1038/nrmicro2937

Daba GM, Elkhateeb WA. Bacteriocins of lactic acid bacteria as biotechnological tools in food and pharmaceuticals: current applications and future prospects. Biocatal Agric Biotechnol. 2020 Sep;28(28):101750. https://doi.org/10.1016/j.bcab.2020.101750

David OM, Onifade OE. Effects of partially purified enterocins from *Enterococcus faecalis* strains on the growth of some phytopathogenic fungi. Ruhuna J Sci. 2018 Dec 31;9(2):160–168. https://doi.org/10.4038/rjs.v9i2.44

De Giani A, Bovio F, Forcella M, Fusi P, Sello G, Di Gennaro P. Identification of a bacteriocin-like compound from *Lactobacillus plantarum* with antimicrobial activity and effects on normal and cancerogenic human intestinal cells. AMB Express. 2019 Dec;9(1):88. https://doi.org/10.1186/s13568-019-0813-6

de la Fuente-Salcido N, Guadalupe Alanís-Guzmán M, Bideshi DK, Salcedo-Hernández R, Bautista-Justo M, Barboza-Corona JE. Enhanced synthesis and antimicrobial activities of bacteriocins produced by Mexican strains of *Bacillus thuringiensis*. Arch Microbiol. 2008 Dec;190(6):633–640. https://doi.org/10.1007/s00203-008-0414-2

Dobson A, Cotter PD, Ross RP, Hill C. Bacteriocin production: a probiotic trait? Appl Environ Microbiol. 2012 Jan 01;78(1):1–6. https://doi.org/10.1128/AEM.05576-11

Drissi F, Buffet S, Raoult D, Merhej V. Common occurrence of antibacterial agents in human intestinal microbiota. Front Microbiol. 2015 May 07;6:441. https://doi.org/10.3389/fmicb.2015.00441

Feliatra F, Muchlisin ZA, Teruna HY, Utamy WR, Nursyirwani N, Dahliaty A. Potential of bacteriocins produced by probiotic bacteria isolated from tiger shrimp and prawns as antibacterial to *Vibrio*, *Pseudomonas*, and *Aeromonas* species on fish. F1000 Res. 2018;7:415. https://doi.org/10.12688/f1000research.13958.1

Gabrielsen C, Brede DA, Nes IF, Diep DB. Circular bacteriocins: biosynthesis and mode of action. Appl Environ Microbiol. 2014 Nov 15;80(22):6854–6862. https://doi.org/10.1128/AEM.02284-14

Gálvez A, Abriouel H, López RL, Omar NB. Bacteriocin-based strategies for food biopreservation. Int J Food Microbiol. 2007 Nov;120(1–2):51–70. https://doi.org/10.1016/j.ijfoodmicro.2007.06.001

Gebhart D, Lok S, Clare S, Tomas M, Stares M, Scholl D, Donskey CJ, Lawley TD, Govoni GR. A modified R-type bacteriocin specifically targeting *Clostridium difficile* prevents colonization of mice without affecting gut microbiota diversity. MBio. 2015 May 01;6(2):e02368-14. https://doi.org/10.1128/mBio.02368-14

Ghequire MGK, De Mot R. The tailocin tale: peeling off phage tails. Trends Microbiol. 2015 Oct;23(10):587–590. https://doi.org/10.1016/j.tim.2015.07.011

Ghequire MGK, De Mot R. Turning over a new leaf: bacteriocins going green. Trends Microbiol. 2018 Jan;26(1):1–2. https://doi.org/10.1016/j.tim.2017.11.001

Ghequire MGK, Öztürk B, De Mot R. Lectin-like bacteriocins. Front Microbiol. 2018a Nov 12;9:2706. https://doi.org/10.3389/fmicb.2018.02706

Ghequire MGK, Swings T, Michiels J, Buchanan SK, De Mot R. Hitting with a BAM: selective killing by lectin-like bacteriocins. MBio. 2018b Mar 20;9(2):e02138-17. https://doi.org/10.1128/mBio.02138-17

Gillor O, Etzion A, Riley MA. The dual role of bacteriocins as anti- and probiotics. Appl Microbiol Biotechnol. 2008 Dec;81(4):591–606. https://doi.org/10.1007/s00253-008-1726-5

Gilmore MS, Rauch M, Ramsey MM, Himes PR, Varahan S, Manson JM, Lebreton F, Hancock LE. Pheromone killing of multidrug-resistant *Enterococcus faecalis* V583 by native commensal strains. Proc Natl Acad Sci USA. 2015 Jun 09;112(23):7273–7278. https://doi.org/10.1073/pnas.1500553112

Grinter R, Milner J, Walker D. Bacteriocins active against plant pathogenic bacteria. Biochem Soc Trans. 2012 Dec 01;40(6):1498–1502. https://doi.org/10.1042/BST20120206

Guralp SA, Murgha YE, Rouillard JM, Gulari E. From design to screening: a new antimicrobial peptide discovery pipeline. PLoS One. 2013 Mar 19;8(3):e59305. https://doi.org/10.1371/journal.pone.0059305

Hahn-Löbmann S, Stephan A, Schulz S, Schneider T, Shaverskyi A, Tusé D, Giritch A, Gleba Y. Colicins and salmocins – New classes of plant-made non-antibiotic food antibacterials. Front Plant Sci. 2019 Apr 9;10:437. https://doi.org/10.3389/fpls.2019.00437

Hegemann JD, Zimmermann M, Xie X, Marahiel MA. Lasso peptides: an intriguing class of bacterial natural products. Acc Chem Res. 2015 Jul 21;48(7):1909–1919. https://doi.org/10.1021/acs.accounts.5b00156

Helal MMI, Hashem AM, Ghobashy MOI, Shalaby SG. Some physiological and biological studies on reuterin production from *Lactobacillus reuteri*. J Prob Health. 2016;04(03):1–8. https://doi.org/10.4172/2329-8901.1000156

Helbig S, Braun V. Mapping functional domains of colicin M. J Bacteriol. 2011 Feb 15;193(4):815–821. https://doi.org/10.1128/JB.01206-10

Hibbing ME, Fuqua C, Parsek MR, Peterson SB. Bacterial competition: surviving and thriving in the microbial jungle. Nat Rev Microbiol. 2010 Jan;8(1):15–25. https://doi.org/10.1038/nrmicro2259

Hols P, Ledesma-García L, Gabant P, Mignolet J. Mobilization of microbiota commensals and their bacteriocins for therapeutics. Trends Microbiol. 2019 Aug;27(8):690–702. https://doi.org/10.1016/j.tim.2019.03.007

Huang T, Zhang X, Pan J, Su X, Jin X, Guan X. Purification and characterization of a novel cold shock protein-like bacteriocin synthesized by *Bacillus thuringiensis*. Sci Rep. 2016 Dec 16;6(1):35560. https://doi.org/10.1038/srep35560

Huo L, Ökesli A, Zhao M, van der Donk WA. Insights into the biosynthesis of duramycin. Appl Environ Microbiol. 2017 Feb 01;83(3):e02698-16. https://doi.org/10.1128/AEM.02698-16

Hurst MRH, Beattie A, Jones SA, Laugraud A, van Koten C, Harper L. *Serratia proteamaculans* strain AGR96X encodes an antifeeding prophage (tailocin) with activity against grass grub (*Costelytra giveni*) and manuka beetle (*Pyronota species*) larvae. Appl Environ Microbiol. 2018 Mar 16;84(10):e02739-17. https://doi.org/10.1128/AEM.02739-17

Iseppi R, Pilati F, Marini M, Toselli M, de Niederhäusern S, Guerrieri E, Messi P, Sabia C, Manicardi G, Anacarso I, et al. Antilisterial activity of a polymeric film coated with hybrid coatings doped with Enterocin 416K1 for use as bioactive food packaging. Int J Food Microbiol. 2008 Apr;123(3):281–287. https://doi.org/10.1016/j.ijfoodmicro.2007.12.015

Ivanov D, Emonet C, Foata F, Affolter M, Delley M, Fisseha M, Blum-Sperisen S, Kochhar S, Arigoni F. A serpin from the gut bacterium *Bifidobacterium longum* inhibits eukaryotic elastase-like serine proteases. J Biol Chem. 2006 Jun;281(25):17246–17252. https://doi.org/10.1074/jbc.M601678200

Juturu V, Wu JC. Microbial production of bacteriocins: latest research development and applications. Biotechnol Adv. 2018 Dec;36(8): 2187–2200. https://doi.org/10.1016/j.biotechadv.2018.10.007

Kaur Maan P, Garcha S. Bacteriocins from Gram-negative *Rhizobium* spp. Adv Biores. Jan 2018;9(1):36–43. https://doi.org/10.15515/abr.0976-4585.9.1.3643

Kaur S, Kaur S. Bacteriocins as potential anticancer agents. Front Pharmacol. 2015 Nov 10;6:272. https://doi.org/10.3389/fphar.2015.00272

Kerr B, Riley MA, Feldman MW, Bohannan BJM. Local dispersal promotes biodiversity in a real-life game of rock-paper-scissors. Nature. 2002 Jul;418(6894):171–174. https://doi.org/10.1038/nature00823

Kierończyk B, Sassek M, Pruszyńska-Oszmałek E, Kołodziejski P, Rawski M, Świątkiewicz S, Józefiak D. The physiological response of broiler chickens to the dietary supplementation of the bacteriocin nisin and ionophore coccidiostats. Poult Sci. 2017 Nov;96(11):4026–4037. https://doi.org/10.3382/ps/pex234

Kim JG, Park BK, Kim SU, Choi D, Nahm BH, Moon JS, Reader JS, Farrand SK, Hwang I. Bases of biocontrol: sequence predicts syn-

thesis and mode of action of agrocin 84, the Trojan Horse antibiotic that controls crown gall. Proc Natl Acad Sci USA. 2006 Jun 06;103(23):8846–8851. https://doi.org/10.1073/pnas.0602965103

Kjos M, Nes IF, Diep DB. Mechanisms of resistance to bacteriocins targeting the mannose phosphotransferase system. Appl Environ Microbiol. 2011 May 15;77(10):3335–3342. https://doi.org/10.1128/AEM.02602-10

Kohoutova D, Smajs D, Moravkova P, Cyrany J, Moravkova M, Forstlova M, Cihak M, Rejchrt S, Bures J. Escherichia colistrains of phylogenetic group B2 and D and bacteriocin production are associated with advanced colorectal neoplasia. BMC Infect Dis. 2014 Dec;14(1):733. https://doi.org/10.1186/s12879-014-0733-7

Kruszewska D, Sahl HG, Bierbaum G, Pag U, Hynes SO, Ljungh Å. Mersacidin eradicates methicillin-resistant Staphylococcus aureus (MRSA) in a mouse rhinitis model. J Antimicrob Chemother. 2004 Sep 01;54(3):648–653. https://doi.org/10.1093/jac/dkh387

Kumar B, Balgir PP, Kaur B, Mittu B, Chauhan A. In vitro cytotoxicity of native and rec-Pediocin CP2 against cancer cell lines: a comparative study. Pharm Anal Acta. 2012;03(08):1–4. https://doi.org/10.4172/2153-2435.1000183

Kumar M, Dhaka P, Vijay D, Vergis J, Mohan V, Kumar A, Kurkure NV, Barbuddhe SB, Malik SVS, Rawool DB. Antimicrobial effects of Lactobacillus plantarum and Lactobacillus acidophilus against multidrug-resistant enteroaggregative Escherichia coli. Int J Antimicrob Agents. 2016 Sep;48(3):265–270. https://doi.org/10.1016/j.ijantimicag.2016.05.014

Ladjouzi R, Lucau-Danila A, Benachour A, Drider D. A leaderless two-peptide bacteriocin, enterocin DD14, is involved in its own self-immunity: evidence and insights. Front Bioeng Biotechnol. 2020 Jun 26;8:644. https://doi.org/10.3389/fbioe.2020.00644

Latham RD, Gell DA, Fairbairn RL, Lyons AB, Shukla SD, Cho KY, Jones DA, Harkness NM, Tristram SG. An isolate of Haemophilus haemolyticus produces a bacteriocin-like substance that inhibits the growth of nontypeable Haemophilus influenzae. Int J Antimicrob Agents. 2017 Apr;49(4):503–506. https://doi.org/10.1016/j.ijantimicag.2016.12.010

Lavermicocca P, Lonigro SL, Valerio F, Evidente A, Visconti A. Reduction of olive knot disease by a bacteriocin from Pseudomonas syringae pv. ciccaronei. Appl Environ Microbiol. 2002 Mar;68(3):1403–1407. https://doi.org/10.1128/AEM.68.3.1403-1407.2002

Lee NK, Paik HD. Partial characterization of lacticin NK24, a newly identified bacteriocin of Lactococcus lactis NK24 isolated from Jeot-gal. Food Microbiol. 2001 Feb;18(1):17–24. https://doi.org/10.1006/fmic.2000.0368

Li JZ, Zhou LY, Peng YL, Fan J. Pseudomonas bacteriocin syringacin M released upon desiccation suppresses the growth of sensitive bacteria in plant necrotic lesions. Microb Biotechnol. 2020 Jan;13(1):134–147. https://doi.org/10.1111/1751-7915.13367

Liu G, Lv Y, Li P, Zhou K, Zhang J. Pentocin 31–1, an anti-Listeria bacteriocin produced by Lactobacillus pentosus 31–1 isolated from Xuan-Wei Ham, a traditional China fermented meat product. Food Control. 2008 Apr;19(4):353–359. https://doi.org/10.1016/j.foodcont.2007.04.010

Liu X, Basu U, Miller P, McMullen LM. Stress response and adaptation of Listeria monocytogenes 08-5923 exposed to a sublethal dose of carnocyclin A. Appl Environ Microbiol. 2014 Jul 01;80(13):3835–3841. https://doi.org/10.1128/AEM.00350-14

López-Cuellar MR, Rodríguez-Hernández AI, Chavarría-Hernández N. LAB bacteriocin applications in the last decade. Biotechnol Biotechnol Equip. 2016 Nov 01;30(6):1039–1050. https://doi.org/10.1080/13102818.2016.1232605

Maldonado-Barragán A, Caballero-Guerrero B, Martín V, Ruiz-Barba JL, Rodríguez JM. Purification and genetic characterization of gassericin E, a novel co-culture inducible bacteriocin from Lacto-

bacillus gasseri EV1461 isolated from the vagina of a healthy woman. BMC Microbiol. 2016 Dec;16(1):37. https://doi.org/10.1186/s12866-016-0663-1

Marín-Cevada V, Muñoz-Rojas J, Caballero-Mellado J, Mascarúa-Esparza MA, Castañeda-Lucio M, Carreño-López R, Estrada-de los Santos P, Fuentes-Ramírez LE. Antagonistic interactions among bacteria inhabiting pineapple. Appl Soil Ecol. 2012 Oct;61:230–235. https://doi.org/10.1016/j.apsoil.2011.11.014

McCaughey LC, Grinter R, Josts I, Roszak AW, Waløen KI, Cogdell RJ, Milner J, Evans T, Kelly S, Tucker NP, et al. Lectin-like bacteriocins from Pseudomonas spp. utilise D-rhamnose containing lipopolysaccharide as a cellular receptor. PLoS Pathog. 2014 Feb 6; 10(2):e1003898. https://doi.org/10.1371/journal.ppat.1003898

McCaughey LC, Ritchie ND, Douce GR, Evans TJ, Walker D. Efficacy of species-specific protein antibiotics in a murine model of acute Pseudomonas aeruginosa lung infection. Sci Rep. 2016 Sep; 6(1):30201. https://doi.org/10.1038/srep30201

Michel-Briand Y, Baysse C. The pyocins of Pseudomonas aeruginosa. Biochimie. 2002 May;84(5–6):499–510. https://doi.org/10.1016/S0300-9084(02)01422-0

Miclotte L, Van de Wiele T. Food processing, gut microbiota and the globesity problem. Crit Rev Food Sci Nutr. 2020 Jun 16;60(11): 1769–1782. https://doi.org/10.1080/10408398.2019.1596878

Mignolet J, Fontaine L, Sass A, Nannan C, Mahillon J, Coenye T, Hols P. Circuitry rewiring directly couples competence to predation in the gut dweller Streptococcus salivarius. Cell Rep. 2018 Feb; 22(7):1627–1638. https://doi.org/10.1016/j.celrep.2018.01.055

Miller P, McMullen LM. Mechanism for temperature-dependent production of piscicolin 126. Microbiology. 2014 Aug 01;160(8): 1670–1678. https://doi.org/10.1099/mic.0.078030-0

Mills S, Griffin C, O'Connor PM, Serrano LM, Meijer WC, Hill C, Ross RP. A multibacteriocin cheese starter system, comprising nisin and lacticin 3147 in Lactococcus lactis, in combination with plantaricin from Lactobacillus plantarum. Appl Environ Microbiol. 2017 Jul 15;83(14):e00799-17. https://doi.org/10.1128/AEM.00799-17

Mitkowski P, Jagielska E, Nowak E, Bujnicki JM, Stefaniak F, Niedziałek D, Bochtler M, Sabała I. Structural bases of peptidoglycan recognition by lysostaphin SH3b domain. Sci Rep. 2019 Dec; 9(1):5965. https://doi.org/10.1038/s41598-019-42435-z

Molloy EM, Casjens SR, Cox CL, Maxson T, Ethridge NA, Margos G, Fingerle V, Mitchell DA. Identification of the minimal cytolytic unit for streptolysin S and an expansion of the toxin family. BMC Microbiol. 2015 Dec;15(1):141. https://doi.org/10.1186/s12866-015-0464-y

Monteiro CA, Levy RB, Claro RM, de Castro IRR, Cannon G. Increasing consumption of ultra-processed foods and likely impact on human health: evidence from Brazil. Public Health Nutr. 2010 Dec 20;14(1):5–13. https://doi.org/10.1017/S1368980010003241

Moubarac JC, Martins APB, Claro RM, Levy RB, Cannon G, Monteiro CA. Consumption of ultra-processed foods and likely impact on human health. Evidence from Canada. Public Health Nutr. 2013 Dec;16(12):2240–2248. https://doi.org/10.1017/S1368980012005009

Naz SA, Jabeen N, Sohail M, Rasool SA. Biophysicochemical characterization of Pyocin SA189 produced by Pseudomonas aeruginosa SA189. Braz J Microbiol. 2015 Dec;46(4):1147–1154. https://doi.org/10.1590/S1517-838246420140737

Nazari M, Smith DL. A PGPR-produced bacteriocin for sustainable agriculture: a review of thuricin 17 characteristics and applications. Front Plant Sci. 2020 Jul 7;11:916. https://doi.org/10.3389/fpls.2020.00916

Neish AS. Microbes in gastrointestinal health and disease. Gastroenterology. 2009 Jan;136(1):65–80. https://doi.org/10.1053/j.gastro.2008.10.080

Nguyen C, Nguyen VD. Discovery of azurin-like anticancer bacteriocins from human gut microbiome through homology modeling and molecular docking against the tumor suppressor p53. BioMed Res Int. 2016;2016:1–12. https://doi.org/10.1155/2016/8490482

Noinaj N, Kuszak AJ, Balusek C, Gumbart JC, Buchanan SK. Lateral opening and exit pore formation are required for BamA function. Structure. 2014 Jul;22(7):1055–1062. https://doi.org/10.1016/j.str.2014.05.008

Oliveira MM, Ramos ETA, Drechsel MM, Vidal MS, Schwab S, Baldani JI. Gluconacin from *Gluconacetobacter diazotrophicus* PAL5 is an active bacteriocin against phytopathogenic and beneficial sugarcane bacteria. J Appl Microbiol. 2018 Dec;125(6):1812–1826. https://doi.org/10.1111/jam.14074

Oluyombo O, Penfold CN, Diggle SP. Competition in biofilms between cystic fibrosis isolates of *Pseudomonas aeruginosa* is shaped by R-pyocins. MBio. 2019 Jan 29;10(1):e01828-18. https://doi.org/10.1128/mBio.01828-18

Ongey EL, Yassi H, Pflugmacher S, Neubauer P. Pharmacological and pharmacokinetic properties of lanthipeptides undergoing clinical studies. Biotechnol Lett. 2017 Apr;39(4):473–482. https://doi.org/10.1007/s10529-016-2279-9

Paiva AD, Breukink E, Mantovani HC. Role of lipid II and membrane thickness in the mechanism of action of the lantibiotic bovicin HC5. Antimicrob Agents Chemother. 2011 Nov;55(11):5284–5293. https://doi.org/10.1128/AAC.00638-11

Palamidi I, Fegeros K, Mohnl M, Abdelrahman WHA, Schatzmayr G, Theodoropoulos G, Mountzouris KC. Probiotic form effects on growth performance, digestive function, and immune related biomarkers in broilers. Poult Sci. 2016 Jul;95(7):1598–1608. https://doi.org/10.3382/ps/pew052

Parnasa R, Sendersky E, Simkovsky R, Waldman Ben-Asher H, Golden SS, Schwarz R. A microcin processing peptidase-like protein of the cyanobacterium *Synechococcus elongatus* is essential for secretion of biofilm-promoting proteins. Environ Microbiol Rep. 2019 Jun;11(3):456–463. https://doi.org/10.1111/1758-2229.12751

Parret AHA, Temmerman K, De Mot R. Novel lectin-like bacteriocins of biocontrol strain *Pseudomonas fluorescens* Pf-5. Appl Environ Microbiol. 2005 Sep;71(9):5197–5207. https://doi.org/10.1128/AEM.71.9.5197-5207.2005

Patz S, Becker Y, Richert-Pöggeler KR, Berger B, Ruppel S, Huson DH, Becker M. Phage tail-like particles are versatile bacterial nanomachines – a mini-review. J Adv Res. 2019 Sep;19:75–84. https://doi.org/10.1016/j.jare.2019.04.003

Perez RH, Zendo T, Sonomoto K. Circular and leaderless bacteriocins: Biosynthesis, mode of action, applications, and prospects. Front Microbiol. 2018 Sep 4;9:2085. https://doi.org/10.3389/fmicb.2018.02085

Perez RH, Zendo T, Sonomoto K. Novel bacteriocins from lactic acid bacteria (LAB): various structures and applications. Microb Cell Fact. 2014;13(Suppl 1):S3. https://doi.org/10.1186/1475-2859-13-S1-S3

Pimentel-Filho NJ, Mantovani HC, de Carvalho AF, Dias RS, Vanetti MCD. Efficacy of bovicin HC5 and nisin combination against *Listeria monocytogenes* and *Staphylococcus aureus* in fresh cheese. Int J Food Sci Technol. 2014 Feb;49(2):416–422. https://doi.org/10.1111/ijfs.12316

Pogány Simonová M, Chrastinová Ľ, Lauková A. Autochtonous strain *Enterococcus faecium* EF2019(CCM7420), its bacteriocin and their beneficial effects in broiler rabbits – a review. Animals (Basel). 2020 Jul 14;10(7):1188. https://doi.org/10.3390/ani10071188

Price R, Jayeola V, Niedermeyer J, Parsons C, Kathariou S. The *Listeria monocytogenes* key virulence determinants *hly* and *prf*A are involved in biofilm formation and aggregation but not colonization of fresh produce. Pathogens. 2018 Feb 01;7(1):18. https://doi.org/10.3390/pathogens7010018

Príncipe A, Fernandez M, Torasso M, Godino A, Fischer S. Effectiveness of tailocins produced by *Pseudomonas fluorescens* SF4c in controlling the bacterial-spot disease in tomatoes caused by *Xanthomonas vesicatoria*. Microbiol Res. 2018 Jul;212-213:94–102. https://doi.org/10.1016/j.micres.2018.05.010

Rebuffat S. Microcins and other bacteriocins: Bridging the gaps between killing strategies, ecology and applications. In: Dorit RL, Roy SM, Riley MA, editors. The Bacteriocins: Current knowledge and future prospects. Norfolk (UK): Caister Academic Press; 2016. p. 11–34. https://doi.org/10.21775/9781910190371.02

Redero M, López-Causapé C, Aznar J, Oliver A, Blázquez J, Prieto AI. Susceptibility to R-pyocins of *Pseudomonas aeruginosa* clinical isolates from cystic fibrosis patients. J Antimicrob Chemother. 2018 Oct 01;73(10):2770–2776. https://doi.org/10.1093/jac/dky261

Riboulet-Bisson E, Sturme MHJ, Jeffery IB, O'Donnell MM, Neville BA, Forde BM, Claesson MJ, Harris H, Gardiner GE, Casey PG, et al. Effect of *Lactobacillus salivarius* bacteriocin Abp118 on the mouse and pig intestinal microbiota. PLoS One. 2012 Feb 17;7(2):e31113. https://doi.org/10.1371/journal.pone.0031113

Rihakova J, Cappelier JM, Hue I, Demnerova K, Fédérighi M, Prévost H, Drider D. *In vivo* activities of recombinant divercin V41 and its structural variants against *Listeria monocytogenes*. Antimicrob Agents Chemother. 2010 Jan;54(1):563–564. https://doi.org/10.1128/AAC.00765-09

Riley MA. Bacteriocins, biology, ecology, and evolution. In: Schaechter M, editor. Encyclopedia of Microbiology. Cambridge (USA): Academic Press; 2009. p. 32–44. https://doi.org/10.1016/B978-012373944-5.00065-1

Rodrigues G, Silva GGO, Buccini DF, Duque HM, Dias SC, Franco OL. Bacterial proteinaceous compounds with multiple activities toward cancers and microbial infection. Front Microbiol. 2019 Aug 6;10:1690. https://doi.org/10.3389/fmicb.2019.01690

Roh E, Park TH, Kim M, Lee S, Ryu S, Oh CS, Rhee S, Kim DH, Park BS, Heu S. Characterization of a new bacteriocin, Carocin D, from *Pectobacterium carotovorum* subsp. *carotovorum* Pcc21. Appl Environ Microbiol. 2010 Nov 15;76(22):7541–7549. https://doi.org/10.1128/AEM.03103-09

Rooney WM, Grinter RW, Correia A, Parkhill J, Walker DC, Milner JJ. Engineering bacteriocin-mediated resistance against the plant pathogen *Pseudomonas syringae*. Plant Biotechnol J. 2020 May; 18(5):1296–1306. https://doi.org/10.1111/pbi.13294

Russel J, Røder HL, Madsen JS, Burmølle M, Sørensen SJ. Antagonism correlates with metabolic similarity in diverse bacteria. Proc Natl Acad Sci USA. 2017 Oct 03;114(40):10684–10688. https://doi.org/10.1073/pnas.1706016114

Salazar-Marroquín EL, Galán-Wong LJ, Moreno-Medina VR, Reyes-López MÁ, Pereyra-Alférez B. Bacteriocins synthesized by *Bacillus thuringiensis*: generalities and potential applications. Rev Med Microbiol. 2016 Jul;27(3):95–101. https://doi.org/10.1097/MRM.0000000000000076

Salgado PR, Ortiz CM, Musso YS, Di Giorgio L, Mauri AN. Edible films and coatings containing bioactives. Curr Opin Food Sci. 2015 Oct;5:86–92. https://doi.org/10.1016/j.cofs.2015.09.004

Salvucci E, Saavedra L, Hebert EM, Haro C, Sesma F. Enterocin CRL35 inhibits *Listeria monocytogenes* in a murine model. Foodborne Pathog Dis. 2012 Jan;9(1):68–74. https://doi.org/10.1089/fpd.2011.0972

Sánchez-Hidalgo M, Montalbán-López M, Cebrián R, Valdivia E, Martínez-Bueno M, Maqueda M. AS-48 bacteriocin: close to perfection. Cell Mol Life Sci. 2011 Sep;68(17):2845–2857. https://doi.org/10.1007/s00018-011-0724-4

Sand SL, Nissen-Meyer J, Sand O, Haug TM. Plantaricin A, a cationic peptide produced by *Lactobacillus plantarum*, permeabilizes eukaryotic cell membranes by a mechanism dependent on negative

surface charge linked to glycosylated membrane proteins. Biochim Biophys Acta (BBA) – Biomembranes. 2013 Feb;1828(2):249–259. https://doi.org/10.1016/j.bbamem.2012.11.001

Sarantinopoulos P, Leroy F, Leontopoulou E, Georgalaki MD, Kalantzopoulos G, Tsakalidou E, Vuyst LD. Bacteriocin production by *Enterococcus faecium* FAIR-E 198 in view of its application as adjunct starter in Greek Feta cheese making. Int J Food Microbiol. 2002 Jan;72(1–2):125–136.
https://doi.org/10.1016/S0168-1605(01)00633-X

Sarika AR, Lipton AP, Aishwarya MS. Biopreservative efficacy of bacteriocin gp1 of *Lactobacillus rhamnosus* gp1 on stored fish filets. Front Nutr. 2019 Mar 22;6:29.
https://doi.org/10.3389/fnut.2019.00029

Schneider T, Hahn-Löbmann S, Stephan A, Schulz S, Giritch A, Naumann M, Kleinschmidt M, Tusé D, Gleba Y. Plant-made *Salmonella* bacteriocins salmocins for control of *Salmonella* pathovars. Sci Rep. 2018 Dec;8(1):4078.
https://doi.org/10.1038/s41598-018-22465-9

Scholz R, Vater J, Budiharjo A, Wang Z, He Y, Dietel K, Schwecke T, Herfort S, Lasch P, Borriss R. Amylocyclicin, a novel circular bacteriocin produced by *Bacillus amyloliquefaciens* FZB42. J Bacteriol. 2014 May 15;196(10):1842–1852.
https://doi.org/10.1128/JB.01474-14

Shanker E, Federle M. Quorum sensing regulation of competence and bacteriocins in *Streptococcus pneumoniae* and *mutans*. Genes (Basel). 2017 Jan 05;8(1):15. https://doi.org/10.3390/genes8010015

Shi F, Wang Y, Li Y, Wang X. Mode of action of leucocin K7 produced by *Leuconostoc mesenteroides* K7 against *Listeria monocytogenes* and its potential in milk preservation. Biotechnol Lett. 2016 Sep;38(9):1551–1557. https://doi.org/10.1007/s10529-016-2127-y

Shin JM, Gwak JW, Kamarajan P, Fenno JC, Rickard AH, Kapila YL. Biomedical applications of nisin. J Appl Microbiol. 2016 Jun;120(6):1449–1465. https://doi.org/10.1111/jam.13033

Silva CCG, Silva SPM, Ribeiro SC. Application of bacteriocins and protective cultures in dairy food preservation. Front Microbiol. 2018 Apr 9;9:594. https://doi.org/10.3389/fmicb.2018.00594

Simons A, Alhanout K, Duval RE. Bacteriocins, antimicrobial peptides from bacterial origin: overview of their biology and their impact against multidrug-resistant bacteria. Microorganisms. 2020 Apr 27;8(5):639. https://doi.org/10.3390/microorganisms8050639

Sindhu SS, Sehrawat A, Sharma R, Dahiya A. Biopesticides: use of rhizosphere bacteria for biological control of plant pathogens. Def Life Sci J. 2016 Oct 07;1(2):135–148.
https://doi.org/10.14429/dlsj.1.10747

Soltani S, Hammami R, Cotter PD, Rebuffat S, Said LB, Gaudreau H, Bédard F, Biron E, Drider D, Fliss I. 2021. Bacteriocins as a new generation of antimicrobials: toxicity aspects and regulations. EMS Microbiol Rev. 2021 Jan 8;45(1):fuaa039.
https://doi.org/10.1093/femsre/fuaa039

Stoyanova LG, Ustyugova EA, Netrusov AI. Antibacterial metabolites of lactic acid bacteria: their diversity and properties. Appl Biochem Microbiol. 2012 May;48(3):229–243.
https://doi.org/10.1134/S0003683812030143

Subramanian S, Smith DL. Bacteriocins from the rhizosphere microbiome – from an agriculture perspective. Front Plant Sci. 2015 Oct 30;6:909. https://doi.org/10.3389/fpls.2015.00909

Sun Z, Wang X, Zhang X, Wu H, Zou Y, Li P, Sun C, Xu W, Liu F, Wang D. Class III bacteriocin Helveticin-M causes sublethal damage on target cells through impairment of cell wall and membrane. J Ind Microbiol Biotechnol. 2018 Mar 01;45(3):213–227.
https://doi.org/10.1007/s10295-018-2008-6

Teneva-Angelova T, Hristova I, Pavlov A, Beshkova D. Chapter 4 – Lactic acid bacteria – From nature through food to health. In:

Holban AM, Grumezescu AM, editors. Handbook of Food Bioengineering, Advances in Biotechnology for Food Industry. Cambridge (USA): Academic Press; 2018. p. 91–133.
https://doi.org/10.1016/B978-0-12-811443-8.00004-9

Todorov SD. Bacteriocin production by *Lactobacillus plantarum* AMA-K isolated from Amasi, a Zimbabwean fermented milk product and study of the adsorption of bacteriocin AMA-K to *Listeria* sp. Braz J Microbiol. 2008 Mar;39(1):178–187.
https://doi.org/10.1590/S1517-83822008000100035

Turovskiy Y, Ludescher RD, Aroutcheva AA, Faro S, Chikindas ML. Lactocin 160, a bacteriocin produced by vaginal *Lactobacillus rhamnosus*, targets cytoplasmic membranes of the vaginal pathogen, *Gardnerella vaginalis*. Probiotics Antimicrob Proteins. 2009 Jun;1(1):67–74.
https://doi.org/10.1007/s12602-008-9003-6

Um S, Kim YJ, Kwon H, Wen H, Kim SH, Kwon HC, Park S, Shin J, Oh DC. Sungsanpin, a lasso peptide from a deep-sea streptomycete. J Nat Prod. 2013 May 24;76(5):873–879.
https://doi.org/10.1021/np300902g

van Staden ADP, Heunis T, Smith C, Deane S, Dicks LMT. Efficacy of lantibiotic treatment of *Staphylococcus aureus*-induced skin infections, monitored by *in vivo* bioluminescent imaging. Antimicrob Agents Chemother. 2016 Jul;60(7):3948–3955.
https://doi.org/10.1128/AAC.02938-15

Veening JW, Blokesch M. Interbacterial predation as a strategy for DNA acquisition in naturally competent bacteria. Nat Rev Microbiol. 2017 Oct;15(10):621–629.
https://doi.org/10.1038/nrmicro.2017.66

Vijay Simha B, Sood SK, Kumariya R, Garsa AK. Simple and rapid purification of pediocin PA-1 from *Pediococcus pentosaceous* NCDC 273 suitable for industrial application. Microbiol Res. 2012 Oct;167(9):544–549. https://doi.org/10.1016/j.micres.2012.01.001

Villarante KI, Elegado FB, Iwatani S, Zendo T, Sonomoto K, de Guzman EE. Purification, characterization and *in vitro* cytotoxicity of the bacteriocin from *Pediococcus acidilactici* K2a2–3 against human colon adenocarcinoma (HT29) and human cervical carcinoma (HeLa) cells. World J Microbiol Biotechnol. 2011 Apr; 27(4):975–980. https://doi.org/10.1007/s11274-010-0541-1

Vivarelli S, Salemi R, Candido S, Falzone L, Santagati M, Stefani S, Torino F, Banna GL, Tonini G, Libra M. Gut microbiota and cancer: from pathogenesis to therapy. Cancers (Basel). 2019 Jan 03;11(1):38. https://doi.org/10.3390/cancers11010038

Yang SC, Lin CH, Sung CT, Fang JY. Antibacterial activities of bacteriocins: application in foods and pharmaceuticals. Front Microbiol. 2014 May 26;5:241. https://doi.org/10.3389/fmicb.2014.00241

Yao GW, Duarte I, Le TT, Carmody L, LiPuma JJ, Young R, Gonzalez CF. A broad-host-range tailocin from *Burkholderia cenocepacia*. Appl Environ Microbiol. 2017 May 15;83(10):e03414-16.
https://doi.org/10.1128/AEM.03414-16

Zelezetsky I, Tossi A. Alpha-helical antimicrobial peptides – using a sequence template to guide structure-activity relationship studies. Biochim Biophys Acta (BBA) – Biomembranes. 2006 Sep;1758(9): 1436–1449. https://doi.org/10.1016/j.bbamem.2006.03.021

Zhang ZF, Kim IH. Effects of multistrain probiotics on growth performance, apparent ileal nutrient digestibility, blood characteristics, cecal microbial shedding, and excreta odor contents in broilers. Poult Sci. 2014 Feb;93(2):364–370.
https://doi.org/10.3382/ps.2013-03314

Zhou W, Wang G, Wang C, Ren F, Hao Y. Both IIC and IID components of mannose phosphotransferase system are involved in the specific recognition between immunity protein PedB and bacteriocin-receptor complex. PLoS One. 2016 Oct 24;11(10):e0164973.
https://doi.org/10.1371/journal.pone.0164973

ORIGINAL PAPER

First Description of Various Bacteria Resistant to Heavy Metals and Antibiotics Isolated from Polluted Sites in Tunisia

SAMAR BEN MILOUD[1,2,3], OLFA DZIRI[1,2], SANA FERJANI[3], MUNTASIR MD ALI[4], MOHAMED MYSARA[4],
ILHEM BOUTIBA[3], ROB VAN HOUDT[4] and CHEDLY CHOUCHANI[1,2]*

[1] Research Laboratory of Environmental Sciences and Technologies, Higher Institute of Environmental Sciences
and Technologies of Borj-Cedria, University of Carthage, Hammam-Lif, Tunisia
[2] Laboratory of Microorganisms and Active Biomolecules, Faculty of Sciences of Tunis,
University of Tunis El-Manar, Tunis El-Manar, Tunisia
[3] Research Laboratory Antibiotic Resistance, Faculty of Medicine of Tunis, Tunisia
[4] Microbiology Unit, Belgian Nuclear Research Centre (SCK CEN), Mol, Belgium

Abstract

Environmental bacteria belonging to various families were isolated from polluted water collected from ten different sites in Tunisia. Sites were chosen near industrial and urban areas known for their high degree of pollution. The aim of this study was to investigate cross-resistance between heavy metals (HM), i.e., silver, mercury and copper (Ag, Hg, and Cu), and antibiotics. In an initial screening, 80 isolates were selected on ampicillin, and 39 isolates, retained for further analysis, could grow on a Tris-buffered mineral medium with gluconate as carbon source. Isolates were identified based on their 16S rRNA gene sequence. Results showed the prevalence of antibiotic resistance genes, especially all isolates harbored the bla_{TEM} gene. Some of them (15.38%) harbored bla_{SHV}. Moreover, several were even ESBLs and MBLs-producers, which can threaten the human health. On the other hand, 92.30%, 56.41%, and 51.28% of the isolates harbored the heavy metals resistance genes $silE$, $cusA$, and $merA$, respectively. These genes confer resistance to silver, copper, and mercury. A cross-resistance between antibiotics and heavy metals was detected in 97.43% of our isolates.

Introduction

Since the industrial revolution, new ecological niches have emerged following the release of toxic industrial wastes, which often consist of a mixture of heavy metals, organic compounds, and hydrocarbons, into the environment. Environmental pollution is a significant problem, affecting many environments in a negative and almost irreversible way (Filali et al. 2000). In particular, heavy metal contamination of surface waters directly impacts both the environment and public health (Chihomvu et al. 2015). Environmental bacteria that are resistant to heavy metals, as well as multiple antibiotics, are of great concern in many areas of the world.

Bacteria-heavy metal interactions have been studied in many and extreme environments. Some metals are essential cofactors of specific proteins; others cause oxidative stress because of their redox potential. Heavy metals are naturally occurring, but with excessive anthropogenic activities, they are shown in large quantities, then become toxic at high concentration. Soil, water, and air are the major environmental compartments, which are affected by heavy metals pollution leading to many adverse impacts (Tchounwou et al. 2012).

In this study, we focused on copper, silver, and mercury. These heavy metals are more and more used in many applications and are also found in different areas worldwide (Kerfoot et al. 2002; 2004).

* Corresponding author: Ch. Chouchani, Research Laboratory of Environmental Sciences and Technologies, Higher Institute of Environmental Sciences and Technologies of Borj-Cedria, University of Carthage, Hammam-Lif, Tunisia; Laboratory of Microorganisms and Active Biomolecules, Faculty of Sciences of Tunis, University of Tunis El-Manar, Tunis El-Manar, Tunisia;
  e-mail: chedly.chouchani@gmail.com

Copper is an essential element that is toxic at high concentrations (Chihomvu et al. 2015). High cytoplasmic copper concentrations can lead to dysfunctional proteins (Kershaw et al. 2005), or damage lipids, DNA, and other molecules (Harrison et al. 2000). Microorganisms have developed several copper resistance mechanisms to survive in contaminated environments.

Silver is used as an antimicrobial agent in various medical products, such as catheters, and for burns wound treatments (Silver and Phung 1996; Klasen 2000; Jung et al. 2008). Bacteria can develop resistance to silver via efflux mechanisms encoded by the *sil-* or *pco/cop*-genes (Gupta et al. 1999).

The mercury ion has been known to be effective against a broad range of microorganisms. It has no beneficial functions in living organisms, and this toxic compound can accumulate in the food chain (Jan et al. 2009). The mercury resistance system is encoded by the *mer* operon, which reduces Hg^{2+} into elemental mercury via the mercuric reductase enzyme (MerA) (Boyd and Barkay 2012; Fatimawali et al. 2014).

Furthermore, many reports suggested that heavy metal contamination could directly or indirectly impact the maintenance and proliferation of antibiotic resistance (Summers 2002). Several studies reported the co-occurrence of heavy metal and antibiotic resistance. It has been proven that heavy metals in environmental reservoirs, water, wastewater, and soil, may contribute to the selection of antibiotic-resistant strains through co-resistance and cross-resistance mechanisms (Nguyen et al. 2019). It is important to underline that co-resistance occurs when genes coding for the resistance phenotypes are present on the same mobile genetic elements (i.e., plasmids, transposons, and integrons) (Mandal et al. 2016). Mercury, copper, and silver resistance genes are located on mobile genetic elements, e.g., on class II transposons with various antibiotic resistance genes. For instance, *Salmonella* plasmid pMG101 carries silver, mercury, and tellurite resistance genes and genes conferring resistance against chloramphenicol, ampicillin, tetracycline, streptomycin, and sulphonamide. Plasmid-encoded mercury resistance operons are frequently associated with class II transposons. In addition, P-type ATPases are indispensable for the transport of ions, such as copper and silver from cells, acting as a resistance mechanism to actively efflux heavy metal cations. These PIB-type ATPase genes have been found to occur on plasmids and transposons in both Gram-positive and Gram-negative bacteria and be prone to horizontal gene transfer (HGT) (Aminov 2011).

In this report, we were interested in studying the contamination of ten sites in Tunisia by silver, copper, and mercury and detecting a cross-resistance between them and antibiotics in water environmental isolates.

It was done to understand better whether heavy metal contamination could contribute to the proliferation and the spread of antibiotic resistance.

Experimental

Materials and Methods

Sampling sites. Samples were collected from ten different geographic areas from the north to the south of Tunisia (Table I). Sampling sites were chosen because of their geographic situation near urban, industrial, and agricultural areas. Sample locations were based on a previous study that determined the degree of pollution (Ben Miloud et al. 2020).

Sample collection and HM resistant bacteria screening. A plankton net was used to recover water samples, which were transferred into sterile bottles and transported at 4°C to the laboratory. After a first filtration step to remove insoluble solids, a nitrocellulose filter (0.45 μm) was used to collect microorganisms. Filters were directly placed on Lysogeny Broth (LB) agar plates with ampicillin (AMP) 64 μg/ml and incubated for 24–48 hrs. at 37°C. Ampicillin was used to counter select sensitive isolates. In the next step, growth on Tris-buffered mineral agar supplemented with 0.2% (w/v) sodium gluconate (MM284) (Mergeay et al. 985) was scored. Finally, 39 isolates were stored on 15% glycerol at –80°C.

Total DNA extraction. According to the manufacturer's protocol, the total DNA of each isolate was extracted from bacterial cultures using the QIAamp DNA Maxi kit. DNA concentration (ng/μl) was measured with the Nano Drop Microvolume Quantitation of Nucleic Acids. (Thermo Scientific, NanoDrop 1000).

Amplification of the 16S rRNA gene. The 16S rRNA gene was amplified using 50–100 ng of total DNA, 25 μl of DreamTaq Green PCR Master Mix (2X), 0.1–1 μM of the universal primers 8F (5'-AGAGTTTGATCCTG-GCTCAG-3') and 1492R (5'-TACGGTTACCTTGT-TACGACTT-3') (Galkiewicz and Kellogg 2008), and adjusted to 50 μl with nuclease-free water. Amplification was performed in an Eppendorf Master cycler thermocycler (Hamburg, Germany) using the following conditions: initial denaturation at 95°C for 10 min, 30 cycles of 95°C for 30s, 56°C for 30s, 72°C for 2 min, and a final extension at 72°C for 10 min. The 16S rRNA gene amplicons were purified (Promega SV Gel and PCR clean-up system kit) and sequenced (Eurofins Genomics, Germany). Isolates were identified using 16S rRNA sequence according to Greengenes Database.

Phylogenetic analysis. The 16S rRNA gene sequences were aligned to silva, trimmed to the same region removed those shorter than 900 bp (6 sequences),

Table I
Sampling sites characteristics, locations, and their corresponding geographic coordinates.

Sites/numeration	Geographic coordinates	Location	Characteristics
Menzel Jemil, Bizerte: Site I	37°14′19″N, 9°54′59″E	Industrial area	Waste and contamination from the textile industry and wiring throwing inside the Bizerte lagoon
Menzel Bourguiba, Bizerte: Site II	37°09′N, 9°47′E	Unit manufacturing printed circuits. In the Iron factory	Contamination by HM from the iron factory in the Bizerte lagoon. Urban and agricultural pollution
Tinjah wedi, Bizerte: Site III	37°10′N, 9°45′E	Near the lagoon of Bizerte	Agricultural pollution and compost contamination.
Beja: Site IV	36°43′30″N, 9°10′55″E	Southwest of the city of Tunis Near the CWTP*	Urban and industrial area, the most known are wastewater and yeast factory
Essijoumi Lagoon: Site V	36°45′52″N, 10°08′49″E	Contribution in the Gulf of Tunis	Lagoon receiving contamination from wastewater contamination and wastes from the capital Tunis.
Rades Milian River: Site VI	36°46′N, 10°17′E	Industrial zone of Rades	High load alluvial estimated at 25 grams per liter. Receiving wastewater from two towns Rades and Ezzahra.
Majerda River: Site VII	37°7′0″N, 10°13′0″E	A peninsula in far north-eastern Tunisia	Used for irrigation of the region's agriculture
Lebna River: Site VIII	36°45′N, 10°54′E	Inlet manifold sewage treatment plant	Agricultural coastal Plans can be found in the area of Cap Bon
Om Larayes, Gafsa: Site IX	34°28′59″N, 8°16′01″E	The industrial platforms of phosphgyps activity	One of the known mining towns in Gafsa
Gulf of Gabes: Site X	34°05′37″N, 10°26′13″E	The junction between the Eastern and Central Basin	Known by industry for the transformation of merchantable phosphate into Phosphoric Acid (H_3PO_4) and Chemical Fertilizers

* – CWTP: Collector between wastewater treatment plant.

reported the phylogeny based on both filtered and complete set of sequences. The phylogenetic tree was built by the MEGA clustal algorithm, and distances calculated using "Maximum Likelihood" in MEGA X. The evolutionary history was inferred by using Maximum Likelihood and Tamura-Nei model (Tamura and Nei 1993; Kumar et al. 2016). Evolutionary analyses were conducted in MEGAX.

Antibiotic susceptibility testing. The disk diffusion agar technique determined susceptibility to antimicrobial agents. The following antibiotic disks (supplied by BioMerieux) were used: amoxicillin (10 µg), amoxicillin/clavulanic acid (20 µg/10 µg), piperacillin (100 µg), piperacillin/tazobactam (100 µg/10 µg), cephalothin (30 µg), cefotaxime (30 µg), ceftazidime (30 µg), aztreonam (30 µg), imipenem (10 µg), nalidixic acid (30 µg), ciprofloxacin (5 µg), chloramphenicol (30 µg), gentamicin (10 µg), kanamycin (30 µg), streptomycin (10 µg), sulfamethoxazole/trimethoprim (25 µg), and tetracycline (30 µg) (Vicente et al. 1990).

Determination of heavy metal minimal inhibitory concentration. To determine the MIC of heavy metals, a stationary phase culture (OD_{600} of ca. 1.0 representing 10^9 CFU/ml) of each isolate grown in Tris-buffered mineral medium (MM284) supplemented with gluconate was diluted 50 times in 2 × concentrated MM284 medium. 100 µl of each culture was added to

a 96-well plate containing 100 µl of a heavy metal ion solution (Cu^{2+}, Hg^{2+}, and Ag^+) at increasing concentration. Plates were incubated at 30°C for 48 h in the dark on a rotary shaker. At different time points, bacterial growth was measured by determining the optical density at 595 nm. The minimal inhibitory concentration (MIC) was determined for Cu^{2+}, Hg^{2+}, and Ag^+. *Cupriavidus metallidurans* CH34 and *Escherichia coli* K38 were used as references (Monsieurs et al. 2011). Isolates showing higher MICs than both reference strains were considered as resistant.

PCR amplification of antibiotic resistance genes. β-lactamases encoding-genes were screened as previously described (Dallenne et al. 2010) using multiplex PCR 1 for the detection of the bla_{TEM}, bla_{SHV}, and $bla_{OXA-1-like}$ genes; multiplex PCR 2 for the detection of the bla_{CTX-M} subgroups ($bla_{CTX-M-1}$, $bla_{CTX-M-2}$, $bla_{CTX-M-9}$, $bla_{CTX-M-8}$, $bla_{CTX-M-25}$), and a separate simplex PCR for the detection of the bla_{OXA-48} gene. Primers, amplification conditions and expected fragment sizes are shown in Table II. Fluoroquinolone resistance genes were screened using multiplex PCR 3 (*qnrA, qnrB, qnrC,qnrD, qnrS,* and *oqxAB*), as previously described (CLSI 2013). Primers, amplification conditions, and expected fragment sizes are shown in Tables II and III.

PCR amplification and sequencing of the *silE*, *merA*, and *cusA* genes. The *silE* gene, coding for

Table II
Primers, expected fragment size and conditions of PCR experiments used for β-lactams resistance encoding genes.

Mul-tiplex	Target	Primers sequences (5′–3′)	Size (pb)	Concen-tration (pmol/μl)	Volume (μl)	Amplification conditions
1	TEM	MultiTSO-T_F CATTTCCGTGTCGCCCTTATTC	800	0.4	0.4	94°C 10 min 94°C 40 sec 60°C 40 sec 30 cycles 72°C 1 min 72°C 7 min
		MultiTSO-T_R CGTTCATCCATAGTTGCCTGAC		0.4	0.4	
	SHV	MultiTSO-S_F AGCCGCTTGAGCAAATTAAAC	713	0.4	0.4	
		MultiTSO-S_R ATCCCGCAGATAAATCACCAC		0.4	0.4	
	OXA-1-like	MultiTSO-O_F GGCACCAGATTCAACTTTCAAG	564	0.4	0.4	
		MultiTSO-O_R GACCCCAAGTTTCCTGTAAGTG		0.4	0.4	
2	CTX-M group 1	MultiCTXMGp1_F TTAGGAARTGTGCCGCTGTA	688	0.4	0.4	
		MultiCTXMGp1_R CGATATCGTTGGTGGTCCCAT		0.2	0.2	
	CTX-M group 2	MultiCTXMGp2_F CGTTAACGGCACGATGAC	404	0.2	0.2	
		MultiCTXMGp1_R CGATATCGTTGGTGGTTCCAT		0.2	0.2	
	CTX-M group 9	MultiCTXMGp9_F TCAAGCCTGCCGATCTGGT	561	0.4	0.4	
		MultiCTXMGp9_R TGATTCTCGCCGCTGAAG		0.4	0.4	
	CTX-M group 8	CTX-Mg8/25_F AACTCCCAGACGCTCTAC	326	0.4	0.4	
		CTX-Mg8/25_R TCGAGCCGGAASGTGTAAT		0.4	0.4	
Sim-plex	Target	Primers sequences (5′–3′)	Size (pb)	Concen-tration (pmol/μl)	Volume (μl)	Amplification conditions
1	OXA-48	MultiOXA-48_F GCTTGATCGCCCTCGATT	281	0.4	0.4	94°C 10 min 94°C 40 sec 57°C 40 sec 30 cycles 72°C 1 min 72°C 7 min
		MultiOXA-48_R GATTTGCTCCGTGGCCGAAA		0.4	0.4	

Table III
Primers, expected fragment size, and conditions of PCR experiments used
for quinolones resistance encoding genes.

Multiplex	Target	Sequence of primer (5′–3′)	Size (bp)	Amplification conditions
3	qnrA	qnrA_FCAGCAAGAGGATTTCTCACG	630	95°C 15 min 94°C 30 sec 63°C 40 sec 30 cycles 72°C 90 sec 72°C 10 min
		qnrA_RAATCCGGCAGCACTATTACTC		
	qnrB	qnrB_FGGCTGTCAGTTCTATGATCG	488	
		qnrB_RGAGCAACGATGCCTGGTAG		
	qnrC	qnrC_FGCAGAATTCAGGGGTGTGAT	118	
		qnrC_RAACTGCTCCAAAAGCTGCTC		
	qnrD	qnrD_FCGAGATCAATTTACGGGGAATA	581	
		qnrD_RAACAAGCTGAAGCGCCTG		
	qnrS	qnrS_FGCAAGTTCATTGAACAGGGT	428	
		qnrS_RTCTAAACCGTCGAGTTCGGCG		

a periplasmic heavy metal binding protein involved in silver resistance, the *cusA* gene, part of the RND-driven system effluxing copper, and the *merA* gene, coding for a mercury reductase detoxifying mercury stress, were amplified by PCR. The following reaction mixture (50 μl) was used: 25 μl of DreamTaq Green PCR Master Mix (2X), 0.1–1 μM of reverse and forward primer (50–100 ng) genomic DNA as previously described (Silver and Phung 1996; Besaury et al. 2013).

PCR products were purified by PCR Clean-up and sequenced (Eurofins Genomics, Germany).

Protein prediction and analyses. The *silE, cusA,* and *merA* genes sequences were translated to their corresponding protein using Expasy website, then aligned using BioEdit with SilE from pMG101 (SilE AAD1171743), *Escherichia coli* (CusA P30854), and *Enterobacter cloacae* (MerA EU081910), respectively.

Results

Sample collection and identification of bacterial isolates. Ten filters placed on LB plates, each belonging to a sample collected from the ten sites, showed multiple colonies. The choice of colonies was based on shape and color. Therefore, 80 colonies were chosen from the ten plates to determine the prevalence of heavy metal- and antibiotic-resistant bacteria. In the next step, only the 39 isolates that grew on Tris-buffered mineral agar supplemented with 0.2% (w/v) sodium gluconate (MM284) (Mergeay et al. 1985) were retained. MM284 contained HM trace was used to test heavy metal resistance. Subsequently, the selected isolates were identified using the 16S rRNA gene amplification followed by sequencing, and the corresponding phylogenetic tree was dressed and presented in Fig. 1. Despite the sampling locations, the phylogenetic tree showed a similarity between species. Therefore, six clusters were shown.

Antibiotic resistance profiles and genes. Disk diffusion tests showed that the isolates' antibiotic resistance profiles were diverse (tested according to EUCAST 2018 guidelines). Resistance was detected against different families, including β-lactams, fluoroquinolones, aminoglycosides, tetracycline, and macrolides. We noted that isolate *Aeromonas salmonicida* 32 was only resistant to ampicillin by the production of TEM-1β-lactamase. The other isolates were resistant to less than two antibiotics by the production of different resistance enzymes, like CTX-M-1, OXA-48, SHV-1, CTX-M-9, or OXA-1. Only two isolates, *E. coli* 3 and *Klebsiella pneumoniae* 39 were resistant to quinolones by the expression of *qnrB*.

Heavy metal resistance profiles. Growth of all strains was inhibited at silver nitrate, copper, and mercury at concentrations starting from 0.032 to 0.064 mM, 1.5 to 6 mM, and from 0.02 to 0.08 mM, respectively. A high MIC value for silver was observed for 92.30% of the isolates collected from the ten sites. Only three isolates were sensitive to silver, two from Beja and Essijoumi Lagoon, and one from Melian Rades Wedi.

The growth of strains was inhibited at the copper concentrations starting from 3 to 6 mM. Copper resistance in relation with sites was as follows: 100% of sensible isolates were detected in Majerda River
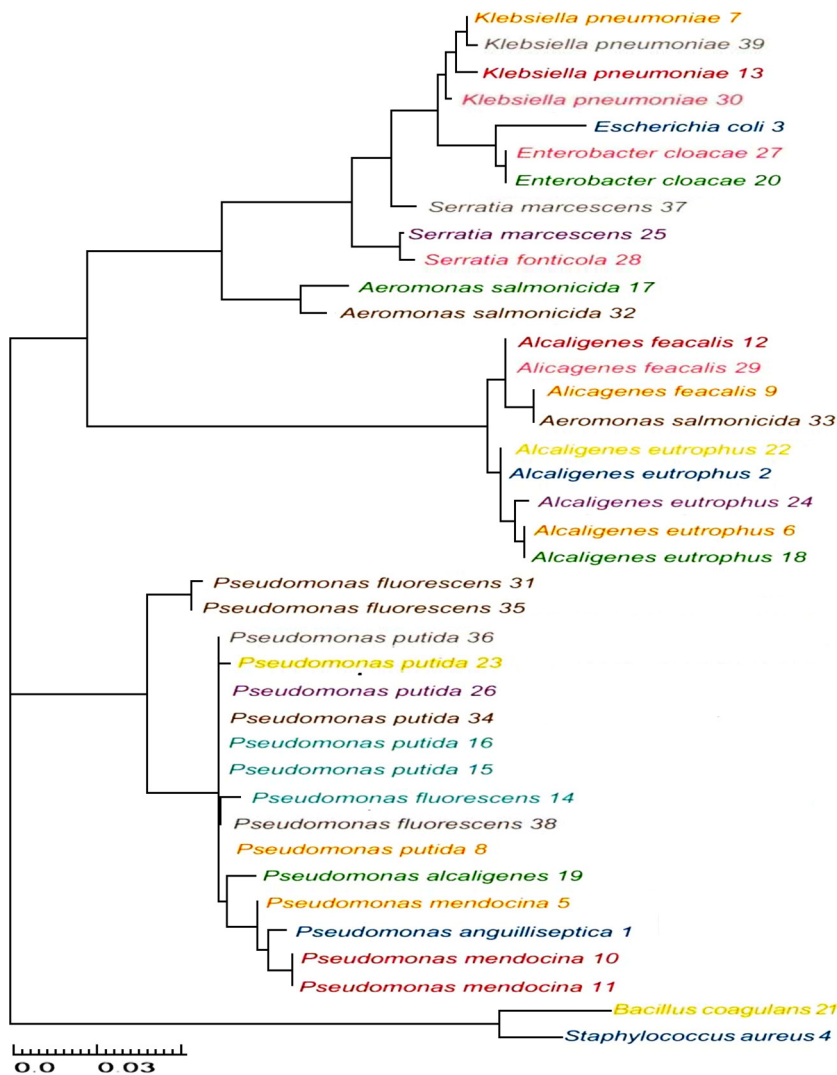
Fig. 1. Phylogenetic tree based on the partial 16S rRNA gene sequences of the 39 isolates. Ten colors used to distinguish ten different sampling sites classified from north to south of Tunisia: Dark blue: Menzel Jemil; Orange: Iron factory; Red: Tinjahwedi Bizerte; Cyan: Collector between wastewater treatment plant (CWTP) of Beja; Green: Marsh Sejoumi; Yellow: Milian Rades Wedi; Light purple: Majerda River; Pink: Lebnawedi Cap Bon; Dark purple: Om Larayes Gafsa; Grey: Golf of Gabes.

showing MIC values from 0.75 to 1.5 mM; < 80% of sensible isolates were detected in Gafsa (about four from a total of five isolates), which demonstrated the lowest MIC values from 0.625 to 1.5 mM; < 50% of sensible isolates were detected in Essijoumi Lagoon with MIC values similar to that of the isolates from Gafsa; < 25% of isolates were detected in each site with MIC values ranged from 0.625 to 1.5 mM. As a result, 75% of isolates resistant to copper were detected in the following Sites: I, II, III, IV, VI, IX, and X followed by 50% of the resistant isolates detected in Site V, and 20% of the isolates were detected in Gafsa (Site VIII). However, none of the isolates resistant to copper were detected in Majerda River (Site VII). Resistant and sensible isolates were detected with different percentages from one site to another as follows: 100% of isolates were detected in Lebna wedi Cab Bon with a low MIC: equal to 0.005 mM; < 75% of isolates detected in Gulf of Gabes were sensible to mercury with the MIC values ranged from 0.0025 to 0.008 mM; < 50% of sensible isolates were isolates from Bizerte (Site I, II, and III) with the MIC values ranged from 0.0025 to 0.005 mM; < 40% of isolates were sensible to mercury with the MIC values equal to 0.005 mM belonged to Site VIII; < 33% sensible isolates collected from Collector between wastewater treatment plant (CWTP) of Beja, Melian Rades Wedi, and Majerda River. All isolates collected from Essoujimi River were resistant to mercury with the MIC values equal to 0.08 mM.

A high percentage of resistance to silver was shown for 92.30% of the total isolates. Furthermore, 22 isolates (56.41%) showed high resistance to copper, and about half of the isolates (51.28%) showed high resistance to mercury.

Identification of the heavy metal resistance encoding genes. PCR amplification using the specific primers provided three different amplicons with a size of 400 bp for the *silE* gene, 410 bp for the *cusA* gene, and 280 bp for the *merA* gene (Fig. 2). Sequencing confirmed amplification of the correct fragment and showed that *silE* was the most common. The silver binding protein gene *silE* was detected in all isolates collected from the ten sites except for one isolate from each Site (IV, V, and VI), which was deprived of it. Reported MICs of silver for resistant isolates did not inhibit colony growth at 0.032 mM to 0.064 mM (Table IV). The copper resistance gene *cusA* was detected in 100% isolates from Site III, 80% of isolates from Site II, 75% isolates from Site (I, VIII and X), 66% of isolates from Site IV, 50% of isolates from the Site V, 33% of isolates isolated from Site VI, and absent in isolates collected from Sites VII and XI. Reported MICs of copper for resistant isolates did not inhibit colony growth at 3 mM to 6 mM.

The mercuric reductase gene *merA* were detected in 100%, 75%, 66%, 50%, 40%, 33%, and 25% isolates
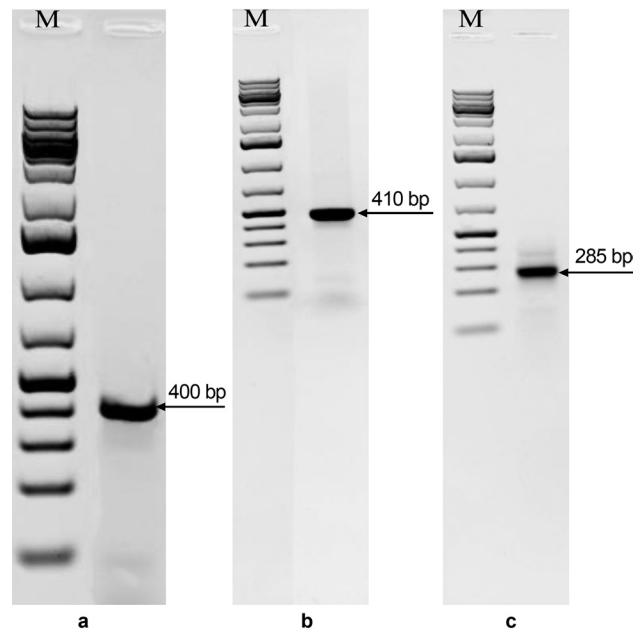
Fig. 2. Detection by PCR of heavy metal resistance genes.
a – Amplicon of *silE* of *Enterobacter cloacae* 27 (400 bp);
b – Amplicon of *cusA* of *Klebsiella pneumoniae* 13 (410 bp);
c – Amplicon of *merA* of *Pseudomonas putida* 26 (285 bp);
M – Size Marker 1 kb Plus.

collected from Site V, IX, (IV, VI), (I, III), II, VII, X, respectively. No gene was detected in the isolates collected from Site VIII. Reported MIC of mercury for resistant isolates did not inhibit colony growth at 0.02 to 0.08 mM. Ten isolates harbored *silE*, *cusA*, and *merA*. For only one isolate, identified as *Pseudomonas putida* 23, no amplification was observed. Therefore, we observed a significant correlation between the detection of resistance genes and MIC determinations.

Structural and functional analyses of protein binding site. The complete sequence of the extracellular heavy metal-binding protein SilE of pMG101 from *Salmonella* (AAD1171743) is composed of 143 amino acids (Asiani et al. 2016). Sequence alignment of the partial SilE sequence obtained from the 39 isolates (this study) and the SilE of pMG101 showed that 84.6% of the SilE sequences were 100% identical to each other and the SilE of pMG101. The rest (15.4%) showed some sequence variation from the SilE of pMG101 (Fig. 3). Nevertheless, all isolates showed the conserved histidine and methionine residues in their sequences and the Ag⁺ binding motif characteristic to SilE (Asiani et al. 2016).

The complete sequence of CusA efflux pump of the *E. coli* (CusA P30854) is composed of 1,047 amino acids. Sequence alignment of the partial CusA protein from ten isolates with CusA from *E. coli* (CusA P30854) showed various mutations. A minor difference detected between partial CusA sequence from *E. coli* 3 and the consensus E149G and V267I.

Fig. 3. Sequence alignment of the partial SilE protein from 39 isolates with SilE from pMG101 (SilE AAD11743). Letters shows residues different from the consensus. Conserved histidine and methionine residues are marked above with either a circle or a square, respectively.

Table IV

Phenotypic and molecular characteristics of antibiotic and heavy metal resistant isolates collected from polluted water in Tunisia.

Strains	Sites	MICs of HM (µg/ml) Ag^{2+} Cu^{2+} Hg^{2+}	HM resistance genes	AB resistance profile	AB resistance genes
Pseudomonas anguilliseptica 1	MJ. Bizerte	0.064 (R) 0.625(S) 0.08 (R)	*silE, merA*	AMP, ATM, FOS	bla_{TEM}
Alcaligenes eutrophus 2	MJ. Bizerte	0.064 (R) 3 (R) 0.005 (S)	*silE, cusA*	AMP, CAZ	bla_{TEM}
Escherichia coli. 3	MJ. Bizerte	0.064 (R) 6 (R) 0.0025 (S)	*silE, cusA*	AMP, TIC, PIP,CXM, CFM, CAZ, ATM, GMN, NET, TOB, CTX	bla_{TEM}, $bla_{CTX-M-1}$, *qnrB*
Staphylococcus aureus 4	MJ. Bizerte	0.064 (R) 3(R) 0.08 (R)	*silE, cusA, merA*	AMP, ATM, FOS, CIP, LEV	bla_{TEM}
Pseudomonas mendocina 5	IF of Bizerte MB	0.032 (R) 3(R) 0.08 (R)	*silE, cusA, merA*	AMP, ATM, FOS	bla_{TEM}
Alcaligenes eutrophus 6	IF of Bizerte MB	0.064 (R) 6(R) 0.005 (S)	*silE, cusA*	AMP, CAZ, SXT, CHL	bla_{TEM}
Klebsiella pneumoniae 7	IF of Bizerte MB	0.064 (R) 3(R) 0.08 (R)	*silE, cusA, merA*	AMP, TIC, FOX, FEP, ETP, AMC, CAZ, IMP, SXT, CTX, FOS, CLS, NOR, CIP, GMN, AKN, NET, TOB, NFE, MNO, TET	bla_{TEM}, bla_{SHV}, $bla_{CTX-M-1}$, bla_{OXA8}, *qnrB*
Pseudomonas putida 8	IF of Bizerte MB	0.064 (R) 1.5 (S) 0.005 (S)	*silE*	AMP, TIC, TCC, PIP, FEP, CAZ, ATM, FOS	bla_{TEM}
Alcaligenes faecalis 9	IF of Bizerte MB	0.064 (R) 3 (R) 0.005 (S)	*silE, cusA*	AMP, CAZ	bla_{TEM}
Pseudomonas mendocina 10	Tinjah wedi, Bizerte	0.064 (R) 1.5 (S) 0.08 (R)	*silE, cusA, merA*	AMP, ATM, FOS	bla_{TEM}
Pseudomonas mendocina 11	Tinjah wedi, Bizerte	0.032 (R) 3 (R) 0.005 (S)	*silE, cusA*	AMP, TCC, FOS	bla_{TEM}
Alcaligenes faecalis 12	Tinjah wedi, Bizerte	0.064 (R) 3 (R) 0.005 (S)	*silE, cusA*	AMP, CAZ, CHL	bla_{TEM}
Klebsiella pneumoniae 13	Tinjah wedi, Bizerte	0.032 (R) 3 (R) 0.04 (R)	*silE, cusA, merA*	AMP, TIC, AMC, NAL, NOR, CHL ,TGC, MNO, TET	bla_{TEM}, bla_{SHV}
Pseudomonas fluorescens 14	CWTP of Beja	0.064 (R) 3 (R) 0.005 (S)	*silE, cusA*	AMP, TIC, ATM, FOS, IMP, MEM,	bla_{TEM}
Pseudomonas putida 15	CWTP of Beja	0.064 (R) 1.5 (S) 0.08 (R)	*silE, merA*	AMP, TIC, TCC	bla_{TEM}
Pseudomonas putida 16	CWTP of Beja	0.008 (S) 3 (R) 0.04 (R)	*cusA, merA*	AMP, TIC, TCC, PIP, FEP, CAZ, ATM, FOS	bla_{TEM}
Aeromonas salmonicida 17	Marsh Sejoumi	0.032 (R) 1.5 (S) 0.08 (R)	*silE, merA*	AMP, TIC	bla_{TEM}
Alcaligenes eutrophus 18	Marsh Sejoumi	0.008 (S) 0.625 (S) 0.08 (R)	*merA*	AMP, CAZ	bla_{TEM}
Pseudomonas alcaligenes 19	Marsh Sejoumi	0.0064(R) 3 (R) 0.08 (R)	*silE, cusA, merA*	AMP, TIC, PIP, TCC, FOS	bla_{TEM}
Enterobacter cloacae 20	Marsh Sejoumi	0.064 (R) 6 (R) 0.08 (R)	*silE, cusA, merA*	AMP, TIC, FOX, AMC, CTX	bla_{TEM}, bla_{OXA-1}, bla_{SHV}, $bla_{CTX-M-9}$

Table IV
Continued

Strains	Sites	MICs of HM (µg/ml) Ag^{2+} Cu^{2+} Hg^{2+}	HM resistance genes	AB resistance profile	AB resistance genes
Bacillus coagulans 21	Milian Rades Wedi	0.064 (R) 3 (R) 0.02 (R)	*silE, cusA, merA*	AMP, TIC, TCC, PIP, FEP, CAZ, ATM, FOS	bla_{TEM}
Alcaligenes eutrophus 22	Milian Rades Wedi	0.064 (R) 0.625 (S) 0.08 (R)	*silE, merA*	AMP, CAZ, SXT, CHL	bla_{TEM}
Pseudomonas putida 23	Milian Rades Wedi	0.004 (S) 0.625 (S) 0.005 (S)	–	AMP, ATM, FOS	bla_{TEM}, bla_{SHV}
Alcaligenes eutrophus 24	Majerda River	0.064 (R) 1.5 (S) 0.005 (S)	*silE*	AMP, CAZ	bla_{TEM}
Serratia marcescens 25	Majerda River	0.064 (R) 1.5 (S) 0.02 (R)	*silE, merA*	AMP, TIC, FOX, AMC	bla_{TEM}, bla_{OXA-1}, bla_{SHV}
Pseudomonas putida 26	Majerda River	0.032 (R) 0.75 (S) 0.02 (R)	*silE, merA*	AMP, FOS, ATM, LEV	bla_{TEM}
Enterobacter cloacae 27	Lebna wedi C.B	0.064 (R) 3 (R) 0.005 (S)	*silE, cusA*	AMP, TIC, FOX, AMC, TGC, MNO, TET	bla_{TEM}, bla_{OXA-1}
Serratia fonticola 28	Lebna wedi C.B	0.064 (R) 1.5 (S) 0.005 (S)	*silE*	AMP, TIC, AMC, CTX, CLS	bla_{TEM}, $bla_{CTX-M-9}$
Alcaligenes faecalis 29	Lebna wedi C.B	0.032 (R) 3 (R) 0.005 (S)	*silE, cusA*	AMP, CAZ	bla_{TEM}
Klebsiella pneumoniae 30	Lebna wedi C.B	0.064 (R) 6 (R) 0.005 (S)	*silE, cusA*	AMP, TIC, AMC	bla_{TEM}, bla_{SHV}
Pseudomonas fluorescens 31	Om Larayes, Gafsa	0.064 (R) 3 (R) 0.08 (R)	*silE, cusA, merA*	AMP, TIC, TCC, PIP, FEP, ATM, IMP, MEM, FOS	bla_{TEM}
Aeromonas salmonicida 32	Om Larayes, Gafsa	0.064 (R) 0.625 (S) 0.005 (S)	*silE*	AMP	bla_{TEM}
Aeromonas salmonicida 33	Om Larayes, Gafsa	0.064 (R) 1.5 (S) 0.08 (R)	*silE, merA*	AMP, TIC, FEP, CAZ, ATM	bla_{TEM}
Pseudomonas putida 34	Om Larayes, Gafsa	0.032 (R) 1.5 (S) 0.08 (R)	*silE, merA*	AMP, TIC, TCC, PIP, TZP, CAZ, ATM	bla_{TEM}
Pseudomonas fluorescens 35	Om Larayes, Gafsa	0.0064 (R) 0.75 (S) 0.005 (S)	*silE*	AMP, TIC, TCC, ATM, MEM	bla_{TEM}
Pseudomonas putida 36	Gulf of Gabes	0.064 (R) 3 (R) 0.008 (S)	*silE, cusA*	AMP, TIC, TCC, PIP, TZP, ATM, MEM	bla_{TEM}
Serratia marcescens 37	Gulf of Gabes	0.064 (R) 1.5 (S) 0.005 (S)	*silE*	AMP, FOX, AMC, TGC, MNO, TET	bla_{TEM}
Pseudomonas fluorescens 38	Gulf of Gabes	0.0064 (R) 6 (R) 0.08 (R)	*silE, cusA, merA*	AMP, TIC, TCC, PIP, TZP, FEP, CAZ, ATM, MEM, LEV, FOS	bla_{TEM}
Klebsiella pneumoniae 39	Gulf of Gabes	0.032 (R) 3 (R) 0.0025 (S)	*silE, cusA*	AMP, TIC, TCC, PIP, CFN, CXM, CFM, CAZ, FEP, ATM, GMN, NET, TOB	bla_{SHV}, $bla_{CTX-M-1}$, *qnrB*

AKN – Amikacin; AMC – Amoxicillin-Clavulanic acid; ATM – Aztreonam; CAZ – Ceftazidim; CFM – Cefixim; CFN – Cefalexin; CHL – Chlorampenicol; CIP – Ciprofloxacin; CLS – Colistin; CTX – Cefotaxim; CXM – Cefuroxim; ETP – Ertapenem; FEP – Cefepim; FOS – Fosfomicin; FOX – Cefoxitin; GMN – Gentamicin; IMP – Imipenem; LEV – Levofloxacin; MEP – Meropenem; MNO – Minocyclin; NAL – Nalidixic acid; NET – Netilmecin; NMN – Neomycin; PIP – Piperacillin; SXT – Trimethoprim-Sulfamethoxazole; TCC – Ticarcillin-Clavulanic acid; TET – Tetracycline; TGC – Tigecyclin; TIC – Ticarcillin; TOB – Tobramycin; TZP – Piperacillin-Tazobactam; *silE* – silver-binding protein; *merA* – mercury II reductase; *cusA* – cation efflux system protein CusA

Fig. 4. Sequence alignment of the partial Cation efflux system protein CusA from 10 isolates with *E. coli* P30854. Different residues from the consensus are showed by one letter. Conserved residues are represented by points.

Fig. 5. Sequence alignment of the partial mercuric reductase protein MerA from 8 isolates with *E. cloacae* (MerA EU081910). Different residues from the consensus are showed by one letter. Conserved residues are represented by points.

A similar partial CusA sequences from *E. cloacae* 27, *Alcaligenes feacalis* 9, *Bacillus coagulans* 21, and *K. pneumoniae* (7, 13, 30 and 39) were different by 26% residues with the consensus.

Similar partial CusA sequence was showed for *Pseudomonas alcaligenes* 19 and *P. putida* 36. Nevertheless, both of them detected a low sequence homology with 42% of different residues comparing with the consensus (Fig. 4).

Five hundred sixty-one amino acids compose the complete sequence of the mercuric reductase MerA protein of *E. cloacae* (MerA EU081910). Similar partial MerA sequences of *P. alcaligenes* 19 and *P. putida* 34 were different by seven residues comparing with the consensus (*E. cloacae* (MerA EU081910). Moreover, *K. pneumoniae* (7 and 13) showed the seven different residues mentioned previously for *P. alcaligenes* 19 and *P. putida* 34, and showed another different extra residue R55V N37K, respectively (Fig. 5).

Same different residues like in *P. alcaligenes* 19 and *P. putida* 34 except for one residue S1A was detected in *Alcaligenes eutrophus* 22.

Discussion

In order to investigate the spread and emergence of environmental bacteria resistant to heavy metals in contaminated waters, we studied the heavy metal-resistant phenotype and selected marker genes for resistance to silver, mercury, and copper. In addition, we scored antibiotic resistance to evaluate the impact of heavy metal

contamination as a selective agent in the spreading of antibiotic resistance. The heavy metals in the collected contaminated waters from ten sites over Tunisia mainly originated from anthropogenic activities. Sites I, II, and III, located near and surround the Lagoon of Bizerte, were subjected to urban and agricultural pollutions. As described by Dellali et al. (2001), agricultural origin wastes reach the lagoon due to leaching of inland cultivated and devoted to cereal activities (Banni et al. 2009). With the thirteen isolates collected from Sites I, II, and III, the highest resistance was recorded for silver; 100% of isolates showed the high MIC values for Ag^+ ranging from 0.032 to 0.064 mM, and harbored the *silE* gene in the same time.

Prevalence of multidrug-resistant bacteria in the North of Tunisia. Ten resistant isolates from Sites I, II, and III harbored the CusA efflux pump. The *cusA* gene was found in 84.6% of the isolates in I, II, and III Sites. All of these isolates showed high MICs of copper ranging from 3 to 6 mM, except for only one isolate, which was able to grow in a concentration of 1.5 mM, and harbored the gene simultaneously. The contents of copper of the superficial sediments of the Lagoon of Bizerte suggested by Dellali et al. (2001), Ouakad et al. (2007), and Ben Garali et al. (2010) showed a remarkable increase of the concentrations 45 parts-per-million (ppm), 58 ppm, and 67 ppM respectively. These values are beyond the admissible limit of the National Network of Observation (RNO 2007) with 30 ppm, and therefore, they are considered contaminated. Those results can explain the high level of resistance against copper, shown by isolates from this work.

On the other hand, we found the *merA* gene in only 46.15% of the isolates that could grow in concentrations higher than 0.04 mM. This low resistance against mercury can be explained by the low concentration of mercury in the lagoon and surrounding areas, such as Bizerte, Menzel Bourguiba (0.41 ppm) (Mzoughi et al. 2002).

Data recorded in Essijoumi Lagoon showed that 50% of isolates collected in this site harbored the *cusA* gene and were able to grow until a concentration of Cu ranged from 3 to 6 mM. The copper concentration recorded in this site corresponds to a high concentration (359 ppm) (Marzougui and Ben Mammou 2006); it is much higher than the critical values given by the European norm (30 ppm) (Rademacher 2001). Moreover, 75% of the isolates for which the MIC values of Ag^+ were above 0.032 mM, harbored the *silE* gene. Zhang et al. (2019) reported that copper ions (Cu^{2+}) could stimulate the conjugative transfer of silver via resistance nodulation-cell division (RND-type) Ag^+/Cu^+ efflux transporter that exports Ag^+/Cu^+ from the periplasm via an antiport (Randall et al. 2015).

No data in the literature evokes the contamination of this site by mercury. Nevertheless, 100% of isolates in this site harbored the *merA* gene with the high MIC value between 0.04 and 0.08 mM. Those high values are considered as the first values reported in the literature.

Site VI and VII are located on the west coast of Tunis's gulf and exposed to heavy metals, mainly transported to the marine environment (Ben Amor et al. 2019). The geoaccumulation index value for copper (10 ppm) recorded by Ben Amor et al. (2019) has indicated that all samples were uncontaminated. Those results explained in the present work, the lowest proportion (20%) of isolates that harbored the *cusA* gene, while 83% and 60% of them showed resistance to silver and mercury, respectively.

Trace heavy metal, like mercury, is among the most severe pollutants in nature due to its toxicity. Luckily, it was reported by Ennouri et al. (2008) at a very low concentration (0.33 ppm) in the Lebna River (Site VIII). Regarding Hg, the concentrations are relatively low. It may be why isolates did not develop any resistance, especially that we did not detect the *merA* gene among our isolates. The metal at a concentration of only 0.005 mM could have inhibited their growth.

Prevalence of multidrug-resistant bacteria in South of Tunisia. The lowest (20%) and the highest (100%) percentages of the resistant isolates against copper and silver, respectively, were collected from Gafsa (Site IX). Copper inhibited the growth of 20% of isolates at a concentration of 3 mM. Site IX was exposed to a high degree of phosphoric and heavy metals contamination due to the anthropogenic activities i.e., mining, manufacturing, and the use of synthetic products

(Mekki and Sayedi 2017). It can explain why growth was inhibited for all isolates at a high silver nitrate concentration starting from 0.032 up to 0.064 mM, and that 60% of isolates harbored merA to resist the mercury presence. They were able to grow in the presence of Hg^+ at a concentration of 0.08 mM.

The leading cause of contamination of waters in Gabes (Site X) is the acidic industrial effluent that originated from the phosphate treatment factory. Effluents contain phosphogypsum particles and cause ecological risk to marine organisms and human health (Naifar et al. 2018). 75% of isolates from Gabes harbored the cusA gene with the MIC value for copper of 3 mM. When we compare our results with Naifar et al. (2018) results, we could say that the copper concentration of 0.5 ppm is lower than Tunisian standards (1.5 ppm). It can stimulate the resistance against copper with high MICs. The co-stimulation may explain those results by other heavy metals present with high concentrations, i.e., iron (16 ppm) and Zn (18 ppm). Both values exceeded the Tunisian standards (1 ppm) and (10 ppm), respectively.

The present study provided new information about silver contamination, notably the highest resistance in the ten sites was recorded to silver. The *silE* gene was harbored by 36 isolates (92.30%) of the total 39 isolates. Moreover, the silver resistance prevalence was higher than those observed by Edwards-Jones (2009), who recorded only 3.5% isolates possessing the silver resistance genes *silE* of 172 bacterial isolates from wounds. The considerable difference between these studies may be explained by the fact that the environment always brings the most significant risk of being exposed to HM contamination.

Molecular analysis of multi-drug resistance. The latter encodes the extracellular heavy metal-binding protein (periplasmic space) SilE. Observed amino acid sequence variations did not concern conserved histidine and methionine residues nor the Ag^+ binding motif characteristic to SilE, described by Asiani et al. (2016). It allowed the corresponding isolate to maintain its ability to resist silver presence by producing an active SilE, and conserved the protein functionality in absorbing heavy metal ions. These results confirmed again that mutations observed here had no impact on the MIC value of silver.

Long et al. (2010) suggest a crystal structure of the CusA efflux pump methionine mediated CuI but also AgI heavy metal transport. The *cusA* gene was harbored by 43.4% of our isolates.

The heavy metal binding-sites are formed by three methionines (M573, M623, and M672) and found above this horizontal helix (Long et al. 2010). The partial sequence aligned with consensus started from AA^{149} to AA^{280} with conserved M^{230} and M^{271}. The latter is one of the four channel pairs, which includes the four methionine pairs (M410 and M501, M403 and M486, M391

and M1009, and M271 and M755) as well as the heavy metal binding-sites formed by the three methionines, facilitating heavy metal transport. The mutations that affected the other residues, which did not touch the heavy metal binding-sites or the channel, conserved their functionality in absorbing AgI and CuI ions.

The mercury reductase MerA is known as an enzyme, reducing the ionic mercury Hg (II) to elemental mercury. In bacteria, the mercury resistance is specified by operon (*mer*) that can transport Hg (II) and organo-mercury to the cytosol for degradation and reduction to Hg (0). MerA catalase, a flavin oxidoreductase, reduces Hg (II) to NAD(P)H dependent reaction. MerA or mercury reductase can play an important role in the biogeochemical cycling of mercury in contaminated environments by partitioning mercury to the atmosphere (Ní Chadhain et al. 2006).

The MerA amino acid sequences' multiple alignments in the present study revealed a minor difference in sequence patterns between our MerA protein isolates and the consensus (Fig. 5). Thus, the partial MerA sequence did not contain both motifs. Despite the few mutations, mercuric reductase from our resistant isolates retained the ability to reduce mercury. We suppose that FAD/NADP and mercury binding sites were well conserved in our eight resistant isolates. Among 51.2% of mercury-resistant isolates,, which detected the *merA* gene, only 20% of them expressed the MerA protein; however, the remaining isolates expressed ABC Transporter, TeTR family, ATP-ase super-family, and ATP binding family.

Molecular aspects of cross-resistance. To better understand the bacterial cross-resistance and its ecological risk, it was essential to elucidate the bacterial resistance against heavy metals and antibiotics.

The overuse of antibiotics in clinics and hospitals raises the emergence of resistant bacteria. Environmental bacteria, especially, showed resistance to antibiotics, which were detected in different environmental compartments such as soils, surface water, sediments ground water, and waste-water (Kümmerer 2004).

In the present study, the environmental strains isolated from the ten sites showed high resistance to a large number of antibiotics, and some were even ESBLs and MBLs-producers, which is a global health concern. This ubiquitous detection of antibiotic resistance and resistant genes in isolates indicates the emergence of antibiotic-resistant strains in the golf of Tunis and Gulf of Gabes, which threatens the health of animals and people throughout Tunisia.

Substantial reports suggest that heavy metal contamination represents an indirect selection agent that contributes to the maintenance and spread of antibiotic resistance factors (Baker-Austin et al. 2006). The *silE* gene can be harbored on plasmids (Ben Miloud et al.

2020) carrying antibiotic resistance genes, and silver can thereby have an indirect selective pressure. Even more directly, silver can select for porin deficiency and consequently mediate a cross-resistance to β-lactams (Sütterlin et al. 2014). In addition, contamination by heavy metals such as cadmium, zinc, copper, and mercury affected soil or water environment, besides they are toxic to bacteria. They also initiate the co-selection of antibiotic resistance using different mechanisms, i.e., agricultural soils amended with copper co-select resistance to ampicillin, chloramphenicol, and tetracycline (Oves and Hussain 2016).

Conclusion

It is the first work describing contaminations by copper, silver, and mercury in ten sites in Tunisia. Such data were almost absent in the literature. Moreover, a high degree of heavy metal and antibiotic resistance were found in our isolates. They develop some new mechanisms to eliminate or reduce heavy metals or antibiotics' impact.

The resistant environmental bacteria in Tunisia are more prevalent than we expected for both antibiotic and heavy metal resistance. The cross-resistance between them made the bacteria better fitted to the environment. It also enhances the danger and the risk of public health. Even though the detailed mechanisms of cross-resistance are unclear, it will be recommended to study the impact of heavy metals on antibiotic resistance in environmental microorganisms. With the extent of pollution, it is valid to study the co-existence of antibiotics and heavy metal resistance and their particular influence on bacteria.

ORCID
    Chedly Chouchani https://orcid.org/0000-0002-8294-8289

Conflict of interest
    The authors do not report any financial or personal connections with other persons or organizations, which might negatively affect the contents of this publication and/or claim authorship rights to this publication.

Literature

Aminov RI. Horizontal gene exchange in environmental microbiota. Front Microbiol. 2011 Jul 26;2:158. https://doi.org/10.3389/fmicb.2011.00158

Asiani KR, Williams H, Bird L, Jenner M, Searle MS, Hobman JL, Scott DJ, Soultanas P. SilE is an intrinsically disordered periplasmic "molecular sponge" involved in bacterial silver resistance. Mol Microbiol. 2016 Sep;101(5):731–742. https://doi.org/10.1111/mmi.13399

Baker-Austin C, Wright MS, Stepanauskas R, McArthur JV. Co-selection of antibiotic and metal resistance. Trends Microbiol. 2006 Apr;14(4):176–182. https://doi.org/10.1016/j.tim.2006.02.006

Banni M, Bouraoui Z, Ghedira J, Clearandeau C, Jebali J, Boussetta H. Seasonal variation of oxidative stress biomarkers in clams *Ruditapes decussatus* sampled from Tunisian coastal areas. Environ Monit Assess. 2009 Aug;155(1-4):119–128. https://doi.org/10.1007/s10661-008-0422-3

Ben Amor R, Yahyaoui A, Abidi M, Chouba L, Gueddari M. Bioavailability and assessment of metal contamination in surface sediments of Rades-Hamam Lif Coast, around Meliane River (Gulf of Tunis, Tunisia, Mediterranean Sea). J Chem. 2019 Apr 15;2019:1–11. https://doi.org/10.1155/2019/4284987

Ben Garali A, Ouakad M, Gueddari M. Contamination of superficial sediments by heavy metals and iron in the Bizerte lagoon, northern Tunisia. Arab J Geosci. 2010;3:295–306. https://doi.org/10.1007/s12517-009-0082-9

Ben Miloud S, Ali Md Muntasir, Boutiba I, Van Houdt R, Chouchani C. First report of cross resistance to silver and antibiotics in *Klebsiella pneumoniae* isolated from patients and polluted water in Tunisia. Water and Enviro J. 2020;0:1–10. https://doi.org/10.1111/wej.12665

Besaury L, Bodilis J, Delgas F, Andrade S, De la Iglesia R, Ouddane B, Quillet L. Abundance and diversity of copper resistance genes *cusA* and *copA* in microbial communities in relation to the impact of copper on Chilean marine sediments. Mar Pollut Bull. 2013 Feb;67(1-2):16–25. https://doi.org/10.1016/j.marpolbul.2012.12.007

Boyd ES, Barkay T. The mercury resistance operon: from an origin in a geothermal environment to an efficient detoxification machine. Front Microbiol. 2012;3:349. https://doi.org/10.3389/fmicb.2012.00349

Chihomvu P, Stegmann P, Pillay M. Characterization and structure prediction of partial length protein sequences of *pcoA*, *pcoR* and *chrB* genes from heavy metal resistant bacteria from the Klip River, South Africa. Int J Mol Sci. 2015 Apr 01;16(12):7352–7374. https://doi.org/10.3390/ijms16047352

CLSI. M100-S23 performance standards for antimicrobial susceptibility testing. Twenty-third informational supplement. Wayne (USA): Clinical and Laboratory Standards Institute; 2013.

Dallenne C, Da Costa A, Decré D, Favier C, Arlet G. Development of a set of multiplex PCR assays for the detection of genes encoding important β-lactamases in Enterobacteriaceae. J Antimicrob Chemother. 2010 Mar;65(3):490–495. https://doi.org/10.1093/jac/dkp498

Dellali M, Gnassia Barelli M, Romeo M, Aissa P. The use of acetylcholinesterase activity in *Ruditapes decussatus* and *Mytilus galloprovincialis* in the biomonitoring of Bizerta lagoon. Comp Biochem Physiol C Toxicol Pharmacol. 2001 Oct;130(2):227–235. https://doi.org/10.1016/S1532-0456(01)00245-9

Edwards-Jones V. The benefits of silver in hygiene, personal care and healthcare. Lett Appl Microbiol. 2009 Aug;49(2):147–152. https://doi.org/10.1111/j.1472-765X.2009.02648.x

Ennouri R, Chouba L, Kraiem MM. [Evaluation de la contamination chimique par les métaux traces (Cd, Pb, Hg et Zn) du zooplancton et de la sardinelle (*Sardinella aurita*) dans le golfe de Tunis] (in French). Bull. Inst. Nat. Scien. Tech. Mer de salambo. 2008;35:87–94.

Fatimawali, Kepel B, Yusuf I, Badaruddin F, Natsir R, Retnoningrum D. Isolation and characterization of partial sequence of *merA* gene from mercury resistant bacterium *Klebsiella pneumoniae* isolated from Sario River Estuary Manado. J Environ Earth Sci. 2014;6(3):156–160. https://doi.org/10.19026/rjees.6.5754

Filali BK, Taoufik J, Zeroual Y, Dzairi FZ, Talbi M, Blaghen M. Waste water bacterial isolates resistant to heavy metals and antibiotics. Curr Microbiol. 2000 Sep;41(3):151–156. https://doi.org/10.1007/s0028400

Galkiewicz JP, Kellogg CA. Cross-kingdom amplification using bacteria-specific primers: complications for studies of coral microbial ecology. Appl Environ Microbiol. 2008 Dec 15;74(24):7828–7831. https://doi.org/10.1128/AEM.01303-08

Gupta A, Matsui K, Lo JF, Silver S. Molecular basis for resistance to silver cations in *Salmonella*. Nat Med. 1999 Feb;5(2):183–188. https://doi.org/10.1038/5545

Harrison M, Jones C, Solioz M, Dameron C. Intracellular copper routing: the role of copper chaperones. Trends Biochem Sci. 2000 Jan 01;25(1):29–32. https://doi.org/10.1016/S0968-0004(99)01492-9

Jan AT, Murtaza I, Ali A, Rizwanul Haq QM. Mercury pollution: an emerging problem and potential bacterial remediation strategies. World J Microbiol Biotechnol. 2009 Sep;25(9):1529–1537. https://doi.org/10.1007/s11274-009-0050-2

Jung WK, Koo HC, Kim KW, Shin S, Kim SH, Park YH. Antibacterial activity and mechanism of action of the silver ion in *Staphylococcus aureus* and *Escherichia coli*. Appl Environ Microbiol. 2008 Apr 01;74(7):2171–2178. https://doi.org/10.1128/AEM.02001-07

Kerfoot WC, Harting SL, Jeong J, Robbins JA, Rossmann R. Local, regional, and global implications of elemental mercury in metal (copper, silver, gold, and zinc) ores: insights from Lake Superior sediments. J Great Lakes Res. 2004 Jan;30:162–184. https://doi.org/10.1016/S0380-1330(04)70384-6

Kerfoot WC, Harting, SL, Rossmann, R, Robbins, JA. Elemental mercury in copper, silver and gold ores: an unexpected contribution to Lake Superior sediments with global implications. Geochem Explor Environ Anal. 2002 May;2(2):185–202. https://doi.org/10.1144/1467-787302-022

Kershaw CJ, Brown NL, Constantinidou C, Patel MD, Hobman JL. The expression profile of *Escherichia coli* K-12 in response to minimal, optimal and excess copper concentrations. Microbiology. 2005 Apr 01;151(4):1187–1198. https://doi.org/10.1099/mic.0.27650-0

Klasen HJ. Historical review of the use of silver in the treatment of burns. I. Early uses. Burns. 2000 Mar;26(2):117–130. https://doi.org/10.1016/S0305-4179(99)00108-4

Kumar S, Stecher G, Tamura K. MEGA 7: molecular Evolutionary Genetics Analysis version 7.0 for bigger datastes. Mol Biol Evol. 2016 Jul;33(7):1870–1874. https://doi.org/10.1093/molbev/msw054

Kümmerer K. Resistance in the environment. J Antimicrob Chemother. 2004 Jul 01;54(2):311–320. https://doi.org/10.1093/jac/dkh325

Long F, Su CC, Zimmermann MT, Boyken SE, Rajashankar KR, Jernigan RL, Yu EW. Crystal structures of the CusA efflux pump suggest methionine-mediated metal transport. Nature. 2010 Sep;467(7314):484–488. https://doi.org/10.1038/nature09395

Mandal S, Nath Das S, Mandal M. Plasmid mediated antibiotic and heavy metal co-resistance in bacterial isolates from Mahananda River water (Malda, India). Transl Med (Sunnyvale). 2016;06(04):185. https://doi.org/10.4172/2161-1025.1000185

Marzougui A, Ben Mammou A. Impacts of the dumping site on the environment: Case of the Henchir El Yahoudia Site, Tunis, Tunisia. C R Geosci. 2006 Dec;338(16):1176–1183. https://doi.org/10.1016/j.crte.2006.09.020

Mekki A, Sayadi S. Study of heavy metal accumulation and residual toxicity in soil saturated with phosphate processing wastewater. Water Air Soil Pollut. 2017 Jun;228(6):215. https://doi.org/10.1007/s11270-017-3399-0

Mergeay M, Nies D, Schlegel HG, Gerits J, Charles P, Van Gijsegem F. *Alcaligenes eutrophus* CH34 is a facultative chemolithotroph with plasmid-bound resistance to heavy metals. J Bacteriol. 1985; 162(1):328–334. https://doi.org/10.1128/JB.162.1.328-334.1985

Monsieurs P, Moors H, Van Houdt R, Janssen PJ, Janssen A, Coninx I, Mergeay M, Leys N. Heavy metal resistance in *Cupriavidus metallidurans* CH34 is governed by an intricate transcriptional network. Biometals. 2011 Dec;24(6):1133–1151. https://doi.org/10.1007/s10534-011-9473-y

Mzoughi N, Stoichev T, Dachraoui M, El Abed A, Amouroux D, Donard OFX. Inorganic mercury and methylmercury in surface sediments and mussel tissues from a microtidal lagoon (Bizerte, Tunisia). J Coast Conserv. 2002;8(2):141–145. https://doi.org/10.1652/1400-0350(2002)008[0141:IMAMIS]2.0.CO;2

Naifar I, Pereira F, Zmemla R, Bouaziz M, Elleuch B, Garcia D. Spatial distribution and contamination assessment of heavy metals in marine sediments of the southern coast of Sfax, Gabes Gulf, Tunisia. Mar Pollut Bull. 2018 Jun;131(Pt A):53–62. https://doi.org/10.1016/j.marpolbul.2018.03.048

Nguyen CC, Hugie CN, Kile ML, Navab-Daneshmand T. Association between heavy metals and antibiotic-resistant human pathogens in environmental reservoirs: A review. Front Environ Sci Eng. 2019 Jun;13(3):46. https://doi.org/10.1007/s11783-019-1129-0

Ní Chadhain SM, Schaefer JK, Crane S, Zylstra GJ, Barkay T. Analysis of mercuric reductase (*merA*) gene diversity in an anaerobic mercury-contaminated sediment enrichment. Environ Microbiol. 2006 Oct;8(10):1746–1752. https://doi.org/10.1111/j.1462-2920.2006.01114.x

Ouakad M. Genèse et évolution des milieux laguno-lacustres du nord-est de la Tunisie (Garaet Ichkeul, Lagunes de Bizerte et de Ghar el Melh) [Thèse Doct. ès.]. Sciences Géologiques, Université de Tunis el Manar, Tunis, Tunisie. 2007. p. 453.

Oves M, Mabood Hussain F. Antibiotics and heavy metal resistance emergence in water borne bacteria. J Invest Genomics. 2016 Sep 28; 3(2):23–25. https://doi.org/10.15406/jig.2016.03.00045

Rademacher P. Atmospheric heavy metals and forest ecosystems. Geneva (Switzerland): UN/ECE, Federal Research Centre for Forestry and Forest Products (BFH); 2001. p. 75.

Randall CP, Gupta A, Jackson N, Busse D, O'Neill AJ. Silver resistance in Gram-negative bacteria: a dissection of endogenous and exogenous mechanisms. J Antimicrob Chemother. 2015 Jan 06;70(4):1037–1046. https://doi.org/10.1093/jac/dku523

RNO. Tendances temporelles des teneurs en contaminants dans les mollusques du littoral français. Surveillance du Milieu Marin. Édition 2000. Travaux du Réseau National d'Observation de la qualité du milieu marin (RNO). Ifremer et Ministère de l'Aménagement du territoire et de l'Environnement; 2007. p. 9–32.

Silver S, Phung LT. Bacterial heavy metal resistance: new Surprises. Annu Rev Microbiol. 1996 Oct;50(1):753–789. https://doi.org/10.1146/annurev.micro.50.1.753

Summers AO. Generally overlooked fundamentals of bacterial genetics and ecology. Clin. Infect. 2002 Jun 1;34(Suppl 3):S85–S92. https://doi.org/10.1086/340245

Sütterlin S, Edquist P, Sandegren L, Adler M, Tängdén T, Drobni M, Olsen B, Melhus Å. Silver resistance genes are overrepresented among *Escherichia coli* isolates with CTX-M production. Appl Environ Microbiol. 2014 Nov 15;80(22):6863–6869. https://doi.org/10.1128/AEM.01803-14

Tamura K, Nei M. Estimation of the number of nucleotide substitutions in the control region of mitochondrial DNA in humans and chimpanzees. Mol Biol Evol. 1993 May;10(3):512–526. https://doi.org/10.1093/oxfordjournals.molbev.a040023

Tchounwou PB, Yedjou CG, Patlolla AK, Sutton DJ. Heavy metal toxicity and the environment. In: Luch A, editor. Molecular, clinical and environmental toxicology. Basel (Switzerland): Springer; 2012. p. 133–164. https://doi.org/10.1007/978-3-7643-8340-4_6

Vicente A, Avilés M, Codina JC, Borrego JJ, Romero P. Resistance to antibiotics and heavy metals of *Pseudontonas aeruginosa* isolated from natural waters. J Appl Bacteriol. 1990 Jun;68(6):625–632. https://doi.org/10.1111/j.1365-2672.1990.tb05228.x

Zhang S, Wang Y, Song H, Lu J, Yuan Z, Guo J. Copper nanoparticles and copper ions promote horizontal transfer of plasmid-mediated multi-antibiotic resistance genes across bacterial genera. Environ Int. 2019 Aug;129:478–487. https://doi.org/10.1016/j.envint.2019.05.054

Comparative Analysis of the Microbiota Between Rumen and Duodenum of Twin Lambs Based on Diets of Ceratoides or Alfalfa

ZACCHEAUS PAZAMILALA AKONYANI[#], FENG SONG[#], YING LI, SUDE QIQIGE and JIANGHONG WU[*]

College of Animal Science and Technology, Inner Mongolia University for the Nationalities, Tongliao, China

Abstract

In our previous study, diet directly impacted the microbiota of the rumen in twin lambs. The duodenum is the first part of the small intestine, so we seek to determine whether there is a difference in the digesta between the two feed groups HFLP (high fiber, low protein) and LFHP (low fiber, high protein), and its impact on the biodiversity and metabolism of the duodenum. Results showed that the number of Operational Taxonomic Units (OTUs) in the duodenum (2,373 OTUs) was more than those in the rumen (1,230 OTUs), and 143 OTUs were significantly different in the duodenum between the two groups. The two most predominant phyla were *Bacteriodetes* and *Firmicutes*, but this ratio was reversed between the rumen and duodenum of lambs fed different feedstuffs. The difference in the digesta that greatly changed the biodiversity of the rumen and duodenum could affect the microbial community in the gastrointestinal tract (GIT). Sixteen metabolites were significantly different in the duodenum between the two groups based on the metabolome analysis. The relationships were built between the microbiome and the metabolome based on the correlation analysis. Some metabolites have a potential role in influencing meat quality, which indicated that the diet could affect the microbiota community and finally change meat quality. This study could explain how the diet affects the rumen and duodenum's microbiota, lay a theoretical basis for controlling feed intake, and determine the relationship between the duodenum's microbiota and metabolism.

Introduction

Many environmental factors such as nutrition, habitat, and host genetics impact the components and functions within the gut microbiome (Ussar et al. 2016). The rumen of sheep envelops a complicated microbiota and acts as the primary location for fermentation of consumed feed (McCann et al. 2017), which directly impacts sheep's health and physiological functions.

The rumen is the largest compartment of ruminants where plant cell walls and other herbage materials are degraded by intricate microbial communities predominated by bacteria (Sirohi et al. 2012). The bacteria systematically decompose plant cell materials (Flint and Bayer 2008) and break down plant biomass, serving as a link between the sheep and the nutrients absorbed by the sheep. The succeeding rumen fermentation manufactures ammonia and short-chain fatty acids (SCFAs), including acetate, butyrate, and propionate. In a previous study, we found that diet directly impacts the microbiota structure of the rumen and affects the metabolic process in sheep muscle (Wu et al. 2020). However, the nutritional components that entered the small intestines were not analyzed.

The duodenum, the first part of the small intestines, is where absorption of nutrients begins due to its ability to receive partially degraded food from the stomach. The duodenum is the most proximal phase of degradation, and it represents the most oversized diameter, the densest villi, and the deepest part within the small intestines. The duodenum takes fluid and bile produced by the pancreas and the liver, thereby assisting the intestines in breaking fat, protein, and starch (Faichney 1969; DeGregorio et al. 1982; Lewis and Dehority 1985). Few studies have been done regarding the microbiota of the duodenum, and there is a need to analyze the metabolome of the duodenum, compare it with the microbiota of the rumen, to determine the structure of the bacterial community in the lambs based on two different feeds.

Zaccheaus P. Akonyani and Feng Song contribute equally to this work and are co-first authors.
* Corresponding author: J. Wu, College of Animal Science and Technology, Inner Mongolia University for the Nationalities, Tongliao, China; e-mail: wujianghonglong@126.com

Experimental

Materials and Methods

Preparation of feed pellets. In our previous study (Wu et al. 2020), two categories of feed pellets were prepared. One category was alfalfa (Medicago sativa) which belongs to the LFHP group. The other category was ceratoides (*Ceratoides arborescens*) belonging to the HFLP group.

Experimental animals. To avoid the influence of genetic background, four pairs of 3 months old twins Sunit lambs with an average weight of 24 ± 2.3 kg were used in the experiment. The details of how the twin lambs were grouped, monitored, fed, slaughtered, and their genomic DNA extracted can be seen in Wu et al. (2020). For microbiome analysis, the liquid phases of duodenum content were separated by squeezing them through four gauze layers (1 mm mesh). The fluid was divided into two parts, centrifuged at 500 g for 30 min at 4°C to isolate residual particles and preserved at –80°C.

16S rRNA sequencing of duodenum and rumen. To determine the structure of the bacterial community in the lambs fed based on two different dietary requirements, the 16S rRNA microbiome in the duodenum was sequenced. Microbiome DNA was extracted using the E.Z.N.A.® Stool DNA Kit according to the manufacturer's instructions. Bacterial 16S genes were enlarged from microbiome DNA using V3-V4 region primers and arranged in sequence using the Illumina MiSeq PE300. A total of 181,562 tags were obtained from 8 specimens, with an average of 22,695.25 tags per specimen after being filtered and merged. The UCLUST (Edgar 2010) algorithm of QIIME (version 1.8.0) (Caporaso et al. 2010) was used to group the various tags with 97% of similarity and to obtain the Operational Taxonomic Units (OTUs). The OTUs were carefully annotated and carried out by the Silva database (Quast et al. 2013). The Mothur software version 1.30 (Schloss et al. 2009) and UniFrac techniques (Lozupone and Knight 2005) were used in calculating the alpha and beta diversity. The 16S rRNA microbiome in the rumen was obtained from the NCBI SRA data under BioProject PRJNA659928. The same analysis pipeline was used for rumen microbiome.

Duodenum metabolome analysis. In this research, metabolites were separated from the sheep's duodenum and analyzed with liquid chromatography combined with mass spectrometry (LC/MS). An untargeted metabolic analysis was done on the duodenum of the four pairs of the twin lambs. The variation between the two groups (HFLP and LFHP) was identified by using principal components analysis (PCA) and orthogonal partial least squares discriminant analysis (PLS-DA) (Bylesjö et al. 2006): p-value $\leq 0.05 +$ VIP ≥ 1. The p-value was tested by Mann-Whitney-Wilcoxon Test/Student's t-test, and the VIP (Variable Important in the Projection) is the PLS-DA first principal component. To increase the sample size for metabolic analysis, two new samples in each group were created and averagely mixed to produce more sample size. Sample A and B were mixed to produce E (1:1, v/v), and samples C and D were mixed to form F (1:1, v/v). Ions were assigned to metabolites based on online databases, including Human Metabolome Database (HMDB; https://www.hmdb.ca), Biofluid Metabolites Database (http://metlin.scripps.edu), mzCloud (https://www.mzcloud.org), Lipid Maps (https://www.lipidmaps.org), and MassBank (https://www.massbank.jp).

Joint analysis of microbiota and metabolome. Spearman's correlation analysis between the microbiota and metabolites was carried out, coefficients were produced (Looney and Hagan 2007), and was significant ($p \leq 0.05$). The screening condition was |rho| > 0.8. Based on the corresponding relationship between the final metabolite and OTUs, the information was inputted into Cytoscape software (https://cytoscape.org) to draw a network diagram.

Results

The microbial diversity of the rumen and duodenum. Based on Simpsons and Shannon indices, there was a significant difference in the rumen's microbial diversity between the HFLP and the LFHP groups ($p < 0.05$). This could be the effect of the high fiber content in the HFLP diet (Table II). However, there was no significant difference in the duodenum's microbial diversity between the two groups (Table III). The diversity of the microbiota in the HFLP group was higher

Table I
Nutritional components of two feed stuffs.

	DM (%)	GE (MJ/kg DM)	CP (% DM)	CF (% DM)	ADF (% DM)	NDF (% DM)
LFHP	89.4	16.3	16.1	2.4	25.2	46.2
HFLP	90.5	15.8	11.8	2.2	29.6	57.5

LFHP – low fiber high protein level, HFLP – high fiber low protein level, ADF – acid detergent fiber, CF – crude fat,
CP – crude protein, DM – dry matter, GE – gross energy, NDF – neutral detergent fiber

Table II
The diversity analysis of the rumen microbiota of twin lambs.

Items	HFLP	LFHP	p-value
Shannon	5.055 ± 0.1589	4.235 ± 0.181	0.014
Simpsons	0.019 ± 0.004	0.066 ± 0.041	0.116
Observed species (Obs)	992.000 ± 68.474	930.000 ± 18.037	0.154
Ace	1051.658 ± 64.182	992.341 ± 26.875	0.102
Chao 1	1059.470 ± 67.920	1017.360 ± 29.399	0.165

The HFLP group was fed with ceratioids and the LFHP group of twin lambs was fed with alfalfa in the phylum of the rumen. Presented parameters are sample estimators of total species with sample identifications (Sample ID). While Obs, Ace, and richness (Chao 1) are used to describe the species number, Simpson and Shannon's indices are used to indicate how diverse the rumen microbiota is.

Table III
The diversity analysis of duodenum microbiota of twin lambs.

Items	HFLP	LFHP	p-value
Shannon	7.855 ± 0.880	7.828 ± 0.838	0.964
Simpsons	0.985 ± 0.006	0.986 ± 0.005	0.391
Observed species (Obs)	966.750 ± 293.842	905.000 ± 247.818	0.781
Chao 1	1278.063 ± 241.678	1223.815 ± 327.198	0.843

The HFLP group was fed with ceratoides, the LFHP group of twin lambs was fed with alfalfa in the phylum of the duodenum. Presented parameters are sample estimators of total species with sample identifications (Sample ID). While Obs and richness (Chao 1) are used to describe the species number, Simpsons and Shannon's indices are used to indicate how diverse the duodenum microbiota is.

than the LFHP group in the rumen. However, that pattern could not be entirely detected in the duodenum. The diversity of the microbiota in the duodenum was higher than those in the two groups' rumen.

Phylum community distribution of the rumen and duodenum. On the phylum level, the abundance of 11 phyla of the rumen and duodenum was calculated and used to draw histograms for comparisons. A greater number of sequences obtained from the phylum class pertained to the phyla *Bacteroidetes*, and *Firmicutes* but at the duodenum's phylum level, a larger proportion of the sequences obtained related to *Firmicutes,* and *Bacteroidetes*. The major bacteria in the rumen's phylum level were *Bacteriodetes*, but were replaced with *Firmicutes* in the duodenum. The major bacteria were higher in the LFHP group than the HFLP group for the rumen and duodenum (Fig. 1 and 2).

Genus community distribution of the rumen and duodenum. A detailed examination of the relative abundance of bacterial OTUs showed that the two different feeds have a varied influence on both the rumen and duodenum's microbiota. According to the 16s rRNA gene of the rumen and duodenum bacteria sequences, 1,230 OTUs and 2,373 OTUs among eight rumen and duodenum samples were identified. In the duodenum, 143 OTUs were significantly different between the two groups.

Ninety-two non-identical genera were designated from the sequences at the genus level. The genera were among almost all specimens. *Prevotella* was abundant in the rumen of the LFHP group compared to the HFLP group (Fig. 3a). Unclassified *Lachnospiraceae* were prevalent in the LFHP group's duodenum compared to the HFLP group (Fig. 3b). The high protein in the LFHP feed increases the genera *Prevotella* and unclassified *Lachnospiraceae* of the rumen and duodenum.

Comparison between the microbiota of ceratoides (HFLP) and alfalfa (LFHP) feeds, and their *Firmicutes/Bacteriodetes* (F:B) ratio in the rumen and duodenum. The F:B ratio in the rumen microbiota of the twin lambs fed on the LFHP pellets was 0.104, and that of the HFLP pellets was 0.275 (Fig. 4a and 4b). The F:B ratio in the duodenum microbiota of the twin lambs fed on the LFHP pellets was 6.419, and that of the HFLP pellets was 5.356 (Fig. 4c and 4d). There was a change in the F:B ratios in the rumen and duodenum even under the different feeds.

Differential expression metabolites between two groups. After the data was filtered, 3,696 stable metabolic features were detected. A partial least squares discriminant analysis (PLS-DA) was performed between the two groups to identify metabolic differences in duodenum of twin sheep fed different diets (Fig. 5). The results showed that 407 significantly different metabolites

Duodenum Phylum	A1	B1	C1	D1	A2	B2	C2	D2
Actinobacteria	1.71	4.93	3.45	6.91	1.15	0.80	1.49	10.21
Bacteroidetes	12.46	0.37	7.95	1.88	1.62	21.04	11.33	0.14
Cyanobacteria	0.04	0.05	0.03	0.22	0.21	0.11	0.24	0.41
Elusimicrobia	0.06	0.00	0.01	0.00	0.00	0.02	0.00	0.00
Firmicutes	71.23	74.94	65.81	43.86	88.03	66.20	68.63	74.56
Lentisphaerae	0.04	0.00	0.08	0.03	0.00	0.07	0.01	0.00
Proteobacteria	2.47	0.08	2.46	1.33	0.33	1.73	1.00	0.15
Spirochaetes	0.40	0.01	0.47	1.23	0.09	0.78	0.56	0.00
Synergistetes	0.00	0.01	0.12	0.10	0.00	0.05	0.06	0.00
Tenericutes	0.42	0.02	0.29	0.12	0.17	0.38	0.24	0.01
Others	11.168	19.579	19.325	44.301	8.3986	8.83	16.45	14.52
Rumen Phylum								
Actinobacteria	0.12	0.66	1.71	0.29	0.03	0.13	0.06	0.01
Bacteroidetes	73.88	68.19	68.22	70.14	86.20	85.20	89.14	85.65
Cyanobacteria	0.18	0.15	0.12	0.02	0.06	0.01	0.03	0.03
Elusimicrobia	0.04	0.02	0.02	0.00	0.04	0.01	0.01	0.04
Firmicutes	12.58	15.84	23.98	24.91	8.75	11.16	7.81	8.33
Lentisphaerae	1.47	2.75	0.73	1.28	0.60	0.38	0.52	0.61
Proteobacteria	9.09	10.20	2.37	1.18	1.48	0.55	0.36	1.05
Spirochaetes	0.19	0.15	0.19	0.64	0.40	0.23	0.20	0.41
Synergistetes	0.08	0.40	0.10	0.05	0.02	0.02	0.02	0.01
Tenericutes	1.60	0.69	0.91	0.79	1.93	1.13	1.17	2.81
Others	0.77	0.95	1.65	0.69	0.49	1.19	0.67	1.07

Fig. 1. This figure shows a comparison between the phylum composition of the bacteria in the rumen and duodenum of twin lambs. The letters A1-D1 represent HFLP group, and A2-D2 represent LFHP group.
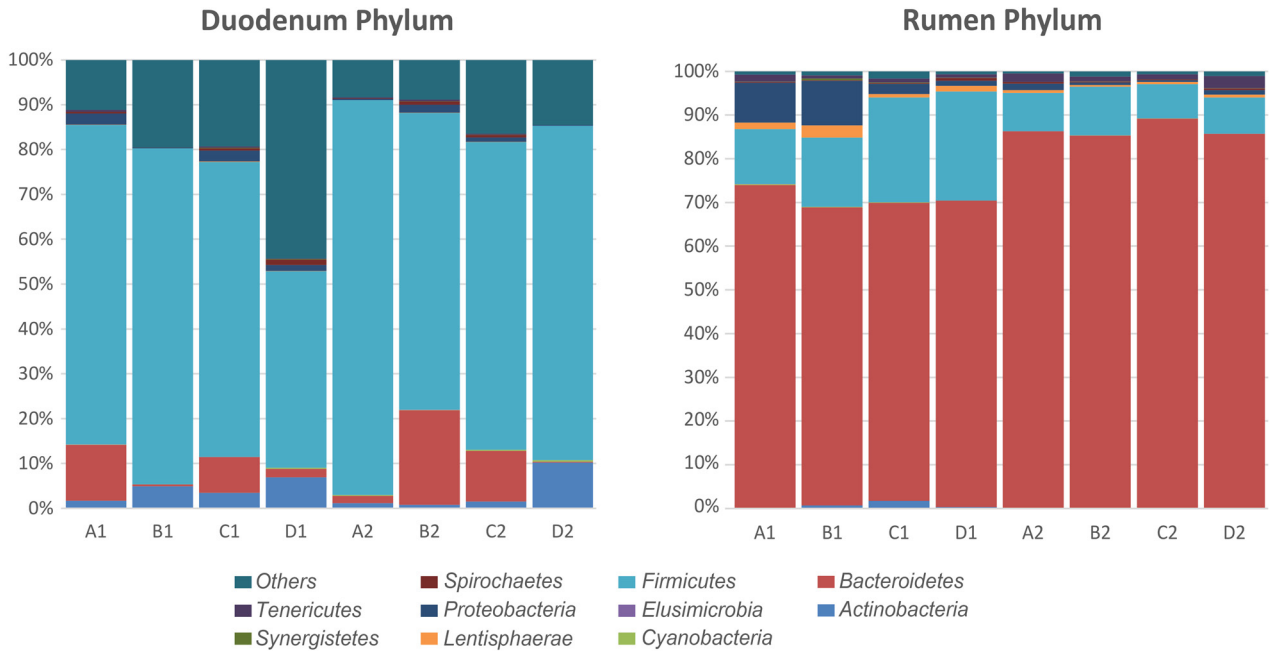
Fig. 2. The phylum composition of rumen and duodenum of twin lambs. The letters A1-D1 represent the HFLP group, and the A2-D2 represent the LFHP group of phylum and duodenum, respectively.

(p-value ≤ 0.05) were screened between the two groups. In the HFLP group, 273 of the metabolites showed a lower expression, and 134 of the metabolites showed a higher expression. Tandem mass spectrometry (MS/MS) was used to detect 16 significantly different metabolites indicated in the heat map (Fig. 6). The HFLP group increased 7 of the metabolites while that of the LFHP group influenced 9 of the metabolites. Some of the metabolites discussed are adenosine, taurine, L-alanine, and nicotinic acid (Fig. 7). It was detected that there was a significant difference between the HFLP diet and the LFHP diet (p-value ≤ 0.05).

The correlation analysis indicated that the abundance of 5,6-dihydrouracil correlated positively with
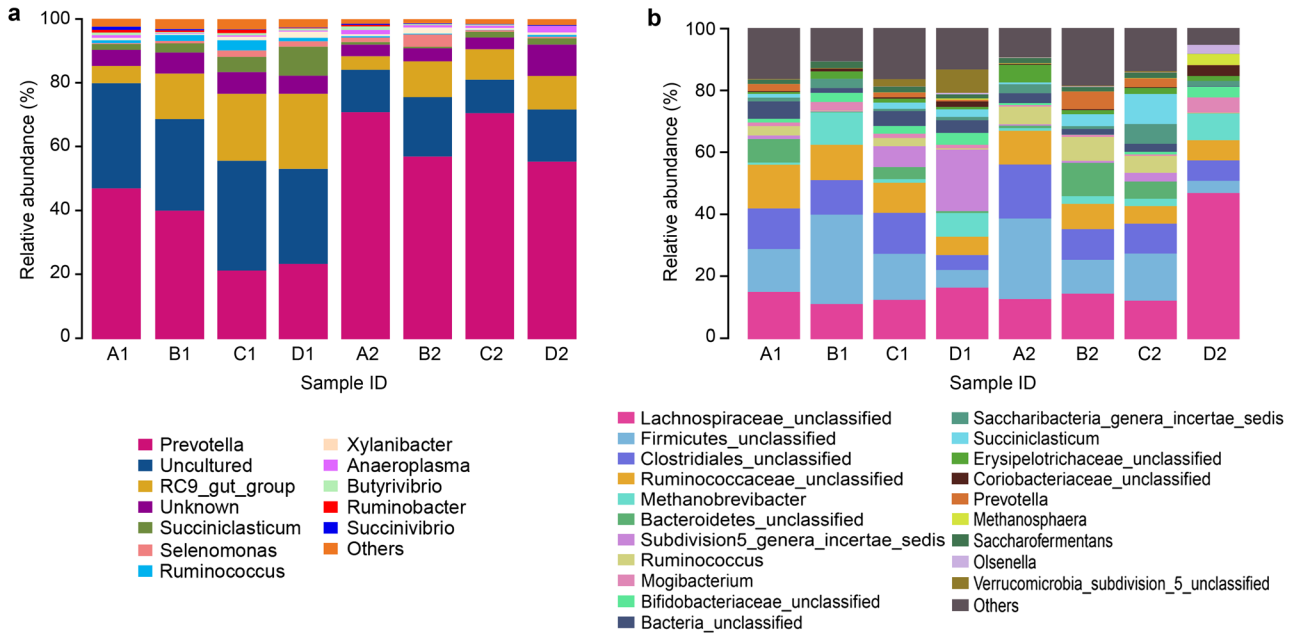
Fig. 3. The genus community distribution of rumen and duodenum.

a) The genus community distribution of rumen. The letters A1-D1 represent the first group fed with HFLP and A2-D2 represents the second group of twin lambs fed with LFHP in the genus. b) The genus community distribution of duodenum. The letters A1-D1 represent the first group fed with HFLP and A2-D2 represents the second group of twin lambs fed with LFHP in the genus.
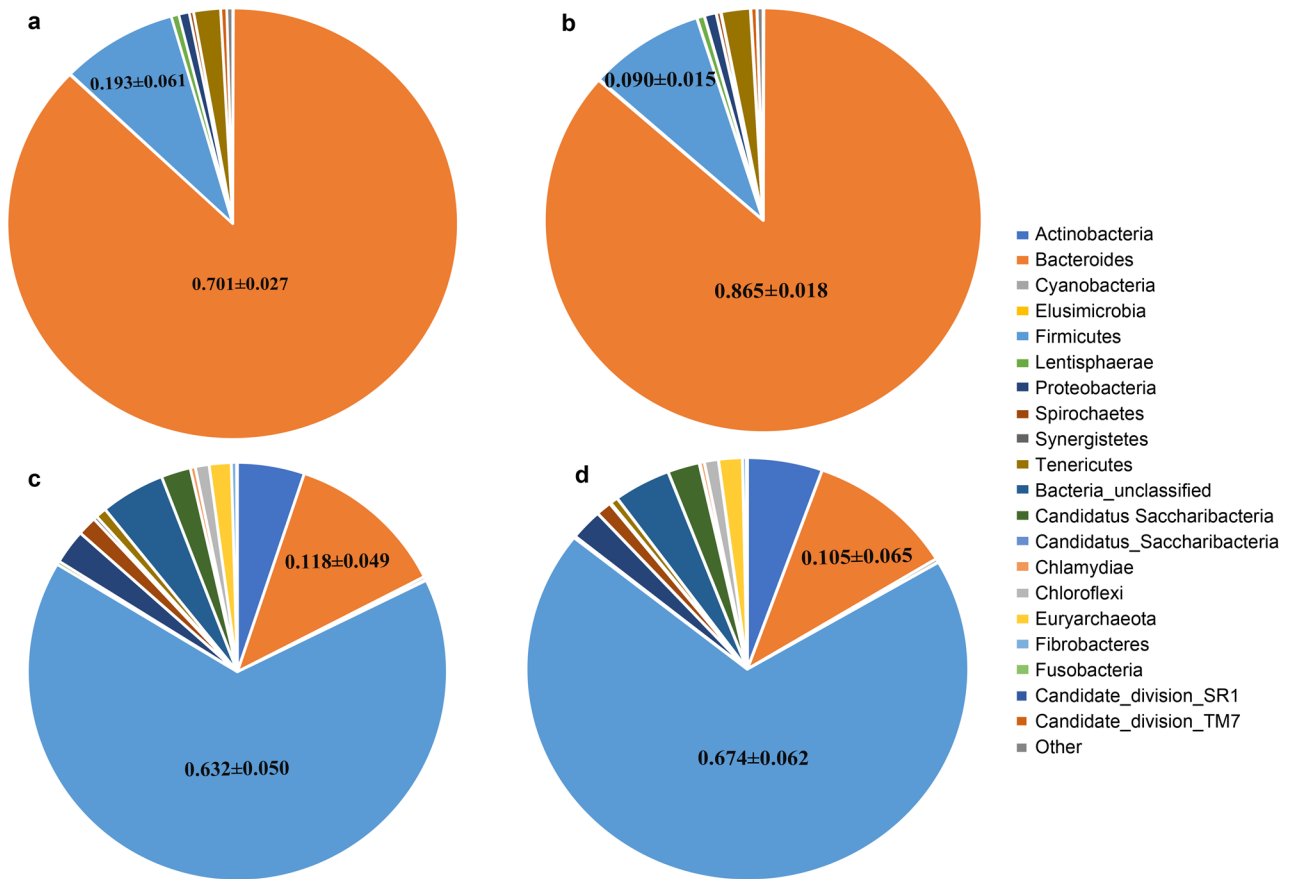
Fig. 4. Comparison between HFLP and LFHP's microbiota and their F:B ratio in the rumen and duodenum.

The letters a) and b) represent HFLP pellets and LFHP pellets, respectively, of the rumen. Enterotypes were strongly associated with feeds a) and b) which show LFHP pellets (*Bacteroidetes*) against HFLP pellets (*Firmicutes*). LFHP pellets displayed a substantial increase in *Bacteroidetes* and a reduction in *Firmicutes*. The letters c) and d) represent HFLP and LFHP pellets, respectively, of the duodenum. Enterotypes were strongly associated with feeds c) and d) which show LFHP pellets (*Bacteroidetes*) against HFLP pellets (*Firmicutes*). HFLP pellets displayed an increase in *Firmicutes* and a reduction in *Bacteroidetes*.

Fig. 5. PLS-DA score plot came from liquid chromatography combined with mass spectrometry (LC/MS) spectra for the HFLP group (blue dots) and the LFHP group (red dots).

Fig. 6. Heat map built by the 407 significantly different metabolites (p-value ≤ 0.05) in the HFLP and LFHP groups. The red color represents the LFHP group, and the blue represents the HFLP group.

adenosine, and negatively correlated with 9(R)-HODE and acrylic acid. Adenosine was observed to be positively correlated with 5,6-dihydrouracil, and correlated

negatively with 9(R)-HODE and acrylic acid. 9(R)-HODE had a positive correlation with acrylic acid, and correlated negatively with 5,6-dihydrouracil and

Fig. 7. The relationship between the two feed (LFHP and HFLP) groups and the metabolites.

adenosine. Also, acrylic acid was seen to be correlated positively with 9(R)-HODE but negatively correlated with 5,6-dihydrouracil, and adenosine (Fig. 8).

Relationship between duodenal microbiota and metabolites. Correlation analysis between the microbiota and metabolites was carried out to find the possible coexistence. 79 correlations were related positively ($|rho| > 0.8$, p-value ≤ 0.05) while 194 correlations were related negatively ($|rho| > 0.8$, p-value ≤ 0.05) between the OTUs and the metabolites. *Prevotella* and 1-amino-cyclohexanecarboxylic acid had the greatest positive correlations ($r = 0.84$, p-value ≤ 0.05). *Methanobrevibacter* and 3-deshydroxysappanol trimethyl ether were detected to have the greatest negative correlations ($r = -0.79$, p-value ≤ 0.05) between the bacteria and metabolites.

The bacterium *Candidatus saccharibacteria* (OTU31, OTU970) is positively correlated with the metabolites 9(R)-HODE and acrylic acid and correlated negatively with 5,6-dihydrouracil, adenosine, and L-alanine. The bacterium *Cyanobacteria sreptophyta* (OUT217) was found to be correlated positively with 9(R)-HODE and acrylic acid but correlated negatively with 5,6-dihydrouracil, adenosine, and L-alanine. The bacteria *Firmicutes blautia*, *Firmicutes Firmicutes* unclassified, and *Firmicutes Eubacterium* sp. C2 (OTU224, OTU769, OTU798) which all belong to phylum *Firmicutes* were positively correlated with 9(R)-HODE and acrylic acid but negatively correlated with 5,6-dihydrouracil, adenosine, and L-alanine. The bacterium *Planctomycees planctomycetaceae* (OTU1882) correlated
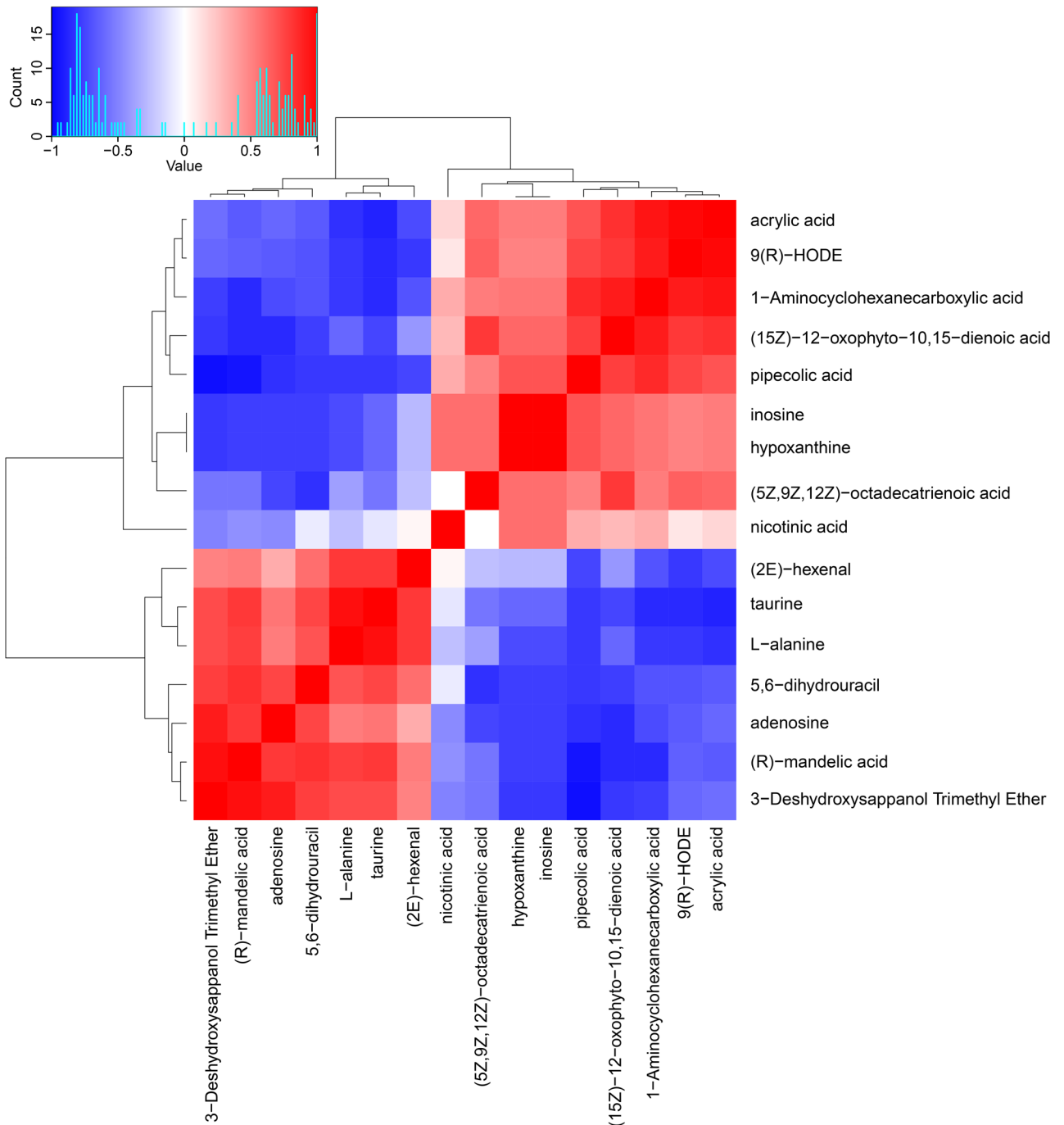
Fig. 8. Metabolites correlation heat map. The rows and columns in the figure represent different metabolites, and different colors represent different correlations. The red color represents a positive correlation, and the blue represents a negative correlation among the metabolites. The deeper the color in the heat map, the better the metabolism.

positively with 5,6-dihydrouracil, adenosine, and L-alanine but correlated negatively with 9(R)-HODE and acrylic acid (Fig. 9).

Discussion

Many former researchers on ruminants only concentrate on the rumen microbiomes. However, we decided to compare the rumen and duodenum micro-biomes using two feed types and the duodenal metabolism to investigate the relationship between microbiota and metabolome because metabolites can influence the meat quality and health of the host (Xu et al. 2013; Muroya et al. 2019).

The biodiversity of the rumen and duodenum microbiota. The biodiversity of the rumen was higher when fed with ceratoides (HFLP) than when fed with alfalfa pellets (LFHP) (Table II). The outcome of this work is compatible with our previous research, which

Fig. 9 This figure shows the relationship between OTUs, metabolites, and the microbiota. The nodes represent different OTUs related to bacteria, which belong to *Firmicutes*, *Bacteriodetes*, and other phyla. The orange diamonds indicate 16 metabolites detected. The lines indicate the correlations between the OTUs, bacteria, and metabolites. The solid red connecting lines show a positive correlation, and the blue connecting dot line indicates a negative correlation between the OTUs, bacteria, and metabolites. The line thickness shows how strong the correlation was.

reveals that the microbiota in the lambs' rumen fed a high fiber diet (HFLP) were more diverse than those fed a low fiber diet (LFHP) (Wu et al. 2020). A study shows that *Firmicutes* and *Bacteroidetes* are the major predominant phyla of microorganisms in the gut community of terrestrial animals (Qin et al. 2010). In this research, the most predominant phyla in the rumen's microbiota of the twin lambs were *Bacteroidetes* and *Firmicutes* (Fig. 1 and 2), which are more associated with the breakdown of carbohydrates and proteins. Results of this kind have been revealed in earlier reports (Hook et al. 2011). *Bacteroidetes* aids in the degradation of starch in the rumen (Stevenson and Weimer 2007).

The LFHP diet influenced the genus *Prevotella* and the phylum *Bacteroides* of the rumen (Fig. 3). Results of this kind have been detected in earlier research (Zhang et al. 2014). The genus *Prevotella* plays a signifi-

cant role in breaking down dietary protein to ammonia, which can reduce the utilization of dietary amino acids. The degradation of peptides in the rumen is associated with the breakdown approach in which dietary protein is disintegrated into ammonia, thereby leading to an inexpedient utilization of dietary amino acids (Walker et al. 2005).

There was no significant difference between the two diets in the duodenum in this study (Table III). Regardless of diet, amino acid profiles of the duodenal digesta were similar due to the presence of forage (Merchen et al. 1986). In this study, *Firmicutes* was relatively abundant in the duodenum's phylum level, which confirms a research study where *Firmicutes* were the predominant phylum among all the bacterial groups across the GIT besides those within the omasum and abomasum, in which *Bacteroidetes* were more prevalent (Wang

et al. 2017). The *Lachnospiraceae* was found to be the most abundant genus in the duodenum (Fig. 3). This finding agrees with a research study that revealed that other *Firmicutes* members showing a great abundance in lamb's gut were *Lachnospiraceae* (Palomba et al. 2017).

The Firmicutes/Bacteroidetes ratio (F:B) in the rumen and duodenum's microbiota. The microbiota's F:B ratio was reversed between the rumen and the duodenum due to differences in the organs and functions. The most potent organ, which degrades and converts plant materials to SCFAs in the ruminants, is the rumen (Wang et al. 2020). It possesses the complex microbiota that plays a vital role in the fermentation of feed and energy metabolism, and the SCFAs provide more than 70% of the energy to guarantee host growth and reproduction performance (Flint et al. 2007). Several researchers suggested that bacteria detected in intestinal contents as they go through the abomasum could come from lysed cells (Waghorn et al. 1990; Koenig et al. 1997; Hristov 2007), and the role of the duodenal microbiota in terms of its function in feed degradation is likely to be different from that of the ruminal bacterial community.

A study revealed that including dried distillers' grains with solubles (DDGS) at the detriment of corn bran decreased the flow of bacteria from the rumen (Castillo-Lopez et al. 2014). The DDGS consists of about 31% crude protein, 34% neutral detergent fiber, 12% fat, and 5% starch (Paz et al. 2013). Also, the rumen's microbiota clustered differently compared to that of the duodenum showing different bacterial diversity between ruminal bacteria and the duodenal digesta. Therefore, including the DDGS in the feeds would increase the flow of saturated fatty acids to the duodenum and cause a shift in the rumen and duodenum's bacterial diversity (Castillo-Lopez et al. 2014).

The small intestine, which comprises the duodenum, is a long and coiled tube where the remaining degradable activities occur. Villi that line the small intestine are the main site where nutrients are absorbed and are distributed to the whole body. Amino acids, fatty acids, and sugars which are the end products of digestion, are absorbed from the small intestines, enters the lymph, and distributed (National Research Council 2007). Another study revealed that when fat was injected into the duodenum of lambs, it was absorbed quickly, but when introduced to the rumen, absorption was slow and took several days (Heath and Morris 1962).

The feed delivered plays a crucial function in the F:B ratio (Ramirez Ramirez et al. 2012). The F:B ratio of the microbiota appreciably changed in the rumen when the twin lambs consumed either LFHP or HFLP feeds (5.356 and 6.419), respectively (Fig. 4a and 4b). There was also a change in the F:B ratio of microbiota in the duodenum when the twin lambs consumed either

LFHP or HFLP feeds (0.275 and 0.104), respectively (Fig. 4c and 4d).

The more significant F:B ratio in fecal specimens is related to an increase in human weight (Ley et al. 2006), and a study found that the frequency of particular microbial phylotypes could be affected within the offspring of farm animals such as cattle due to the sire breed when utilizing disparate feeds (Hernandez-Sanabria et al. 2013). Also, the changes of the F:B ratios in this current research agrees with a previous study that analyzed the F:B ratio in mice and humans, where changes in the GIT were demonstrated to affect obesity and the capability of the host to harvest energy (Krajmalnik-Brown et al. 2012). It implies that the shift in the F:B ratio in this study could result from the different kinds of feed.

The relationship between the two feed (LFHP and HFLP) groups and the metabolites. Adenosine can influence meat quality. Apart from influencing the components of the gut microbiota, the type of diet can also regulate metabolic homeostasis in twin lambs. In the presence of low protein, meat quality improves in the HFLP group (Fig. 7a). A study summarized that Tibetan sheep meat was preferred to Small-tailed Han sheep meat even though variations between the breeds were not much; however, meat quality was enhanced in the two breeds with the growth of the nutritional energy level when a low-protein feed was given (Jiao et al. 2020). The presence of adenosine in this study could influence the health and regulate the sheep's immune system. It reduces the production of tumor necrosis factor (TNF), induces the manufacture of Nitric Oxide (NO), and plays a vital role in maintaining tissue perfusion (Adanin et al. 2002).

Taurine was influenced by the HFLP feed (Fig. 7b). Taurine present in this study is vital when inspecting the relationship between taurine and palatability. A study mentioned that ribose 5-phosphate, and pyrrolidone carboxylic acid or taurine were natural antecedents of 4-hydroxy-5-methyl-3(2H)-furanone, which is a taste part removed from beef broth and has a caramel-like and burnt chicory smell (Tonsbeek et al. 1968; Weenen et al. 2005). The abundance of taurine in lambs and much more in beef could also enhance the beef's nutritional value apart from contributing to flavor (Purchas et al. 2004). Taurine is important for meat quality, and increasing the concentration of taurine in mutton could be a future breeding objective for Sunit sheep.

The metabolite L-alanine, which was influenced by HFLP diet (Fig. 7c) could benefit the host by reducing tuberculosis. Tuberculosis is caused by *Mycobacterium tuberculosis*, and it is a major health issue globally. A study discovered that exogenous L-alanine can lead to the manufacturing of reactive oxygen species in *Mycobacterium smegmatis* by accelerating the tricarboxylic

cid cycle and/or primary metabolism synergizing with fluoroquinolones, which, in the long run, results in the destruction of *M. smegmatis* (Zhen et al. 2020).

The LFHP diet could increase nicotinic acid in the twin lambs (Fig. 7d). A study showed that replacing dietary protein with non-protein nitrogen depresses nicotinic acid (Buziassy and Tribe 1960). Another study revealed that both nicotinamide and insulin-induced hypoglycemia reductions in free fatty acid enhanced growth hormones released in dairy cows, and each of these cases provided a possible function for glucose and free fatty acid in modulating the growth hormone-releasing factor, which stimulates the release of growth hormones in ruminants (Reynaert et al. 1975; Sartin et al. 1988).

The joint analysis of metabolites and microbiota in the duodenum. The bacteria, which all belong to phylum *Firmicutes* (OTU224, OTU769, and OTU798) correlated negatively with adenosine (Fig. 9). The bacteria *Planctomycetes planctomycetaceae* (OTU1882) correlated positively with adenosine and L-alanine. Early research states that *Planctomycetes* contain a strong proline- and cysteine-rich proteins envelope and not a peptidoglycan cell wall (Liesack et al. 1986). Also, *Candidatus saccharibacteria* (OTU31, OTU970), and *Cyanobacteria sreptophyta* (OUT217) correlated negatively with adenosine and L-alanine. Recently, whole genomes of *Saccharibacteria*, acquired via metagenomics, reported that a few members ferment metabolites, glucose, and various sugars and produce lactate (Albertsen et al. 2013). *Cyanobacteria* has various unique roles that include the ability to restore nitrogen, synthesize vitamin B and K21, syntrophically manufacture hydrogen, and obligate anaerobic fermentation (Di Rienzi et al 2013).

Based on the relationship between the bacteria and metabolites, *Methanobrevibacter* can produce methane in the gut. Methanogenic archaea represented by *Methanobrevibacter ruminantium* produce ruminant's methane and is found in ruminants fed on varied kinds of feeds worldwide (Leahy et al. 2010).

Conclusions

This study shows how 16S rRNA sequencing combined with metabolome analysis may be used in discovering new and significant influences on the functions of a microbe inside the host. The results showed that the diet could directly affect the diversity of rumens' microbiota but not the microbiota in duodenum. There was a shift in the F:B ratio in the rumen and duodenum of the twin lambs even under the different feeds. We found that some bacteria had a relationship with the metabolites. In summary, these findings could provide

knowledge of how the diet affects the microbiota of the rumen and duodenum, lay a theoretical basis for controlling feed intake, and determine the relationship between the duodenum's microbiota and metabolism.

Literature

Adanin S, Yalovetskiy IV, Nardulli BA, Sam AD 2nd, Jonjev ZS, Law WR. Inhibiting adenosine deaminase modulates the systemic inflammatory response syndrome in endotoxemia and sepsis. Am J Physiol Regul Integr Comp Physiol. 2002 May;282(5):R1324–R1332. https://doi.org/10.1152/ajpregu.00373.2001

Albertsen M, Hugenholtz P, Skarshewski A, Nielsen KL, Tyson GW, Nielsen PH. Genome sequences of rare, uncultured bacteria obtained by differential coverage binning of multiple metagenomes. Nat Biotechnol. 2013 Jun;31(6):533–538. https://doi.org/10.1038/nbt.2579

Buziassy C, Tribe DE. The synthesis of vitamins in the rumen of sheep. I. The effect of diet on the synthesis of thiamine, riboflavin, and nicotinic acid. Aust J Agr Res. 1960;11(6):989–1001. https://doi.org/10.1071/AR9600989

Bylesjö M, Rantalainen M, Cloarec O, Nicholson JK, Holmes E, Trygg J. OPLS discriminant analysis: combining the strengths of PLS-DA and SIMCA classification. J Chemometrics. 2006;20:341–351. https://doi.org/10.1002/cem.1006

Caporaso JG, Kuczynski J, Stombaugh J, Bittinger K, Bushman FD, Costello EK, Fierer N, Peña AG, Goodrich JK, Gordon JI, et al. QIIME allows analysis of high-throughput community sequencing data. Nat Methods. 2010 May;7(5):335–336. https://doi.org/10.1038/nmeth.f.303

Castillo-Lopez E, Ramirez Ramirez HA, Klopfenstein TJ, Anderson CL, Aluthge ND, Fernando SC, Jenkins T, Kononoff PJ. Effect of feeding dried distillers grains with solubles on ruminal biohydrogenation, intestinal fatty acid profile, and gut microbial diversity evaluated through DNA pyro-sequencing. J Anim Sci. 2014 Feb;92(2):733–743. https://doi.org/10.2527/jas.2013-7223

DeGregorio RM, Tucker RE, Mitchell GE Jr, Gill WW. Carbohydrate fermentation in the large intestine of lambs. J Anim Sci. 1982 Apr;54(4):855–862. https://doi.org/10.2527/jas1982.544855x

Di Rienzi SC, Sharon I, Wrighton KC, Koren O, Hug LA, Thomas BC, Goodrich JK, Bell JT, Spector TD, Banfield JF, et al. The human gut and groundwater harbor non-photosynthetic bacteria belonging to a new candidate phylum sibling to Cyanobacteria. Elife. 2013 Oct 1;2:e01102. https://doi.org/10.7554/eLife.01102

Edgar RC. Search and clustering orders of magnitude faster than BLAST. Bioinformatics. 2010 Oct 1;26(19):2460–2461. https://doi.org/10.1093/bioinformatics/btq461

Faichney GJ. Production of volatile fatty acids in the sheep caecum. Aust J Agr Res. 1969;20(3):491–498. https://doi.org/10.1071/AR9690491

Flint HJ, Bayer EA. Plant cell wall breakdown by anaerobic microorganisms from the Mammalian digestive tract. Ann N Y Acad Sci. 2008 Mar;1125:280–288.
https://doi.org/10.1196/annals.1419.022

Flint HJ, Duncan SH, Scott KP, Louis P. Interactions and competition within the microbial community of the human colon: links between diet and health. Environ Microbiol. 2007 May;9(5):1101–1111.
https://doi.org/10.1111/j.1462-2920.2007.01281.x

Heath TJ, Morris B. The absorption of fat in sheep and lambs. Q J Exp Physiol Cogn Med Sci. 1962 Apr;47:157–169.
https://doi.org/10.1113/expphysiol.1962.sp001587

Hernandez-Sanabria E, Goonewardene LA, Wang Z, Zhou M, Moore SS, Guan LL. Influence of sire breed on the interplay among rumen microbial populations inhabiting the rumen liquid of the progeny in beef cattle. PLoS One. 2013;8(3):e58461.
https://doi.org/10.1371/journal.pone.0058461

Hook SE, Steele MA, Northwood KS, Dijkstra J, France J, Wright AD, McBride BW. Impact of subacute ruminal acidosis (SARA) adaptation and recovery on the density and diversity of bacteria in the rumen of dairy cows. FEMS Microbiol Ecol. 2011 Nov;78(2):275–284.
https://doi.org/10.1111/j.1574-6941.2011.01154.x

Hristov AN. Comparative characterization of reticular and duodenal digesta and possibilities of estimating microbial outflow from the rumen based on reticular sampling in dairy cows. J Anim Sci. 2007 Oct;85(10):2606–2613.
https://doi.org/10.2527/jas.2006-852

Jiao J, Wang T, Zhou J, Degen AA, Gou N, Li S, Bai Y, Jing X, Wang W, Shang Z. Carcass parameters and meat quality of Tibetan sheep and Small-tailed Han sheep consuming diets of low-protein content and different energy yields. J Anim Physiol Anim Nutr (Berl). 2020 Jul;104(4):1010–1023.
https://doi.org/10.1111/jpn.13298

Koenig KM, Rode LM, Cohen RD, Buckley WT. Effects of diet and chemical form of selenium on selenium metabolism in sheep. J Anim Sci. 1997 Mar;75(3):817–827. https://doi.org/10.2527/1997.753817x

Krajmalnik-Brown R, Ilhan ZE, Kang DW, DiBaise JK. Effects of gut microbes on nutrient absorption and energy regulation. Nutr Clin Pract. 2012 Apr;27(2):201–214.
https://doi.org/10.1177/0884533611436116

Leahy SC, Kelly WJ, Altermann E, Ronimus RS, Yeoman CJ, Pacheco DM, Li D, Kong Z, McTavish S, Sang C, et al. The genome sequence of the rumen methanogen *Methanobrevibacter ruminantium* reveals new possibilities for controlling ruminant methane emissions. PLoS One. 2010 Jan 28;5(1):e8926.
https://doi.org/10.1371/journal.pone.0008926

Lewis SM, Dehority BA. Microbiology and ration digestibility in the hindgut of the ovine. Appl Environ Microbiol. 1985 Aug;50(2):356–363. https://doi.org/10.1128/AEM.50.2.356-363

Ley RE, Turnbaugh PJ, Klein S, Gordon JI. Microbial ecology: human gut microbes associated with obesity. Nature. 2006 Dec 21;444(7122):1022–1023. https://doi.org/10.1038/4441022a

Liesack W, König H, Schlesner H, Hirsch P. Chemical composition of the peptidoglycan-free cell envelopes of budding bacteria of the *Pirella/Planctomyces* group. Arch Microbiol. 1986;145:361–366.
https://doi.org/10.1007/BF00470872

Looney SW, Hagan JL. 4 statistical methods for assessing biomarkers and analyzing biomarker data. In: Rao CR, Miller JP, Rao DC, editors. Handbook of statistics. Amsterdam (The Netherlands): Elsevier; 2007;27. p.109–147.
https://doi.org/10.1016/S0169-7161(07)27004-X

Lozupone C, Knight R. UniFrac: a new phylogenetic method for comparing microbial communities. Appl Environ Microbiol. 2005 Dec;71(12):8228–8235.
https://doi.org/10.1128/AEM.71.12.8228-8235.2005

McCann JC, Elolimy AA, Loor JJ. Rumen microbiome, probiotics, and fermentation additives. Vet Clin North Am Food Anim Pract. 2017 Nov;33(3):539–553.
https://doi.org/10.1016/j.cvfa.2017.06.009

Merchen NR, Firkins JL, Berger LL. Effect of intake and forage level on ruminal turnover rates, bacterial protein synthesis and duodenal amino acid flows in sheep. J Anim Sci. 1986 Jan;62(1):216–225.
https://doi.org/10.2527/jas1986.621216x

Muroya S, Oe M, Ojima K, Watanabe A. Metabolomic approach to key metabolites characterizing postmortem aged loin muscle of Japanese Black (Wagyu) cattle. Asian-Australas J Anim Sci. 2019 Aug;32(8):1172–1185.
https://doi.org/10.5713/ajas.18.0648

National Research Council. Nutrient requirements of small ruminants: sheep, goats, cervids, and New World camelids. Washington (USA): The National Academies Press; 2007.
https://doi.org/10.17226/11654

Palomba A, Tanca A, Fraumene C, Abbondio M, Fancello F, Atzori AS, Uzzau S. Multi-omic biogeography of the gastrointestinal microbiota of a pre-weaned lamb. Proteomes. 2017 Dec 18; 5(4):36.
https://doi.org/10.3390/proteomes5040036

Paz HA, Castillo-Lopez E, Ramirez-Ramirez HA, Christensen DA, Kononoff PJ. Invited review: Ethanol co-products for dairy cows: there goes our starch … now what? Can J Anim Sci. 2013;93(4):407–425.
https://doi.org/10.4141/cjas2013-048

Purchas RW, Rutherfurd SM, Pearce PD, Vather R, Wilkinson BH. Concentrations in beef and lamb of taurine, carnosine, coenzyme Q(10), and creatine. Meat Sci. 2004 Mar;66(3):629–637.
https://doi.org/10.1016/S0309-1740(03)00181-5

Qin J, Li R, Raes J, Arumugam M, Burgdorf KS, Manichanh C, Nielsen T, Pons N, Levenez F, Yamada T, et al. A human gut microbial gene catalogue established by metagenomic sequencing. Nature. 2010 Mar 4;464(7285):59–65. https://doi.org/10.1038/nature08821

Quast C, Pruesse E, Yilmaz P, Gerken J, Schweer T, Yarza P, Peplies J, Glöckner FO. The SILVA ribosomal RNA gene database project: improved data processing and web-based tools. Nucleic Acids Res. 2013 Jan;41(Database issue):D590–D596.
https://doi.org/10.1093/nar/gks1219

Ramirez Ramirez HAR, Nestor K, Tedeschi LO, Callaway TR, Dowd SE, Fernando SC, Kononoff PJ. The effect of brown midrib corn silage and dried distillers' grains with solubles on milk production, nitrogen utilization and microbial community structure in dairy cows. Can J Anim Sci. 2012; 92(3):365–380.
https://doi.org/10.4141/cjas2011-133

Reynaert R, De Paepe M, Marcus S, Peeters G. Influence of serum free fatty acid levels on growth hormone secretion in lactating cows. J Endocrinol. 1975 Aug;66(2):213–224.
https://doi.org/10.1677/joe.0.0660213

Sartin JL, Bartol FF, Kemppainen RJ, Dieberg G, Buxton D, Soyoola E. Modulation of growth hormone-releasing factor stimulated growth hormone secretion by plasma glucose and free fatty acid concentrations in sheep. Neuroendocrinology. 1988 Dec; 48(6): 627–633. https://doi.org/10.1159/000125073

Schloss PD, Westcott SL, Ryabin T, Hall JR, Hartmann M, Hollister EB, Lesniewski RA, Oakley BB, Parks DH, Robinson CJ, et al. Introducing Mothur: open-source, platform-independent, community-supported software for describing and comparing microbial communities. Appl Environ Microbiol. 2009 Dec;75(23):7537–7541.
https://doi.org/10.1128/AEM.01541-09

Sirohi SK, Singh N, Dagar SS, Puniya AK. Molecular tools for deciphering the microbial community structure and diversity in rumen ecosystem. Appl Microbiol Biotechnol. 2012 Sep;95(5):1135–1154.
https://doi.org/10.1007/s00253-012-4262-2

Stevenson DM, Weimer PJ. Dominance of *Prevotella* and low abundance of classical ruminal bacterial species in the bovine rumen

revealed by relative quantification real-time PCR. Appl Microbiol Biotechnol. 2007 May;75(1):165–174. https://doi.org/10.1007/s00253-006-0802-y

Tonsbeek CHT, Plancken AJ, Weerdhof TVD. Components contributing to beef flavor. Isolation of 4-hydroxy-5-methyl-3(2H)-furanone and its 2,5-dimethyl homolog from beef broth. J Agr Food Chem. 1968;16(6):1016–1021 https://doi.org/10.1021/jf60160a008

Ussar S, Fujisaka S, Kahn CR. Interactions between host genetics and gut microbiome in diabetes and metabolic syndrome. Mol Metab. 2016 Jul 18;5(9):795–803. https://doi.org/10.1016/j.molmet.2016.07.004

Waghorn GC, Shelton ID, Sinclair BR. Distribution of elements between solid and supernatant fractions of digesta in sheep given six diets. New Zeal J Agr Res. 1990;33(2):259–269. https://doi.org/10.1080/00288233.1990.10428418

Walker ND, McEwan NR, Wallace RJ. A pepD-like peptidase from the ruminal bacterium, *Prevotella albensis*. FEMS Microbiol Lett. 2005 Feb 15;243(2):399–404. https://doi.org/10.1016/j.femsle.2004.12.032

Wang J, Fan H, Han Y, Zhao J, Zhou Z. Characterization of the microbial communities along the gastrointestinal tract of sheep by 454 pyrosequencing analysis. Asian-Australas J Anim Sci. 2017 Jan; 30(1):100–110. https://doi.org/10.5713/ajas.16.0166

Wang Q, Wang Y, Wang X, Dai C, Tang W, Li J, Huang P, Li Y, Ding X, Huang J, et al. Effects of dietary energy levels on rumen fermentation, microbiota, and gastrointestinal morphology in growing ewes. Food Sci Nutr. 2020 Nov 10;8(12):6621–6632. https://doi.org/10.1002/fsn3.1955

Weenen H, Kerler J, van der Ven JGM. The Maillard reaction in flavour formation. In: Swift KAD, editor. Flavours and fragrances. Woodhead Publishing Series in Food Science, Technology and Nutrition. Cambridge (England): Woodhead Publishing; 2005. p. 153–170. https://doi.org/10.1533/9781845698249.3.153

Wu J, Yang D, Gong H, Qi Y, Sun H, Liu Y, Liu Y, Qiu X. Multiple omics analysis reveals that high fiber diets promote gluconeogenesis and inhibit glycolysis in muscle. BMC Genomics. 2020 Sep 24;21(1):660. https://doi.org/10.1186/s12864-020-07048-1

Xu X, Xu P, Ma C, Tang J, Zhang X. Gut microbiota, host health, and polysaccharides. Biotechnol Adv. 2013 Mar-Apr;31(2):318–37. https://doi.org/10.1016/j.biotechadv.2012.12.009

Zhang R, Zhu W, Zhu W, Liu J, Mao S. Effect of dietary forage sources on rumen microbiota, rumen fermentation and biogenic amines in dairy cows. J Sci Food Agric. 2014 Jul;94(9):1886–1895. https://doi.org/10.1002/jsfa.6508

Zhen J, Yan S, Li Y, Ruan C, Li Y, Li X, Zhao X, Lv X, Ge Y, Moure UAE, et al. L-Alanine specifically potentiates fluoroquinolone efficacy against *Mycobacterium* persisters via increased intracellular reactive oxygen species. Appl Microbiol Biotechnol. 2020 Mar;104(5):2137–2147. https://doi.org/10.1007/s00253-020-10358-9

Genomic Analysis of the Mycoparasite *Pestalotiopsis* sp. PG52

DENGYUN ZHANG[1] , JINDE YU[1], CHANGLE MA[2], LEI KONG[1], CHENGZHONG HE[1*] and JING LI[1*]

[1] College of Life Science, Southwest Forestry University, Kunming, China
[2] School of Landscape Architecture and Horticulture Science, Southwest Forestry University, Kunming, China

Abstract

Pestalotiopsis sp. is a mycoparasite of the plant pathogen *Aecidium wenshanense*. To further understand the mycoparasitism mechanism of *Pestalotiopsis* sp., we assembled and analyzed its genome. The genome of *Pestalotiopsis* sp. strain PG52 was assembled into 335 scaffolds and had a size of 58.01 Mb. A total of 20,023 predicted genes and proteins were annotated. This study compared PG52 with the mycoparasites *Trichoderma harzianum*, *Trichoderma atroviride,* and *Trichoderma virens*. This study reveals the entirely different mycoparasitism mechanism of *Pestalotiopsis* compared to *Trichoderma* and reveals this mycoparasite's strong ability to produce secondary metabolites.

K e y w o r d s: genome, DNA sequencing, *Pestalotiopsis* sp., mycoparasite

Introduction

Pestalotiopsis sp. is a mitosporic fungus with spore-forming conidia. This fungus has a wide distribution and a variety of life habits, including pathogenicity (Wang et al. 2019), saprophytic (Zi 2015), and endophytic characteristics (Tanapichatsakul et al. 2019; Liao et al. 2020). It is an important plant pathogen and an asexual fungus with specific economic value (Taylor et al. 2001). The types of compounds isolated from *Pestalotiopsis* in recent years include alkaloids, polyols, cyclic peptides, terpenes, isocoumarins, coumarins, quinones, semiquinones, chromones, simple phenols, phenolic acids, esters, and other novel compounds (Yang et al. 2012; Xie et al. 2015). Many of these compounds have important application prospects. Among the reported *Pestalotiopsis* species, most are pathogens, saprophytes, or endophytes, but there has been little research on the mycoparasitism of these species.

Mycoparasitism is the most critical form of antagonism involving direct physical contact with the host mycelium (Pal et al. 2006). It involves typical growth of biocontrol fungal mycelia toward the target pathogen followed by extensive coiling and secretion of various hydrolytic enzymes, leading to the dissolution of the pathogen's cell wall or membrane. This mycoparasitism is common among *Trichoderma*. However, the mycoparasitism of *Pestalotiopsis* species is utterly different from that of *Trichoderma* based on microscopic observation. The aeciospores' outer walls appear deformed and completely broken after treatment with *Trichoderma* (Li et al. 2014). *Pestalotiopsis* concentrates the contents of rust spores by producing toxins, and the cell walls sag inward. The contents of the affected rust spores are concentrated, and most of the spores are empty shells (Li et al. 2017).

Mycoparasitic *Pestalotiopsis* species produce secondary metabolites different from those of endophytic or pathogenic *Pestalotiopsis* species (Xie et al. 2015), and these species have yet to be developed and used as important fungal resources. Both the lifestyle and secondary metabolite richness of mycoparasitic fungi are not comprehensively understood. In this study, the genome of the mycoparasite *Pestalotiopsis* sp. PG52 isolated from *Aecidium wenshanense* was sequenced and annotated. A large set of genes involved in secondary metabolism was identified. The purpose of this research was to investigate the possible mechanisms of mycoparasitism, potential active secondary substances (antifungal or antibacterial substances), and gene resources for resistance breeding against fungal diseases using genomic sequencing.

* Corresponding authors: Ch. He, College of Life Science, Southwest Forestry University, Kunming, China; **e-mail:hcz70@163.com**
  J. Li, College of Life Science, Southwest Forestry University, Kunming, Yunnan, China; **e-mail: lijingcas@163.com**

Experimental

Materials and Methods

Microbial material. The aeciospores of *A. wenshanense* were collected in Kunming, Yunnan Province, People's Republic of China, in September 2012. The species was mistakenly identified as *Aecidium pourthiaea* Syd. (Cai and Wu 2008) and has been corrected to *A. wenshanense* (Zhuang and Wei 2016; Zhu et al. 2020). The aeciospores were incubated on distilled filter paper at 25°C and cultured until mycelium or colony formation was observed. After being cultured for approximately one week, strain PG52 was isolated from the aeciospores, identified as *Pestalotiopsis kenyana* (Sui et al. 2020), and preserved at Southwest Forest University, Kunming, China.

Mycelial sample preparation. The conidia of *Pestalotiopsis* sp. PG52 were cultured on modified Fries culture agar. After incubation at room temperature for three days, the mycelium was carefully scraped off and stored in liquid nitrogen for later use.

DNA extraction and WGS library construction. *Pestalotiopsis* sp. PG52 DNA was extracted using a TIANGEN (Tiangen, Beijing, China) Bacterial Genomic DNA Extraction Kit and sheared into fragments between 100 and 800 bp in size by a Covaris E220 ultrasonicator (Covaris, Brighton, UK). High-quality DNA was selected using AMPure XP beads (Agencourt, Beverly, MA, USA). After repair using T4 DNA polymerase (Enzymatics, Beverly, MA, USA), the selected fragments were ligated at both ends to T-tailed adapters and amplified using KAPA HiFi HotStart ReadyMix (Kapa Biosystems, Wilmington, NC, USA). Then, amplification products were subjected to a single-strand circularization process using T4 DNA ligase (Enzymatics) to generate a single-stranded circular DNA library.

Genome sequencing and assembly. The NGS library was loaded and sequenced on the BGISEQ-500 platform. Raw data are available in the GenBank. The raw reads with a high proportion of Ns (ambiguous bases) and low-quality bases were filtered out using SOAPnuke (v1.5.6) (Chen et al. 2018) with the parameters "-l 15 -q 0.2 -n 0.05 -Q 2 -c 0". Then, the clean NGS ("Next-generation" sequencing technology) data were assembled using Canu (Koren et al. 2017) with the parameters "-useGrid = false maxThreads = 30 maxMemory = 60 g -nanopore-raw *.fastq -p -d". BUSCO (v3.0.1) was used to assess the confidence of the assembly with *Pestalotiopsis* sp. PG52.

Identification of Repetitive Elements and Non-Coding RNA Genes. Repetitive sequences were identified using multiple tools. TEs were identified by aligning against the Repbase (Bao et al. 2015) database using RepeatMasker (v4.0.5) (Tarailo-Graovac and Chen 2009) with parameters "-nolow -no_is -norna -engine wublast" and RepeatProteinMasker (v4.0.5) with parameters "-noLowSimple -pvalue 0.0001" at DNA and protein levels respectively. Meanwhile, the de novo repeat library was detected using RepeatModeler (v1.0.8) and LTR-FINDER (v1.0.6) (Xu and Wang 2007) with default parameters. Based on the de novo identified repeats, repeat elements were classified using RepeatMasker (v4.0.5) (Tarailo-Graovac and Chen 2009) with the same parameters. Furthermore, the tandem repeats were identified using Tandem Repeat Finder (v4.07) (Benson 1999) with parameters "-Match 2 -Mismatch 7 -Delta 7 -PM 80 -PI 10 -Minscore 50 -MaxPeriod 2000".

For non-coding RNA (ncRNA), the tRNA genes were predicted using tRNAscan-SE (v1.3.1) (Lowe and Eddy 1997) with default parameters. The rRNA fragments were identified using RNAmmer (v1.2). The snRNA and miRNA genes were predicted using CMsearch (v1.1.1) (Cui et al. 2016) with default parameters after aligning against the Rfam database (Kalvari et al. 2018) with a blast (v2.2.30).

Gene prediction and genome annotation. The predicted genes were aligned to the KEGG (Kanehisa 1997; Kanehisa et al. 2004; Kanehisa et al. 2006), Swiss-Prot (Magrane and UniProt Consortium 2011), COG (Tatusov et al. 1997; 2003), CAZy (Cantarel et al. 2009), NR and GO (Ashburner et al. 2000) databases using blastall (v2.2.26) (Altschul et al. 1990) with the parameters "-p blastp -e 1e-5 -F F -a 4 -m 8". The *Pestalotiopsis* sp. PG52 assembly was uploaded to the antiSMASH (v5.0) (Medema et al. 2011) website to identify the secondary metabolite gene cluster.

Transcriptome analysis. In order to define secondary metabolite clusters using transcriptional data, *Pestalotiopsis* sp. PG52 was inoculated on modified Fries medium for experiment. Abundant secondary metabolites were detected in the study. Total RNA was extracted from tissue samples. The mRNA was purified and then reverse transcribed into cDNA, and the library was constructed according to the large-scale parallel signature scheme. They were then sequenced using Illumina's technology. The genomic annotation results were compared with transcriptome data, and if mRNA of a gene was detected, the gene was considered to be expressed.

Results

***Pestalotiopsis* sp. PG52 genome extraction and quality inspection.** The quality and concentration of the extracted *Pestalotiopsis* sp. PG52 genomic DNA were measured using a Qubit fluorometer, and then the DNA was subjected to 1% agarose gel electrophoresis. The sample volume was 1 µl. The test results are shown in Fig. 1 and indicate that the extracted genomic DNA had
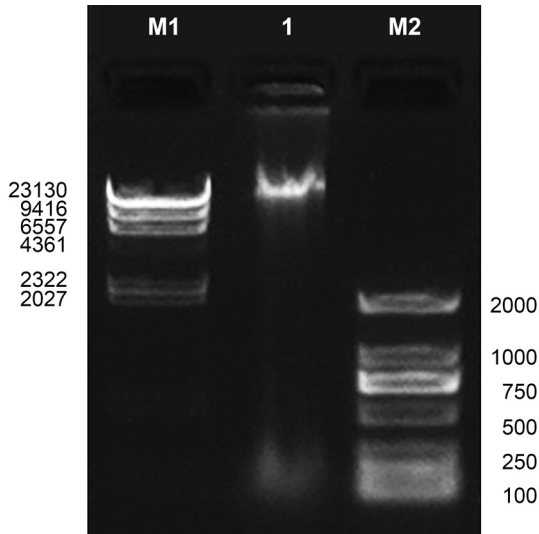
Fig. 1. Electrophoresis pattern of *Pestalotiopsis kenyana* PG52 genome. Agarose concentration (%): 1; voltage: 180 V; time: 35 min.; molecular weight standard name: M1: λ-Hind III digest (Takara), M2: D2000 (Tiangen); sample volume: M1: 3 μl, M2: 6 μl.

good integrity. BD Image Lab software was used to calculate the amounts of DNA in the electrophoresis image. The total amount of DNA in the samples was 3.78 μg, which meets the requirements for library construction and sequencing; this amount could meet the requirements for two or more samples for library construction.

Genomic sequencing quality analysis. Fqcheck software was used to evaluate the quality of the data. Fig. 2 and 3 show the base composition and quality of PG52.

The slight fluctuation at the beginning of the curve is typical of the BGI-seq 500 sequencing platform and does not affect the data. Normally, the distribution curves of the A and T and the C and G bases should coincide with each other. If an abnormality occurs in the sequencing process, it may cause abnormal fluctuations in the middle of the curve. If a particular library construction method or library is used, the base distribution may also be changed (Fig. 2).

The base quality distribution reflects the accuracy of the sequencing reads. The sequencer, sequencing reagents, and sample quality can all affect base quality. Overall, the low-quality (< 20) base proportion was low, indicating that the sequencing quality of the lane was relatively good (Fig. 3).

Genome assembly and gene prediction. The long fragment of *Pestalotiopsis* sp. PG52 was sequenced on the Nanopore platform, and a total of 12.18 Gb of data was generated. Before assembly, k-mer was selected as 15, and k-mer analysis was performed based on the second-generation data to estimate the genome's size (assembly results indicate the true genome size), degree of heterozygosity, and repeatability. Using Jellyfish software to process the filtered data, the results showed that the genome size of the PG52 strain was 50.7 Mb. We used Canu to assemble the Nanopore data and then with Pilon used the second-generation data for base error correction to obtain the final assembly result. BUSCO integrity assessment was conducted using the genome database (SordariomycetA_ODB9). More than 97.0% of core genes could be annotated in the genome, reflecting the high integrity of assembly results. A total of 335 scaffolds were assembled by genome stitching. The genome size was 58.01 Mbp, and the values of N50 and N90 were 6,598,051 bp and 55,791 bp, respectively. The entire genome's size was larger than those of the *Pestalotiopsis fici* (51.91 Mbp), *Pestalotiopsis* sp. JCM 9685 (48.23 Mbp) and *Pestalotiopsis* sp. NC0098 (46.41 Mbp) genomes, which have been sequenced.
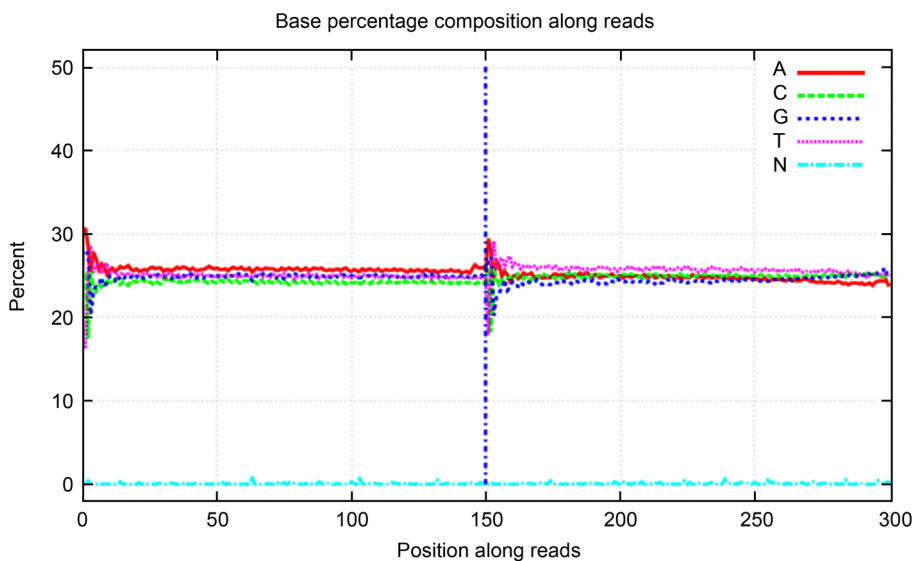

Fig. 2. *Pestalotiopsis kenyana* PG52 base composition distribution map. The X axis represents the position on reads, and the Y axis represents the percentage of bases.
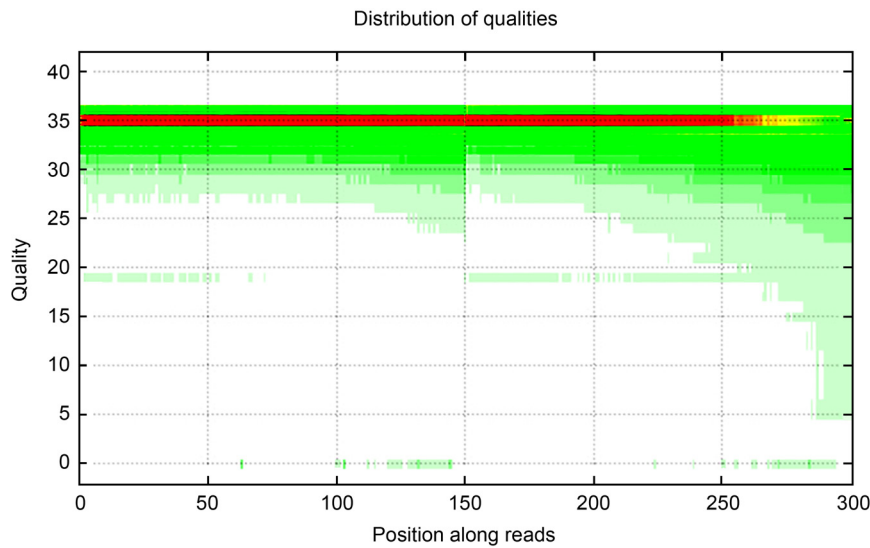
Fig. 3. *Pestalotiopsis kenyana* PG52 base mass distribution map. The X axis is the position of the base in reads, and the Y axis is the base quality value. Each point in the figure represents the total number of bases at this position that reach a certain.

A total of 20,023 genes were predicted in the *Pestalotiopsis* sp. PG52 genome, with an average length of 1,714.03 bp, an average CDS length of 1,478.29 bp, an average of 3.13 exons per gene, an average exon length of 472.00 bp, and an average intron length of 110.57 bp. The reported average length of the predicted genes of *P. fici* (Wang et al. 2015) is 1,683.88 bp, and the average number of exons contained in each gene is 3. Another reported average length of the predicted genes of *Pestalotiopsis* sp. NC0098 is 1864 bp, and the average number of exons contained in each gene is 2.83. The above comparison results indicate the reliability of the sequencing data for the *Pestalotiopsis* sp. PG52 genome and the similarity to the other two *Pestalotiopsis* strain genomes (Table I).

Gene prediction and functional annotation. The NCBI NR database was used to annotate the predicted genes, with a total of 17,500 genes annotated (accounting for 87.40% of the total predicted genes), and the KEGG database was used to annotate the predicted genes, with a total of 11,847 genes annotated (account-

ing for 59.17% of the total predicted genes). Using the GO database to annotate the predicted genes, a total of 10,454 genes were annotated (accounting for 52.21% of the total predicted genes).

KEGG (Kyoto Encyclopedia of Genes and Genomes). KEGG enrichment analysis showed that 11,847 genes that corresponded to KEGG pathways were enriched in 129 metabolic pathways, and most of these genes were involved in metabolic pathways (ko01100) (4,306 genes), biosynthesis of secondary metabolites (ko01110) (1,677 genes), biosynthesis of antibiotics (ko01130) (1,267 genes) and biosynthesis of amino acids (ko01230) (495 genes) (Fig. 4).

GO (Gene Ontology). A total of 10,454 genes can be used to extract GO annotation information with Blast2GO. Based on function, the genes can be divided into three subcategories, namely, biological process (25 branches), cellular component (14 branches) and molecular function (13 branches), with a total of 52 branches (Fig. 5: 1 – metabolic process, 2 – cellular process, 3 – localization, 4 – biological regulation, 5 – cellular component organization or biogenesis, 6 – regulation of biological process, 7 – response to stimulus, 8 – signaling, 9 – negative regulation of biological process, 10 – positive regulation of biological process, 11 – reproduction, 12 – reproductive process, 13 – developmental process, 14 – multi-organism process, 15 – growth, 16 – biological adhesion, 17 – detoxification, 18 – nitrogen utilization, 19 – cell aggregation, 20 – carbon utilization, 21 – biological phase, 22 – cell proliferation, 23 – immune system process, 24 – pigmentation, 25 – rhythmic process, 26 – membrane, 27 – membrane part, 28 – cell, 29 – cell part, 30 – organelle, 31 – macromolecular complex,

Table I
The comparison of *Pestalotiopsis* genome sequences.

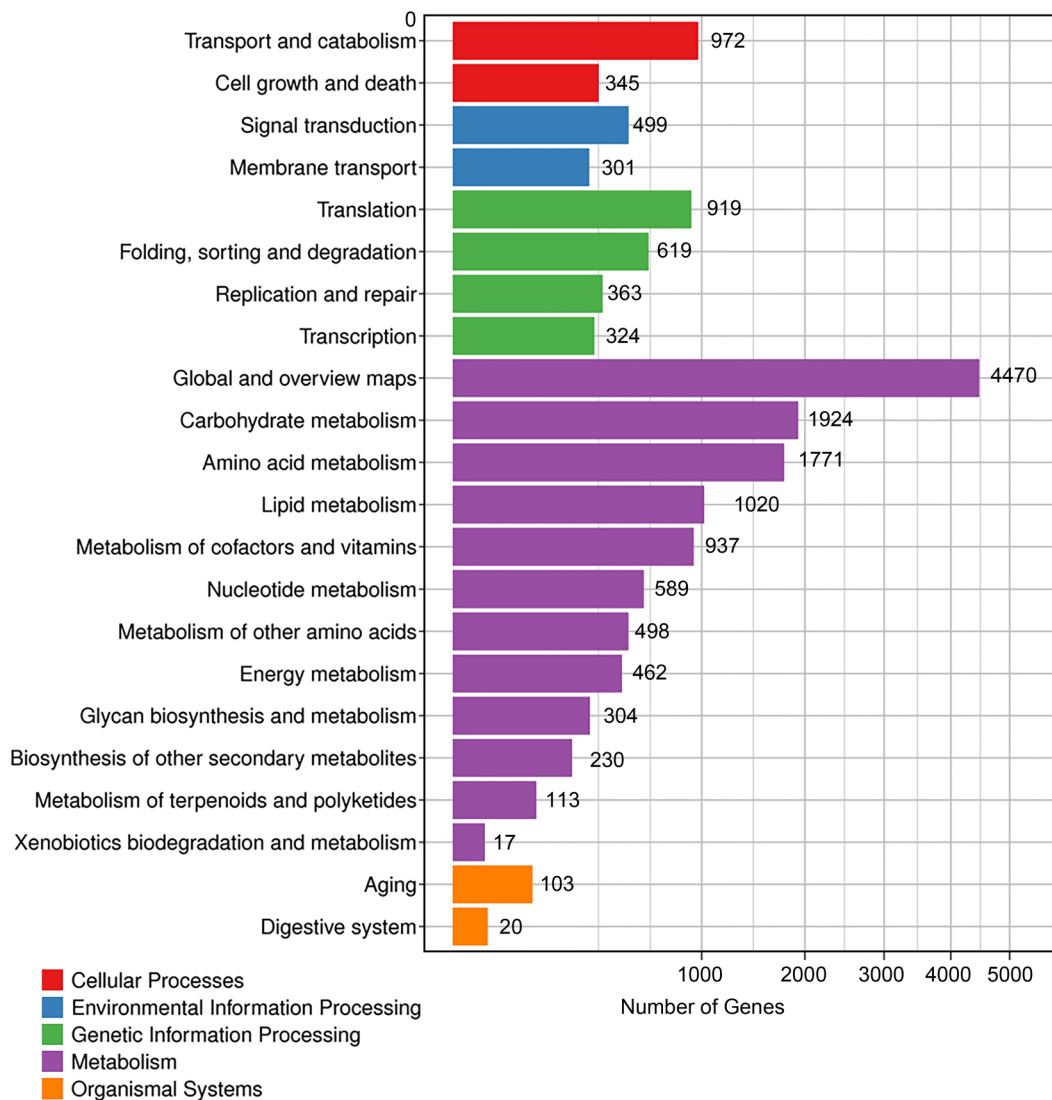|	PG52	FICI	NC0098
Assembly size (Mb)	55	52	46.61
Scaffold N50 (Mb)	6.6	4.0	5
Coverage (fold)	335.0	24.5	24
GC content (%)	53.30	48.73	51.28
Protein-coding genes	20,023	15,413	15,180
Gene density (genes per Mb)	345.22	296.90	327.08
Exons per gene	3.13	2.76	2.83

Fig. 4. KEGG function analysis.

32 – organelle part, 33 – membrane-enclosed lumen, 34 – extracellular region, 35 – supramolecular complex, 36 – virion, 37 – virion part, 38 – nucleoid, 39 – extracellular region part, 40 – catalytic activity, 41 – binding, 42 – transporter activity, 43 – transcription regulator activity, 44 – structural molecule activity, 45 – molecular function regulator, 46 – signal transducer activity, 47 – antioxidant activity, 48 – molecular transducer activity, 49 – molecular carrier activity, 50 – nutrient reservoir activity, 51 – protein tag, 52 – translation regulator activity). Most of the genes in the biological process category are involved in the metabolic processes and cellular processes, most of the genes in the cellular component category are involved in membrane and membrane part, and highest number of the genes in the molecular function category are involved in catalytic activity and binding.

COG (Cluster of Orthologous Groups of proteins). In the COG classification prediction of *Pestalotiopsis* sp. PG52 obtained by sequencing, a total of 8,975 genes were divided into 24 categories. In addition to the general function prediction category, the five categories with the greatest number of genes were amino acid transport and metabolism (905 genes, accounting for 10.08%), energy production and conversion (737 genes, accounting for 8.21%), carbohydrate transport and metabolism (709 genes, accounting for 7.90%), lipid transport and metabolism (657 genes, accounting for 7.32%), and secondary metabolite biosynthesis, transport and catabolism (516 genes, 5.75%) (Fig. 6: A – Cell cycle control, cell division, chromosome partitioning, B – Cell motility, C – Cell wall/membrane/envelope biogenesis, D – Defense mechanisms, E – Extracellular structures, F – Intracellular trafficking, secretion, and vesicular transport, G – Posttranslational modification, protein turnover, chaperones, H – Signal transduction mechanisms, I – Chromatin structure and dynamics, J – Replication, recombination and repair, K – RNA processing and modification, L – Transcription, M – Translation, ribosomal structure
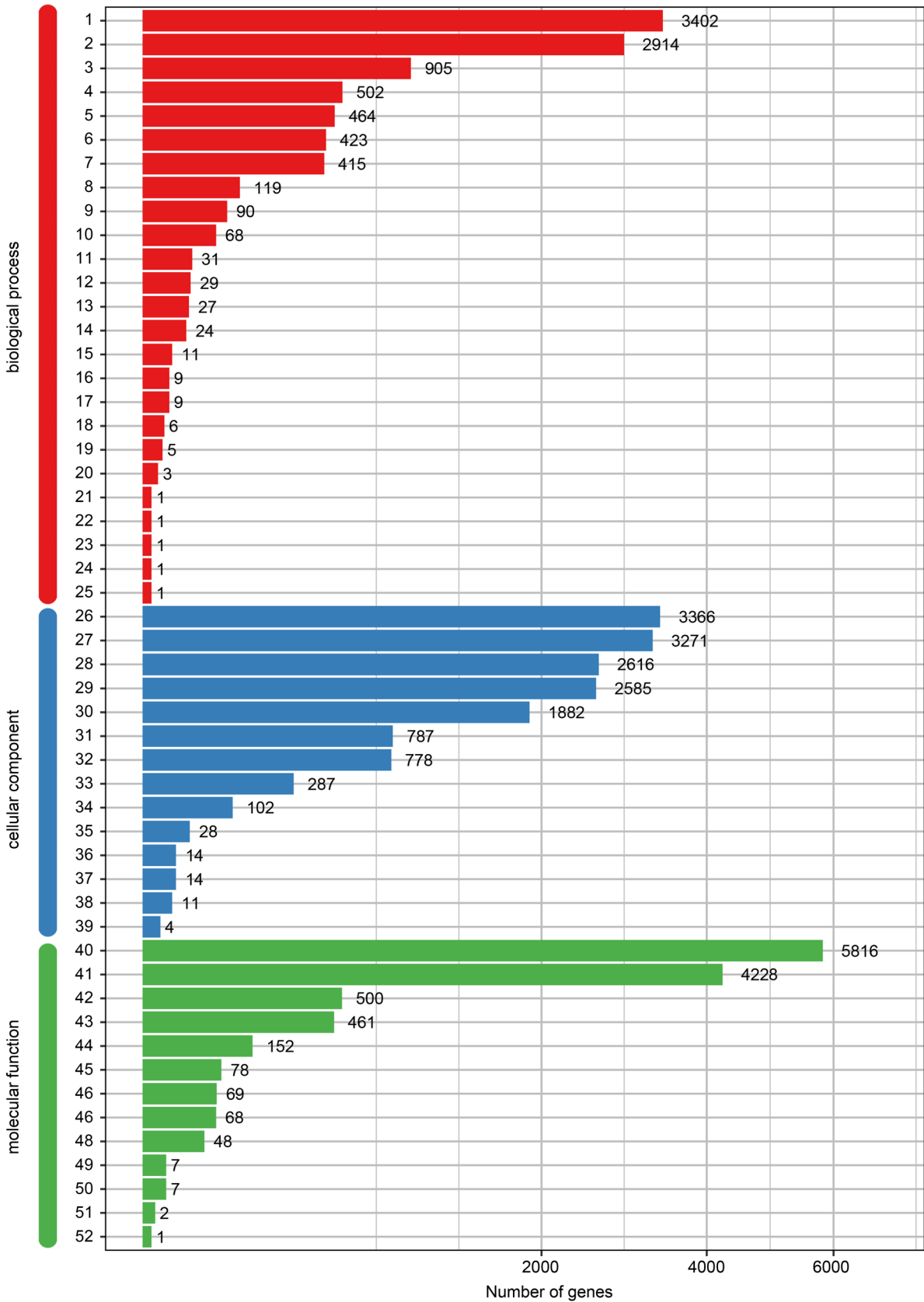
Fig. 5. GO functional classification map of all unigenes with GO annotation.

and biogenesis, N – Amino acid transport and metabolism, O – Carbohydrate transport and metabolism, P – Coenzyme transport and metabolism, Q – Energy production and conversion, R – Inorganic ion transport and metabolism, S – Lipid transport and metabolism, T – Mobilome – rophages, transposons, U – Nucleotide

COG Function Classification (PG52)
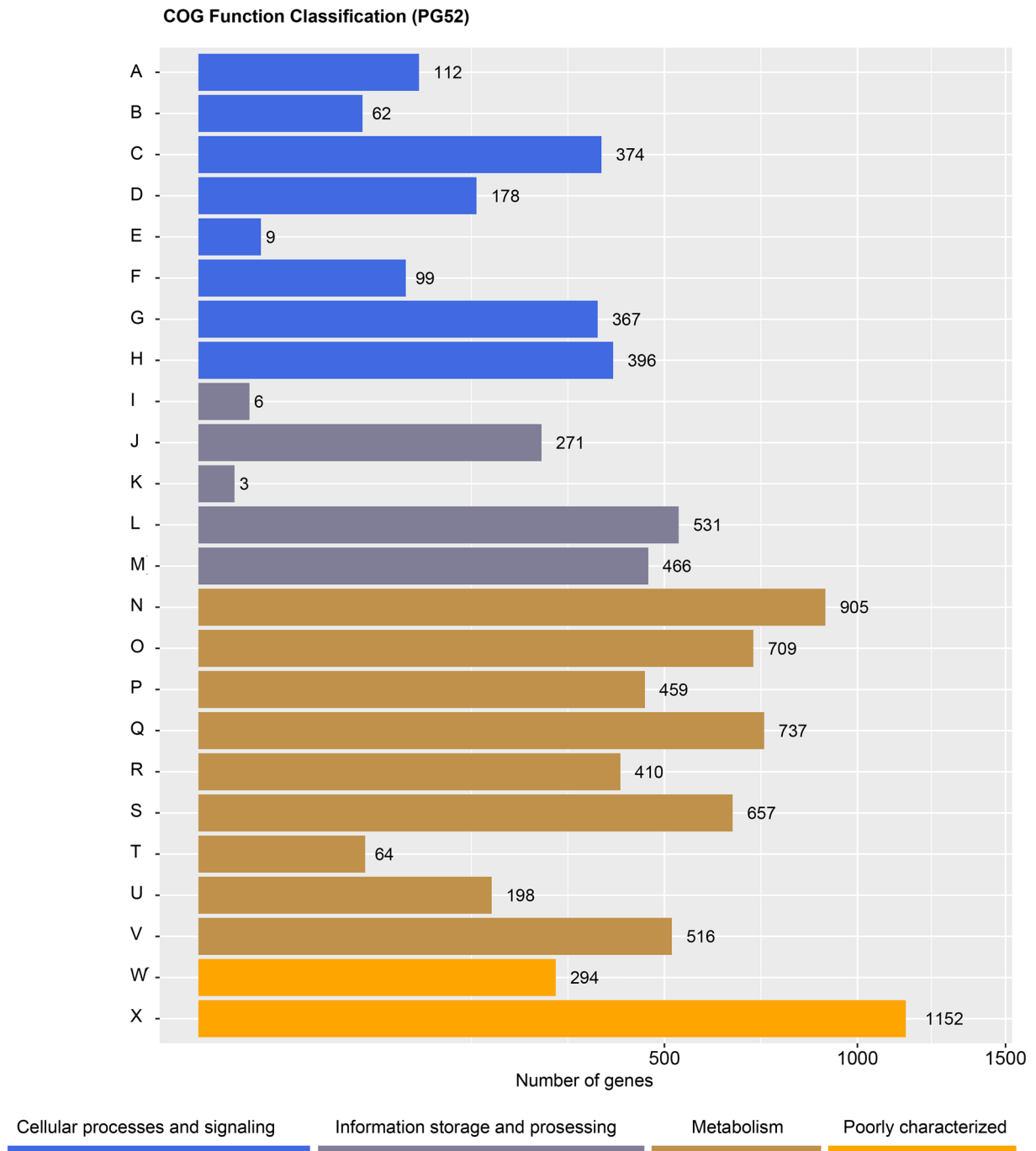
Fig. 6. COG function analysis.

transport and metabolism, V – Secondary metabolites biosynthesis, transport and catabolism, W – Function unknown, X – General function prediction only).

CAZy (Carbohydrate-Active enZYmes) database. Carbohydrate-active enzymes participate in many important biological processes, including cell wall synthesis and signal and energy production, which are related to the fungal nutritional mode and infection mechanism (Zhao et al. 2014). The *Pestalotiopsis* sp. PG52 genome contains 345 hydrolase family genes (GHs), 150 glycosyltransferase family-like genes (GTs), 17 polysaccharide lyase family genes (PLs), 61 carbohy-

drate esterase family genes (CEs) and 196 carbohydrate-binding domain family genes (CBMs).

Further analysis of the GHs of mycoparasites is shown in Table II. *Pestalotiopsis* sp. PG52 has three GH18 and seven GH19 families (mainly chitinase) genes, significantly fewer than the number in the other three mycoparasites. This species contains 31 β-1,3-glucanase genes (GH17, GH55, GH64, and GH81 families), of which the GH55 gene is significantly redundant with those of *Trichoderma harzianum* (Antal et al. 2002; Steindorff et al. 2014; Baroncelli et al. 2015), *Trichoderma atroviride* (Kubicek et al. 2011; Shi-Kunne et al.

Table II
Glycosyl hydrolase families related to mycoparasitic in mycoparasites.

Species	GH18	GH75	GH17	GH55	GH64	GH81
Pestalotiopsis sp. PG52	3	6	7	19	3	2
Trichoderma harzianum	20	4	4	5	3	2
Trichoderma atroviride	29	5	5	8	3	2
Trichoderma virens	36	5	4	10	3	1

Table III
The number of polyketide synthases and nonribosomal peptide synthetases
of *P. fici*, *Pestalotiopsis* sp. NC0098 and mycoparasites.

Secondary metabolites	*Pestalotiopsis* sp. PG52	*P. fici*	*Pestalotiopsis* sp. NC0098	*T. harzianum*	*T. atroviride*	*T. virens*
NRPS	13	12	12	17	16	28
PKS	102	27	21	27	18	18
Total	115	39	33	44	34	46

2015) and *Trichoderma virens* (Kubicek et al. 2011); GH75 family chitosanase has been reported to degrade the host cell wall, and this process was also greatly enhanced (Cuomo et al. 2007). There are six GH75 genes in *Pestalotiopsis* sp. PG52, which is more than the number in the other three mycoparasites. The above results showed that the number of carbohydrate enzymes in *Pestalotiopsis* sp. PG52 is comparable to that of other mycoparasites, but the number of hydrolytic enzymes associated with mycoparasitism is similar to that in *T. harzianum* and lower than in *T. atroviride* and *T. virens*.

Others. The numbers of polyketide synthases (PKSs) and nonribosomal peptide synthetases (NRPSs) in *Pestalotiopsis* sp. PG52, *Pestalotiopsis* sp. NC0098, *P. fici* and *Trichoderma* were compared. The results showed that the total numbers of PKSs and NRPSs from *Pestalotiopsis* sp. NC0098, *P. fici*, *T. virens*, *T. harzianum* and *T. atroviride* were similar but significantly lower than those from *Pestalotiopsis* sp. PG52 (Table III). We compared the number of NRPSs and PKSs in PG52 with that in *Pestalotiopsis* sp. NC0098, *P. fici* and 3 other mycoparasites. The results showed that the total number of the above enzymes in PG52 was much larger than that in *Pestalotiopsis* sp. NC0098, *P. fici* and *Trichoderma*, indicating that there may be more secondary metabolites in mycoparasitic *Pestalotiopsis* species. In

our previous study, four novel PKs were isolated from PG52. Their configurations were identified, and their toxic activities against human tumor cells were tested (Xie et al. 2015). Cytochrome P450 is a kind of multifunctional oxidase that is closely related to secondary metabolism (Črešnar and Petrič 2011). There are 317 cytochrome P450-coding genes in the *Pestalotiopsis* sp. PG52 genome, which is higher than the number reported in *T. harzianum*, *T. atroviride* and *T. virens*. A total of 175 proteases were found in the genome of *Pestalotiopsis* sp. PG52, which is significantly higher than the numbers in the genomes of *T. harzianum*, *T. atroviride* and *T. virens* (Table IV). There are more cytochromes and proteases in PG52 than in the other three *Trichoderma* mycoparasites. In addition, transcription factors (TFs) play a vital role in the fungal regulatory network. A total of 202 transcription factors were found in the genome sequencing results, including 19 genes encoding C2H2-type transcription factors and Zn2/Cys6-type transcription factors. There are 4 Zn2/Cys6-type transcription factor genes, which is significantly less than the number of such genes in *T. atroviride* and *T. virens* (Table IV).

Transcriptome analysis. The whole genome results of the *Pestalotiopsis* sp. PG52 were compared with the transcription group data (Table V), and 82 of the

Table IV
Numbers of P450, protease and Zn2/Cys6 transcription factor genes
of mycoparasites.

	Pestalotiopsis sp. PG52	*T. harzianum*	*T. atroviride*	*T. virens*
Cytochrome P450	317	50	15	40
Zn2/Cys6 transcription factor	4	7	69	95
Protease	175	53	23	28

Genes	Transcription groups	Genome	Expression rate
PKS	82	102	80.39%
NRPS	10	13	76.92%
Protease	137	175	78.29%
Cytochrome P450	245	317	77.29%
Zn2Cys6 transcription factor	1	4	25.00%

102 PKs genes found in the genome were detected in the transcription group with an expression rate of 80.39%. Ten NRPS genes were detected in the transcription group with an expression rate of 76.92%. Protease, Cytochrome P450 and Zn2Cys6 transcription factor have expression rates of 78.29 percent, 77.29 and 25.00 percent, respectively.

Discussion

Long fragments of *Pestalotiopsis* sp. PG52 were sequenced and assembled to obtain the complete genome sequence using BGISEQ-500 and Oxford Nanopore NGS technology, and this sequence was compared with relevant genome-wide information for *P. fici* and *Pestalotiopsis* sp. NC0098. The results showed that the genomes of similar *Pestalotiopsis* species are similar. Genes related to mycoparasitism and secondary metabolism were analyzed and compared with *T. harzianum*, *T. atroviride,* and *T. virens*. The results showed differences in the characteristics of mycoparasites in terms of parasitic ability and secondary metabolism.

In *Pestalotiopsis* sp. PG52, the number of mycoparasitism-related hydrolases, including chitinase (GH18), is less than that in *Trichoderma*, but the total number of β-1,3-glucanases (GH17, GH55, GH64, GH81) is greater than that in *Trichoderma*. All the chitinase genes in *Trichoderma* belong to the GH18 family (Seidl-Seiboth et al. 2014); however, a new chitinase family, GH19, was found in *Pestalotiopsis*; this family is always found in bacteria and higher plants (Suginta et al. 2016). The expression of this gene was also detected in transcriptome data analysis. The number of chitinase genes in *Pestalotiopsis* is far less than that in *Trichoderma* in general, which is consistent with the mycoparasitism characteristics of *Pestalotiopsis* and *Trichoderma*. *Pestalotiopsis* may produce toxins to concentrate the pathogenic bacterial content and generate dents in the cell wall, while *Trichoderma* produces enzymes (mainly chitinase) to destroy the cell wall of the pathogenic bacteria and cause pathogen lysis (Gruber et al. 2011).

A large number of protease genes were detected in the gene annotation results of *Pestalotiopsis* sp. PG52.

There are many proteins containing polysaccharides in the outermost layer of the cell wall of host fungi, and the expression of a large number of proteases in PG52 may enhance its parasitic ability to the host fungi. It has been reported that aspartic acid proteases may be involved in mycoparasitism, and some subtilisin-like serine proteases are homology of *Metarhizium anisopliae* PR1c and are involved in corneous degradation (Hu and Leger 2004, Herrera-Estrella 2014). These findings may be important in the involvement of proteases in the initial stages of mycoparasitism.

Mycoparasites produce secondary metabolites, proteases, and gene transcription regulation factors that are all closely related to mycoparasitism. Polyketide synthases (PKSs) and nonribosomal peptide synthetases (NRPSs) are large multimodular enzymes involved in polyketide and peptide biosynthesis toxins produced by fungi. PKS is a key enzyme that regulates the synthesis of polyketides, mainly catalyzing the synthesis of secondary metabolites and pigments; NRPS can catalyze the synthesis of antimicrobial peptides (Gallo et al. 2013). Cytochrome P450 can catalyze some endogenous substances' biosynthesis with important physiological functions, such as hormones, fatty acids, and terpenoids, and play an important role in the modification of secondary metabolites (Črešnar and Petrič 2011). The higher amount of cytochrome P450 indicates that there may be more types of secondary metabolites in PG52. Some proteins secreted by fungi can play an important role in the process of infecting plant pathogenic fungi, reduce the defense capacity of plant pathogenic fungi and destroy pathogenic fungal cells, but their role in the process of mycoparasitism is still unclear (Mueller et al. 2008; Doehlemann et al. 2009). There are a high number of secreted proteins in the PG52 genome, and these proteins may play an important role in the process of mycoparasitism. Transcription factors can regulate gene expression and participate in fungi's secondary metabolic process (Schoberle et al. 2014). A Zn2/Cys6-type transcription factor found in PG52 can upregulate the β-glucosidase gene expression (Nitta et al. 2012). The number of Zn2/Cys6-type transcription factors in different mycoparasites varies greatly, and further research on this aspect is needed.

In this article, we report for the first time the complete genome information for the mycoparasite *Pestalotiopsis* sp. PG52, identifying a large number of genes related to mycoparasitism. We also show a preliminary comparison and analysis of four mycoparasite genomes, laying the foundation for studying the systematic evolution and revealing the mechanism of mycoparasitism of *Pestalotiopsis*. Additionally, this study provides reference information for genomic research on other filamentous fungi.

ORCID

Dengyun Zhang https://orcid.org/0000-0002-8077-4721

Conflict of interest

The authors do not report any financial or personal connections with other persons or organizations, which might negatively affect the contents of this publication and/or claim authorship rights to this publication.

Literature

Altschul SF, Gish W, Miller W, Myers EW, Lipman DJ. Basic local alignment search tool. J Mol Biol. 1990 Oct;215(3):403–410. https://doi.org/10.1016/S0022-2836(05)80360-2

Antal Z, Manczinger L, Kredics L, Kevei F, Nagy E. Complete DNA sequence and analysis of a mitochondrial plasmid in the mycoparasitic *Trichoderma harzianum* strain T95. Plasmid. 2002 Mar; 47(2):148–152. https://doi.org/10.1006/plas.2001.1559

Ashburner M, Ball CA, Blake JA, Botstein D, Butler H, Cherry JM, Davis AP, Dolinski K, Dwight SS, Eppig JT, et al.; The Gene Ontology Consortium. Gene Ontology: tool for the unification of biology. Nat Genet. 2000 May;25(1):25–29. https://doi.org/10.1038/75556

Bao W, Kojima KK, Kohany O. Repbase Update, a database of repetitive elements in eukaryotic genomes. Mob DNA. 2015 Dec; 6(1):11. https://doi.org/10.1186/s13100-015-0041-9

Baroncelli R, Piaggeschi G, Fiorini L, Bertolini E, Zapparata A, Pè ME, Sarrocco S, Vannacci G. Draft Whole-Genome Sequence of the Biocontrol Agent *Trichoderma harzianum* T6776. Genome Announc. 2015 Jun 25;3(3):e00647–15. https://doi.org/10.1128/genomeA.00647-15

Benson G. Tandem repeats finder: a program to analyze DNA sequences. Nucleic Acids Res. 1999 Jan 01;27(2):573–580. https://doi.org/10.1093/nar/27.2.573

Cai C, Wu JR. Preliminary study on *Aecidium pourthiaea* Syd. of heather rust. North Horticult. 2008;1:208–210.

Cantarel BL, Coutinho PM, Rancurel C, Bernard T, Lombard V, Henrissat B. The Carbohydrate-Active EnZymes database (CAZy): an expert resource for Glycogenomics. Nucleic Acids Res. 2009 Jan 01;37 Database:D233–D238. https://doi.org/10.1093/nar/gkn663

Chen Y, Chen Y, Shi C, Huang Z, Zhang Y, Li S, Li Y, Ye J, Yu C, Li Z, et al. SOAPnuke: a MapReduce acceleration-supported software for integrated quality control and preprocessing of high-throughput sequencing data. Gigascience. 2018 Jan 01;7(1):1–6. https://doi.org/10.1093/gigascience/gix120

Črešnar B, Petrič Š. Cytochrome P450 enzymes in the fungal kingdom. Biochimica et Biophysica Acta (BBA) – Proteins and Proteomics. 2011 Jan;1814(1):29–35. https://doi.org/10.1016/j.bbapap.2010.06.020

Cui X, Lu Z, Wang S, Jing-Yan Wang J, Gao X. CMsearch: simultaneous exploration of protein sequence space and structure space improves not only protein homology detection but also protein structure prediction. Bioinformatics. 2016 Jun 15;32(12):i332–i340. https://doi.org/10.1093/bioinformatics/btw271

Cuomo CA, Güldener U, Xu JR, Trail F, Turgeon BG, Di Pietro A, Walton JD, Ma LJ, Baker SE, Rep M, et al. The *Fusarium graminearum* genome reveals a link between localized polymorphism and pathogen specialization. Science. 2007 Sep 07;317(5843):1400–1402. https://doi.org/10.1126/science.1143708

Doehlemann G, van der Linde K, Aßmann D, Schwammbach D, Hof A, Mohanty A, Jackson D, Kahmann R. Pep1, a secreted effector protein of *Ustilago maydis*, is required for successful invasion of plant cells. PLoS Pathog. 2009 Feb 6;5(2):e1000290–e1000290. https://doi.org/10.1371/journal.ppat.1000290

Gallo A, Ferrara M, Perrone G. Phylogenetic study of polyketide synthases and nonribosomal peptide synthetases involved in the biosynthesis of mycotoxins. Toxins (Basel). 2013 Apr 19;5(4):717–742. https://doi.org/10.3390/toxins5040717

Gruber S, Kubicek CP, Seidl-Seiboth V. Differential regulation of orthologous chitinase genes in mycoparasitic *Trichoderma* species. Appl Environ Microbiol. 2011 Oct;77(20):7217–7226. https://doi.org/10.1128/AEM.06027-11

Herrera-Estrella A. Chapter 33 – Genome-wide approaches toward understanding mycotrophic *Trichoderma* species. In: Gupta VK, Schmoll M, Herrera-Estrella A, Upadhyay RS, Druzhinina I, Tuohy MG, editors. Biotechnology and Biology of *Trichoderma*. Amsterdam (The Netherlands): Elsevier; 2014. p. 455–464. https://doi.org/10.1016/B978-0-444-59576-8.00033-3

Hu G, Leger RJS. A phylogenomic approach to reconstructing the diversification of serine proteases in fungi. J Evol Biol. 2004 Nov;17(6):1204–1214. https://doi.org/10.1111/j.1420-9101.2004.00786.x

Kalvari I, Nawrocki EP, Argasinska J, Quinones-Olvera N, Finn RD, Bateman A, Petrov AI. Non-coding rna analysis using the rfam database. Curr Protoc Bioinformatics. 2018 Jun;62(1):e51. https://doi.org/10.1002/cpbi.51

Kanehisa M, Goto S, Hattori M, Aoki-Kinoshita KF, Itoh M, Kawashima S, Katayama T, Araki M, Hirakawa M. From genomics to chemical genomics: new developments in KEGG. Nucleic Acids Res. 2006 Jan 01;34(90001):D354–D357. https://doi.org/10.1093/nar/gkj102

Kanehisa M, Goto S, Kawashima S, Okuno Y, Hattori M. The KEGG resource for deciphering the genome. Nucleic Acids Res. 2004 Jan 01;32(90001):277D–280. https://doi.org/10.1093/nar/gkh063

Kanehisa M. A database for post-genome analysis. Trends Genet. 1997 Sep;13(9):375–376. https://doi.org/10.1016/S0168-9525(97)01223-7

Koren S, Walenz BP, Berlin K, Miller JR, Bergman NH, Phillippy AM. Canu: scalable and accurate long-read assembly via adaptive *k*-mer weighting and repeat separation. Genome Res. 2017 May;27(5):722–736. https://doi.org/10.1101/gr.215087.116

Kubicek CP, Herrera-Estrella A, Seidl-Seiboth V, Martinez DA, Druzhinina IS, Thon M, Zeilinger S, Casas-Flores S, Horwitz BA, Mukherjee PK, et al. Comparative genome sequence analysis underscores mycoparasitism as the ancestral life style of *Trichoderma*. Genome Biol. 2011 Apr;12(4):R40. https://doi.org/10.1186/gb-2011-12-4-r40

Li J, Xie J, Li XN, Zhou ZF, Liu FL, Chen YH. [Isolation, identification and antimicrobial activity of mycoparasites (*Pestalotiopsis*) from *Aecid-*

ium pourthiaea] (in Chinese). Biotechnol Bull. 2017;33(3):122–127. https://doi.org/10.13560/j.cnki.biotech.bull.1985.2017.03.018

Li J, Yang YH, Zhou L, Cheng LJ, Chen YH. Destructive effects of a mycoparasite *Trichoderma atroviride* SS003 on aeciospores of *Cronartium ribicola*. J Phytopathol. 2014 Jun;162(6):396–401. https://doi.org/10.1111/jph.12202

Liao G, Wu P, Liu Z, Xue J, Li H, Wei X. 2*H*-pyranone and isocoumarin derivatives from the endophytic fungus *Pestalotiopsis microspora* SC3082 derived from *Scaevola taccada* (Gaertn.) Roxb. Nat Prod Res. 2020 Jan 30:1–8. https://doi.org/10.1080/14786419.2020.1719488

Lowe TM, Eddy SR. tRNAscan-SE: a program for improved detection of transfer RNA genes in genomic sequence. Nucleic Acids Res. 1997 Mar 01;25(5):955–964. https://doi.org/10.1093/nar/25.5.955

Magrane M, UniProt Consortium. UniProt Knowledgebase: a hub of integrated protein data. Database (Oxford). 2011 Mar 29; 2011(0): bar009. https://doi.org/10.1093/database/bar009

Medema MH, Blin K, Cimermancic P, de Jager V, Zakrzewski P, Fischbach MA, Weber T, Takano E, Breitling R. antiSMASH: rapid identification, annotation and analysis of secondary metabolite biosynthesis gene clusters in bacterial and fungal genome sequences. Nucleic Acids Res. 2011 Jul 01;39(Web Server issue) suppl_2:W339–W346. https://doi.org/10.1093/nar/gkr466

Mueller O, Kahmann R, Aguilar G, Trejo-Aguilar B, Wu A, de Vries RP. The secretome of the maize pathogen *Ustilago maydis*. Fungal Genet Biol. 2008 Aug;45 Suppl 1:S63–S70. https://doi.org/10.1016/j.fgb.2008.03.012

Nitta M, Furukawa T, Shida Y, Mori K, Kuhara S, Morikawa Y, Ogasawara W. A new Zn(II)2Cys6-type transcription factor BglR regulates *β-glucosidase* expression in *Trichoderma reesei*. Fungal Genet Biol. 2012 May;49(5):388–397. https://doi.org/10.1016/j.fgb.2012.02.009

Pal KK, Scholar V, Gardener BBM. Biological Control of Plant Pathogens. Plant Health Instructor. 2006. https://doi.org/10.1094/phi-a-2006-1117-02

Schoberle TJ, Nguyen-Coleman CK, Herold J, Yang A, Weirauch M, Hughes TR, McMurray JS, May GS. A novel C_2H_2 transcription factor that regulates *gliA* expression interdependently with GliZ in *Aspergillus fumigatus*. PLoS Genet. 2014 May 1;10(5): e1004336. https://doi.org/10.1371/journal.pgen.1004336

Seidl-Seiboth V, Ihrmark K, Druzhinina I, Karlsson M. Chapter 5 – Molecular Evolution of *Trichoderma* Chitinases. In: Gupta VK, Schmoll M, Herrera-Estrella A, Upadhyay RS, Druzhinina I, Tuohy MG, editors. Biotechnology and Biology of *Trichoderma*. Amsterdam (The Netherlands): Elsevier; 2014. p. 67–78. https://doi.org/10.1016/B978-0-444-59576-8.00005-9

Shi-Kunne X, Seidl MF, Faino L, Thomma BPHJ. Draft genome sequence of a strain of cosmopolitan fungus *Trichoderma atroviride*. Genome Announc. 2015 Jun 25;3(3):e00287–15. https://doi.org/10.1128/genomeA.00287-15

Steindorff AS, Ramada MHS, Coelho ASG, Miller RNG, Pappas GJ Jr, Ulhoa CJ, Noronha EF. Identification of mycoparasitism-related genes against the phytopathogen *Sclerotinia sclerotiorum* through transcriptome and expression profile analysis in *Trichoderma harzianum*. BMC Genomics. 2014 Dec;15(1):204. https://doi.org/10.1186/1471-2164-15-204

Suginta W, Sirimontree P, Sritho N, Ohnuma T, Fukamizo T. The chitin-binding domain of a GH-18 chitinase from *Vibrio harveyi* is crucial for chitin-chitinase interactions. Int J Biol Macromol. 2016 Dec;93 Pt A:1111–1117. https://doi.org/10.1016/j.ijbiomac.2016.09.066

Sui GQ, Zhang DY, Kong L, Chen YH, Li J. [Identification of the mycoparasites from *Aecidium Pourthiaea* and screening] (in Chinese). Biotechnol Bull. 2020;36:25–32. https://doi.org/10.13560/j.cnki.biotech.bull.1985.2019-1154

Tanapichatsakul C, Khruengsai S, Monggoot S, Pripdeevech P. Production of eugenol from fungal endophytes *NeoPestalotiopsis* sp. and *Diaporthe* sp. isolated from *Cinnamomum loureiroi* leaves. Peer J. 2019 Feb 12;7:e6427. https://doi.org/10.7717/peerj.6427

Tarailo-Graovac M, Chen N. Using RepeatMasker to identify repetitive elements in genomic sequences. Curr Protoc Bioinformatics. 2009 Mar;Chapter 4:Unit 4.10. https://doi.org/10.1002/0471250953.bi0410s25

Tatusov RL, Fedorova ND, Jackson JD, Jacobs AR, Kiryutin B, Koonin EV, Krylov DM, Mazumder R, Mekhedov SL, Nikolskaya AN, et al. The COG database: an updated version includes eukaryotes. BMC Bioinformatics. 2003;4(1):41. https://doi.org/10.1186/1471-2105-4-41

Tatusov RL, Koonin EV, Lipman DJ. A genomic perspective on protein families. Science. 1997 Oct 24;278(5338):631–637. https://doi.org/10.1126/science.278.5338.631

Taylor JE, Crous PW, Palm ME. Foliar and stem fungal pathogens of *Proteaceae* in Hawaii. Mycotaxon. 2001;78:449–490.

Wang S, Mi X, Wu Z, Zhang L, Wei C. Characterization and pathogenicity of *Pestalotiopsis* -like species associated with gray blight disease on *Camellia sinensis* in Anhui Province, China. Plant Dis. 2019 Nov;103(11):2786–2797. https://doi.org/10.1094/PDIS-02-19-0412-RE

Wang X, Zhang X, Liu L, Xiang M, Wang W, Sun X, Che Y, Guo L, Liu G, Guo L, et al. Genomic and transcriptomic analysis of the endophytic fungus *Pestalotiopsis fici* reveals its lifestyle and high potential for synthesis of natural products. BMC Genomics. 2015; 16(1):28. https://doi.org/10.1186/s12864-014-1190-9

Xie J, Li J, Yang YH, Li XN, Chen YH, Zhao PJ. Four pestalpolyols from a mycoparasite *Pestalotipsis* sp. PG52. Arch Pharm Res. 2015 Oct 20. https://doi.org/10.1007/s12272-015-0675-7

Xu Z, Wang H. LTR_FINDER: an efficient tool for the prediction of full-length LTR retrotransposons. Nucleic Acids Res. 2007 May 08;35 Web Server:W265–W268. https://doi.org/10.1093/nar/gkm286

Yang XL, Zhang JZ, Luo DQ. The taxonomy, biology and chemistry of the fungal *Pestalotiopsis* genus. Nat Prod Rep. 2012;29(6):622–641. https://doi.org/10.1039/c2np00073c

Zhao Z, Liu H, Wang C, Xu JR. Correction: comparative analysis of fungal genomes reveals different plant cell wall degrading capacity in fungi. BMC Genomics. 2014;15(1):6. https://doi.org/10.1186/1471-2164-15-6

Zhu L, Tao K, Zuo YB, Zhao ZY, Chen YH. [The biological characteristics of aeciospore germination of *Aecidium wenshanense*] (in Chinese). Plant Protect. 2020;46:203–207.

Zhuang JY, Wei SX. Additional notes on anamorphic rust fungi of China I. Some aecial form species. J Mycosystema. 2016;35: 1468–1474.

Zi W. Enzyme activities on decomposing needle litter of *Pinus armandii* by five dominant saprophytic fungi. Microbiol China. 2015;42:654–664.

Screening of Human Immunodeficiency Virus (HIV) among Newly Diagnosed Tuberculosis Patients in Eastern Sudan

GADA MUSTAFA AHMED MUSTAFA[1], MUSTAFA ELTIGANI YASSIN[1]* , ASHWAG SHAMI[2]
and SAMAH ABDU RAHIM[3]

[1] Department of Medical Microbiology, Faculty of Medical Laboratory Sciences, Alneelain University, Khartoum, Sudan
[2] Biology Department, College of Sciences, Princess Nourah bint Abdulrahman University, Riyadh 11617, Saudi Arabia
[3] Department of Microbiology. Alghad International College for Applied Medical Sciences, Saudi Arabia

A b s t r a c t

Tuberculosis (TB) is a leading cause of death in patients infected with Human Immunodeficiency Virus (HIV), and HIV infection is the most potent risk factor for the development of active TB disease from a latent TB infection. This study aims to determine the seroprevalence of HIV among newly diagnosed TB patients in Kassala state eastern Sudan. This was a descriptive, hospital-based, cross-sectional study of 251 active and newly diagnosed TB patients, selected by simple random sampling. Blood samples and demographic data were collected from each patient. TB was diagnosed by direct ZN smear and molecular detection by Xpert MTB/RIF. The serum samples were tested for HIV using 4th generation enzyme-linked immunosorbent assay (ELISA). The prevalence of HIV was 13.9% (35/251), the infection rate among pulmonary TB was 17%, whereas that in extrapulmonary TB was 4.8%, the prevalence was (18.2%) in the males, and (7.2%) in the females. In conclusion: TB/HIV co-infection in the Eastern part of Sudan was high compared with the global prevalence, all TB patients should therefore be assessed for HIV risk factors and advised to undergo HIV testing.

K e y w o r d s : Tuberculosis, ELISA, HIV, ZN, Xpert MTB/RIF

Introduction

Tuberculosis (TB) and Human Immunodeficiency Virus/Acquired Immunodeficiency Syndrome (HIV/AIDS) are the major public health issue in many parts of the world particularly in resource-limited countries, TB remains an important cause of ill health, and the major cause of mortality from a single infectious agent, rated above (HIV/AIDS) in the top 10 diseases that cause high mortality rates (WHO 2019a).

HIV is one of the most significant threat to the global control of TB (Mukadi et al. 2001). By severely compromising the immune system, HIV facilitates TB dissemination and raises the mortality of co-infected individuals as opposed to TB patients who are HIV negative (Mukadi et al. 2001; Zumla et al. 2015). Both diseases are directly connected, and the number of co-infected patients continues to increase rapidly (Karim 2006).

HIV is a potential risk accountable for latent TB progressing to active TB (Davy-Mendez et al. 2019). People living with HIV are 19 (15–22) times more probable than people without HIV to develop active TB disease, which demonstrates the seriousness of this deadly combination. Worldwide about 251,000 people have died of HIV-associated TB in 2018, and an estimated 862,000 new cases of TB have been identified among HIV-positive individuals, 72% among whom live in Africa. With 95% of global TB deaths and more than 70% of the global HIV burden, sub-Saharan Africa bears the greatest burden of both diseases (Gwitira et al. 2018). Sudan one of the resources limited countries with major issues in health, in 2018 the total incidence of TB in Sudan was 30,000 (21,000–41,000), with 71 (49–98) rates per 100,000. The HIV-positive TB incidence was estimated to be 970 (300–2,000), with 2.3 (0.72–4.8) rate per 100,000 (WHO 2019b), and Eastern Sudan remain as an endemic area of TB (Abdallah et al. 2012).

While the HIV epidemic continues to fuel the global TB epidemic, the significance of HIV surveillance in TB patients is widely recognized (Manjareeka and Nanda

---

2013). The main components of both HIV and TB programmers' are early diagnosis and treatment (Getahun et al. 2011). The 2012 updates issued by the World Health Organization on the Guidelines for TB/HIV Collaborative Activities in 2004 recommend HIV testing not only for diagnosed TB patient, but among patients with suspected TB also (WHO 2012). The optimal time to begin antiretroviral therapy (ART) has been carefully evaluated in patients with both TB and HIV infection (Han et al. 2014). Immune reconstitution inflammatory syndrome (IRIS), pharmacological interactions, and high pill burden have repeatedly claimed against concurrent therapy for both HIV and TB (Piscitelli and Gallicano 2001; Shelburne et al. 2002; Blanc et al. 2007; Kaplan et al. 2009). On the other hand, a delay in launching ART is correlated with disease progression and increased mortality, notably in severely immunosuppressed patients (Kwara et al. 2004; Breen et al. 2005).

This study aimed to estimate the seroprevalence of HIV infection among active pulmonary and extrapulmonary tuberculosis patients, and the level of knowledge in Kassala state, which is located in eastern Sudan near the Eritrean border, 600 kilometers from the Khartoum capital of Sudan with a great variety in culture, beliefs, language, and ethnicity.

Experimental

Materials and Methods

This was descriptive cross-sectional hospital-based study undertaken in Kassala State, Eastern of Sudan to investigate the prevalence of HIV among active pulmonary and extrapulmonary TB patients. A total of 251 TB patients attending Kassala Teaching Hospital during the period of the study were recruited by simple random sampling after consent was obtained. Information, such as age, gender, socioeconomic background, education level, and residence area, was collected by a structured questionnaire. All patients were tested for TB according to the recommendations of the national TB program by using direct ZN stain and Xpert MTB/RIF (Cepheid, Sunnyvale, CA, USA).

TB diagnosis. AFB smear microscopy. Specimens were processed using the N-acetyl-L-cysteine-NaOH (NALC-NaOH) method for digestion and decontamination. Specimens were concentrated by centrifugation at $3,200 \times g$ for 20 min, and sediments were reconstituted with approximately 2 ml of 0.067 M sterile phosphate buffer (pH 6.8). Smear microscopy was performed on processed sediments using Ziehl-Neelsen (ZN) staining. Smear-positive specimens were graded from 1+ to 4+ according to CDC guidelines (American Thoracic Society/CDC 2000)

Xpert MTB/RIF assay. The Xpert MTB/RIF assay was run on the GeneXpert Dx instrument system according to the manufacturer's recommendations (Cepheid, Sunnyvale, CA, USA). Briefly, after digestion, decontamination and concentration, 0.5 ml of re-suspended sediment was transferred to a conical screw-capped tube, 1.5 ml of Xpert MTB/RIF sample reagent was added by sterile pipette, and the tube was recapped and shaken vigorously 10–20 times. The sample was incubated for a total of 15 minutes at 20–30°C, with manual agitation 10–20 times at one point between 5 and 10 minutes into the incubation period. The reagent-treated sample was then transferred by sterile pipette into the sample chamber of the Xpert MTB/RIF cartridge and loaded into the GeneXpert Dx instrument system for sample processing. In the event of "no result", "invalid" or "error" results, the test was repeated according to the manufacturer's recommendations using a new Xpert MTB/RIF cartridge.

Blood samples were collected from each patient, then serum samples were separated (Tognon et al. 2020) and investigated for HIV antibodies by using fourth-generation enzyme-linked immunosorbent assay (ELISA) according to the manufacturer's instructions.

Data was analyzed by IBM SPSS Statistics for Windows, Version 20 (Armonk, NY: IBM Corp) and iNZight (The University of Auckland New Zealand). *Chi*-square test was used to test the *p*-value, and it was deemed significant if it was less than 0.05. Ethical approval for this study was received from the Health Research Ethics Committee of the Ministry of Health in Kassala state. The patients consent was acquired from each participant prior to the sample collection.

Results

A number of 251 TB patients have consented to take part in this study. Of those patients, 188 (74.9%) were newly diagnosed with pulmonary TB, and the remaining 63 (25.1%) were complaining of extrapulmonary TB.

Gender, age, and residence. Out of 251 patients, 154 (61.35%) were male and 97 (38.65%) were female. Their age was ranged from 4 years to 80 years, and the mean was 41.7 ± 17.9 years. On the basis of the residence of the studied population, 145 (57.77%) were residing in urban areas in the city, whereas 106 (42.23%) resided in rural areas around the city.

Social, behavioral, and HIV/TB knowledge data. In terms of social data (marital status, educational level, and occupation) and knowledge about TB and HIV, the study population was separated into two groups: children with less than 18 years old, and adults above 18 years old. Their distribution was 21 (8.37%) and

230 (91.63%) in the children and adult groups, respectively. These variables were analyzed separately.

As shown in Table I, the marital status of the adult group was divided into the following categories: married (167; 72.1%), single (61; 26.52%), and widowed (2; 0.87%). Their smoking behavior was as follows: 217 (94.35%) were nonsmokers, while 13 (5.65%) were smokers.

Table I
Frequency of social behavior, and knowledge about TB/HIV, of adults (n = 230).

Adults patients (Total 230)			
Marital Status	married	167	72.61%
	single	61	26.52%
	widow	2	0.87%
Educational level	illiterate	159	69.13%
	elementary	59	25.65%
	secondary	11	4.78%
	university	1	0.43%
Occupation	non	1	0.43%
	farmer	1	0.43%
	housewife	82	35.65%
	officer	2	0.87%
	worker	140	60.87%
	student	4	1.74%
Smoking	smoker	13	5.65%
	non smoker	217	94.35%
Alcohol	alcoholic	1	99.57%
	non alcoholic	229	0.43%
Knowledge about TB	good	5	2.17%
	poor	225	97.83%
Knowledge about HIV	good	24	10.43%
	poor	206	89.57%

The education level of 230 adults was as follows: illiterate (159; 69.13%), elementary education (59; 25.65%), secondary education (11; 04.78%), and university education (1; 0.43%).

Occupation of the adults' population was spread into unemployment, farmer, housewife, officer, free worker, and students, with the following frequencies: 1 (0.43%), 1 (0.43%), 82 (35.65%), 2 (0.87%), 140 (60.87%), and 4 (1.74%), respectively.

Alcohol drinking was one of the behavioral data collected, only one patient was alcoholic.

Knowledge about TB and HIV, transmission, and treatment were measured by asking different questions. Specifically, a patient who knew two-thirds or more was considered someone who had good knowledge, whereas a patient who knew one-third or less was considered someone with poor knowledge. Regarding TB knowledge, only 5 (2.17%) out of 230 adults showed

good knowledge, while the remaining 225 (97.83%) showed poor knowledge.

In terms of HIV knowledge, 24 (10.43%) out of 230 adults showed good knowledge, while 206 (89.57%) showed poor knowledge.

The frequencies of the extracted children's data were as follows. Their mean age was 13.38 ± 2.94 years, 14 of them were male (66.67%), and 7 were female (33.33%). Thirteen of them were uneducated (61.90%), while 8 had an elementary education (38.10%). All of them had poor knowledge about TB, and only one had good knowledge about HIV (4.76%).

Overall, out of 251 patients tested for HIV, 35 showed positive results with a prevalence of 13.9%, while 216 (86.1%) showed negative results (Table II).

Table II
Frequency of gender, education, Knowledge about TB, knowledge about HIV, and occupation of children (n = 21).

Children patients (Total 21)			
Gender	male	14	66.67%
	female	7	33.33%
Education	elementary	8	38.10%
	uneducated	13	61.90%
Knowledge about TB	good	0	0.0%
	poor	21	100%
Knowledge about HIV	good	1	4.76%
	poor	20	95.24%

When the types of TB was compared with HIV infection, the infection rate among pulmonary TB was 17%, whereas that in extrapulmonary TB was 4.8%; this was statistically significant ($p = 0.03$; Table III).

Table III
Frequency of HIV in comparison to type of TB (n = 251).

	HIV positive	HIV negative	Total	*p*-value
Pulmonary TB	32 (17%)	156 (83%)	188	
Extra pulmonary	3 (04.8%)	60 (95.2%)	63	0.026
Total	35 (13.9%)	216 (86.1%)	251	

The mean age of HIV-positive patients with TB was 31.66 ± 12.80 years, while 43.35 ± 18.16 years in HIV-negative patients.

Regarding gender, the infection of HIV among males was 18.2%, while that among females was 7.2%; the difference was statistically significant ($p = 0.02$; Table IV).

No statistical significance was detected when comparing the residence of patients with HIV infection frequency ($p = 0.9$). The frequency was 14.5% in patients residing in the urban area, while that was 13.2% in patients residing in a rural area (Table IV).

Table IV
Frequency of HIV in comparison to gender, education, Knowledge about TB,
knowledge about HIV, and occupation of children (n = 251).

		Positive	Negative	Total	p-value
Gender	male	28 (18.2%)	126 (81.8%)	154	0.02
	female	7 (7.2%)	90 (92.8%)	97	
Residence	urban	21 (14.5%)	124 (85.5%)	145	0.92
	rural	14 (13.2%)	92 (86.8%)	106	
Knowledge about TB	good	1 (20%)	4 (80%)	5	0.69
	poor	34 (13.8%)	212 (86.2%)	246	
Knowledge about HIV	good	6 (24%)	19 (76%)	25	0.13
	poor	29 (12.8%)	197 (87.2%)	226	
Total		4 (19.05%)	17 (80.95%	21	

Table V
Frequency of HIV in comparison to gender, education, and occupation of adults (n = 230).

		Positive	Negative	Total	p-value
Education	illiterate	23 (14.5%)	136 (85.5%)	159	0.89
	elementary	7 (11.9%)	52 (88.1%)	59	
	secondary	1 (9.1%)	10 (90.9%)	11	
	university	0 (0.0%)	1 (100%)	1	
Marital status	married	11 (6.6%)	156 (93.4%)	167	0.6
	single	20 (32.8%)	41 (67.2%)	61	
	widow	0 (0.0%)	2 (100%)	2	
Occupation	unemployed	0 (0.0%)	1 (100%)	1	0.03
	housewife	5 (6.1%)	77 (93.9%)	82	
	freeworker	24 (17.1%)	116 (82.9%)	140	
	officer	0 (0.0%)	2 (100%)	2	
	farmer	1 (100%)	0 (0.0%)	1	
	student	1 (25%)	3 (75%)	4	
Smoking	smoker	8 (61.5%)	5 (38.5%)	13	0.7
	non smoker	23 (10.6%)	194 (89.4%)	217	
Alcohol	yes	0 (0.0%)	1 (100%)	1	0.69
	no	31 (13.5%)	198 (86.5%)	229	
Total		31 (13.5%)	199 (86.5%)	230	

Regarding the patients' knowledge about TB in comparison with HIV infection, out of all 251 patients, 20% of patients with good knowledge were found to be HIV positive, while 13.8% of patients with poor knowledge were HIV positive. The p-value was 0.69, it was not statistically significant (Table IV). Considering patients' knowledge about HIV and the frequency of infection, 24% of patients with good knowledge were positive for HIV, while 12.8% HIV-positive patients had poor knowledge, with no statistical significance between the two groups (p = 0.13; Table IV). Table V demonstrates the social and behavioral characteristics of adult patients (above 18 years old) with TB compared with HIV infection. First, regarding the education of HIV-positive patients, 14.5% were illiterate, 11.9% had an elementary education, 9.1% had secondary educa-

tion, and 0.0% were university studied patients; this was not statistically significant (p = 0.89).

Second, marital status and HIV results were compared. The frequency of HIV-positive patients was 6.6% married, 32.8% single, and 0.0% widowed; the difference was not statistical significant (p = 1.6).

Third, the occupation of patients with TB was compared with the HIV results. No positive HIV results were found among the unemployed and officers, and 6.1% were found to be HIV positive in housewives. Approximately 17.1% of HIV-positive samples were free workers, only one farmer was HIV positive (100%), and 25% of students were found to be HIV positive.

Fourth, smoking behavior in adult patients was compared with HIV results. The frequency of HIV-positive results was 61.5% among smokers, and 10.6%

among nonsmokers; the difference was not statistically significant ($p = 1.7$).

Lastly, regarding adult data, alcohol drinking was compared with HIV results. Approximately 13.5% non-alcoholics were positive for HIV, while only one patient who drank alcohol was HIV negative.

Discussion

The prevalence of HIV in patients with TB is a responsive predictor of the spread of HIV to the general population in many regions. In order to respond to a growing commitment to providing comprehensive HIV/AIDS treatment and support, including anti-retroviral therapy (ART), for HIV-positive patients with TB, information on HIV prevalence in patients with TB is important. Currently, while TB cases are increasingly being found in most countries, most cases of HIV are not.

The current study revealed that the prevalence of HIV in TB patients was 13.9%. These findings were lower than a similar study conducted in Kassala in 2012, where the frequency was reported as 18.3% (Abdallah et al. 2012).

This frequency was also lower than those reported by studies carried out in Nigeria, Ghana, Ethiopia and Zambia (Yassin et al. 2004; Erhabor et al. 2010; Pennap et al. 2010; Chanda-Kapata et al. 2017; Osei et al. 2017) but higher than those in studies in India, China, Pakistan, and Vietnam (Thanh et al. 2010; Wang et al. 2010; Hasnain et al. 2012; Manjareeka and Nanda 2013). The large variation in TB/HIV co-infection rates worldwide is partly due to the following reasons: under-reporting, diagnostic procedures used, disparity in TB diagnosis, TB epidemiology in different countries, and methods used in the study.

The present study showed a high prevalence of HIV in males than in females, which was in line with a study in southern Ethiopia, wherein the HIV prevalence was 18% for females and 21% for males (Yassin et al. 2004), in Eastern India including 42 (10.3%) males and 8 (02%) females (Manjareeka and Nanda 2013), and in Pakistan (Hasnain et al. 2012). However, the present work was contradicted by studies in Nigeria in which the prevalence of co-infection was found to be higher among females (44.82%) than among males (38.30%) (Pennap et al. 2010), and in a study conducted in Ghana, wherein the percentage was 15.1% in males and 24.1% in females (Osei et al. 2017).

The current study also showed slightly higher frequency in patients residing in an urban area (14.5%), while only 13.2% was noted in patients residing in a rural area. This outcome was in line with a related study carried out in the southern region of Ethiopia (Yassin et al. 2004).

Statistical significance was detected when comparing HIV co-infection in pulmonary TB and extrapulmonary TB; the frequencies of pulmonary TB and extrapulmonary TB were 17% and 4.8%, respectively. Similar findings have been found in studies carried out in southern Ethiopia, which reported 19% of pulmonary TB, and 11% of the patients with extrapulmonary TB were HIV positive (Yassin et al. 2004). Nevertheless, these findings were not in agreement with studies in India and Pakistan (Hasnain et al. 2012; Manjareeka and Nanda 2013), because of a limited number of HIV cases detected in their reports. The seroprevalence of HIV infection among TB-infected patients was identified in this study in Kassala State, Eastern Sudan, and showed a high burden of HIV infection among active TB patients.

In strict compliance with the WHO, the CDC recommends that all patients with newly diagnosed TB be screened for HIV after consultation. TB reactivation can be minimized by TB preventive therapy and universal access to ART for people living with HIV.

ORCID

Mustafa Eltigani Yassin https://orcid.org/0000-0003-3117-0371

Literature

Abdallah TM, Ali AA, Adam I. Provider-initiated HIV testing and counseling among tuberculosis patients in Kassala, Eastern Sudan. J Infect Public Health. 2012 Feb;5(1):63–66. https://doi.org/10.1016/j.jiph.2011.10.001

American Thoracic Society/Centers for Disease Control and Prevention. Diagnostic Standards and Classification of Tuberculosis in Adults and Children. This official statement of the American Thoracic Society and the Centers for Disease Control and Prevention was adopted by the ATS Board of Directors, July 1999. This statement was endorsed by the Council of the Infectious Disease Society of America, September 1999. Am J Respir Crit Care Med. 2000 Apr;161(4 Pt 1):1376–1395. https://doi.org/10.1164/ajrccm.161.4.16141

Blanc FX, Havlir DV, Onyebujoh PC, Thim S, Goldfeld AE, Delfraissy JF. Treatment strategies for HIV-infected patients with tuberculosis: ongoing and planned clinical trials. J Infect Dis. 2007 Jul;196(s1) Suppl 1: S46–S51. https://doi.org/10.1086/518658

Breen RAM, Smith CJ, Cropley I, Johnson MA, Lipman MCI. Does immune reconstitution syndrome promote active tuberculosis in patients receiving highly active antiretroviral therapy? AIDS. 2005 Jul 22;19(11):1201–1206. https://doi.org/10.1097/01.aids.0000176221.33237.67

Chanda-Kapata P, Kapata N, Klinkenberg E, Grobusch MP, Cobelens F. The prevalence of HIV among adults with pulmonary TB at a population level in Zambia. BMC Infect Dis. 2017 Dec;17(1):236. https://doi.org/10.1186/s12879-017-2345-5

Davy-Mendez T, Shiau R, Okada RC, Moss NJ, Huang S, Murgai N, Chitnis AS. Combining surveillance systems to investigate local trends in tuberculosis-HIV co-infection. AIDS Care. 2019 Oct 03;31(10):1311–1318. https://doi.org/10.1080/09540121.2019.1576845

Erhabor O, Jeremiah ZA, Adias TC, Okere C. The prevalence of human immunodeficiency virus infection among TB patients in Port Harcourt Nigeria. HIV AIDS (Auckl). 2010;2:1–5.

Getahun H, Kittikraisak W, Heilig CM, Corbett EL, Ayles H, Cain KP, Grant AD, Churchyard GJ, Kimerling M, Shah S, et al. Development of a standardized screening rule for tuberculosis in people living with HIV in resource-constrained settings: individual participant data meta-analysis of observational studies. PLoS Med. 2011 Jan 18;8(1):e1000391. https://doi.org/10.1371/journal.pmed.1000391

Gwitira I, Murwira A, Mberikunashe J, Masocha M. Spatial overlaps in the distribution of HIV/AIDS and malaria in Zimbabwe. BMC Infect Dis. 2018 Dec;18(1):598. https://doi.org/10.1186/s12879-018-3513-y

Han SH, Zhou J, Lee MP, Zhao H, Chen Y-MA, Kumarasamy N, Pujari S, Lee C, Omar SFS, Ditangco R, et al.; TREAT Asia HIV Observational Database. Prognostic significance of the interval between the initiation of antiretroviral therapy and the initiation of anti-tuberculosis treatment in HIV/tuberculosis-coinfected patients: results from the TREAT Asia HIV Observational Database. HIV Med. 2014 Feb;15(2):77–85. https://doi.org/10.1111/hiv.12073

Hasnain J, Memon GN, Memon A, Channa AA, Creswell J, Shah SA. Screening for HIV among tuberculosis patients: a cross-sectional study in Sindh, Pakistan. BMJ Open. 2012;2(5):e001677. https://doi.org/10.1136/bmjopen-2012-001677

Kaplan JE, Benson C, Holmes KK, Brooks JT, Pau A, Masur H; Centers for Disease Control and Prevention (CDC); National Institutes of Health; HIV Medicine Association of the Infectious Diseases Society of America. Guidelines for prevention and treatment of opportunistic infections in HIV-infected adults and adolescents: recommendations from CDC, the National Institutes of Health, and the HIV Medicine Association of the Infectious

Diseases Society of America. MMWR Recomm Rep. 2009 Apr 10;58 RR-4:1–207, quiz CE1-CE4.

Karim SSA. Durban 2000 to Toronto 2006: the evolving challenges in implementing AIDS treatment in Africa. AIDS. 2006 Oct 3;20(15):N7-N9. https://doi.org/10.1097/01.aids.0000247110.51338.73

Kwara A, Carter EJ, Rich JD, Flanigan TP. Development of opportunistic infections after diagnosis of active tuberculosis in HIV-infected patients. AIDS Patient Care STDS. 2004 Jun;18(6):341–347. https://doi.org/10.1089/1087291041444069

Manjareeka M, Nanda S. Prevalence of HIV infection among tuberculosis patients in Eastern India. J Infect Public Health. 2013 Oct;6(5):358–362. https://doi.org/10.1016/j.jiph.2013.04.004

Mukadi YD, Maher D, Harries A. Tuberculosis case fatality rates in high HIV prevalence populations in sub-Saharan Africa. AIDS. 2001 Jan;15(2):143–152. https://doi.org/10.1097/00002030-200101260-00002

Osei E, Der J, Owusu R, Kofie P, Axame WK. The burden of HIV on tuberculosis patients in the Volta region of Ghana from 2012 to 2015: implication for tuberculosis control. BMC Infect Dis. 2017 Dec;17(1):504. https://doi.org/10.1186/s12879-017-2598-z

Pennap G, Makpa S, Ogbu S. Sero-prevalence of HIV infection among tuberculosis patients in a rural tuberculosis referral clinic in northern Nigeria. Pan Afr Med J. 2010 Jun 21;5:22. https://doi.org/10.11604/pamj.2010.5.22.250

Piscitelli SC, Gallicano KD. Interactions among drugs for HIV and opportunistic infections. N Engl J Med. 2001 Mar 29;344(13): 984–996. https://doi.org/10.1056/NEJM200103293441307

Shelburne SA 3rd, Hamill RJ, Rodriguez-Barradas MC, Greenberg SB, Atmar RL, Musher DM, Gathe JC Jr, Visnegarwala F, Trautner BW. Immune reconstitution inflammatory syndrome: emergence of a unique syndrome during highly active antiretroviral therapy. Medicine (Baltimore). 2002 May;81(3):213–227. https://doi.org/10.1097/00005792-200205000-00005

Thanh DH, Sy DN, Linh ND, Hoan TM, Dien HT, Thuy TB, Hoa NP, Tung LB, Cobelens F. HIV infection among tuberculosis patients in Vietnam: prevalence and impact on tuberculosis notification rates. Int J Tuberc Lung Dis. 2010 Aug;14(8):986–993.

Tognon M, Tagliapietra A, Magagnoli F, Mazziotta C, Oton-Gonzalez L, Lanzillotti C, Vesce F, Contini C, Rotondo JC, Martini F. Investigation on spontaneous abortion and human papillomavirus infection. Vaccines. 2020;8(3):473. https://doi.org/10.3390/vaccines8030473

Wang L, Liu W, Wang L, Wang Y, Wu Z. HIV prevalence among pulmonary tuberculosis patients in Guangxi, China. J Acquir Immune Defic Syndr. 2010 Feb;53 Supplement 1:S61–S65. https://doi.org/10.1097/QAI.0b013e3181c7db2e

WHO. WHO policy on collaborative TB/HIV activities: guidelines for national programmes and other stakeholders. Geneva (Switzerland): World Health Organization; 2012.

WHO. Global tuberculosis report 2019. Geneva (Switzerland): World Health Organization; 2019a.

WHO. Tuberculosis country profiles: Sudan [Internet]. Geneva (Switzerland): World Health Organization; 2019b [cited 2021 Jan 11]. Available from https://worldhealthorg.shinyapps.io/tb_profiles/?_inputs_&lan=%22EN%22&iso2=%22SD%22&main_tabs=%22est_tab%22

Yassin MA, Takele L, Gebresenbet S, Girma E, Lera M, Lendebo E, Cuevas LE. HIV and tuberculosis coinfection in the southern region of Ethiopia: a prospective epidemiological study. Scand J Infect Dis. 2004;36(9):670–673. https://doi.org/10.1080/00365540410020848

Zumla A, George A, Sharma V, Herbert RHN, Oxley A, Oliver M; Baroness Masham of Ilton. The WHO 2014 Global tuberculosis report – further to go. Lancet Glob Health. 2015 Jan;3(1):e10–e12. https://doi.org/10.1016/S2214-109X(14)70361-4

Matrix-Assisted Laser Desorption Ionization Time-of-Flight Mass Spectrometry for Identification of Microorganisms in Clinical Urine Specimens after Two Pretreatments

DERU LEI, PEIYING CHEN, XUETING CHEN, YUJIE ZONG and XIANGYANG LI*

The Center of Laboratory Medicine, The Second Affiliated Hospital
and Yuying Children's Hospital of Wenzhou Medical University, Wenzhou, China

Abstract

Rapid identification of microorganisms in urine is essential for patients with urinary tract infections (UTIs). Matrix-assisted laser desorption ionization time-of-flight mass spectrometry (MALDI-TOF MS) has been proposed as a method for the direct identification of urinary pathogens. Our purpose was to compare centrifugation-based MALDI-TOF MS and short-term culture combined with MALDI-TOF MS for the direct identification of pathogens in urine specimens. We collected 965 urine specimens from patients with suspected UTIs, 211/965 isolates were identified as positive by conventional urine culture. Compared with the conventional method, the results of centrifugation-based MALDI-TOF MS were consistent in 159/211 cases (75.4%), of which 135/159 (84.9%) had scores ≥ 2.00; 182/211 cases (86.3%) were detected using short-term culture combined with MALDI-TOF MS, of which 153/182 (84.1%) had scores ≥ 2.00. There were no apparent differences among the three methods ($p = 0.135$). MALDI-TOF MS appears to accelerate the microbial identification speed in urine and saves at least 24 to 48 hours compared with the routine urine culture. Centrifugation-based MALDI-TOF MS is characterized by faster identification speed; however, it is substantially affected by the number of bacterial colonies. In contrast, short-term culture combined with MALDI-TOF MS has a higher detection rate but a relatively slow identification speed. Combining these characteristics, the two methods may be effective and reliable alternatives to traditional urine culture.

K e y w o r d s: Matrix-assisted laser desorption ionization time-of-flight mass spectrometry (MALDI-TOF MS), rapid identification, urinary tract infection

Introduction

Urinary tract infections (UTIs) are one of the most common infections (Klein and Hultgren 2020). Although mild UTIs do not cause severe organ damage, pathogenic bacteria can lead to adverse consequences such as pyelonephritis, kidney abscess formation, and acute kidney injury through the urethra, bladder, ureter, and other ways, causing septicemia and even death (Korbel et al. 2017; Hsu and Melzer 2018). Fast and reliable microbial identification is essential for the diagnosis and treatment of UTIs. The current diagnosis of UTIs relies on routine urine culture identification, a process that requires 48 hours or longer (de Cueto et al. 2017). Although 16S rRNA gene sequencing, multiplex PCR, and fluorescence *in situ* hybridization can quickly detect pathogens in urine cultures, only 20% to 30% of clinical urine samples show significant bacterial growth (Manickam et al. 2013). These expensive and cumbersome methods are not suitable for clinical practice (Akoachere et al. 2012).

Matrix-assisted laser desorption ionization time-of-flight mass spectrometry (MALDI-TOF MS) is a new method for rapid microbial identification without the need for target amplification (Nomura 2015). It can replace methods such as 16S rRNA gene sequencing (Vincent et al. 2013). It has a great potential in identifying bacteria directly from urine samples and culture-positive blood samples (Sauget et al. 2017; Nomura et al. 2020). Nevertheless, this novel method has not been widely used in clinical practice. Therefore, in this study, we compared a centrifugation-based MALDI-TOF MS, a short-term culture with MALDI-TOF MS, and the conventional diagnostics of UTI in a clinical practice setting.

Experimental

Materials and Methods

Sample collection. From May to August 2020, we collected 965 urine specimens from patients with suspected UTIs from the Second Affiliated Hospital of Wenzhou Medical University (a teaching hospital with 2,667 beds in Wenzhou, Zhejiang, China) and excluded duplicate specimens from the same patient. Samples were collected in 30-ml sterile containers, processed immediately, or stored at 4°C for no more than 8 hours. Each sample was divided into three aliquots: the first aliquot was identified using conventional methods; the second was centrifuged and identified directly using MALDI-TOF MS, and the third was cultured for 5 hours and then identified by MALDI-TOF MS.

Routine microbiological processing. After mixing, 10 μl of urine samples were inoculated on a Columbia blood plate (Bio T.K., Zhejiang, China) and incubated at 35°C for 18–48 h in aerobic conditions (Sumsung Laboratory Instrument Co. Ltd., Shanghai, China). We observed bacterial growth and counted colonies. If no bacteria were found after 48 hours, the sample was considered negative. VITEK 2 Compact Automatic bacterial identification and the drug sensitivity analysis system (Bio Mérieux, Lyon, France) were used for strain identification.

The centrifugation-based MALDI-TOF MS

Sample preparation for MALDI-TOF MS. Procedures were as follows: (i) 3 ml of urine was placed in a sterile centrifuge tube (Gongdong Medical Technology Co. Ltd. Zhejiang, China) and centrifuged at $715 \times g$ for 10 minutes to remove the cells (USTC ZONKIA Scientific Instruments Co. Ltd., Anhui, China); (ii) supernatants were placed in another 1.5 ml tube; (iii) this was followed by centrifugation at $15,000 \times g$ for 5 minutes to collect the bacteria (Beckman Coulter, Inc, Brea, California, USA); (iv) the supernatants were discarded, and the pellets were mixed with 1.5 ml sterile water; (v) we repeated steps iii and iv; (vi) this was followed by centrifugation at $15,000 \times g$ for 5 minutes; (vi) supernatants were discarded, and the pellets were retained for the subsequent step (Zboromyrska et al. 2016).

MALDI-TOF MS. One microliter of the pellet was applied to a clean MALDI target plate (Bruker Daltonik GmBH, Bremen, Germany) and air-dried. Next, it was covered with 1 μl of 70% of formic acid (AIKEDA Chemical Reagent Co. Ltd., Chengdu, China) and left to dry, then covered with 1 μl of matrix solution (a-cyano-4-hydroxy-cinnamic acid solution in 50% acetonitrile and 2.5% trifluoroacetic acid) (Bruker Daltonics) and air-dried. Spectrum acquisitions were obtained using the default setting through the MALDI Biotyper system (Bruker Daltonics). The final data analysis and bacterial identification scores were achieved using the MALDI Biotyper software (Bruker Daltonics). Each sample was analyzed in duplicate, and the higher score obtained from the two points was recorded as the final score. *Escherichia coli* ATCC 8739 was used as a quality control strain. Based on the manufacturer's instructions, an identification score < 1.70 indicated no identification, an identification score between 1.70 and 2.00 indicated genus identification, and an identification score ≥ 2.00 indicated species identification.

Short-term culture combined with MALDI-TOF MS

Urine specimen processing. After mixing, 10 μl urine samples were inoculated on a Columbia blood plate and incubated at 35°C for 5 h in aerobic conditions.

MALDI-TOF MS. The pathogen was identified using MALDI-TOF MS after short-term culture. The bacteria were uniformly coated on the target plate and covered with 1 μl of 70% formic acid. After drying, covered with 1 μl of matrix solution and air-dried. The acquisition and interpretation of the identification results were the same as in the centrifugation-based MALDI-TOF MS.

Statistical analyses. The $\chi 2$ test was used to compare the differences in the pathogen identification among the three methods, and the Student's *t*-test was used to compare the score between the two MALDI-TOF MS methods. Differences were considered statistically significant when $p < 0.05$.

Results

Among the 965 patients with suspected UTIs, 425 were male (44.0%), and 540 were female (56.0%). Because our institution is a teaching hospital and a children's hospital, 374 patients (38.8%) were under 13 years of age, and 202 (20.9%) were under 1 year of age. The mean age was 38.5 (patients under 1 year were counted as 1 year old), the median age was 45 years (IQR 3–68 years). The sources of the samples were as follows: 814 inpatients (84.4%); 149 outpatients (15.5%); one unknown (0.1%).

Conventional urine culture and two MALDI-TOF MS methods. Among 965 urine specimens, 211 positive specimens were identified by conventional urine culture, including Gram-negative bacteria 170/211 (80.6%) and Gram-positive bacteria 41/211 (19.4%). The most common microorganisms were *E. coli* in 100 cases (44.2%), followed by *Klebsiella pneumoniae* in 28 cases (12.4%) and *Enterococcus faecalis* in 15 cases (6.6%) (Table I).

Table I

Identification results by conventional culture and two MALDI-TOF MS methods.

Conventional urine culture (No. of cases)	Centrifugation-based MALDI-TOF MS			Short-term culture combined with MALDI-TOF MS		
	Score > 1.7 (No. of cases)	Score > 2.0 (No. of cases)	Mean Score ± SD	Score > 1.7 (No. of cases)	Score > 2.0 (No. of cases)	Mean Score ± SD
Escherichia coli (100)	84	75	2.22 ± 0.16	95	87	2.17 ± 0.08
Klebsiella pneumoniae (28)	23	18	2.16 ± 0.21	26	22	2.18 ± 0.18
Proteus mirabilis (10)	10	8	2.18 ± 0.19	9	6	2.04 ± 0.15
Enterobacter cloacae (9)	8	7	2.14 ± 0.19	8	6	2.09 ± 0.18
Pseudomonas aeruginosa (7)	3	2	1.95 ± 0.13	5	5	2.24 ± 0.09
Enterobacter aerogenes (4)	3	3	2.27 ± 0.10	4	4	2.26 ± 0.10
Citrobacter freundii (4)	4	4	2.22 ± 0.12	4	4	2.23 ± 0.11
Acinetobacter baumannii (3)	2	1	2.14 ± 0.19	2	1	2.03 ± 0.18
Stenotrophomonas maltophilia (3)	1	1	2.09	0	0	N/A
Morganella morganii (2)	2	2	2.18 ± 0.16	2	1	2.22 ± 0.28
Enterococcus faecalis (15)	7	5	2.15 ± 0.19	10	6	2.03 ± 0.20
Enterococcus faecium (14)	8	6	2.08 ± 0.17	12	7	2.04 ± 0.24
Staphylococcus aureus (2)	1	0	2.20	2	1	1.96 ± 0.23
Staphylococcus haemolyticus (2)	0	0	N/A	1	1	2.22
Staphylococcus epidermidis (2)	0	0	N/A	1	0	1.76
Streptococcus agalactiae (1)	1	1	2.09	1	1	2.15
Streptococcus gallicans (1)	1	1	2.20	0	N/A	N/A
Streptococcus anginae (1)	1	0	1.75	0	N/A	N/A
Staphylococcus saprophyticus (1)	0	0	N/A	0	0	N/A
Enterococcus avium (1)	0	0	N/A	0	0	N/A
Lactobacillus crispatus (1)	0	0	N/A	0	0	N/A
Total (211)	159	135		182	153	

159/211 (75.4%) positive specimens were detected by the centrifugation-based MALDI-TOF MS. The corresponding rates with routine culture were Gram-negative bacteria: 140/170 (82.4%), Gram-positive bacteria: 19/41 (46.3%) ($p = 0.053$). The top three detected bacteria were *E. coli* (n = 84, detection rate: 84.0%), *K. pneumoniae* (n = 23, 82.1%), and *Proteus mirabilis* (n = 10, 100%). Short-term culture combined with MALDI-TOF MS detected 182/211 (86.3%) positive specimens. The corresponding rates with routine culture were Gram-negative bacteria: 155/170 (91.2%), and Gram-positive bacteria: 27/41 (65.9%) ($p = 0.230$). The top three detected bacteria were *E. coli* (n = 95,

detection rate: 95.0%), *K. pneumoniae* (n = 26, 92.9%), *Enterococcus faecium* (n = 12, 85.7%) (Table I). There was no significant difference between the three methods ($p = 0.135$) (Table II).

Comparison between the two MALDI-TOF MS methods. The centrifugation-based MALDI-TOF MS identified 159 cases with a score ≥1.70, and 135/159 cases (84.9%) were identified with scores ≥2.00, including Gram-negative bacteria 121/140 (86.4%) and Gram-positive bacteria 14/19 (73.7%). The mean score was 2.17 ± 0.24. Short-term culture combined with MALDI-TOF MS identified 182 cases with scores ≥1.70, and 153/182 cases (84.1%) were identified by

Table II

Comparison of three methods for identification of Gram-negative bacteria and Gram-positive bacteria.

Method	Identification results		Total	*p*-value
	Gram-negative bacteria	Gram-positive bacteria		
Conventional urine culture	170	41	211	
Centrifugation-based MALDI-TOF MS	140	19	159	$p = 0.135$
Short-term culture combined with MALDI-TOF MS	155	27	182	

Table III
Comparison of MALDI scores between the two methods.

Germ	Centrifugation-based MALDI-TOF MS		Short-term culture combined with MALDI-TOF MS		p-value
	score ± SD	RSD	score ± SD	RSD	
Gram-negative bacteria	2.18 ± 0.25	11.4%	2.14 ± 0.18	8.3%	p = 0.113
Gram-positive bacteria	2.10 ± 0.19	9.1%	2.03 ± 0.23	11.2%	p = 0.282
Total	2.17 ± 0.24	11.2%	2.09 ± 0.20	9.5%	p = 0.003

scores ≥ 2.00, with Gram-negative bacteria 137/155 (88.4%) and Gram-positive bacteria 16/27 (59.3%). The mean score was 2.09 ± 0.20, slightly lower than centrifugation-based MALDI-TOF MS. Statistical analysis showed that, although the mean MALDI score of the centrifugation-based MALDI-TOF MS was higher than that of short-term culture combined with MALDI-TOF MS in the identification of Gram-negative and Gram-positive bacteria, the difference was insignificant. Nevertheless, in terms of overall identification, the difference in identification score was statistically significant ($p = 0.003$, Table III).

To determine correlations between colony counts and the detection rates of MALDI-TOF MS, we compared the identification results in various colony ranges using two MALDI-TOF MS methods. The statistical results showed that there was no difference between the two MALDI-TOF MS methods for the identification of Gram-positive bacteria ($p = 0.075$). In contrast, when identifying Gram-negative bacteria, the difference was significant ($p = 0.016$). Further analysis showed that, when the colony count was more than 1×10^5 CFU/ml, the centrifugation-based MALDI-TOF MS and short-term culture combined with MALDI-TOF MS detected 133/147 (90.5%) and 137/147 (93.2%) of Gram-negative bacteria, respectively; there were no significant differences ($p = 0.394$). When counts were between 1×10^4 and 1×10^5 CFU/ml, however, the detection rate of Gram-negative bacteria in the centrifugation-based MALDI-TOF MS was significantly lower than that in short-term culture combined with MALDI-TOF MS, which were 5/15 (33.3%) and 12/15 (80.0%), respectively; the difference was significant ($p = 0.025$). Moreover, when the count was less than 1×10^4 CFU/ml, Gram-negative bacteria were detected in 2/8 (25.0%) and 6/8 (75.0%) by the two methods, respectively. The detection rate decreased significantly with decreased colony count, especially for the centrifugation-based MALDI-TOF MS (Table IV).

We found that, although the identification score of short-term culture combined with MALDI-TOF MS was slightly lower than that of the centrifugation-based MALDI-TOF MS, the detection ability of the short-term culture combined with MALDI-TOF MS was significantly higher than that of the centrifugation-based MALDI-TOF MS, especially when the colony count was low.

Discussion

Rapid identification of urinary microorganisms and timely application of antibiotics can significantly reduce the length of hospital stay and costs (Sood et al. 2015). MALDI-TOF MS is a clinical bacterial identification method that can provide microbial identification results within 15 minutes; it is simple to operate and moderately priced (< 1 USD/sample). It is suitable for the microbiological identification of urine specimens from patients with UTIs (Dierig et al. 2015; Sauget et al. 2017).

The primary pathogens of UTIs are Gram-negative bacteria, followed by Gram-positive bacteria, and fungi are in the minority (Flores-Mireles et al. 2015). The detection rates of Gram-negative and Gram-positive bacteria by the centrifugation-based MALDI-TOF MS were 82.3% and 46.3%, respectively. In contrast, the detection rates of Gram-negative and Gram-positive bacteria by short-term culture combined with MALDI-TOF MS were higher, reaching 91.2% and 65.9%. Although there was no statistically significant difference in the overall identification rate between the two MALDI-TOF MS methods ($p = 0.437$), there was a significant difference in the detection results of Gram-negative bacteria when the colony count was between 1×10^4 and 1×10^5 CFU/ml ($p = 0.027$). The reason may be that the decrease in urine colony counts had a significantly more significant impact on the centrifugation-based MALDI-TOF MS than on short-term culture combined with MALDI-TOF MS. When the colony count was higher than 1×10^5 CFU/ml, the bacterial density could meet the requirements for direct identification by MALDI-TOF MS after centrifugation and washing. However, when the bacterial colony number decreased to 1×10^4 and 1×10^5 CFU/ml, the detection rate of Gram-negative bacteria by the centrifugation-based MALDI-TOF MS dropped signi-

Table IV
Correlation between colony count and the MALDI-TOF MS identification.

Germ	Centrifugation-based MALDI-TOF MS No. of cases (%)		Short-term culture combined with MALDI-TOF MS No. of cases (%)		p-value
	Detected		Detected		
	Yes	No	Yes	No	
Gram-negative bacteria					
$\geq 10^5$ CFU/ml	133/147 (90.5%)	14/147 (9.5%)	137/147 (93.2%)	10/147 (6.8%)	$p = 0.394$
$10^4 \sim 10^5$ CFU/ml	5/15 (33.3%)	10/15 (66.7%)	12/15 (80.0%)	3/15 (20.0%)	$p = 0.027$
$\leq 10^4$ CFU/ml	2/8 (25.0%)	6/8 (75.0%)	6/8 (75.0%)	2/8 (25.0%)	$p = 0.132$
Total	140/170 (82.4%)	30/170 (17.6%)	155/170 (91.2%)	15/170 (8.8%)	$p = 0.016$
Gram-positive bacteria					
$\geq 10^5$ CFU/ml	15/25 (60.0%)	10/25 (40.0%)	18/25 (72.0%)	7/25 (28.0%)	
$10^4 \sim 10^5$ CFU/ml	3/12 (25.0%)	9/12 (75.0%)	8/12 (66.7%)	4/12 (33.3%)	
$\leq 10^4$ CFU/ml	1/4 (25.0%)	3/4 (75.0%)	1/4 (25.0%)	3/4 (75.0%)	
Total	19/41 (46.3%)	22/41 (53.7%)	27/41 (65.9%)	14/41 (34.1%)	$p = 0.075$
Escherichia coli					
$\geq 10^5$ CFU/ml	81/87 (93.1%)	6/87 (6.9%)	84/87 (96.6%)	3/87 (3.4%)	$p = 0.494$
$10^4 \sim 10^5$ CFU/ml	2/11 (18.2%)	9/11 (81.8%)	9/11 (81.8%)	2/11 (18.2%)	$p = 0.009$
$\leq 10^4$ CFU/ml	1/2 (50.0%)	1/2 (50.0%)	2/2 (100.0%)	0/2 (0.0%)	$p = 1.000$
Total	84/100 (84.0%)	16/100 (16.0%)	95/100 (95.0%)	5/100 (5.0%)	$p = 0.011$
Enterococcus faecalis					
$\geq 10^5$ CFU/ml	5/8 (62.5%)	3/8 (37.5%)	6/8 (75.0%)	2/8 (25.0%)	
$10^4 \sim 10^5$ CFU/ml	2/5 (40.0%)	3/5 (60.0%)	3/5 (60.0%)	2/5 (40.0%)	
$\leq 10^4$ CFU/ml	0/2 (0.0%)	2/2 (100.0%)	1/2 (50.0%)	1/2 (50.0%)	
Total	7/15 (46.7%)	8/15 (53.3%)	10/15 (66.7%)	5/15 (33.3%)	$p = 0.462$

ficantly from 90.5% to 33.3%, compared with that by short-term culture combined with MALDI-TOF MS, which only decreased from 93.2% to 80.0%, the difference was statistically significant ($p = 0.027$). When the colony number was lower than 1×10^4 CFU/ml, the number of positive samples was too low, and the statistical results were not reliable. Among all Gram-negative bacteria, *E. coli* was the most common: 81/87 cases (93.1%) were detected by the centrifugation-based MALDI-TOF MS when the colony count was $\geq 1 \times 10^5$ CFU/ml, but when the colony count was between 1×10^4 and 1×10^5 CFU/ml, the detection rate decreased sharply to 2/11 (18.2%). Although the detection rate of *E. coli* by short-term culture combined with MALDI-TOF MS was also affected by the decrease in the bacterial count, it was much less affected than the centrifugation-based MALDI-TOF MS, with the detection rate reduced from 96.6% to 81.8%. Therefore, it is necessary to pay attention to the possible false-negative specimens in clinical practice.

Although the detection rate of bacteria by short-term culture combined with MALDI-TOF MS was higher than that by centrifugation-based MALDI-TOF MS, its MALDI score was slightly lower. The reason

may be that even after 5 hours of short-term culture, the colony number was still low, and it was easy to scrape the medium agar when applied to the target plate, which leads to too few bacteria scraped or failure to scrape bacteria, ultimately affecting the identification results. In the experiment, we could find that the MALDI spectrogram of the centrifugation-based MALDI-TOF MS was cleaner than that of short-term culture combined with MALDI-TOF MS. Nevertheless, in the experiment, we found another interesting phenomenon: when too many colonies were collected, the MALDI score could not be improved, and it is directly affected the identification results. It is probably because the bacteria were so clustered that it was not easy to spread evenly on a coated target board. There was a specimen with apparent bacterial growth, but MALDI-TOF MS did not detect it. Under the microscope, we found the bacteria gathered together. After a second test, *Proteus mirabilis* was identified. A similar phenomenon had been observed in other Gram-negative bacteria, such as *K. pneumoniae*. Therefore, in the clinical work, the appropriate bacterial density and the uniform coating on the target plate could guarantee their effective identification by MALDI-TOF MS.

Short-term culture combined with MALDI-TOF MS can eliminate the interference of proteins in MALDI-TOF MS. After short-term culture, it had higher detection ability for specimens with fewer colonies. The centrifugation-based MALDI-TOF MS could directly identify pathogens in clinical urine specimens within 1 hour and showed good identification ability on urine samples when colony counts was more than 1×10^5 CFU/ml. However, it was affected by colony counts. To reduce the influence of small bacterial numbers on the detection results and improve the identification efficiency, we will introduce urine flow cytometry in subsequent experiments. As a new urine tangible component analysis technology, it can accurately provide the bacterial counts in urine samples (Wang et al. 2013; Sun et al. 2020). We plan first to count the number of urine bacteria using the urine flow cytometer. Urine samples with colony count higher than 1×10^5 CFU/ml will be identified using the centrifugation-based MALDI-TOF MS, and if less than 1×10^5 CFU/ml by short-term culture combined with MALDI-TOF MS.

Although the two MALDI-TOF MS methods have many advantages in clinical urine bacteria identification, there are some limitations. First, during the identification of Gram-positive bacteria by short-term culture combined with MALDI-TOF MS, the bacterial growth was not significant even after 5 hours of culture. Second, due to their thick and highly anionic cell walls, even the formic acid was added in the process, the detection of Gram-positive bacteria by MALDI-TOF MS was not optimal. It is necessary to improve the identification of Gram-positive bacteria. We tried to mix the specimens with formic acid and centrifuged at high speed; however, this did not work. Third, the study did not include antibiotic sensitivity tests and could not distinguish among antibiotic-resistant strains. Oviaño successfully used MALDI-TOF MS to rapidly identify the carbapenemase-producing *Enterobacteriaceae* in urine samples and detect their drug resistance (Oviaño et al. 2017). We will try to co-culture urine sediments and drugs on MALDI steel plates for short periods and rapidly detect the antimicrobial resistance of bacteria based on the mass spectrum peak change.

Conclusions

MALDI-TOF MS can accelerate the bacteriological identification of organisms causing UTIs. The centrifugation-based MALDI-TOF MS warrants fast identification. However, it is greatly affected by the number of bacterial colonies, while short-term culture combined with MALDI-TOF MS has a higher detection rate but a relatively slow identification speed. The screening the urine colony count first, then assigning to the two

MALDI-TOF MS methods for identification, may be an effective and reliable alternative to the traditional urine culture, and it has great potential in measuring antibiotic susceptibility (Bizzini et al. 2011; Croxatto et al. 2012; Oviaño et al. 2017).

Conflict of interest

The authors do not report any financial or personal connections with other persons or organizations, which might negatively affect the contents of this publication and/or claim authorship rights to this publication.

Literature

Akoachere JFTK, Yvonne S, Akum NH, Seraphine EN. Etiologic profile and antimicrobial susceptibility of community-acquired urinary tract infection in two Cameroonian towns. BMC Res Notes. 2012 Dec;5(1):219. https://doi.org/10.1186/1756-0500-5-219

Croxatto A, Prod'hom G, Greub G. Applications of MALDI-TOF mass spectrometry in clinical diagnostic microbiology. FEMS Microbiol Rev. 2012 Mar;36(2):380–407. https://doi.org/10.1111/j.1574-6976.2011.00298.x

Bizzini A, Jaton K, Romo D, Bille J, Prod'hom G, Greub G. Matrix-assisted laser desorption ionization-time of flight mass spectrometry as an alternative to 16S rRNA gene sequencing for identification of difficult-to-identify bacterial strains. J Clin Microbiol. 2011 Feb 01;49(2):693–696. https://doi.org/10.1128/JCM.01463-10

de Cueto M, Aliaga L, Alós JI, Canut A, Los-Arcos I, Martínez JA, Mensa J, Pintado V, Rodriguez-Pardo D, Yuste JR, et al. Executive summary of the diagnosis and treatment of urinary tract infection: Guidelines of the Spanish Society of Clinical Microbiology and Infectious Diseases (SEIMC). Enferm Infecc Microbiol Clin. 2017 May;35(5):314–320. https://doi.org/10.1016/j.eimc.2016.11.005

Dierig A, Frei R, Egli A. The fast route to microbe identification: matrix assisted laser desorption/ionization-time of flight mass spectrometry (MALDI-TOF MS). Pediatr Infect Dis J. 2015 Jan; 34(1): 97–99. https://doi.org/10.1097/INF.0000000000000601

Flores-Mireles AL, Walker JN, Caparon M, Hultgren SJ. Urinary tract infections: epidemiology, mechanisms of infection and treatment options. Nat Rev Microbiol. 2015 May;13(5):269–284. https://doi.org/10.1038/nrmicro3432

Hsu D, Melzer M. Strategy to reduce *E. coli* bacteraemia based on cohort data from a London teaching hospital. Postgrad Med J. 2018 Apr;94(1110):212–215. https://doi.org/10.1136/postgradmedj-2017-135454

Klein RD, Hultgren SJ. Urinary tract infections: microbial pathogenesis, host–pathogen interactions and new treatment strategies. Nat Rev Microbiol. 2020 Apr;18(4):211–226. https://doi.org/10.1038/s41579-020-0324-0

Korbel L, Howell M, Spencer JD. The clinical diagnosis and management of urinary tract infections in children and adolescents. Paediatr Int Child Health. 2017 Oct 02;37(4):273–279. https://doi.org/10.1080/20469047.2017.1382046

Manickam K, Karlowsky JA, Adam H, Lagacé-Wiens PRS, Rendina A, Pang P, Murray BL, Alfa MJ. CHROMagar Orientation medium reduces urine culture workload. J Clin Microbiol. 2013 Apr 01;51(4):1179–1183. https://doi.org/10.1128/JCM.02877-12

Nomura F. Proteome-based bacterial identification using matrix-assisted laser desorption ionization–time of flight mass spectrometry (MALDI-TOF MS): A revolutionary shift in clinical diagnostic microbiology. Biochimica et Biophysica Acta (BBA) – Proteins and Proteomics. 2015 Jun;1854(6):528–537. https://doi.org/10.1016/j.bbapap.2014.10.022

Nomura F, Tsuchida S, Murata S, Satoh M, Matsushita K. Mass spectrometry-based microbiological testing for blood stream infection. Clin Proteomics. 2020 Dec;17(1):14.
https://doi.org/10.1186/s12014-020-09278-7

Oviaño M, Ramírez CL, Barbeyto LP, Bou G. Rapid direct detection of carbapenemase-producing Enterobacteriaceae in clinical urine samples by MALDI-TOF MS analysis. J Antimicrob Chemother. 2017 May 1;72(5):1350–1354.
https://doi.org/10.1093/jac/dkw579

Sauget M, Valot B, Bertrand X, Hocquet D. Can MALDI-TOF mass spectrometry reasonably type bacteria? Trends Microbiol. 2017 Jun;25(6):447–455. https://doi.org/10.1016/j.tim.2016.12.006

Sood A, Penna FJ, Eleswarapu S, Pucheril D, Klett DE, Abd-El-Barr A-E-R, Abdollah F, Lakshmanan Y, Menon M, Trinh Q-D, et al. 503 Incidence, admission rates and economic burden of pediatric emergency department visits for urinary tract infection. Eur Urol Suppl. 2015 Apr;14(2):e503–e503a.
https://doi.org/10.1016/S1569-9056(15)60496-1

Sun C, Zhang X, Wang J, Cheng C, Kang H, Gu B, Ma P. Matrix-assisted laser desorption ionization time-of-flight mass spectrometry combined with UF-5000i urine flow cytometry to directly identify pathogens in clinical urine specimens within 1 hour. Ann Transl Med. 2020 May;8(9):602–611.
https://doi.org/10.21037/atm.2019.10.73

Vincent CR, Thomas TL, Reyes L, White CL, Canales BK, Brown MB. Symptoms and risk factors associated with first urinary tract infection in college age women: a prospective cohort study. J Urol. 2013 Mar;189(3):904–910.
https://doi.org/10.1016/j.juro.2012.09.087

Wang XH, Zhang G, Fan YY, Yang X, Sui WJ, Lu XX. Direct identification of bacteria causing urinary tract infections by combining matrix-assisted laser desorption ionization-time of flight mass spectrometry with UF-1000i urine flow cytometry. J Microbiol Methods. 2013 Mar;92(3):231–235.
https://doi.org/10.1016/j.mimet.2012.12.016

Zboromyrska Y, Rubio E, Alejo I, Vergara A, Mons A, Campo I, Bosch J, Marco F, Vila J. Development of a new protocol for rapid bacterial identification and susceptibility testing directly from urine samples. Clin Microbiol Infect. 2016 Jun;22(6):561.e1–561.e6.
https://doi.org/10.1016/j.cmi.2016.01.025

Environmental Factors Associated with the Eukaryotic Microbial Community and Microalgal Groups in the Mountain Marshes of South Korea

YOUNG-SAENG KIM[1][*][†], HYUN-SIK YUN[2][†], JEA HACK LEE[2], HAN-SOON KIM[2][*]
and HO-SUNG YOON[2, 3][*]

[1] Research Institute of Ulleung-do and Dok-do, Kyungpook National University, Daegu, South Korea
[2] Department of Biology, College of Natural Sciences, Kyungpook National University, Daegu, South Korea
[3] School of Life Sciences, BK21 FOUR KNU Creative BioResearch Group,
Kyungpook National University, Daegu, South Korea

Abstract

The diversity indices of eukaryotic microalgal groups in the Jeonglyeongchi, Waegok, and Wangdeungjae marshes of Mount Jiri, Korea, were measured using Illumina MiSeq and culture-based analyses. Waegok marsh had the highest species richness, with a Chao1 value of 828.00, and the highest levels of species diversity, with Shannon and Simpson index values of 6.36 and 0.94, respectively, while Wangdeungjae marsh had the lowest values at 2.97 and 0.75, respectively. The predominant species in all communities were *Phagocata sibirica* (Jeonglyeongchi, 68.64%), *Aedes albopictus* (Waegok, 34.77%), *Chaetonotus* cf. (Waegok, 24.43%), *Eimeria* sp. (Wangdeungjae, 26.17%), and *Eumonhystera* cf. (Wangdeungjae, 22.27%). Relative abundances of the microalgal groups Bacillariophyta (diatoms) and Chlorophyta (green algae) in each marsh were respectively: Jeonglyeongchi 1.38% and 0.49%, Waegok 7.0% and 0.3%, and Wangdeungjae 10.41% and 4.72%. Illumina MiSeq analyses revealed 34 types of diatoms and 13 types of green algae. Only one diatom (*Nitzschia dissipata*) and five green algae (*Neochloris* sp., *Chlamydomonas* sp., *Chlorococcum* sp., *Chlorella vulgaris*, *Scenedesmus* sp.) were identified by a culture-based analysis. Thus, Illumina MiSeq analysis can be considered an efficient tool for analyzing microbial communities. Overall, our results described the environmental factors associated with geographically isolated mountain marshes and their respective microbial and microalgal communities.

K e y w o r d s: environmental sample, Illumina MiSeq, Mount Jiri marshes, microbial community, microalgal community

Introduction

Mount Jiri (hereafter referred to as Jiri) is located at the southern tip of the Sobaek Mountain ranges in the southern part of the Korean peninsula. It covers a vast area, spanning five cities, and it is the second-highest mountain (1915 m) in South Korea, with slopes of 28°–30° (Kim and Jung 2018). Jiri presents annual average temperature of 13°C and an average annual precipitation of 1,350–1,510 mm, with 69% of the rainfall concentrated between June and September (Kim and Jung 2018). Mountain streams and high marshes have developed depending on groundwater and rainfall. Such freshwater ecosystems may be geographically isolated due to weathering and erosion (Wieringa 1964; Kim and Jung 2018). Jiri has well-developed mountain marshes that can be separated and isolated by the mountain ranges or originated from separate water sources (Wieringa 1964; Kim and Jung 2018). Here, we studied three mountain marshes – Jeonglyeongchi, Waegok, and Wangdeungjae – and their different environmental factors associated with their respective microbial and microalgal communities.

Jiri's high marshes characteristics have been influenced by topography and soil properties (Yang 2008; Kim et al. 2010). In particular, the soil of Jiri's high

marshes presents high water retention and poor permeability, allowing fresh water to flow into the wetlands (Yang 2008; Kim et al. 2010). Because of the low soil permeability, sediments around Mount Jiri tend to build up, influencing the development of soil layers (Yang 2008; Kim et al. 2010). Thus, soil in Mount Jiri is characterized by organic layers and deep O and A soil horizons (Anderson 1988; Bormann et al. 1995; Huggett 1998; Hartemink et al. 2020). The soil supports a thriving vegetation, along with peat deposits (Anderson 1988; Bormann et al. 1995; Huggett 1998). Some microorganisms can use the peat as an energy source, leading to the formation of a unique type of microbial community (Williams and Yavitt 2003; Dobrovol'skaya et al. 2012). This microbial community contains decomposers that can degrade cellulose and/or lignin as well as consumers that utilize the resulting degradation products (Berg and McClaugherty 2003; Berg and Laskowski 2005; Stone et al. 2020), including organic carbon sources, nitrogen, phosphorus, and trace elements (Jewell 1971; Garber 1984; Canfield et al. 2020; Zhang et al. 2020). In addition, microalgal groups consume nitrogen and phosphorus (Di Termini et al. 2011) and are involved in cycling these elements through photosynthesis (McGlathery et al. 2004). Microalgal groups can act as producers (of oxygen), consumers (of organic carbon sources), and decomposers (of cellulose and lignin, using them as energy sources) (Schoenberg et al. 1984; Perez-Garcia et al. 2011; Blifernez-Klassen et al. 2012). Therefore, microalgal groups can play a variety of ecological roles and potentially affect the diversity of the microbial community (Schoenberg et al. 1984; Perez-Garcia et al. 2011; Blifernez-Klassen et al. 2012).

Each of the Jiri marshes possesses unique characteristics, making them attractive sites for the comparative analyses of physicochemical factors and microbial communities (Yang 2008; Kim and Jung 2018). In this study, we investigated three mountain marsh sites by analyzing the microbial community DNA of eukaryotic microalgal groups and other microorganisms based on the amplification of the 18S rRNA gene. In addition, the geographic isolation between the mountain marshes was tested to identify the environmental factors affecting microbial and microalgal communities in the marshes.

Experimental

Materials and Methods

Collection of samples. Samples were collected from Jeonglyeongchi marsh (35°21'52.5"N 127°31'25.5"E, Deokdong-ri, Sannae-myeon, Namwon-si, Jeollabuk-do, South Korea), Waegok marsh (35°22'57.0"N 127°46'49.7"E, Yupyeong-ri, Samjang-myeon, San-

cheong-gun, Gyeongsangnam-do, South Korea), and Wangdeungjae marsh (35°23'21.8"N 127°47'19.0"E, Yupyeong-ri, Samjang-myeon, Sancheong-gun, Gyeongsangnam-do, South Korea) (Fig. 1) in July 2019, at ten different locations within each marsh. Each sample consisted of 500 ml of freshwater. Samples were transported to the laboratory, then shipped to Macrogen Co., Ltd. using the same-day express courier service. All analyses were performed at room temperature. All living materials were immediately examined and then fixed in 5% formalin for permanent preservation and detailed identification (Kim and Jung 2018).

Physicochemical analysis. Temperature, pH, electrical conductivity (EC), salinity, dissolved oxygen (DO), and nephelometric turbidity of the samples were measured on-site using a multiparameter instrument (U-50 Multiparameter Water Quality Meter, HORIBA, Kyoto, Japan). A water test kit (HUMAS, Daejeon, South Korea) was used to measure total nitrogen (TN) and total phosphorus (TP) in each sample.

Microbial community analysis. Illumina MiSeq analyses of the microbial communities were performed by the Macrogen (Macrogen, Seoul, South Korea, https://dna.macrogen.com/kor/), as described previously (Yun et al. 2019). DNA for Illumina MiSeq sequencing was extracted from the samples according to the manufacturer's protocol of the PowerSoil® DNA Isolation Kit (Cat. No. 12888, MO BIO) (Claassen et al. 2013). PicoGreen and Nanodrop were used for quantification and quality measurements of the extracted DNA. Extracted DNA samples were amplified by PCR according to the Illumina 18S Metagenomic Sequencing Library protocols (Vo and Jedlicka 2014). The 18S V4 primer set was used to amplify the 18S rRNA regions (Stoeck et al. 2010). TAReuk454FWD1 (forward primer, 5'-CCAGCA(G/C)C(C/T)GCGG-TAATTCC-3') and TAReukREV3 (reverse primer, 5'-ACTTTCGTTCTTGAT(C/T)(A/G)A-3') were used as the 18S V4 primer set (Stoeck et al. 2010). A subsequent limited-cycle amplification was conducted for the addition of multiplexing indices and Illumina sequencing adapters (Meyer and Kircher 2010). The target DNA fragment size of PCR amplification is approximately 420 bp; the final DNA fragments were pooled and normalized using PicoGreen. TapeStation DNA and D1000 ScreenTape system (Agilent) was used to verify the library size. The sequencing data results were analyzed using the MiSeq™ platform (Illumina, San Diego, USA) (Kozich et al. 2013).

Taxonomic identification and phylogenetic analysis. The raw sequencing data were demultiplexed using the index sequence, and a FASTQ file was generated for each sample (Yun et al. 2019). The adapter sequence was removed using SeqPurge, and the sequencing error correction was performed on the overlapping areas of the
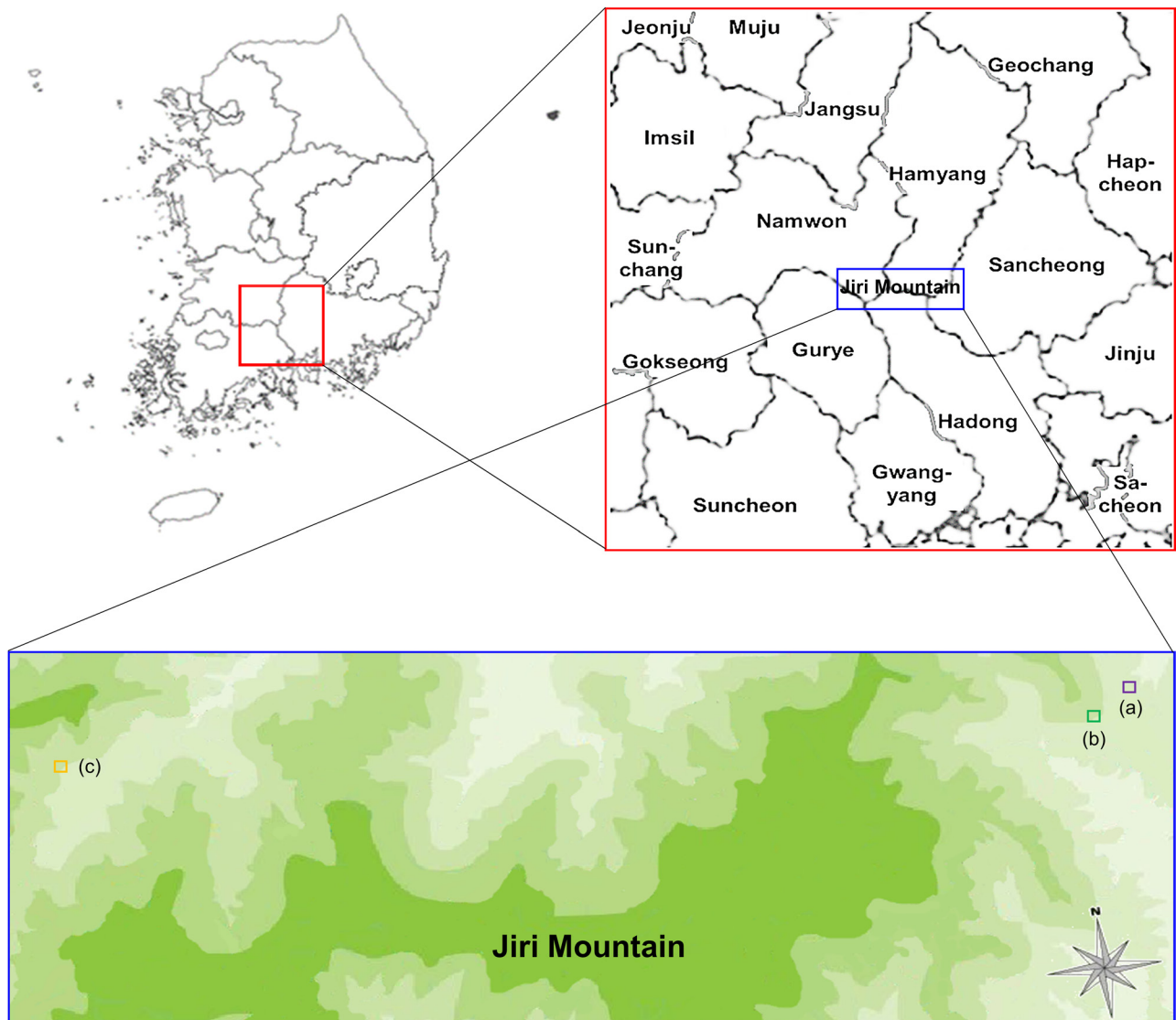
Fig. 1. Location of sampling sites at three mountain marshes. Red box: location of Mountain Jiri, covering five cities in the southern part of the Korean peninsula. Blue box: location of Mountain Jiri and sampling sites marked with small boxes.
a) Purple box, Wangdeungjae marsh, 35°23′21.8″N 127°47′19.0″E. b) Green box, Waegok marsh, 35°22′57.0″N 127°46′49.7″E. c) Orange box, Jeong-lyeongchi marsh, 35°21′52.5″N 127°31′25.5″E.

correct reads (Sturm et al. 2016). Low-quality sequences of barcode sequences were trimmed and filtered (standard: 400 bp < read length or 25 < average quality value). The trimmed and filtered sequencing data were identified using a BLASTN search from the NCBI database, based on their barcode sequences (Zhang et al. 2000). For the unclassified results, "–" was marked to the end of the name for each sublevel. Each operational taxonomic unit (OTU) was analyzed based on the CD-HIT at a 97% sequence similarity level (Li et al. 2012). The rarefaction curves and the diversity indicators (Shannon, Simpson, and Chao1) were calculated using the Mothur platform (Heck Jr et al. 1975; Schloss et al. 2009). Based on the weighted UniFrac distance, Beta diversity (sample diversity information of the comparison group) was calculated and used to visualize the relationship between the

samples using the UPGMA tree (FigTree, http://tree.bio. ed.ac.uk/software/figtree/). Phylogenetic analysis was performed using the software package MEGA version 7.0 (Kumar et al. 2008; Kumar et al. 2016). The identified sequencing data groups were aligned using ClustalW and incorporated in MEGA 7.0 (Kumar et al. 2008; Kumar et al. 2016). The best-fit nucleotide substitution model was selected based on the Bayesian information criterion (Schwarz 1978). The maximum likelihood (ML) phylogenetic tree was built according to the best-fit nucleotide substitution model (Felsenstein 1985).

Culture-based analysis of microalgal groups. To culture microalgae, 1 ml of each sample was inoculated into 100 ml of culture medium in a 250 ml flask (Rippka et al. 1979; Bolch and Blackburn 1996). Four types of culture media were used: Blue Green-11 (BG11)

medium, Optimum *Haematococcus* Medium (OHM), Bold Basal medium (BB), and Diatom Medium (DM) (Agrawal and Sarma 1982; Bolch and Blackburn 1996; Fábregas et al. 2000; Safonova et al. 2007). The cultures were grown under constant shaking (VS-202D orbital shaker, Vision Scientific, Bucheon, South Korea) and exposed to light in an illuminated incubation room (light: dark cycle of 16:8 h, fluorescent lamp, approximately 55 μmol photons) set at 25°C. Microalgae were cultivated for two weeks, and the resulting cultures were spread on agar plates and incubated until algal colonies formed. Then, the latter would be transferred aseptically to fresh medium (Stanier et al. 1971). The number of colonies that formed on the first set of plats was counted, and data were analyzed as described in the next section. An optical microscope (Nikon Eclipse E100 Biological Microscope, Tokyo, Japan) was used for morphological identification and the 18S V4 region of selected cultures was amplified and sequenced for molecular identification (Stoeck et al. 2010).

Statistical analysis. We compared individual data points using the Student's *t*-test. A *p*-value of < 0.05 was considered statistically significant. All data were subjected to one-way analysis of variance (ANOVA). All statistical analyses were performed using the Statistical Package for the Social Sciences software (SPSS). All the experiments were performed at least in triplicate, and all the traditional microbiological data are expressed as mean ± standard deviation (SD) (n = 3).

Results

Environmental factors and species diversity estimates. The physicochemical characteristics of Jeonglyeongchi, Waegok, and Wangdeungjae marshes are summarized in Table I. The registered average temperatures in Jeonglyeongchi, Waegok, and Wangdeungjae were 12.75°C, 16.55°C, and 22.93°C, respectively. The pH values of all marshes were between pH 6 and 7 – pH 6.95 at Jeonglyeongchi, pH 6.84 at Waegok, and pH 6.48 at Wangdeungjae. The EC values at Jeonglyeongchi and Waegok were 32 and 36 μS/cm, respectively, and significantly lower than 96 μS/cm registered at Wangdeungjae. The marshes differed by approximately 3 mg/l in DO, as its values at Jeonglyeongchi, Waegok, and Wangdeungjae were 10.51, 7.98, and 4.71 mg/l, respectively. The turbidity at Waegok averaged 42.30 nephelometric turbidity units (NTU), which was considerably higher than those at Jeonglyeongchi (2.51 NTU) and Wangdeungjae (6.26 NTU). The TP levels at Jeonglyeongchi and Waegok were 1.57 ± 0.16 and 0.94 ± 0.01 mg/l, respec-

Table I
Physicochemical measurements, sequencing results, and ecological diversity analysis
of Mount Jiri marsh samples.

x		Jeonglyeongchi	Waegok	Wangdeungjae
Physico-chemical factors	Temperature (°C)	12.75	16.55	22.93
	pH	6.95	6.84	6.48
	EC (μS/cm)	32	36	96
	Salinity (ppt)	0.0	0.0	0.0
	DO (mg/l)	10.51	7.98	4.71
	Turbidity (NTU)	2.51	42.30	6.26
	TN (mg/l)	0.00 ± 0.00	0.00 ± 0.00	0.00 ± 0.00
	TP (mg/l)	1.57 ± 0.16	0.94 ± 0.01	0.00 ± 0.00
Sequencing results	Total reads	122,953	113,853	121,392
	Validated reads	98,159	80,099	22,249
	Mean read length (bp)	406.28	402.63	401.70
	Maximum read length (bp)	419	407	407
	Number of OTUs[a]	243	828	64
Diversity indicators	Chao1[b]	243.00	828.00	64.00
	Shannon[c]	4.84	6.36	2.97
	Simpson[d]	0.91	0.94	0.75
	Goods Coverage[e]	1.00	1.00	1.00

[a] – OTUs: Operational Taxonomic Units

[b] – Chao1: species richness estimation, a count of the species present

[c] – Shannon: Shannon diversity index (> 0, higher is more diverse)

[d] – Simpson: Simpson diversity index (0 – 1, 1 = most diverse)

[e] – Goods Coverage: number of singleton OTUs/number of sequences (1 = 100% coverage)
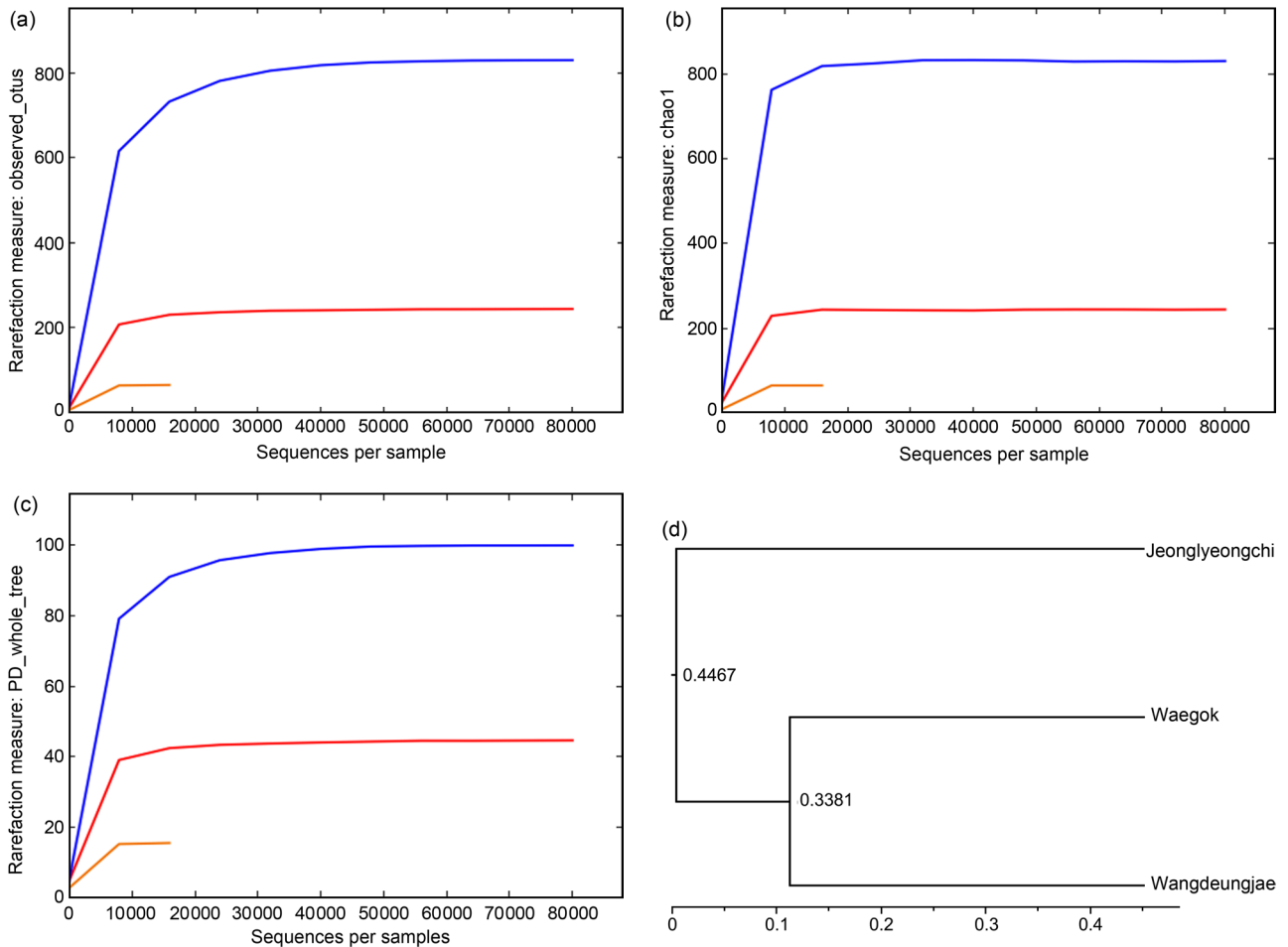
Fig. 2. Rarefaction curves for OTUs representing the eukaryotic microbial communities associated with the marsh samples. The OTUs were analyzed using the cluster database that was set at high identity, with the tolerance (CD-HIT) program set at a 97% sequence similarity. The Mothur platform was used to calculate the rarefaction curves and diversity indices.

a) OTUs. b) Chao1 estimator. c) Whole tree (Waegok, red curve; Jeonglyeongchi, blue curve; Wangdeungjae, orange curve). d) UPGMA tree illustrating the relationships based on weighted UniFrac distances between the eukaryotic microbial communities associated with Jeonglyeongchi, Waegok, and Wangdeungjae marshes.

tively, and undetectable in Wangdeungjae. The salinity and TN levels in all the marshes were below the detection limits. Overall, Jeonglyeongchi and Waegok have shown to have similar physicochemical characteristics.

The analysis of Illumina MiSeq results and taxonomic identifications based on the NCBI database are summarized in supplementary Table SI. The GenBank accession numbers (PRJNA694792) for the microbial community in South Korean Mount Jiri marshes were accepted. In terms of the number of validated reads and their ratio to phylogenetics, Jeonglyeongchi (ratio = 79.83 %) had the highest number and ratio of validated reads, followed by Waegok (ratio = 70.35 %), and Wangdeungjae (ratio = 18.33 %). The mean and maximum read lengths for each marsh were as follows: Jeonglyeongchi, 406.28 and 419 bp; Waegok, 402.63 and 407 bp; and Wangdeungjae, 401.70 and 407 bp. Using a 3% sequence cutoff value, OTUs totaled 243 for Jeonglyeongchi, 828 for Waegok, and 64 for Wangdeungjae. The high numbers of OTUs at Jeonglyeongchi and

Waegok have indirectly confirmed the high diversity of the habitats, especially at Waegok.

We measured the species' richness using the Chao1 estimator, which counts the number of species within a community without considering their abundance levels. Shannon and Simpson's diversity indices measured the species' diversity, both of which account for the evenness of species distribution and their abundance (the number of individuals per species). The Chao1, Shannon, and Simpson index values for Waegok were 828.00, 6.36, and 0.94, respectively, which were remarkably higher than the corresponding Wangdeungjae values of 64.00, 2.97, and 0.75, respectively (Fig. 2). The whole tree was obtained by adding up all the branch lengths of a phylogenetic tree to measure diversity based on Waegok, Jeonglyeongchi, and Wangdeungjae (Fig. 2c). The relationships between sites based on the weighted UniFrac distances were generated from our sequence data. Fig. 2d shows that Waegok and Wangdeungjae were the marshes with the most similarity in
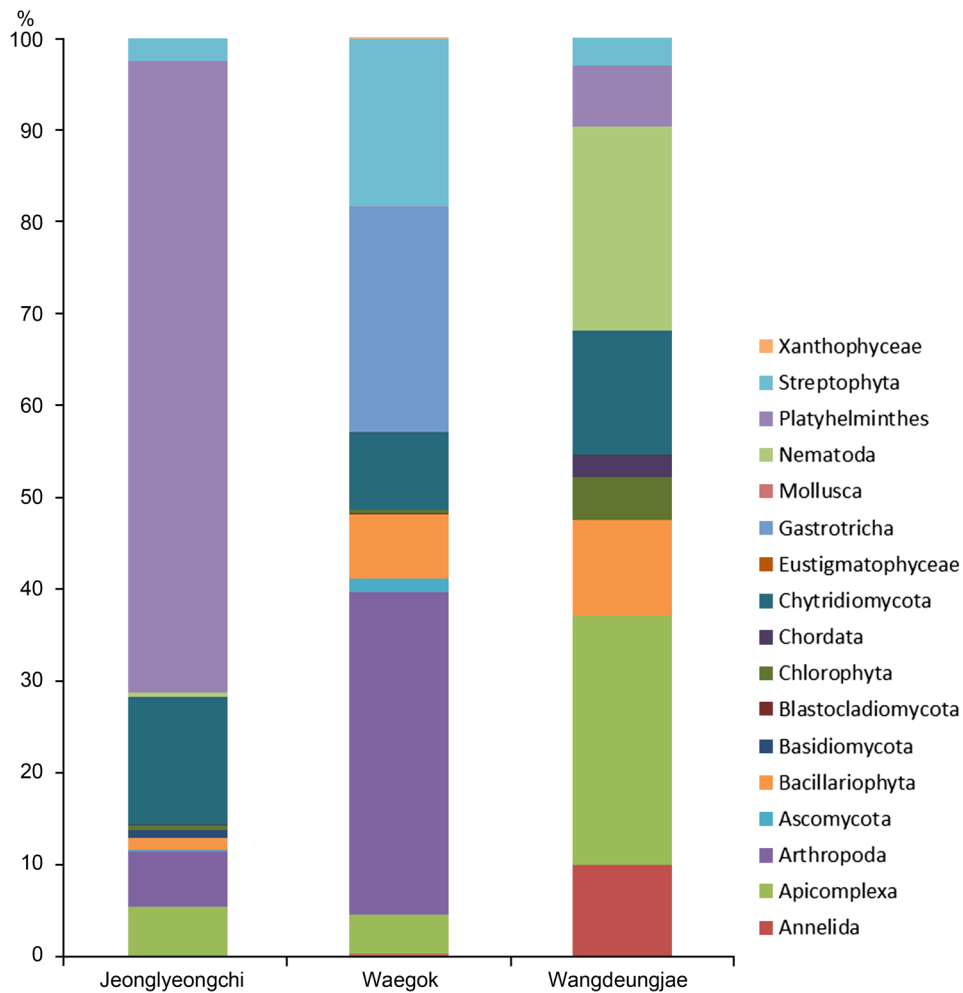
Fig. 3. Taxonomic composition of microalgal and other microbial phyla found in Jeonglyeongchi, Waegok, and Wangdeungjae marsh samples.

eukaryotic communities. Waegok is characterized by moderate environmental conditions and had the highest species richness and diversity among the three sites.

Structure of microbial community and microalgal composition. The taxonomic composition of the eukaryotic microbial communities was analyzed at the phylum level (Fig. 3). Seventeen phyla were detected in the three marshes (Fig. 3), 11 of which were present in Jeonglyeongchi (Table II). Only Chytridiomycota (13.95%) and Platyhelminthes (68.71%) were present at abundance levels greater than 10%. The highest number of phyla was detected in Waegok (15 phyla) (Table II). Of these, Arthropoda (35.01%), Gastrotricha (24.43%), and Streptophyta (18.30%) were present at levels greater than 10%. Nine phyla were detected at Wangdeungjae (Table II), of which Apicomplexa (27.10%), Bacillariophyta (10.41%), Chytridiomycota (13.47%), and Nematoda (22.27%) were present at abundance levels greater than 10%. Phylum distribution was not biased toward a specific phylum. However, Jeonglyeongchi was dominated by phylum Platyhelminthes (among 11 phyla), whereas three-four phyla dominate Waegok

and Wangdeungjae. Among the three marshes, Waegok presented the most diverse eukaryotic community.

We found 123 species of unclassified taxonomic names in the three marshes. Table II and supplementary Table SI summarize the relative abundance levels of species in Jeonglyeongchi (33 species), Waegok (96 species), and Wangdeungjae (21 species). The following species were present at abundance levels greater than 5%: Jeonglyeongchi, four species (*Eimeriidae environmental*, *Hygrobates norvegicus*, *Rhizoclosmatium globosum*, and *Phagocata sibirica*); Waegok, three species (*Aedes albopictus*, *Chaetonotus* cf., and *Stipa narynica*); Wangdeungjae, six species (*Dero* sp. *Eimeria* sp., *Aulacoseira* sp., *Chytriomyces* sp., *Eumonhystera* cf., and *Stenostomum* sp.). The phylogenetic relationships between all species comprising the marsh communities were visualized using the ML tree analysis (Fig. 4a) (Schwarz 1978; Felsenstein 1985; Kumar et al. 2008; Kumar et al. 2016). Samples from Waegok had the highest species richness and diversity, with 96 species representing 78.04% of the total species present in all communities.

Table II

Relative abundance of species in the Jeonglyeongchi, Waegok, and Wangdeungjae samples.

Taxonomy					Relative abundance (%)		
Phylum	Class	Order	Family	Species	Jeonglyeongchi	Waegok	Wangdeungjae
Annelida	–	Haplotaxida	Enchytraeidae	*Mesenchytraeus pelicensis*	0	0.05	0
Annelida	–	Haplotaxida	Naididae	*Dero sp.*	0	0.17	9.98
Apicomplexa	–	–	–	*Apicomplexan Acarus*	0	0.01	0
Apicomplexa	–	–	Sphaerocystidae	*Paraschneideria metamorphosa*	0	0.19	0
Apicomplexa	Coccidia	Eucoccidiorida	Cryptosporidiidae	*Cryptosporidiidae environmental*	0	3.09	0.93
Apicomplexa	Coccidia	Eucoccidiorida	Eimeriidae	*Eimeriidae environmental*	5.43	1.11	0
Apicomplexa	Coccidia	Eucoccidiorida	Eimeriidae	*Eimeria sp.*	0	0	26.17
Arthropoda	–	Cyclopoida	Cyclopidae	*Paracyclops chiltoni*	0	0.16	0
Arthropoda	Arachnida	–	Anystidae	*Anystis sp.*	0	0.03	0
Arthropoda	Arachnida	–	Hygrobatidae	*Hygrobates norvegicus*	5.73	0	0
Arthropoda	Insecta	Diptera	Chironomidae	*Micropsectra sp.*	0.31	0	0
Arthropoda	Insecta	Diptera	Chironomidae	*Monodiamesa sp.*	0	0.05	0
Arthropoda	Insecta	Diptera	Culicidae	*Aedes albopictus*	0	34.77	0
Ascomycota	–	–	–	*Uncultured ascomycete*	0	0.04	0
Ascomycota	Saccharomycetes	Saccharomycetales	Debaryomycetaceae	*[Candida] schatavii*	0.07	0	0
Ascomycota	Sordariomycetes	–	–	*Leptosporella sp.*	0	0.11	0
Ascomycota	Sordariomycetes	Chaetosphaeriales	Chaetosphaeriaceae	*Thozetella pandanicola*	0	1.24	0
Ascomycota	Sordariomycetes	Diaporthales	Diaporthaceae	*Diaporthe amygdali*	0	0.02	0
Ascomycota	Sordariomycetes	Hypocreales	Nectriaceae	*Fusarium oxysporum*	0	0.05	0
Ascomycota	Sordariomycetes	Xylariales	–	*Discosia querci*	0	0.01	0
Bacillariophyta	Bacillariophyceae	–	–	*Achnanthidium daonense*	0	0.04	0
Bacillariophyta	Bacillariophyceae	–	–	*Achnanthidium digitatum*	0	0.11	0
Bacillariophyta	Bacillariophyceae	–	–	*Achnanthidium minutissimum*	0	0.25	0
Bacillariophyta	Bacillariophyceae	–	–	*Achnanthidium straubianum*	0	0.12	0
Bacillariophyta	Bacillariophyceae	–	Bacillariaceae	*Nitzschia acidoclinata*	0	0.04	0
Bacillariophyta	Bacillariophyceae	–	Bacillariaceae	*Nitzschia dissipata*	0	0.18	0
Bacillariophyta	Bacillariophyceae	–	Cymbellaceae	*Cymbella aspera*	0	1.45	0
Bacillariophyta	Bacillariophyceae	–	Cymbellaceae	*Cymbopleura naviculiformis*	0	0.82	0
Bacillariophyta	Bacillariophyceae	–	Cymbellaceae	*Placoneis elginensis*	0	0.09	0
Bacillariophyta	Bacillariophyceae	–	Gomphonemataceae	*Gomphonema affine*	0.57	0.36	0
Bacillariophyta	Bacillariophyceae	–	Gomphonemataceae	*Gomphonema cf.*	0	0.18	0

Table II. Continued.

Phylum	Class	Order	Family	Species	Relative abundance (%)		
					Jeonglyeongchi	Waegok	Wangdeungjae
Bacillariophyta	Bacillariophyceae	Eunotiales	Eunotiaceae	*Eunotia* sp.	0.24	0.14	0.81
Bacillariophyta	Bacillariophyceae	Naviculales	–	*Humidophila australis*	0	0.03	0
Bacillariophyta	Bacillariophyceae	Naviculales	–	Uncultured *Halamphora*	0	0.03	0
Bacillariophyta	Bacillariophyceae	Naviculales	Amphipleuraceae	*Halamphora* sp.	0	0.11	0
Bacillariophyta	Bacillariophyceae	Naviculales	Naviculaceae	*Pinnunavis* sp.	0	0.18	0
Bacillariophyta	Bacillariophyceae	Naviculales	Naviculaceae	*Navicula* sp.	0	0.04	0
Bacillariophyta	Bacillariophyceae	Naviculales	Neidiaceae	*Neidium hitchcockii*	0	0.01	0
Bacillariophyta	Bacillariophyceae	Naviculales	Neidiaceae	*Neidium* sp.	0	0.11	0
Bacillariophyta	Bacillariophyceae	Naviculales	Pinnulariaceae	*Pinnularia* cf.	0	0.11	0
Bacillariophyta	Bacillariophyceae	Naviculales	Pinnulariaceae	*Pinnularia microstauron*	0	0.51	0
Bacillariophyta	Bacillariophyceae	Naviculales	Pinnulariaceae	*Pinnularia subgibba*	0.34	0	0
Bacillariophyta	Bacillariophyceae	Naviculales	Pinnulariaceae	*Pinnularia viridiformis*	0	0.04	0
Bacillariophyta	Bacillariophyceae	Naviculales	Sellaphoraceae	*Sellaphora* cf.	0	0.01	0
Bacillariophyta	Bacillariophyceae	Naviculales	Sellaphoraceae	*Sellaphora pupula*	0	0.04	0
Bacillariophyta	Bacillariophyceae	Surirellales	–	*Surirella brebissonii*	0	0.75	0
Bacillariophyta	Bacillariophyceae	Surirellales	–	*Surirella* cf.	0	0.08	0
Bacillariophyta	Bacillariophyceae	Surirellales	–	*Surirella* sp.	0	0.09	0
Bacillariophyta	Bacillariophyceae	Thalassiophysales	Catenulaceae	*Amphora copulata*	0	0.21	0
Bacillariophyta	Coscinodiscophyceae	–	Aulacoseiraceae	*Aulacoseira alpigena*	0	0.12	1.83
Bacillariophyta	Coscinodiscophyceae	–	Aulacoseiraceae	*Aulacoseira* sp.	0	0	7.77
Bacillariophyta	Coscinodiscophyceae	Chaetocerotales	Chaetocerotaceae	Uncultured *Chaetoceros*	0	0.02	0
Bacillariophyta	Fragilariophyceae	Fragilariales	Fragilariaceae	*Fragilaria vaucheriae*	0	0.29	0
Bacillariophyta	Fragilariophyceae	Tabellariales	Tabellariaceae	*Tabellaria flocculosa*	0.23	0.44	0
Basidiomycota	Agaricomycetes	Agaricales	–	*Inocybe spuria*	0	0.01	0
Basidiomycota	Agaricomycetes	Polyporales	–	*Fibroporia gossypium*	0.11	0.08	0
Basidiomycota	Tremellomycetes	–	–	*Holtermanniella nyarrowii*	0.04	0	0
Basidiomycota	Tremellomycetes	Cystofilobasidiales	Cystofilobasidiaceae	*Cystofilobasidium macerans*	0.31	0.01	0
Basidiomycota	Tremellomycetes	Filobasidiales	–	*Solicoccozyma terricola*	0.21	0	0
Basidiomycota	Tremellomycetes	Filobasidiales	Filobasidiaceae	*Filobasidium magnum*	0.15	0	0
Basidiomycota	Tremellomycetes	Tremellales	–	*Cryptococcus carnescens*	0.02	0	0
Basidiomycota	Tremellomycetes	Tremellales	–	*Papiliotrema flavescens*	0.03	0	0 0

Table II. Continued.

| Taxonomy | | | | | Relative abundance (%) | | |
Phylum	Class	Order	Family	Species	Jeonglyeongchi	Waegok	Wangdeungjae
Blastocladiomycota	–	–	–	Uncultured Blastocladiomycota	0	0.11	0
Chlorophyta	–	–	–	Chlorophyta sp.	0	0.01	0
Chlorophyta	Chlorophyceae	–	Microsporaceae	Microspora sp.	0	0	1.24
Chlorophyta	Chlorophyceae	Chlamydomonadales	Chlamydomonadaceae	Chlamydomonas sp.	0	0.05	1.24
Chlorophyta	Chlorophyceae	Chlamydomonadales	Chlorococcaceae	Chlorococcum sp.	0	0.04	0
Chlorophyta	Chlorophyceae	Sphaeropleales	–	Dictyococcus sp.	0	0.08	0
Chlorophyta	Chlorophyceae	Sphaeropleales	–	Bracteacoccus deserticola	0	0	0.09
Chlorophyta	Chlorophyceae	Sphaeropleales	Neochloridaceae	Neochloris sp.	0.22	0	0
Chlorophyta	Chlorophyceae	Sphaeropleales	Scenedesmaceae	Scenedesmus sp.	0	0	1.71
Chlorophyta	Chlorophyceae	Sphaeropleales	Scenedesmaceae	Asterarcys quadricellulare	0	0.02	0
Chlorophyta	Trebouxiophyceae	–	Coccomyxaceae	Coccomyxa simplex	0.15	0.01	0
Chlorophyta	Trebouxiophyceae	Chlorellales	Chlorellaceae	Chlorella vulgaris	0	0.01	0.44
Chlorophyta	Ulvophyceae	Ulotrichales	–	Tupiella speciosa	0.12	0.03	0
Chlorophyta	prasinophytes	–	–	Monomastix opisthostigma	0	0.05	0
Chordata	Amphibia	Caudata	Salamandridae	Cynops pyrrhogaster	0.05	0	0
Chordata	Mammalia	Cetacea	Delphinidae	Lagenorhynchus obliquidens	0	0	2.45
Chytridiomycota	–	–	–	Uncultured Chytridiomycota	1.31	1.09	0.44
Chytridiomycota	–	–	–	Uncultured rhizosphere	0	0.01	0
Chytridiomycota	–	–	–	Catenomyces sp.	0	0.08	0
Chytridiomycota	Chytridiomycetes	–	–	Rhizophlyctis rosea	0	0	1.58
Chytridiomycota	Chytridiomycetes	Chytridiales	–	Chytridiales sp.	0	0.41	0
Chytridiomycota	Chytridiomycetes	Chytridiales	–	Uncultured Chytridiales	0	0.46	0
Chytridiomycota	Chytridiomycetes	Chytridiales	–	Uncultured Chytriomyces	0	0.23	0
Chytridiomycota	Chytridiomycetes	Chytridiales	–	Chytriomyces sp.	0.12	0.09	10.94
Chytridiomycota	Chytridiomycetes	Chytridiales	–	Obelidium mucronatum	2.62	0.58	0
Chytridiomycota	Chytridiomycetes	Chytridiales	–	Rhizoclosmatium globosum	9.07	0	0
Chytridiomycota	Chytridiomycetes	Chytridiales	Chytridiaceae	Chytridiaceae sp.	0	0.11	0
Chytridiomycota	Chytridiomycetes	Cladochytriales	–	Nowakowskiella elegans	0	0.02	0
Chytridiomycota	Chytridiomycetes	Cladochytriales	–	Nowakowskiella hemisphaerospora	0.43	0.17	0
Chytridiomycota	Chytridiomycetes	Cladochytriales	–	Nowakowskiella multispora	0	1.61	0
Chytridiomycota	Chytridiomycetes	Cladochytriales	–	Nowakowskiella sp.	0	0.16	0

Table II. Continued.

Phylum	Class	Order	Family	Species	Relative abundance (%)		
					Jeonglyeongchi	Waegok	Wangdeungiae
Chytridiomycota	Chytridiomycetes	Cladochytriales	Cladochytriaceae	*Cladochytrium replicatum*	0	0.02	0
Chytridiomycota	Chytridiomycetes	Cladochytriales	Cladochytriaceae	*Cladochytrium tenue*	0	0.01	0
Chytridiomycota	Chytridiomycetes	Rhizophydiales	–	*Rhizophydiales* sp.	0	0.08	0
Chytridiomycota	Chytridiomycetes	Rhizophydiales	–	*Uebelmesseromyces* sp.	0	0.94	0
Chytridiomycota	Chytridiomycetes	Rhizophydiales	Kappamycetaceae	*Kappamyces laurelensis*	0.13	0.01	0
Chytridiomycota	Chytridiomycetes	Rhizophydiales	Rhizophydiaceae	*Rhizophydium planktonicum*	0	0	0.51
Chytridiomycota	Chytridiomycetes	Rhizophydiales	Rhizophydiaceae	*Rhizophydium sphaerotheca*	0	2.14	0
Chytridiomycota	Chytridiomycetes	Spizellomycetales	–	*Fimicolochytrium alabamae*	0.18	0.15	0
Chytridiomycota	Monoblepharidomycetes	Monoblepharidales	–	*Hyaloraphidium curvatum*	0.09	0.02	0
Chytridiomycota	Monoblepharidomycetes	Monoblepharidales	Harpochytriaceae	*Harpochytrium* sp.	0	0.06	0
Chytridiomycota	Monoblepharidomycetes	Monoblepharidales	Oedogoniomycetaceae	*Oedogoniomyces* sp.	0	0.01	0
Eustigmatophyceae	–	–	–	Uncultured eustigmatophyte	0	0.04	0
Gastrotricha	–	Chaetonotida	Chaetonotidae	*Chaetonotus* cf.	0	24.43	0
Mollusca	Bivalvia	Veneroida	Sphaeriidae	*Pisidium walkeri*	0	0.03	0
Nematoda	Chromadorea	Monhysterida	Monhysteridae	*Eumonhystera* cf.	0.46	0	22.27
Platyhelminthes	–	Catenulida	Catenulidae	*Catenula turgida*	0.07	0	0
Platyhelminthes	–	Catenulida	Stenostomidae	*Stenostomum* sp.	0	0.06	6.62
Platyhelminthes	–	Rhabdocoela	Typhloplanidae	*Phaenocora* sp.	0	0.02	0
Platyhelminthes	–	Tricladida	Planariidae	*Phagocata sibirica*	68.64	0	0
Streptophyta	–	Brassicales	Brassicaceae	*Brassica napus*	0	0	0.34
Streptophyta	–	Caryophyllales	Polygonaceae	*Persicaria virginiana*	1.96	0.01	0
Streptophyta	–	Ericales	Styracaceae	*Styrax americana*	0	0.04	0
Streptophyta	–	Malpighiales	Salicaceae	*Populus trichocarpa*	0	2.84	0
Streptophyta	–	Piperales	–	*Aristolochiaceae* environmental	0.16	0	0
Streptophyta	Liliopsida	Poales	Poaceae	*Stipa narynica*	0	15.14	0
Streptophyta	Zygnemophyceae	Desmidiales	–	Uncultured *Closterium*	0.43	0.06	0
Streptophyta	Zygnemophyceae	Desmidiales	Closteriaceae	*Closterium moniliferum*	0	0.21	0
Streptophyta	Zygnemophyceae	Desmidiales	Closteriaceae	*Closterium venus*	0	0	0.62
Streptophyta	Zygnemophyceae	Desmidiales	Desmidiaceae	*Euastrum affine*	0	0	2.02
Xanthophyceae	–	–	–	*Xanthophyceae* sp.	0	0.05	0

The microbial species detected in at least one of the three samples are shown. Unclassified taxonomic names (phylum, class, order, family, and species) are replaced using underlining (–).
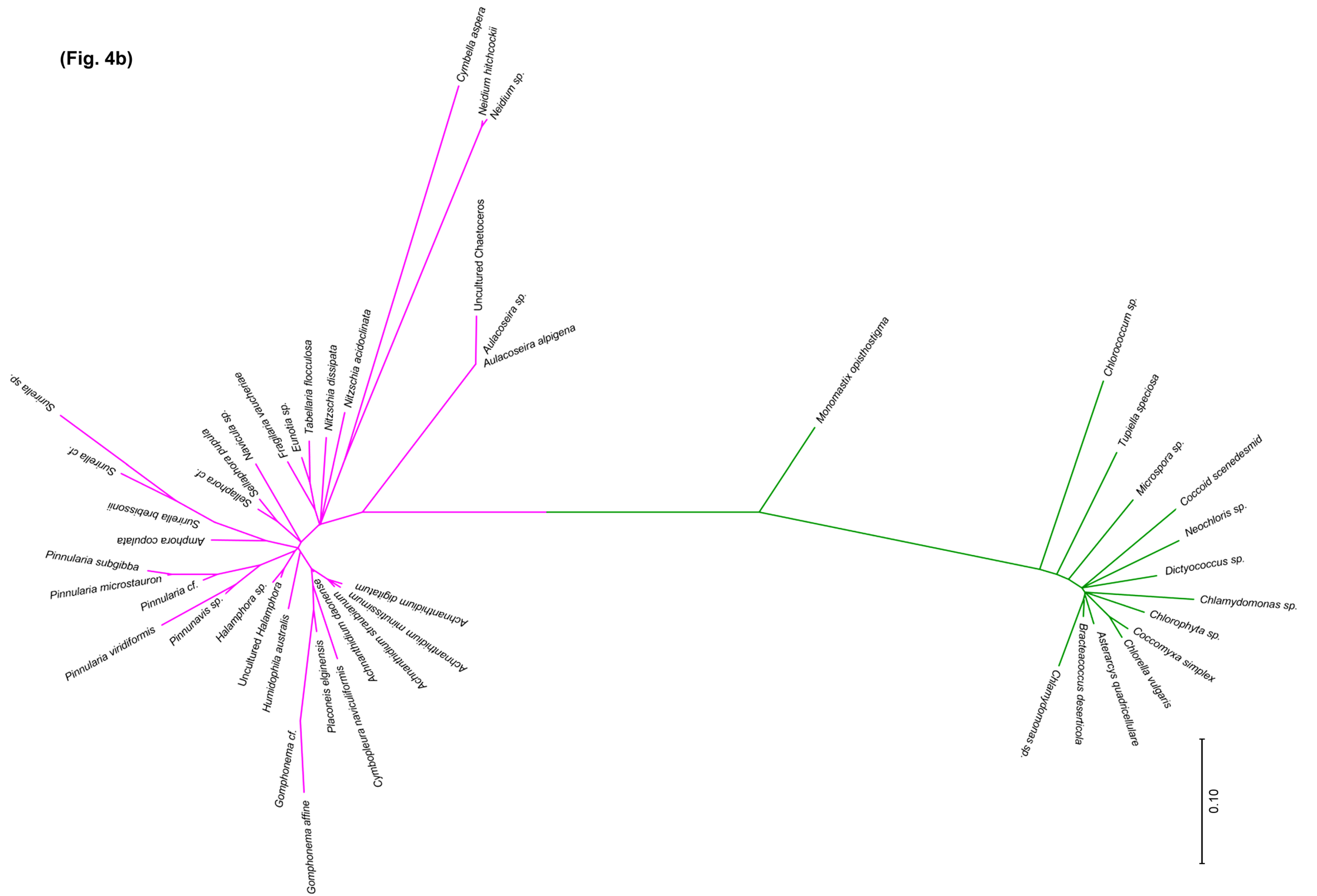
(Fig. 4a)

(Fig. 4b)

Cymbella aspera
Neidium hitchcockii
Neidium sp.
Uncultured Chaetoceros
Aulacoseira sp.
Aulacoseira alpigena
Nitzschia acidoclinata
Tabellaria flocculosa
Eunotia sp.
Fragilaria vaucheriae
Navicula sp.
Sellaphora pupula
Surirella sp.
Surirella cf.
Surirella brebissonii
Amphora copulata
Pinnularia subgibba
Pinnularia microstauron
Pinnularia cf.
Pinnunavis sp.
Pinnularia viridiformis
Halamphora sp.
Uncultured Halamphora
Humidophila australis
Placoneis elginensis
Cymbopleura naviculiformis
Gomphonema cf.
Gomphonema affine
Achnanthidium straubianum
Achnanthidium minutissimum
Achnanthidium digitatum
Achnanthidium delmontense
Monomastix opisthostigma
Chlorococcum sp.
Tupiella speciosa
Microspora sp.
Coccoid scenedesmid
Neochloris sp.
Dictyococcus sp.
Chlamydomonas sp.
Chlorophyta sp.
Coccomyxa simplex
Chlorella vulgaris
Asterarcys quadricellulare
Bracteacoccus deserticola
Chlamydomonas sp.

0.10

Fig. 4. Molecular phylogenetic analysis by the maximum likelihood (ML) tree.
Numbers at the nodes indicate bootstrap probabilities (> 50 v%)
of the ML analyses (1,000 replicates).
a) Phylogenetic relationship between all species identified using a BLASTN search within the
NCBI database. Seventeen phyla corresponded to the species names listed in the phylogenetic tree.
b) Phylogenetic distances between the identified microalgal species (pink branch, Bacillariophyta;
green branch, Chlorophyta).

Microalgal groups represented 6.29% in Jeonglyeongchi (1.38% Bacillariophyta, 0.49% Chlorophyta, 0.00% Eustigmatophyceae, 2.55% Streptophyta, and 0.00% Xanthophyceae); 25.69% in Waegok (7.00% Bacillariophyta, 0.30% Chlorophyta, 0.04% Eustigmatophyceae, 18.30% Streptophyta, and 0.05% Xanthophyceae); and 18.11% in Wangdeungjae (10.41% Bacillariophyta, 4.72% Chlorophyta, 0.00% Eustigmatophyceae, 2.98% Streptophyta, and 0.00% Xanthophyceae) (Fig. 3). The mountain marsh microalgae were composed of 34 Bacillariophyta species, 13 Chlorophyta species, one Eustigmatophyceae species, 10 Streptophyta species, and one Xanthophyceae species (Table II): Jeonglyeongchi contained seven species (four Bacillariophyta and three Chlorophyta), Waegok contained 41 species (32 Bacillariophyta and nine Chlorophyta), and Wangdeungjae contained eight species (three Bacillariophyta and five Chlorophyta). The microalgae in Wangdeungjae were eight times more abundant than those at Jeonglyeongchi, although both marshes shared similar numbers of species (eight and seven, respectively). The phylogenetic distances between the identified microalgal species are represented in Fig. 4b. Waegok, which comprised the highest eukaryotic species richness and diversity, also presented the highest number and abundance of microalgal species. Therefore, the diversity of microalgal groups can be related to the diversity and composition of other groups and species in the eukaryotic microbial communities.

Screening of culturable microalgal species. Microalgae were screened and isolated in four media (BG11, OHM, BB, DM) (Table III, Fig. 5 and supplementary Fig. S1). Although sequencing data identified 34 species of diatom (Bacillariophyta) and 13 species of green algae (Chlorophyta) (Table II), only one species of diatom and five species of green algae were isolated from the four media (Table III). Only *Neochloris* sp. was isolated in all four media inoculated with samples from Jeonglyeongchi. Four species (*Nitzschia dissipata*, *Chlamydomonas* sp., *Chlorococcum* sp., and *Chlorella vulgaris*) were isolated on BG11, BB, and DM from the samples from Waegok, whereas two species were isolated on OHM (*Nitzschia dissipata* and *Chlorococcum* sp.), and *Chlamydomonas* sp. and *Scenedesmus* sp. were isolated from all media inoculated with samples from Wangdeungjae (Fig. 5). Overall, while 47 microalgal species were detected via Illumina MiSeq analysis, only six species (12.77 %) were able to be isolated from cultures.

Discussion

Physicochemical characteristics of Jiri marsh sites. Each marsh presents distinctive environmental characteristics. Jeonglyeongchi marsh had the lowest temperatures registered and the highest DO and TP concentrations (Table I), whereas the temperature at Wangdeungjae marsh (above 20°C) was suitable for the cultivation of microorganisms. The latter marsh also recorded the lowest DO and TP concentrations (Tanner 2007). These mesophilic conditions can promote higher levels of microbial activity compared to low temperatures (Tanner 2007). This increased level of metaolic activity can then change the consumption and overall concentrations of DO and TP (Amon and Benner 1996; Levantesi et al. 2002). In addition, pH and EC, which depend on ion concentrations, vary due to metabolites produced during degradation (Kwabiah et al. 2001; Berg and Laskowski 2005; Rousk et al. 2010). These results support the idea that temperature plays a major role as an environmental factor in all the studied marshes (Witkamp and Frank 1970; Tanner 2007; Kukharenko et al. 2010).

Moreover, Illumina MiSeq analyses were used to characterize the diversity of the microbial communities in the three sites. The sequence analysis revealed a Goods Coverage value of 1.00, which means that our sequencing efforts were 100% effective. Waegok marsh had the highest number of OTUs and diversity index values (Chao1, Shannon, Simpson). By associating the physicochemical characteristics of each site with the corresponding diversity results, we can conclude that the moderate environmental conditions in Waegok marsh, in contrast to the relatively extreme conditions in Jeonglyeongchi and Wangdeungjae, provided a more suitable ecosystem for the microbial community (Zhou et al. 2002; Curtis and Sloan 2004; Roesch et al. 2007). Our research suggests that environmental conditions can determine the degree of diversity of the microbial community, resulting from various adaptation processes. The environmental conditions at each site were influenced by the geographic isolation between the mountain marshes.

Ecological differences and relationships among mountain marsh sites in Jiri mountain. According to the UPGMA tree, which analyzed the relationship between the microbial communities of the investigated mountain marsh sites, it can be concluded that the microbial communities of Weagok and Wangdeungjae, which are geographically close (Fig. 1), presented a higher similarity than the microbial communities of Jeonglyeongchi (Fig. 2). In addition, the physicochemical factors of Jeonglyeongchi were different from those of Weagok and Wangdeungjae (Table I). In Jeonglyeongchi, the measured values for temperature (12.75°C), EC (32 μS/cm), and turbidity (2.51 NTU) were the lowest recorded, whereas higher values were observed for pH (6.95), DO (10.51 mg/l), and TP (1.57 ± 0.16 mg/l). Given these facts, it was possible to explain that the microbial community of Jeonglyeongchi was distinctive

Table III

Illumina MiSeq (M) and culture-based analyses of microalgae from Jeonglyeongchi, Waegok, and Wangdeungjae marsh samples.

| Species	Accession number	Jeonglyeongchi		Waegok		Wangdeungjae	
		M	CB	M	CB	M	CB
Achnanthidium daonense	KJ658413	–	–	+	–	–	–
Achnanthidium digitatum	KX946582	–	–	+	–	–	–
Achnanthidium minutissimum	MH358459	–	–	+	–	–	–
Achnanthidium straubianum	KY863467	–	–	+	–	–	–
Nitzschia acidoclinata	KT072971	–	–	+	–	–	–
Nitzschia dissipata	AJ867018	–	–	+	+	–	–
Cymbella aspera	KJ011615	–	–	+	–	–	–
Cymbopleura naviculiformis	AM501997	–	–	+	–	–	–
Placoneis elginensis	AM501953	–	–	+	–	–	–
Gomphonema affine	MN197879	+	–	+	–	–	–
Gomphonema cf.	AM502005	–	–	+	–	–	–
Eunotia sp.	KJ961696	+	–	+	–	+	–
Humidophila australis	KM116120	–	–	+	–	–	–
Uncultured *Halamphora*	MK656307	–	–	+	–	–	–
Halamphora sp.	MG027261	–	–	+	–	–	–
Pinnunavis sp.	KJ961669	–	–	+	–	–	–
Navicula sp.	MK177604	–	–	+	–	–	–
Neidium hitchcockii	KU674393	–	–	+	–	–	–
Neidium sp.	KU674445	–	–	+	–	–	–
Pinnularia cf.	JN418569	–	–	+	–	–	–
Pinnularia microstauron	AM501981	–	–	+	–	–	–
Pinnularia subgibba	KT072984	+	–	–	–	–	–
Pinnularia viridiformis	AM501985	–	–	+	–	–	–
Sellaphora cf.	EF151967	–	–	+	–	–	–
Sellaphora pupula	AJ544653	–	–	+	–	–	–
Surirella brebissonii	KX120739	–	–	+	–	–	–
Surirella cf.	KX120782	–	–	+	–	–	–
Surirella sp.	KX120781	–	–	+	–	–	–
Amphora copulata	MG027291	–	–	+	–	–	–
Aulacoseira alpigena	AY569578	–	–	+	–	+	–
Aulacoseira sp.	AY569587	–	–	–	–	+	–
Uncultured *Chaetoceros*	MH023058	–	–	+	–	–	–
Fragilaria vaucheriae	AM497736	–	–	+	–	–	–
Tabellaria flocculosa	MH356258	+	–	+	–	–	–
Chlorophyta sp.	MK929233	–	–	+	–	–	–
Microspora sp.	AF387160	–	–	–	–	+	–
Chlamydomonas sp.	MH683856	–	–	+	+	+	+
Chlorococcum sp.	MK954470	–	–	+	+	–	–
Dictyococcus sp.	HM852440	–	–	+	–	–	–
Bracteacoccus deserticola	JQ259938	–	–	–	–	+	–
Neochloris sp.	AB917132	+	+	–	–	–	–
Scenedesmus sp.	MH010849	–	–	–	–	+	+
Asterarcys quadricellulare	MN179327	–	–	+	–	–	–
Coccomyxa simplex	MH196858	+	–	+	–	–	–
Chlorella vulgaris	MK652782	–	–	+	+	+	–
Tupiella speciosa	MF000567	+	–	+	–	–	–
Monomastix opisthostigma	FN562445	–	–	+	–	–	–

+ – detected; – – undetected
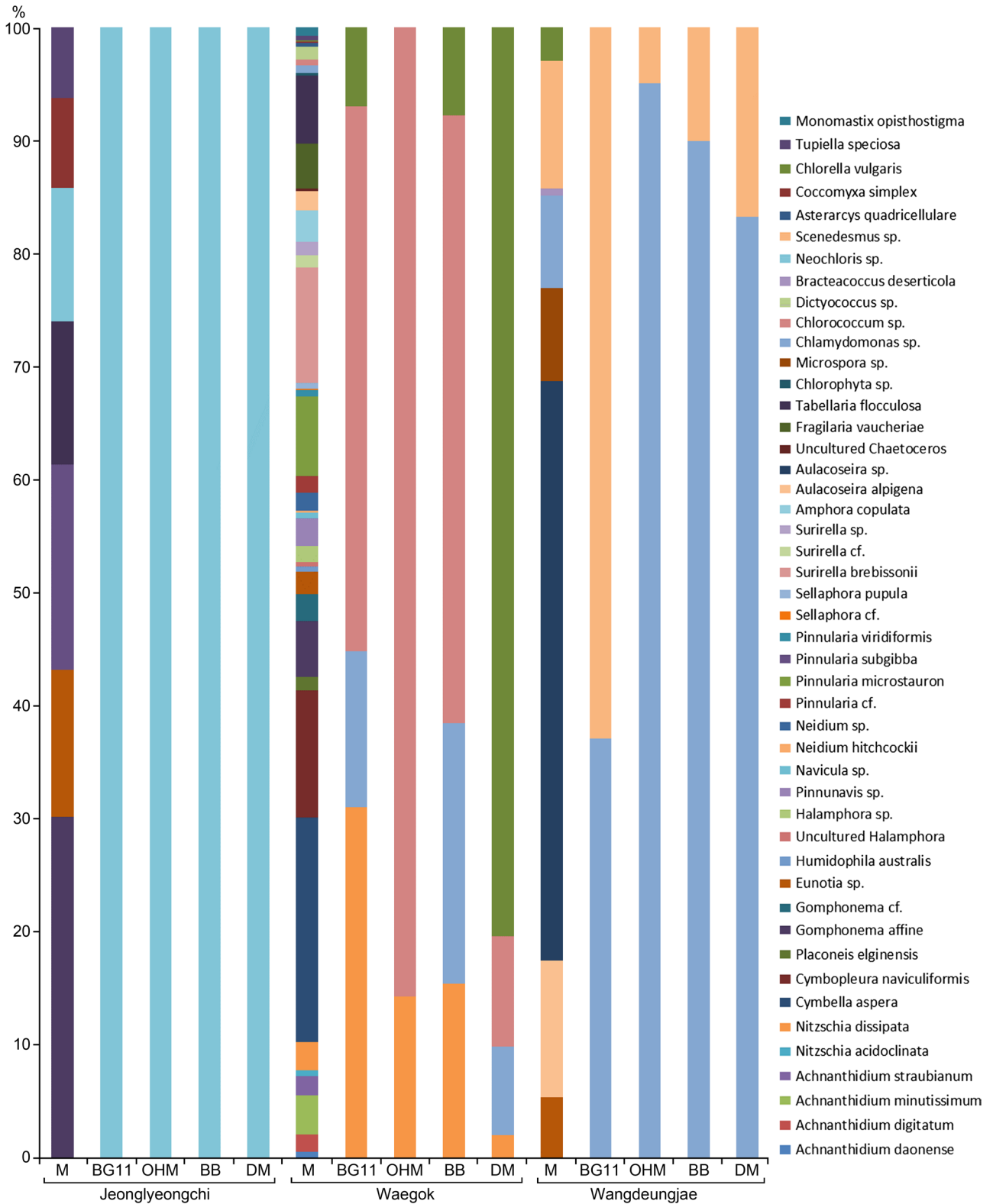
Fig. 5. Composition of microalgal species grown in each culture medium and identified using the Illumina MiSeq analysis (M). Four culture media were used: Blue Green-11 (BG11) medium, Optimum *Haematococus* Medium (OHM), Bold Basal medium (BB), and Diatom Medium (DM).

from other sites, and this was due to the variable inter-marsh physicochemical factors. However, when comparing the differences between microbial communities through the number of OTUs and diversity indicators

(Chao1, Shannon, Simpson), these values showed high similarity between Jeonglyeongchi and Waegok and less to Wangdeungjae (Table I). This fact contradicted the relationship between mountain marshes based

on physicochemical factors. This disparity could be resolved through the composition of the microbial community (supplementary Table SII). While 68.71% of the microbial community in Jeonglyeongchi was dominated by one species belonging to Platyhelminthes, the microbial community of Weagok and Wangdeungjae was composed of several species belonging to 3–4 phyla (Table II). Thus, it is believed that the similarity between microbial communities does not depend on diversity indicators (Miller et al. 2020; Wen et al. 2020). Nonetheless, we support that the comparison between microbial communities should be accompanied by a composition comparison factor (Shi et al. 2020). The composition of microbial communities is thought to be influenced by physicochemical factors, and this way, both studies are complementary (Sun et al. 2020). Thus, the microbial community of mountain marshes, separated due to the topographic features of Mount Jiri, needs diverse research approaches study of physicochemical factors and diversity indicators to understand their microbial community fully.

Taxonomic composition of phyla at mountain marsh sites. The phyla comprising the microbial communities of the three marsh sites is shown in Fig. 3. In addition, the taxonomic compositions from phyla to respective species levels are summarized in Table II. The most abundant phyla (present in more than 10% of the microbiome's taxonomic) included Apicomplexa, Arthropoda, Bacillariophyta, Chytridiomycota, Gastrotricha, Nematoda, Platyhelminthes, and Streptophyta (Fig. 3). Each phylum plays a particular ecological role, either as a producer, decomposer, or consumer. For example, many species of Apicomplexa are parasitic to aquatic animals (Bolland et al. 2020; Laghzaoui et al. 2020). Arthropoda includes animal species such as insects that consume a variety of materials, from living biomass (e.g., algae) to organic carbon sources (e.g., plant byproducts) (Shayanmehr et al. 2020; Sperfeld et al. 2020). Bacillariophyta is composed of autotrophic, photosynthetic organisms such as microalgae that are easily observed in aquatic ecosystems (Al-Handal et al. 2020; Stancheva et al. 2020). Chytridiomycota is a phylum of fungi that includes zoosporic fungal species, which function as heterotrophs in aquatic environments (Jeronimo and Amorim Pires-Zottarelli 2020; McKindles et al. 2020). Gastrotricha comprises various zooplankton species, including predators that feed on phytoplankton (Bosco et al. 2020), whereas Nematoda combines parasitic species and species that consume and decompose organic matter (Jeong et al. 2020; Netherlands et al. 2020). The phylum Platyhelminthes includes species that consume organic matter attached to the bottom and surface, and feed on algae and other microorganisms and plant byproducts (Geraerts et al. 2020; Schadt et al. 2021). Species belonging to Strep-

tophyta include autotrophs capable of photosynthesis (Stamenković et al. 2020; Williamson and Carter 2020). Based on these characteristics, Bacillariophyta and Streptophyta are considered producers (Pushkareva et al. 2016; Shnyukova and Zolotareva 2017); multicellular Arthropoda, Nematoda, and Platyhelminthes and unicellular Chytridiomycota are considered decomposers that decompose and consume organic materials (Berg and McClaugherty 2003; Berg and Laskowski 2005; Gessner et al. 2007; Gulis et al. 2019); and predators (Gastrotricha) and parasites (Apicomplexa) are considered consumers (Norén et al. 1999; Todaro et al. 2006). Most of the major taxa constituting the microbial community of the marshes are decomposers, and their composition differed by region. Jeonglyeongchi comprises more Chytridiomycota and Platyhelminthes, whereas Arthropoda is mostly seen in Waegok, and Chytridiomycota and Nematoda in Wangdeungjae. Among these phyla, only Chytridiomycota exceeded 5% abundance in all investigated regions (Fig. 3). Chytridiomycota is considered a decomposer that can parasitize microalgae (Ibelings et al. 2004; Gessner et al. 2007; Scholz et al. 2014; Gulis et al. 2019). Several species of Chytridiomycota are also parasitic on microalgal populations, thus affecting their growth (Ibelings et al. 2004; Scholz et al. 2014). This parasitic capacity of Chytridiomycota suggested that it may influence the community composition of Bacillariophyta and Chlorophyta in Jiri marshes. Finally, the predatory activity of Gastrotricha (a consumer) suggests that this group may be involved in the predominance of Streptophyta (a producer) by inhibiting the population growth of other microalgae (Todaro et al. 2006).

Our analysis reveals that each major phylum is represented by specific species. The major phyla at Jeonglyeongchi marsh, Chytridiomycota and Platyhelminthes, were represented by *Rhizoclosmatium globosum* and *Phagocata sibirica*, respectively. The major phyla at Waegok marsh, Arthropoda, Gastrotricha, and Streptophyta, were represented by *Aedes albopictus*, *Chaetonotus* cf., and *Stipa narynica*, respectively. The major phyla of Wangdeungjae marsh, Apicomplexa, Bacillariophyta, Chytridiomycota, and Nematoda, were represented by *Eimeria* sp., *Aulacoseira* sp., *Chytriomyces* sp., and *Eumonhystera* cf., respectively. The relative abundances of the predominant species ranged from 65.02% to 100.00%. Bacillariophyta and Chytridiomycota were least likely to be dominated by specific species. Furthermore, Bacillariophyta (34 species) and Chytridiomycota (26 species) were the largest phyla, representing 27.64% and 21.14%, respectively, of a total of 123 detected species. These results suggested that Bacillariophyta and Chytridiomycota were strongly associated with the species richness and diversity of microbial communities in mountain marshes.

Of all the microorganisms recorded in the three studied marshes, producers (Bacillariophyta and Streptophyta) accounted for less than 30% of the total abundance. Because producers were not a significant fraction of the community, consumers were probably dependent on externally derived organic materials (Lu and Wu 1998). For example, Platyhelminthes, a dominant consumer in Jeonglyeongchi, is likely dependent on externally derived organic materials (Roca et al. 1992; Lu and Wu 1998). Although producers were not abundant, their diversity may have had a significant impact on the diversity of the microbial community (Worm et al. 2002; Hillebrand et al. 2007; Cardinale et al. 2011). Bacillariophyta (with the most significant number of species, 34) and Streptophyta (with the fourth-largest number of species, 10) accounted for 35.77% of the total species. The producer group accounted for 17.65–39.58% of the species in the region (17.65% in Jeonglyeongchi, 39.58% in Waegok, and 28.57% in Wangdeungjae). These results discriminated the distribution of species relative to the abundance of the producer group (Hillebrand et al. 2007; Cardinale et al. 2011). Thus, the diversity of producers is highly important in determining the diversity of the local microbial community.

Comparison of marsh sites using culture-based and Illumina MiSeq analyses. We have cultured and identified one-four microalgal species from each marsh site using several types of media (Fig. 5 and supplementary Fig. S1). The following species were isolated and identified: *Neochloris* sp. at Jeonglyeongchi; *Nitzschia dissipata*, *Chlamydomonas* sp., *Chlorococcum* sp., and *Chlorella vulgaris* at Waegok; and *Chlamydomonas* sp. and *Scenedesmus* sp. at Wangdeungjae. Although the species were distributed disproportionately in each medium, only one species tended to be dominant among the few that grew (supplementary Fig. S1). A single species dominated in the BG11 and DM medium but not in the OHM and BB medium (supplementary Fig. S1). We were able to isolate representatives of Bacillariophyta and Chlorophyta, but not Streptophyta, in the culture media (Table III, Fig. 5 and supplementary Fig. 1). Isolated species included *Neochloris* sp., *Nitzschia dissipata*, *Chlamydomonas* sp., *Chlorococcum* sp., *Chlorella vulgaris,* and *Scenedesmus* sp. Only one species, *Nitzschia dissipata,* belonged to Bacillariophyta. The relative abundances of isolated species varied depending on the medium used (Fig. 5 and supplementary Fig. S1) (DiGiulio et al. 2008). It is known that only certain species can be cultivated and their growth depends on the composition of the medium chosen (Harrison and Davis 1979). It suggests that culture-based methods are not suitable for detecting multiple microalgal species, a severe limitation in determining community compositions (Alain and Querellou 2009). Furthermore, the inability to purely

isolate 100% of all microbial species present using existing culture techniques and media means that the identification of unculturable microbes is limited. Therefore, microalgal community research based solely on culture analysis is limited because of the difficulty in identifying unculturable microorganisms (Handelsman 2004; Shokralla et al. 2012; Bodor et al. 2020). In contrast to culture-based methods, Illumina MiSeq can effectively analyze the microbial community structure of environmental samples, including the identification and analysis of unculturable microorganisms. Illumina MiSeq analysis overcomes the limitations of the culture-based analysis, providing a more accurate representation of the diversity of the microbial community.

Characteristics of microalgae in the marshes of Jiri. Most microalgae in aquatic environments with water flow are attached to surfaces (Benito 2020; Plante et al. 2021). Typically, attached algae are dominated by diatoms, including Bacillariophyta and some green algae, including Chlorophyta (Yun et al. 2019; Benito 2020; Plante et al. 2021). Therefore, in an environment with water flow, the floating algae are relatively less abundant (Yun et al. 2019; Prazukin et al. 2020). In an aquatic environment where water flow is weak, floating algae dominate, with its species' composition often determined by environmental factors (Mashwani 2020). The microalgae present in the Jiri marshes were mainly composed of Bacillariophyta and Streptophyta (Ali et al. 2019; Garduño-Solórzano et al. 2020). While it is known that Chlorophyta tends to dominate in other aquatic environments (Amorim and Moura 2021), our results suggest that environmental differences determined the dominant microalgal groups.

Furthermore, to better understand the differences between these regional microalgal groups, a more comprehensive set of environmental factors should be investigated using a multidisciplinary rather than a fragmentary approach (Paquette et al. 2020; Sutherland et al. 2020). Our study provides information on the microbial communities and microalgal groups present in the Jiri marshes. Furthermore, our results suggest that it is important to analyze the taxonomic composition of the microalgae present in mountain marshes.

Conclusion

The highest levels of species richness and diversity among the three Jiri high marshes were found in the Waegok marsh, which may be due to the environment's physicochemical characteristics. Analysis of community composition revealed that species' abundance was concentrated in the decomposer group, whereas species' diversity was based in the producer group. Moreover, the consumer group was related to the producer group.

Based on these results, we suggest that producers do not support the entire microbial community, but they determine phylogenetic diversity. Illumina MiSeq analysis overcame the inherent limitations of the culture-based analysis, i.e., incomplete or biased results. Our analyses provide a clear association between the environmental conditions of three mountain marshes and the properties of their respective microbial and microalgal communities. Further research on the roles and interactions between microbial and microalgal communities should be investigated along with their environmental impacts. The data generated in this study can be used to identify mountain areas based on their microalgal communities and help understand the role of environmental factors in their geography.

Conflict of interest

The authors do not report any financial or personal connections with other persons or organizations, which might negatively affect the contents of this publication and/or claim authorship rights to this publication.

Literature

Agrawal SC, Sarma YSRK. Effects of nutrients present in Bold's basal medium on the green alga *Stigeoclonium pascheri*. Folia Microbiol (Praha). 1982 Mar;27(2):131–137. https://doi.org/10.1007/BF02879772

Alain K, Querellou J. Cultivating the uncultured: limits, advances and future challenges. Extremophiles. 2009 Jul;13(4):583–594. https://doi.org/10.1007/s00792-009-0261-3

Al-Handal AY, Mucko M, Wulff A. *Entomoneis annagodhei* sp. nov., a new marine diatom (Entomoneidaceae, Bacillariophyta) from the west coast of Sweden. Diatom Res. 2020 Jul 02;35(3):269–279. https://doi.org/10.1080/0269249X.2020.1787229

Ali HA, Owaid MN, Ali SF. Recording thirteen new species of phytoplankton in Euphrates River environment in Iraq. Walailak J Sci Technol (WJST). 2019 Jul 22;17(3):200–211. https://doi.org/10.48048/wjst.2020.6217

Amon RMW, Benner R. Photochemical and microbial consumption of dissolved organic carbon and dissolved oxygen in the Amazon River system. Geochim Cosmochim Acta. 1996 May;60(10):1783–1792. https://doi.org/10.1016/0016-7037(96)00055-5

Amorim CA, Moura AN. Ecological impacts of freshwater algal blooms on water quality, plankton biodiversity, structure, and ecosystem functioning. Sci Total Environ. 2021 Mar;758:143605. https://doi.org/10.1016/j.scitotenv.2020.143605

Anderson DW. The effect of parent material and soil development on nutrient cycling in temperate ecosystems. Biogeochemistry. 1988 Feb; 5(1):71–97. https://doi.org/10.1007/BF02180318

Benito X. Benthic Foraminifera and diatoms as ecological indicators. In: Cristóbal G, Blanco S, Bueno G, editors. Modern trends in diatom identification. Cham (Switzerland): Springer; 2020. p. 257–280. https://doi.org/10.1007/978-3-030-39212-3

Berg B, Laskowski R. Decomposers: soil microorganisms and animals. Adv Ecol Res. 2005;38:73–100. https://doi.org/10.1016/S0065-2504(05)38003-2

Berg B, McClaugherty C. Decomposer oganisms. In: Plant litter. Berlin, Heidelberg (Gemany): Springer-Verlag; 2003. p. 31–48. https://doi.org/10.1007/978-3-662-05349-2_3

Blifernez-Klassen O, Klassen V, Doebbe A, Kersting K, Grimm P, Wobbe L, Kruse O. Cellulose degradation and assimilation by the unicellular phototrophic eukaryote *Chlamydomonas reinhardtii*. Nat Commun. 2012 Jan;3(1):1214. https://doi.org/10.1038/ncomms2210

Bodor A, Bounedjoum N, Vincze GE, Erdeiné Kis Á, Laczi K, Bende G, Szilágyi Á, Kovács T, Perei K, Rákhely G. Challenges of unculturable bacteria: environmental perspectives. Rev Environ Sci Biotechnol. 2020 Mar;19(1):1–22. https://doi.org/10.1007/s11157-020-09522-4

Bolch CJS, Blackburn SI. Isolation and purification of Australian isolates of the toxic cyanobacterium *Microcystis aeruginosa* Kütz. J Appl Phycol. 1996 Jan;8(1):5–13. https://doi.org/10.1007/BF02186215

Bolland SJ, Zahedi A, Oskam C, Murphy B, Ryan U. *Cryptosporidium bollandi* n. sp. (Apicomplexa: Cryptosporidiiae) from angelfish (*Pterophyllum scalare*) and Oscar fish (*Astronotus ocellatus*). Exp Parasitol. 2020 Oct;217:107956. https://doi.org/10.1016/j.exppara.2020.107956

Bormann BT, Spaltenstein H, McClellan MH, Ugolini FC, Jr KC, Nay SM. Rapid soil development after windthrow disturbance in pristine forests. J Ecol. 1995 Oct;83(5):747–757. https://doi.org/10.2307/2261411

Bosco I, Lourenço AP, Guidi L, Balsamo M, Hochberg R, Garraffoni ARS. Integrative description of a new species of *Acanthodasys* Remane, 1927 (Gastrotricha, Macrodasyida, Thaumastodermatidae) based on four distinct morphological techniques and molecular data. Zool Anz. 2020 May;286:31–42. https://doi.org/10.1016/j.jcz.2020.03.003

Canfield DE, Bjerrum CJ, Zhang S, Wang H, Wang X. The modern phosphorus cycle informs interpretations of Mesoproterozoic Era phosphorus dynamics. Earth Sci Rev. 2020 Sep;208:103267. https://doi.org/10.1016/j.earscirev.2020.103267

Cardinale BJ, Matulich KL, Hooper DU, Byrnes JE, Duffy E, Gamfeldt L, Balvanera P, O'Connor MI, Gonzalez A. The functional role of producer diversity in ecosystems. Am J Bot. 2011 Mar;98(3):572–592. https://doi.org/10.3732/ajb.1000364

Claassen S, du Toit E, Kaba M, Moodley C, Zar HJ, Nicol MP. A comparison of the efficiency of five different commercial DNA extraction kits for extraction of DNA from faecal samples. J Microbiol Methods. 2013 Aug;94(2):103–110. https://doi.org/10.1016/j.mimet.2013.05.008

Curtis T, Sloan W. Prokaryotic diversity and its limits: microbial community structure in nature and implications for microbial ecology. Curr Opin Microbiol. 2004 Jun;7(3):221–226. https://doi.org/10.1016/j.mib.2004.04.010

Di Termini I, Prassone A, Cattaneo C, Rovatti M. On the nitrogen and phosphorus removal in algal photobioreactors. Ecol Eng. 2011 Jun;37(6):976–980. https://doi.org/10.1016/j.mib.2004.04.010

DiGiulio DB, Romero R, Amogan HP, Kusanovic JP, Bik EM, Gotsch F, Kim CJ, Erez O, Edwin S, Relman DA. Microbial prevalence, diversity and abundance in amniotic fluid during preterm

labor: a molecular and culture-based investigation. PLoS One. 2008 Aug 26;3(8):e3056.
https://doi.org/10.1371/journal.pone.0003056

Dobrovoľskaya TG, Golovchenko AV, Kukharenko OS, Yakushev AV, Semenova TA, Inisheva LA. The structure of the microbial communities in low-moor and high-moor peat bogs of Tomsk oblast. Eurasian Soil Sci. 2012 Mar;45(3):273–281.
https://doi.org/10.1134/S1064229312030039

Fábregas J, Domínguez A, Regueiro M, Maseda A, Otero A. Optimization of culture medium for the continuous cultivation of the microalga *Haematococcus pluvialis*. Appl Microbiol Biotechnol. 2000 May 15;53(5):530–535.
https://doi.org/10.1007/s002530051652

Felsenstein J. Confidence limits on phylogenies: an approach using the bootstrap. Evolution. 1985 Jul;39(4):783–791.
https://doi.org/10.1111/j.1558-5646.1985.tb00420.x

Garber JH. Laboratory study of nitrogen and phosphorus remineralization during the decomposition of coastal plankton and seston. Estuar Coast Shelf Sci. 1984 Jun;18(6):685–702.
https://doi.org/10.1016/0272-7714(84)90039-8

Garduño-Solórzano G, Martínez-García M, Scotta Hentschke G, Lopes G, Castelo Branco R, Vasconcelos VMO, Campos JE, López-Cano R, Quintanar-Zúñiga RE. The phylogenetic placement of *Temnogametum* (Zygnemataceae) and description of *Temnogametum iztacalense* sp. nov., from a tropical high mountain lake in Mexico. Eur J Phycol. 2020 Aug 27;1–15.
https://doi.org/10.1080/09670262.2020.1789226

Geraerts M, Muterezi Bukinga F, Vanhove MPM, Pariselle A, Chocha Manda A, Vreven E, Huyse T, Artois T. Six new species of *Cichlidogyrus* Paperna, 1960 (Platyhelminthes: Monogenea) from the gills of cichlids (Teleostei: Cichliformes) from the Lomami River Basin (DRC: Middle Congo). Parasit Vectors. 2020 Dec;13(1):187.
https://doi.org/10.1186/s13071-020-3927-4

Gessner M, Gulis V, Kuehn K, Chauvet E, Suberkropp K. Fungal decomposers of plant litter in aquatic ecosystems. In: Kubicek CP, Druzhinina IS, editors. Environmental and Microbial Relationships. The Mycota, vol 4. Berlin, Heidelberg (Germany): Springer; 2007. p. 301–324. https://doi.org/10.1007/978-3-540-71840-6_17

Gulis V, Su R, Kuehn KA. Fungal Decomposers in Freshwater Environments. In: Hurst CJ, editor. The Structure and Function of Aquatic Microbial Communities. Advances in Environmental Microbiology, vol 7. Cham (Switzerland): Springer; 2019. p. 121–155.
https://doi.org/10.1007/978-3-030-16775-2_5

Handelsman J. Metagenomics: application of genomics to uncultured microorganisms. Microbiol Mol Biol Rev. 2004 Dec;68(4):669–685.
https://doi.org/10.1128/MMBR.68.4.669-685.2004

Harrison PJ, Davis CO. The use of outdoor phytoplankton continuous cultures to analyse factors influencing species selection. J Exp Mar Biol Ecol. 1979 Oct;41(1):9–23.
https://doi.org/10.1016/0022-0981(79)90078-9

Hartemink A, Zhang Y, Bockheim J, Curi N, Silva S, Grauer-Gray J, Lowe DJ, Krasilnikov P. Chapter Three – Soil horizon variation: A review. In: Sparks DL, editor. Advances in Agronomy. Cambridge (USA): Elsevier Academic Press; 2020;160(1). p. 125–185.
https://doi.org/10.1016/bs.agron.2019.10.003

Heck KL Jr, van Belle G, Simberloff D. Explicit calculation of the rarefaction diversity measurement and the determination of sufficient sample size. Ecology. 1975 Oct;56(6):1459–1461.
https://doi.org/10.2307/1934716

Hillebrand H, Gruner DS, Borer ET, Bracken MES, Cleland EE, Elser JJ, Harpole WS, Ngai JT, Seabloom EW, Shurin JB, et al. Consumer versus resource control of producer diversity depends on ecosystem type and producer community structure. Proc Natl Acad Sci USA. 2007 Jun 26;104(26):10904–10909.
https://doi.org/10.1073/pnas.0701918104

Huggett RJ. Soil chronosequences, soil development, and soil evolution: a critical review. Catena. 1998 Jun;32(3-4):155–172.
https://doi.org/10.1016/S0341-8162(98)00053-8

Ibelings BW, De Bruin A, Kagami M, Rijkeboer M, Brehm M, Donk EV. Host parasite interactions between freshwater phytoplankton and chytrid fungi (Chytridiomycota). J Phycol. 2004 Jun; 40(3):437–453. https://doi.org/10.1111/j.1529-8817.2004.03117.x

Jeong R, Tchesunov AV, Lee W. Two species of Thoracostomopsidae (Nematoda: Enoplida) from Jeju Island, South Korea. PeerJ. 2020 Apr 28;8:e9037. https://doi.org/10.7717/peerj.9037

Jeronimo GH, Amorim Pires-Zottarelli CL. Diversity and distribution of zoosporic fungi (Blastocladiomycota and Chytridiomycota) in three tropical reservoirs. Sydowia. 2020;71:255.

Jewell WJ. Aquatic weed decay: dissolved oxygen utilization and nitrogen and phosphorus regeneration. J Water Pollut Control Fed. 1971 Jul;43(7);1457–1467.

Kim HG, Jeong JY, Koo BH. [The identification and vegetation structure of several mountainous wetlands in Dan-yang and around area] (in in Korean). J Korean Soc Environ Restor Technol. 2010;13(1):1–13.

Kim KH, Jung HR. [Characteristics of step-pool structure in the mountain streams around Mt. Jiri] (in in Korean). J Korean Water Resour Assoc. 2018;51(4):313–322.

Kozich JJ, Westcott SL, Baxter NT, Highlander SK, Schloss PD. Development of a dual-index sequencing strategy and curation pipeline for analyzing amplicon sequence data on the MiSeq Illumina sequencing platform. Appl Environ Microbiol. 2013 Sep 01; 79(17):5112–5120. https://doi.org/10.1128/AEM.01043-13

Kukharenko OS, Pavlova NS, Dobrovoľskaya TG, Golovchenko AV, Pochatkova TN, Zenova GM, Zvyagintsev DG. The influence of aeration and temperature on the structure of bacterial complexes in high-moor peat soil. Eurasian Soil Sci. 2010 May; 43(5):573–579. https://doi.org/10.1134/S106422931005011X

Kumar S, Nei M, Dudley J, Tamura K. MEGA: A biologist-centric software for evolutionary analysis of DNA and protein sequences. Brief Bioinform. 2008 Mar 27;9(4):299–306.
https://doi.org/10.1093/bib/bbn017

Kumar S, Stecher G, Tamura K. MEGA7: molecular evolutionary genetics analysis version 7.0 for bigger datasets. Mol Biol Evol. 2016 Jul;33(7):1870–1874. https://doi.org/10.1093/molbev/msw054

Kwabiah AB, Stoskopf NC, Voroney RP, Palm CA. Nitrogen and phosphorus release from decomposing leaves under sub-humid tropical conditions. Biotropica. 2001 Jun;33(2):229–240.
https://doi.org/10.1111/j.1744-7429.2001.tb00174.x

Laghzaoui EM, Sergiadou D, Perera A, Harris DJ, Abbad A, El Mouden EH. Absence of *Hemolivia mauritanica* (Apicomplexa: Haemogregarinidae) in natural populations of *Testudo graeca* in Morocco. Parasitol Res. 2020 Dec;119(12):4281–4286.
https://doi.org/10.1007/s00436-020-06869-z

Levantesi C, Serafim LS, Crocetti GR, Lemos PC, Rossetti S, Blackall LL, Reis MAM, Tandoi V. Analysis of the microbial community structure and function of a laboratory scale enhanced biological phosphorus removal reactor. Environ Microbiol. 2002 Oct; 4(10):559–569. https://doi.org/10.1046/j.1462-2920.2002.00339.x

Li W, Fu L, Niu B, Wu S, Wooley J. Ultrafast clustering algorithms for metagenomic sequence analysis. Brief Bioinform. 2012 Nov 01;13(6):656–668. https://doi.org/10.1093/bib/bbs035

Lu L, Wu RSS. Recolonization and succession of marine macrobenthos in organic-enriched sediment deposited from fish farms. Environ Pollut. 1998;101(2):241–251.
https://doi.org/10.1016/S0269-7491(98)00041-4

Mashwani ZUR. Environment, climate change and biodiversity. In: Fahad S, Hasanuzzaman M, Alam M, Ullah H, Saeed M, Ali Khan I, Adnan M, editors. Environment, climate, plant and vegetation growth. Cham (Switzerland): Springer; 2020. p. 473–501.
https://doi.org/10.1007/978-3-030-49732-3_19

McGlathery KJ, Sundbäck K, Anderson IC. The importance of primary producers for benthic nitrogen and phosphorus cycling. In: Nielsen SL, Banta GT, Pedersen MF, editors. Estuarine nutrient cycling: the influence of primary producers. Dordrecht (The Netherlands): Springer; 2004. p. 231–261.
https://doi.org/10.1007/978-1-4020-3021-5_9

McKindles KM, Jorge AN, McKay RM, Davis TW, Bullerjahn GS. Isolation and characterization of *Rhizophydiales* sp. (Chytridiomycota), obligate parasite of *Planktothrix agardhii* in a Laurentian Great Lakes Embayment. Appl Environ Microbiol. 2020 Dec 11; 87(4): e02308–20. https://doi.org/10.1128/AEM.02308-20

Meyer M, Kircher M. Illumina sequencing library preparation for highly multiplexed target capture and sequencing. Cold Spring Harb Protoc. 2010 Jun;2010(6):pdb.prot5448.
https://doi.org/10.1101/pdb.prot5448

Miller JI, Techtmann S, Joyner D, Mahmoudi N, Fortney J, Fordyce JA, GaraJayeva N, Askerov FS, Cravid C, Kuijper M, et al. Microbial communities across global marine basins show important compositional similarities by depth. MBio. 2020 Aug 18;11(4): e01448-20. https://doi.org/10.1128/mBio.01448-20

Netherlands EC, Svitin R, Cook CA, Smit NJ, Brendonck L, Vanhove MPM, Du Preez LH. *Neofoleyellides boerewors* n. gen. n. sp. (Nematoda: Onchocercidae) parasitising common toads and mosquito vectors: morphology, life history, experimental transmission and host-vector interaction *in situ*. Int J Parasitol. 2020 Mar; 50(3): 177–194. https://doi.org/10.1016/j.ijpara.2019.11.009

Norén F, Moestrup Ø, Rehnstam-Holm AS. *Parvilucifera infectans* norén et moestrup gen. et sp. nov. (perkinsozoa phylum nov.): a parasitic flagellate capable of killing toxic microalgae. Eur J Protistol. 1999 Oct;35(3):233–254.
https://doi.org/10.1016/S0932-4739(99)80001-7

Paquette AJ, Sharp CE, Schnurr PJ, Allen DG, Short SM, Espie GS. Dynamic changes in community composition of *Scenedesmus*-seeded artificial, engineered microalgal biofilms. Algal Res. 2020 Mar; 46: 101805. https://doi.org/10.1016/j.algal.2020.101805

Perez-Garcia O, Escalante FME, de-Bashan LE, Bashan Y. Heterotrophic cultures of microalgae: metabolism and potential products. Water Res. 2011 Jan;45(1):11–36.
https://doi.org/10.1016/j.watres.2010.08.037

Plante CJ, Hill-Spanik K, Cook M, Graham C. Environmental and spatial influences on biogeography and community structure of saltmarsh benthic diatoms. Estuar Coast. 2020 Jan;44:147–161.
https://doi.org/10.1007/s12237-020-00779-0

Prazukin A, Shadrin N, Balycheva D, Firsov Y, Lee R, Anufriieva E. *Cladophora* spp. (Chlorophyta) modulate environment and create a habitat for microalgae in hypersaline waters. Eur J Phycol. 2020 Oct 06;1–13. https://doi.org/10.1080/09670262.2020.1814423

Pushkareva E, Johansen JR, Elster J. A review of the ecology, ecophysiology and biodiversity of microalgae in Arctic soil crusts. Polar Biol. 2016 Dec;39(12):2227–2240.
https://doi.org/10.1007/s00300-016-1902-5

Rippka R, Stanier RY, Deruelles J, Herdman M, Waterbury JB. Generic assignments, strain histories and properties of pure cultures of cyanobacteria. Microbiology. 1979 Mar 01;111(1):1–61.
https://doi.org/10.1099/00221287-111-1-1

Roca JR, Ribas M, Baguñà J. Distribution, ecology, mode of reproduction and karyology of freshwater planarians (Platyhelminthes; Turbellaria; Tricladida) in the springs of the central Pyrenees. Ecography. 1992 Oct;15(4):373–384.
https://doi.org/10.1111/j.1600-0587.1992.tb00047.x

Roesch LFW, Fulthorpe RR, Riva A, Casella G, Hadwin AKM, Kent AD, Daroub SH, Camargo FAO, Farmerie WG, Triplett EW. Pyrosequencing enumerates and contrasts soil microbial diversity. ISME J. 2007 Aug;1(4):283–290.
https://doi.org/10.1038/ismej.2007.53

Rousk J, Brookes PC, Bååth E. Investigating the mechanisms for the opposing pH relationships of fungal and bacterial growth in soil. Soil Biol Biochem. 2010 Jun;42(6):926–934.
https://doi.org/10.1016/j.soilbio.2010.02.009

Safonova TA, Aslamov IA, Basharina TN, Chenski AG, Vereschagin AL, Glyzina OY, Grachev MA. Cultivation and automatic counting of diatom algae cells in multi-well plastic plates. Diatom Res. 2007 May;22(1):189–195.
https://doi.org/10.1080/0269249X.2007.9705703

Schadt T, Prantl V, Grosbusch AL, Bertemes P, Egger B. Regeneration of the flatworm *Prosthiostomum siphunculus* (Polycladida, Platyhelminthes). Cell Tissue Res. 2021 Mar;383(3):1025-1041.
https://doi.org/10.1007/s00441-020-03302-w

Schloss PD, Westcott SL, Ryabin T, Hall JR, Hartmann M, Hollister EB, Lesniewski RA, Oakley BB, Parks DH, Robinson CJ, et al. Introducing mothur: open-source, platform-independent, community-supported software for describing and comparing microbial communities. Appl Environ Microbiol. 2009 Dec 01;75(23):7537–7541.
https://doi.org/10.1128/AEM.01541-09

Schoenberg SA, Maccubbin AE, Hodson RE. Cellulose digestion by freshwater microcrustacea. Limnol Oceanogr. 1984 Sep;29(5): 1132–1136. https://doi.org/10.4319/lo.1984.29.5.1132

Scholz B, Küpper FC, Vyverman W, Karsten U. Eukaryotic pathogens (Chytridiomycota and Oomycota) infecting marine microphytobenthic diatoms – a methodological comparison. J Phycol. 2014 Dec; 50(6):1009–1019. https://doi.org/10.1111/jpy.12230

Schwarz G. Estimating the dimension of a model. Ann Stat. 1978 Mar 1;6(2):461–464. https://doi.org/10.1214/aos/1176344136

Shayanmehr M, Yoosefi Lafooraki E, Kahrarian M. A new updated checklist of Iranian Collembola (Arthropoda: Hexapoda). JESI. 2020; 39(4):403–445.

Shi A, Zhou X, Yao S, Zhang B. Effects of intensities and cycles of heating on mineralization of organic matter and microbial community composition of a Mollisol under different land use types. Geoderma. 2020 Jan;357:113941.
https://doi.org/10.1016/j.geoderma.2019.113941

Shnyukova EI, Zolotareva EK. Ecological role of exopolysaccharides of Bacillariophyta: a review. Int J Algae. 2017;19(1):5–24.
https://doi.org/10.1615/InterJAlgae.v19.i1.10

Shokralla S, Spall JL, Gibson JF, Hajibabaei M. Next-generation sequencing technologies for environmental DNA research. Mol Ecol. 2012 Apr;21(8):1794–1805.
https://doi.org/10.1111/j.1365-294X.2012.05538.x

Sperfeld E, Nilssen JP, Rinehart S, Schwenk K, Hessen DO. Ecology of predator-induced morphological defense traits in *Daphnia longispina* (Cladocera, Arthropoda). Oecologia. 2020 Mar;192(3): 687–698. https://doi.org/10.1007/s00442-019-04588-6

Stamenković M, Steinwall E, Nilsson AK, Wulff A. Fatty acids as chemotaxonomic and ecophysiological traits in green microalgae (desmids, Zygnematophyceae, Streptophyta): A discriminant analysis approach. Phytochemistry. 2020 Feb;170:112200.
https://doi.org/10.1016/j.phytochem.2019.112200

Stancheva R, Kristan N, Kristan WB 3rd, Sheath RG. Diatom genus *Planothidium* (Bacillariophyta) from streams and rivers in California, USA: diversity, distribution and autecology. Phytotaxa. 2020 Nov 02;470(1):1–30. https://doi.org/10.11646/phytotaxa.470.1.1

Stanier RY, Kunisawa R, Mandel M, Cohen-Bazire G. Purification and properties of unicellular blue-green algae (order Chroococcales). Bacteriol Rev. 1971;35(2):171–205.
https://doi.org/10.1128/BR.35.2.171-205.1971

Stoeck T, Bass D, Nebel M, Christen R, Jones MDM, Breiner HW, Richards TA. Multiple marker parallel tag environmental DNA sequencing reveals a highly complex eukaryotic community in marine anoxic water. Mol Ecol. 2010 Mar;19(Suppl 1):21–31.
https://doi.org/10.1111/j.1365-294X.2009.04480.x

Stone MJ, Shoo L, Stork NE, Sheldon F, Catterall CP. Recovery of decomposition rates and decomposer invertebrates during rain forest restoration on disused pasture. Biotropica. 2020 Mar;52(2): 230–241. https://doi.org/10.1111/btp.12682

Sturm M, Schroeder C, Bauer P. SeqPurge: highly-sensitive adapter trimming for paired-end NGS data. BMC Bioinformatics. 2016 Dec; 17(1):208. https://doi.org/10.1186/s12859-016-1069-7

Sun L, Han X, Li J, Zhao Z, Liu Y, Xi Q, Guo X, Gun S. Microbial community and its association with physicochemical factors during compost bedding for dairy cows. Front Microbiol. 2020 Feb 21; 11:254. https://doi.org/10.3389/fmicb.2020.00254

Sutherland DL, Burke J, Leal E, Ralph PJ. Effects of nutrient load on microalgal productivity and community composition grown in anaerobically digested food-waste centrate. Algal Res. 2020 Oct; 51:102037. https://doi.org/10.1016/j.algal.2020.102037

Tanner RS. Cultivation of bacteria and fungi. In: Hurst CJ, Crawford RL, Garland JL, Lipson DA, and Mills AL, Stetzenbach LD, editors. Manual of Environmental Microbiology, third edition. Washington (USA): ASM Press; 2007. p. 69–78. https://doi.org/10.1128/9781555815882.ch6

Todaro MA, Leasi F, Bizzarri N, Tongiorgi P. Meiofauna densities and gastrotrich community composition in a Mediterranean sea cave. Mar Biol. 2006 Aug;149(5):1079–1091. https://doi.org/10.1007/s00227-006-0299-z

Vo ATE, Jedlicka JA. Protocols for metagenomic DNA extraction and Illumina amplicon library preparation for faecal and swab samples. Mol Ecol Resour. 2014 Nov;14(6):1183–1197. https://doi.org/10.1111/1755-0998.12269

Wen J, LeChevallier MW, Tao W. Microbial community similarity and dissimilarity inside and across full-scale activated sludge processes for simultaneous nitrification and denitrification. Water Sci Technol. 2020 Jan 15;81(2):333–344. https://doi.org/10.2166/wst.2020.112

Wieringa KT. The humification of high-moor peat. Plant Soil. 1964 Dec;21(3):333–344. https://doi.org/10.1007/BF01377748

Williams CJ, Yavitt JB. Botanical composition of peat and degree of peat decomposition in three temperate peatlands. Ecoscience. 2003 Jan;10(1):85–95. https://doi.org/10.1080/11956860.2003.11682755

Williamson DB, Carter CF. A new desmid (Zygnematophyceae, Streptophyta) species from New Zealand, *Cosmarium wilsonii* spec. nov. N Z J Bot. 2020 Jan 02;58(1):62–66. https://doi.org/10.1080/0028825X.2019.1657470

Witkamp M, Frank ML. Effects of temperature, rainfall, and fauna on transfer of ^(137)CS, K, MG, and mass in consumer-decomposer microcosms. Ecology. 1970 May;51(3):465–474. https://doi.org/10.2307/1935381

Worm B, Lotze HK, Hillebrand H, Sommer U. Consumer versus resource control of species diversity and ecosystem functioning. Nature. 2002 Jun;417(6891):848–851. https://doi.org/10.1038/nature00830

Yang H. [The hydrological roles and properties of Wangdeungjae wetland in Jirisan] (in Korean). J Korean Geo Assoc. 2008;15:77–85.

Yun HS, Kim YS, Yoon HS. Illumina MiSeq analysis and comparison of freshwater microalgal communities on Ulleungdo and Dokdo Islands. Pol J Microbiol. 2019 Dec;68(4):527–539. https://doi.org/10.33073/pjm-2019-053

Zhang X, Ward BB, Sigman DM. Global nitrogen cycle: critical enzymes, organisms, and processes for nitrogen budgets and dynamics. Chem Rev. 2020 Jun 24;120(12):5308–5351. https://doi.org/10.1021/acs.chemrev.9b00613

Zhang Z, Schwartz S, Wagner L, Miller W. A greedy algorithm for aligning DNA sequences. J Comput Biol. 2000 Feb;7(1-2):203–214. https://doi.org/10.1089/10665270050081478

Zhou J, Xia B, Treves DS, Wu LY, Marsh TL, O'Neill RV, Palumbo AV, Tiedje JM. Spatial and resource factors influencing high microbial diversity in soil. Appl Environ Microbiol. 2002 Jan; 68(1):326–334. https://doi.org/10.1128/AEM.68.1.326-334.2002

Supplementary materials are available on the journal's website.

The Effect of *Lactobacillus plantarum* BW2013 on the Gut Microbiota in Mice Analyzed by 16S rRNA Amplicon Sequencing

TONG TONG[1], XIAOHUI NIU[1], QIAN LI[1], YUXI LING[1], ZUMING LI[1]*, JIA LIU[2], MICHAEL ZHANG[3], ZHIHUI BAI[4], RAN XIA[3], ZHICHAO WU[3] and XIU LIU[5]

[1] Beijing Key Laboratory of Bioactive Substances and Functional Foods and Department of Food Science,
College of Biochemical Engineering, Beijing Union University, Beijing, China
[2] Internal Trade Food Science and Technology (Beijing) Co., Ltd, Beijing, China
[3] Department of Physics and Astronomy, University of Manitoba, Winnipeg, Canada
[4] Research Center for Eco-Environmental Sciences, Chinese Academy of Sciences, Beijing, China
[5] China National Research Institute of Food and Fermentation Industies Co., Ltd, Beijing, China

A b s t r a c t

Lactobacillus plantarum BW2013 was isolated from the fermented Chinese cabbage. This study aimed to test the effect of this strain on the gut microbiota in BALB/c mice by 16S rRNA amplicon sequencing. The mice were randomly allocated to the control group and three treatment groups of *L. plantarum* BW2013 (a low-dose group of 10^8 CFU/ml, a medium-dose group of 10^9 CFU/ml, and a high-dose group of 10^{10} CFU/ml). The weight of mice was recorded once a week, and the fecal samples were collected for 16S rRNA amplicon sequencing after 28 days of continuous treatment. Compared with the control group, the body weight gain in the treatment groups was not significant. The 16S rRNA amplicon sequencing analysis showed that both the Chao1 and ACE indexes increased slightly in the medium-dose group compared to the control group, but the difference was not significant. Based on PCoA results, there was no significant difference in β diversity between the treatment groups. Compared to the control group, the abundance of *Bacteroidetes* increased in the low-dose group. The abundance of Firmicutes increased in the medium-dose group. At the genus level, the abundance of *Alloprevotella* increased in the low-dose group compared to the control group. The increased abundance of *Ruminococcaceae* and decreased abundance of *Candidatus_Saccharimonas* was observed in the medium-dose group. Additionally, the abundance of Bacteroides increased, and *Alistipes* and *Candidatus_Saccharimonas* decreased in the high-dose group. These results indicated that *L. plantarum* BW2013 could ameliorate gut microbiota composition, but its effects vary with the dose.

K e y w o r d s: *Lactobacillus plantarum*, composition, gut microbiota, 16S rRNA amplicon sequencing, BALB/c mice

Introduction

Gut microbiota, a large and complex microbial community in the gastrointestinal tract, is essential to the host's health and well-being (Koh et al. 2016; Liu et al. 2020). Gut microbiota can not only break down the indigestible carbohydrates in food (Schwalm and Groisman 2017), but also produce short-chain fatty acids (SFAs), which can provide nutrition for gut microbiota (Jia et al. 2020). The disturbance of gut microbiota induces inflammation, insulin resistance, diabetes, and osteoporosis (Ma et al. 2019; Bi et al. 2020). Even the novel coronavirus pneumonia was found associated with gut microbiota disturbance (He et al. 2020a).

Probiotics can modulate gut microbiota and cause favorable changes in the gut microbiota structure and functions (Hasan et al. 2019). When given enough dose, probiotics will reach the intestinal tract in an active state, thus improving intestinal microorganisms' balance and producing beneficial effects on the host (Deng et al. 2020). *Lactobacillus casei* ZX633 may ameliorate the infant diarrhea microbiota, thus reducing the rate of infant bacterial diarrhea (Wang et al. 2020b). After treated with mixed lactic acid bacteria, *Staphylococcus*

aureus infection could be prevented in mice, and the structure of intestinal microbiota could be improved (Ren et al. 2018).

Lactic acid bacteria and *Bifidobacteria* are the most commonly used probiotics (He et al. 2020b). *Lactobacillus plantarum*, a rod-shaped, facultative anaerobic, Gram-positive lactic acid bacterium, can effectively improve the health of the host by decreasing the level of bloodstream cholesterol, managing gastrointestinal disorders, and preventing diarrhea (Liu et al. 2015; Seddik et al. 2017a). Wang et al. (2018) found that *L. plantarum* ZDY2013 remits ulcerative colitis by modifying of intestinal microbiota to regulate both oxidative stress and inflammatory mediators. Some functional activities are strain-specific (Biagioli et al. 2019). Qiu et al. (2018) injected mice with potential probiotic strains, including *L. plantarum* ZDY04 (PLA04) and *L. plantarum* ZDY01 (PLA01). As a result, both serum trimethylamine *N*-oxide and cecal trimethylamine levels was reduced significantly only by *L. plantarum* ZDY04. Li et al. (2019) demonstrated the loss of gut microbiota diversity induced by glycerol monolaurate could be remedied by *L. plantarum* T17, but the same effects were not found in the group of *L. plantarum* T34. *L. plantarum* BW2013 was isolated from fermented Chinese cabbage, and the influence of this strain on the gut microbiota is unknown.

Many methods were used to study the gut microbiota, such as the culture of gut microbiota, polymerase chain reaction denaturing gradient gel electrophoresis (PCR-DGGE), quantitative real-time polymerase chain reaction (qRT-PCR), 16S rRNA amplicon sequencing (Margiotta et al. 2020; Ling et al. 2020). As a relatively new technology, 16S rRNA amplicon sequencing opens out new potential avenues of research and facilitates in-depth studies exploring microbial populations and their dynamics in the animal gut (Peng and Zhang 2009; Kim and Isaacson 2015). The 16S rRNA technology has been widely used in biomedical research, linking the establishment between microbiota disorders and human disease (Evariste et al. 2019). For example, Zhu et al. (2020) used 16S rRNA amplicon sequencing to study the gut microbiota of ulcerative colitis with different glucocorticoid response types and found that they had different bacterial composition and function, which linked the microbiota disorders and ulcerative colitis. Analysis of 16S rRNA amplicon sequencing of intestinal microbiota found that high-calorie diet and lipopolysaccharide atomization synergistically promoted pneumonia process in rat pups, which is related to changes in the structure of intestinal flora (Bai et al. 2020).

Based on 16S rRNA amplicon sequencing, this study investigated the effects of different doses of *L. plantarum* BW2013 on gut microbiota composition in mice.

Experimental

Materials and Methods

Bacterial strains and cultural conditions. *L. plantarum* BW2013 was isolated from fermented Chinese cabbage and preserved by the China General Microbiological Culture Collection Center (CGMCC NO. 9462). *L. plantarum* BW2013 was grown anaerobically in the Man-Rogosa-Sharpe medium broth for 20 h at 37°C, and then centrifuged at 3,000 g for 15 min. The bacteria were washed twice and resuspended in sterile phosphate-buffered saline (PBS, pH 7.4).

Simulate gastrointestinal digestion. The simulated gastrointestinal juice was produced with following Shinde et al. (2019), and amylase, pepsin, bovine bile, and trypsin were purchased from Sigma. First, bacteria (1 ml, 1×10^9 CFU/ml) were suspended in 5 ml simulated salivary juice for 5 min. Then, the samples were resuspended to 10 ml gastric juice and incubated for 2 h. Subsequently, the samples were resuspended to 10 ml intestinal juice and incubated for 2 h. The entire digestion procedure was performed at 37°C, with stirring to simulate peristaltic contraction. After the simulated digestion process, the bacteria cell suspensions were diluted and plated onto MRS agar plates. The number of colonies was counted after 24 h of incubation at 37°C according to the formula:

$$\text{survival rate}(\%) = N1 / N0 \times 100\%$$

where N_1 was the total viable count of strains after treatment and N_0 was the total viable count of strains before treatment.

Adhesion to Caco-2 cell. Caco-2 cell cultures were determined by the method of Fonseca et al. (2021). After cultured in MRS broth for 24 h at 37°C and washed twice with phosphate-buffered solution, the bacteria were resuspended in DMEM approximately 10^9 CFU/ml. Then, 1 ml bacterial suspension was added to cells and incubated for 60 min at 37°C in a 5% CO_2 atmosphere. Subsequently, the cells were washed three times with 1 ml of PBS to remove non-adherent bacterial cells and lysed with 1 ml of Triton-X solution at 37°C for 5 min. After the above procedures, the solution was serial diluted and plated on MRS agar to determine the bacterial counts.

Animal, rearing and grouping. The mice (8-week-old male) used in the experiment were purchased from Vital River Laboratories Inc. (Beijing, China). Mice were singly caged under specific pathogen-free conditions at 20–22°C, and relative humidity of 40–60%. Before intragastric administration, the mice were weighed, and the feces were collected for 16S rRNA gene amplicon sequencing analysis. Then the mice were randomly allocated to four groups (each group n = 10):

control group (NC) and three treatment groups of *L. plantarum* BW2013: a low-dose (10^8 CFU/ml) group (LDG), a medium-dose (10^9 CFU/ml) group (MDG), and a high-dose group (10^{10} CFU/ml) (HDG). From 9 a.m. to 10 a.m. every day, the NC group was given sterile PBS (pH 7.4), and treatment groups were administered the corresponding of *L. plantarum* BW2013 suspension at 400 µl/d once daily over 28 days. All mice were weighed once a week. During the experiment, the mice were fed a normal diet.

16S rRNA gene amplicon sequencing. The fecal genomic DNA was extracted according to the manufacturer's guidelines of DP712-Magnetic Bead Soil and Fecal Genomic DNA Extraction Kit (Tiangen, China). For 16S rRNA gene amplicon sequencing, the DNA samples were amplified with primers 27F (5'-AGAGTTTGATCMTGGCTCAG-3') and 519R (5'-GWATTACCGCGGCKGCTG-3'), which targeted V3-V4 hypervariable regions of the bacterial 16S rRNA gene (Ranasinghe et al. 2012). PCR program was applied, as follows: the initial denaturation at 95°C for 15 min, the amplification of 34 cycles under various conditions (at 95°C for 30 s, 58°C for 30 s and 68°C for 1 min), and the final extension at 68°C for 5 min. Then the purified amplicons were sequenced with an Illumina Miseq sequencing platform at Novogene Bioinformatics Technology Co., Ltd. (Tianjin, China).

The same volume of 1 × loading buffer (contained SYB green) was mixed with PCR products, and electrophoresis was operated on 2% agarose gel for detection. PCR products were mixed in equal density ratios. Then, the mixture of PCR products was purified with Gene JETTM Gel Extraction Kit (Thermo Scientific).

Sequencing libraries were generated using Ion Plus Fragment Library Kit 48 rxns (Thermo Scientific) following the manufacturer's recommendations. The library

quality was assessed on the Qubit@ 2.0 Fluorometer (Thermo Scientific). At last, the library was sequenced on an Ion S5TM XL platform and 400 bp/600 bp single-end reads were generated.

Statistical analysis. The analysis of variance for multiple comparisons was performed in Prisma software (version 5). Statistical differences were evaluated by analysis of variance (ANOVA) and Dunnett-t pairwise comparisons. Cutadapt (V1.9.1) was used for quality control (Martin 2011). Uparse software (Uparse v7.0.1001, http://www.drive5.com/uparse/) was applied to cluster the clean reads to OTUs (Edgar 2013). Species annotation analysis was carried out using the Mothur method and SSSUrRNA database of SILVA132 (http://www.arb-silva.de/) to obtain taxonomic information at each taxonomic level (Quast et al. 2013).

Results

Tolerance to simulated digestion test and adhesion to Caco-2 cell. The survival rate of *L. plantarum* BW2013 after the simulated gastrointestinal digestion process was 2.90%, and the adhesion rates of *L. plantarum* BW2013 was 2.4%.

Effect of *L. plantarum* BW2013 on the body weight gain of mice. Before intragastric administration, the mice were weighed. Then body weight was recorded once a week. The weight changes of mice were shown in Fig. 1. There was no significant difference in body weight gain among the four groups.

Overall sequences and OTUs. An average of 85,386 reads was measured per sample by 16SrRNA amplicon sequencing, and an average of 80,298 clean reads was obtained after quality control. The clean reads of all samples were clustered by OTUs (operational taxonomic units) with 97% identity. A total of 1,120 OTUs were obtained, and 74 OTUs were annotated to the genus level.

Diversity indexes among the NC and treatment groups. Compared with NC group, the Chao 1 and ACE indexes (Table I) were slightly higher than those in the MDG group. But there were no significant differences for all the α-diversity indexes among the NC and treatment groups. Compared with the initial state, the Chao1 index of the NC and MDG groups increased significantly, respectively ($p = 0.0379$, $p = 0.0267$).

The changes in gut microbiota among groups were examined by using principal coordinate analysis (PCoA). Based on weighted unifrac distance, PCoA analysis was conducted to compare the microbial community composition of different samples (Fig. 2). On the weighted unifrac PCoA score plot, the NC group's symbols were separated from those of the treatment groups, which revealed that the microbiome
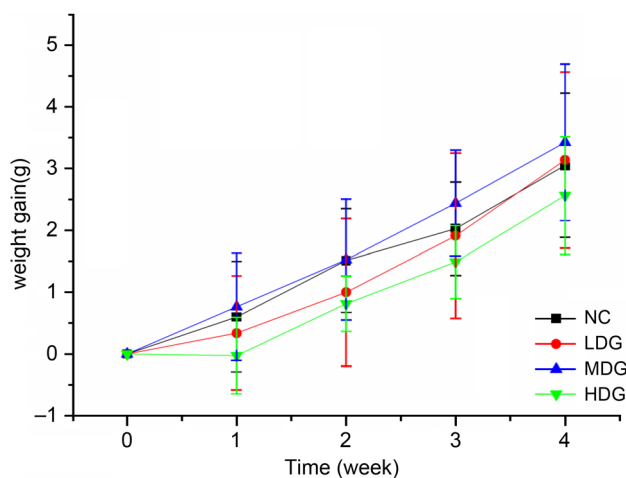

Fig. 1. Body weight variations of the mice after *L. plantarum* BW2013 gavage. The data are represented as mean ± SD.

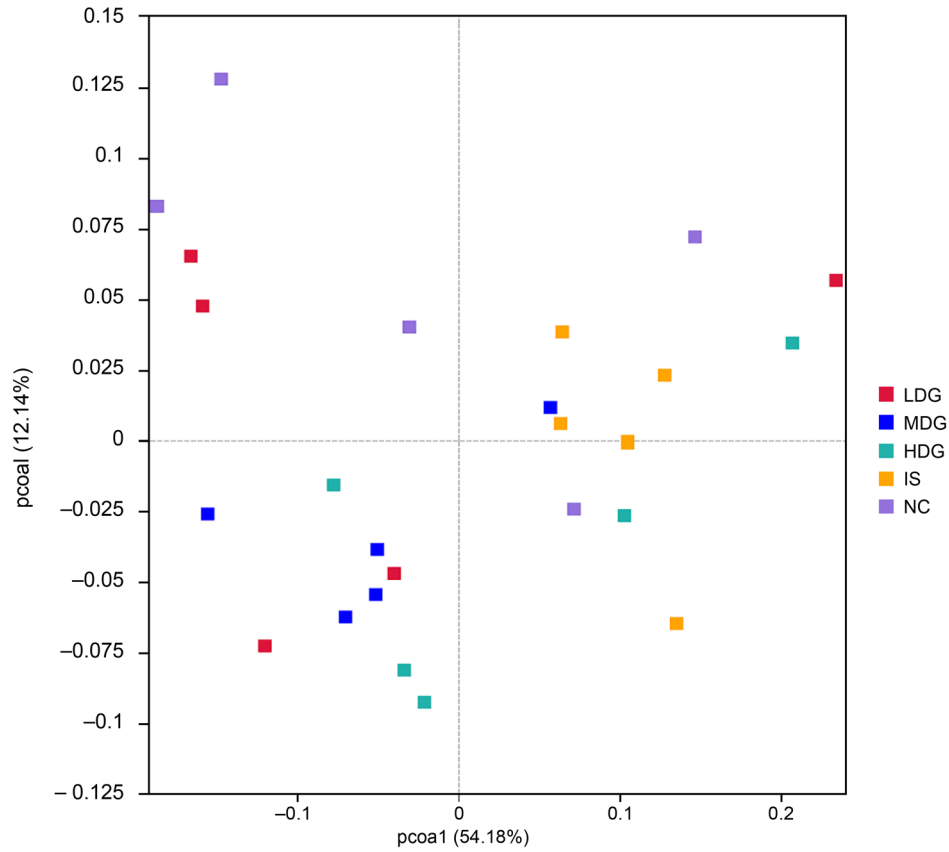NC – control group, LDG – low-dose group, MDG – medium-dose group, HDG – high-dose group.

Fig. 2. Principal co-ordinates analysis (PCoA) of the microbial communities of different groups. Initial state (IS) stands for mice before intragastric administration.

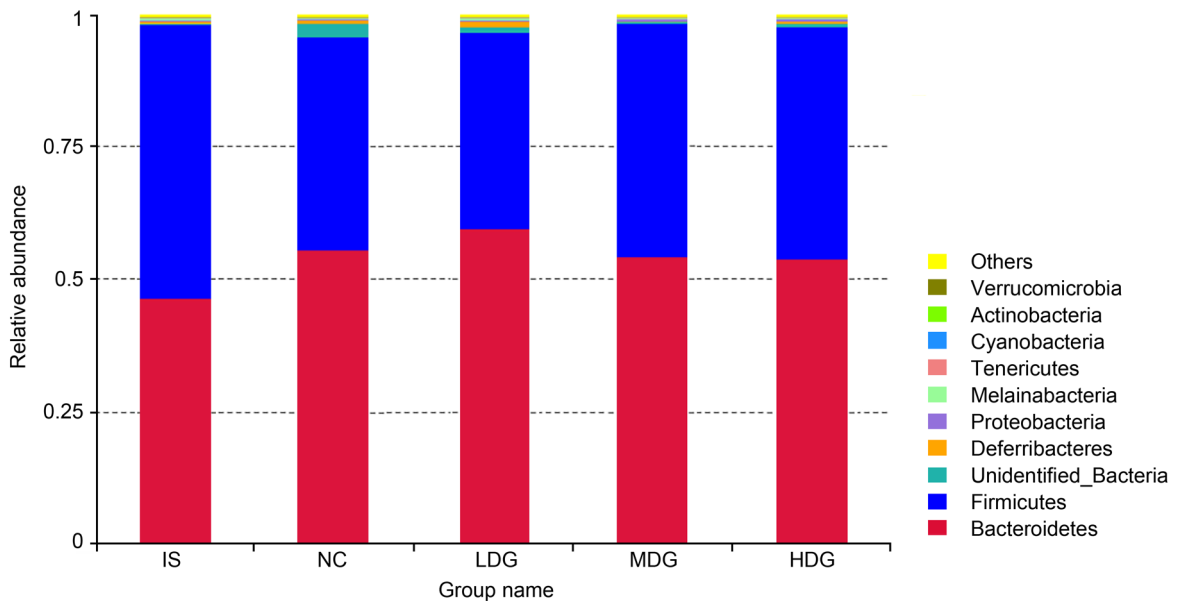NC – control group, LDG – low-dose group, MDG – medium-dose group, HDG – high-dose group.

Fig. 3. Microbial community bar plot at the phylum level. Initial state (IS) stands for mice before intragastric administration.

NC – control group, LDG – low-dose group, MDG – medium-dose group, HDG – high-dose group.

composition of treatment groups was different from those of the NC group, but there was no significant difference. Additionally, there was no significant difference between initial state and NC group.

Relative abundance of gut microbiota at phylum and genus levels. The relative abundance of gut microbiota was measured at the phylum (Fig. 3) and genus (Fig. 4) levels.
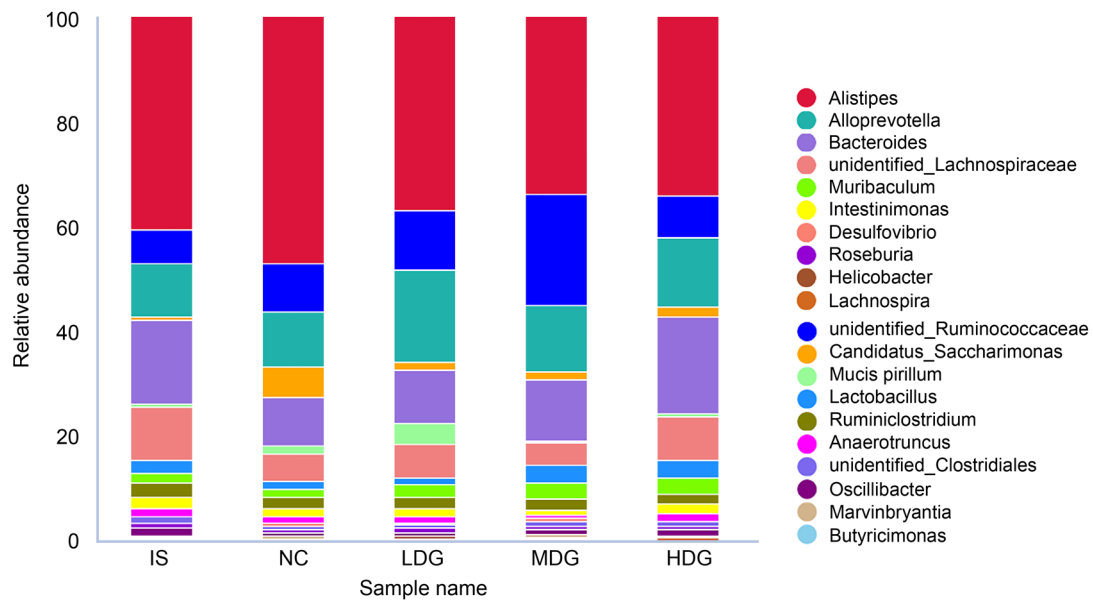
Fig. 4. Microbial community bar plot at the genus level. Initial state (IS) stands for mice before intragastric administration. NC – control group, LDG – low-dose group, MDG – medium-dose group, HDG – high-dose group.

Examining the changes in the gut microbiota, the top ten bacterial phyla of the NC and treatment groups were evaluated. The results showed that Bacteroidetes was the most abundant phylum, followed by Firmicutes, Deferribacteres, and Proteobacteria in the NC and treatment groups. *L. plantarum* BW2013 mainly affected the abundance of Bacteroidetes and Firmicutes, which accounted for 97% of the total bacteria (Fig. 3). Compared with the NC group, the abundance of Bacteroidetes increased significantly in the LDG group ($p = 0.04$). Additionally, the relative abundance of Firmicutes increased significantly in the MDG group compared to the NC group ($p = 0.01$).

The four most prevalent bacterial genera in the guts of the NC and treatment groups were *Alistipes*, *Alloprevotella*, *unidentified_Ruminococcaceae,* and *Bacteroides* (Fig. 4). Compared to the NC group, *Alistipes* exhibited significantly decreased proportions in the HDG group ($p = 0.038$). In addition, the abundance of *Candidatus_Saccharimonas* decreased significantly in the MDG and HDG groups ($p = 0.01$, $p = 0.007$). By contrast, *Alloprevotella*, *unidentified_Ruminococcaceae,* and

Bacteroides showed an upward trend. The abundance of *Alloprevotella* in the LDG group was significantly higher than that in the NC group ($p = 0.001$). Moreover, compared with the NC group, the abundance of *unidentified_Ruminococcaceae* in the MDG group increased significantly ($p = 0.014$), while the abundance of *Lactobacillus* increased slightly, but there was no significant difference. In addition*,* the proportion of *Bacteroides* increased significantly in the HDG group compared to the NC group ($p = 0.038$).

Clustering analysis of species abundance. The heat map showed the relative abundance of the main identified bacteria at the genus level. As shown in Fig. 5, the clustering of gut microbiota was different in the groups. In the initial state, gut microbiota was mainly clustered in Firmicutes. In the NC group, Bacteroidetes were concentrated in the genus of *Desulfovibrio*. Both *Parabacteroides* and *Alloprevotella* from Bacteroidetes dominated the LDG group. In the MDG group, there were large quantities of *Ruminococcaceae* and *Lachnospira* in Firmicutes. In the HDG group, Bacteroidetes were concentrated in the genus of *Bacteroides*.

Table I
The α diversity index of gut microbiota in each group.

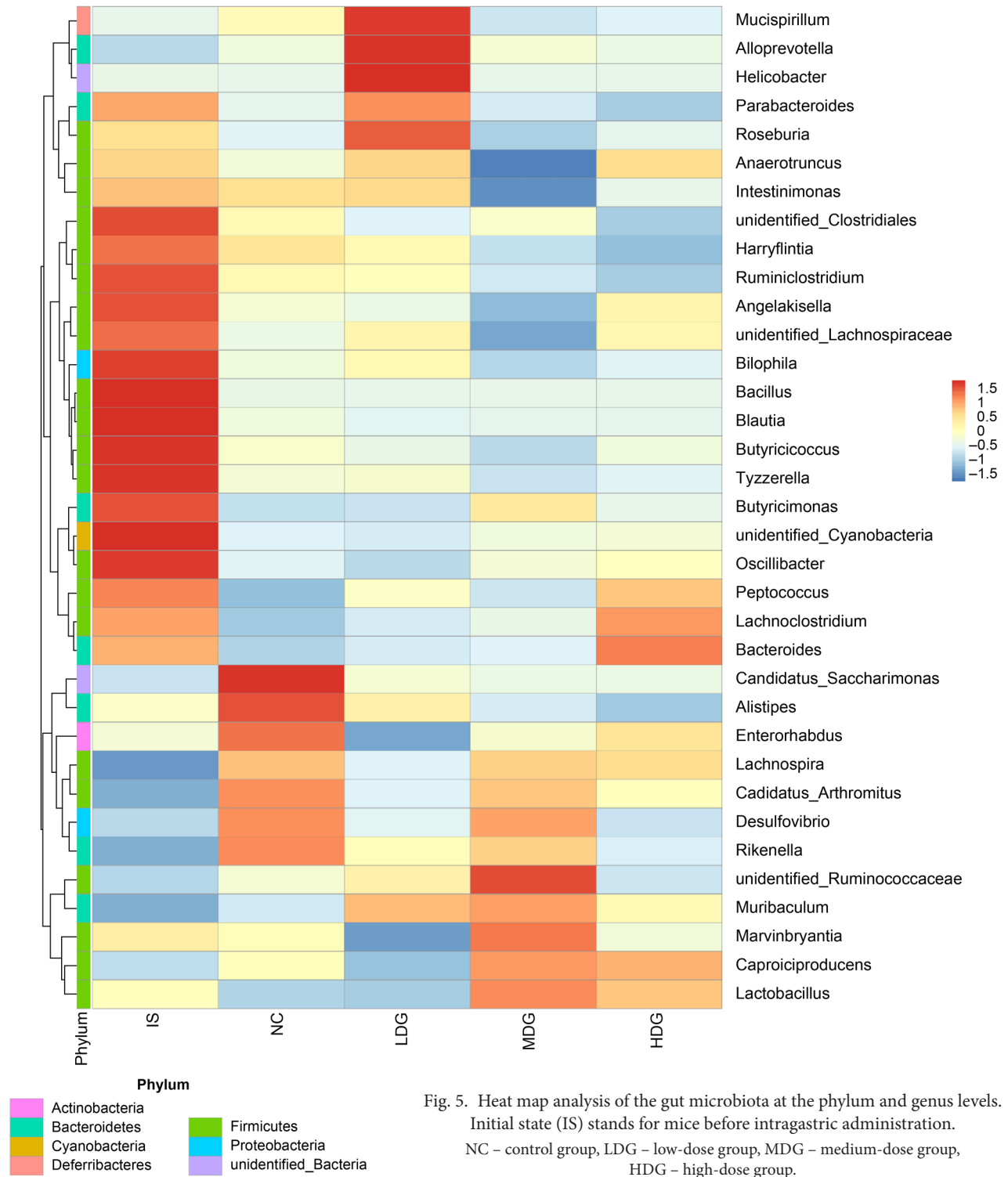| Group	Observed species	Shannon	Simpson	Chao1	ACE	Goods coverage
IS	532	6.566	0.971	534.371	540.911	0.999
NC	535.6	6.433	0.968	538.985	545.437	0.999
LDG	559	6.622	0.976	563.100	570.366	0.999
MDG	580	6.728	0.978	582.440	588.671	0.999
HDG	584.8	6.640	0.971	616.129	619.041	0.999

Fig. 5. Heat map analysis of the gut microbiota at the phylum and genus levels. Initial state (IS) stands for mice before intragastric administration.

NC – control group, LDG – low-dose group, MDG – medium-dose group, HDG – high-dose group.

Phylum

- Actinobacteria
- Bacteroidetes
- Cyanobacteria
- Deferribacteres
- Firmicutes
- Proteobacteria
- unidentified_Bacteria

Discussion

The consumption of probiotics has been reported to modulate the composition and structure of the gut microbiome and treat multiple diseases, but some functional activities are strain-specific (Biagioli et al. 2019; Hsu et al. 2019). There are also various methods for detecting gut microbiota, among which 16S rRNA amplicon sequencing is a faster and cheaper way to study the gut microbiome (Goldfeder et al. 2017). In this study, the effect of *L. plantarum* BW2013 on gut microbiota composition in BALB/c mice was investigated by 16S rRNA amplicon sequencing.

16S rRNA amplicon sequencing could be used to determine all microorganisms' genetic composition and community function in environmental samples (Qi et al. 2019). In our study, the results of 16S rRNA amplicon sequencing showed that the ACE index and Chao1

index slightly increased in the MGD group compared to the NC group, but there was no significant difference. A previous study also showed that the microbial richness (Chao1 and Shannon) was not significantly improved after the *L. plantarum* LIP-1 treatment (Song et al. 2017), which is consistent with our results. Based on PCoA, there was no significant difference in β diversity in the treatment groups compared to the NC group. There was also no significant difference between the initial state and NC group.

At the phylum level, the abundance of Bacteroidetes and Firmicutes accounted for 97% of the total bacteria. Bacteroidetes can regulate the chaotic state of intestinal microorganisms to a balanced state (Wang et al. 2020a). Firmicutes may play important roles in gastrointestinal health, and affect the metabolism and function of gut microbes (Zhao et al. 2018). In this study, the relative abundance of Bacteroidetes in the LDG group was significantly higher than that in the NC group. Li et al. (2017) found that *L. casei* CCFM419 increased the abundance of Bacteroidetes, which is similar to our result. Our study showed that the abundance of Firmicutes increased significantly in the MDG group compared with the NC group. *L. plantarum* 12 increased the relative abundance of Firmicutes (Sun et al. 2020), which is similar to our result. Contrary to our results, a strain of *L. plantarum* decreased the abundance of Firmicutes (Zhang et al. 2019).

At the genus level, *L. plantarum* BW2013 significantly increased the abundance of *Alloprevotella* and *Ruminococcaceae*, and significantly decreased the abundance of both *Alistipes* and *Candidatus_Saccharimonas*. *Alistipes* is pathogenic in colorectal cancer and is associated with mental signs of depression (Parker et al. 2020). *Candidatu_Saccharimonas* has been associated with inflammatory diseases, such as gingivitis and other periodontal dysfunctions (Cruz et al. 2020). *Alloprevotella* can produce vitamin B1 and folic acid, and an increase in the abundance of *Alloprevotella* was associated with the improvement of intestinal disorders Seddik et al. 2017; Qi et al. 2019). Based on our results, the abundance of *Alloprevotella* in the LDG group was significantly higher than in the NC group. Kong et al. (2018) found that the abundance of *Alloprevotella* increased significantly after probiotics treatment. This finding is similar to our result. *Ruminococcaceae* can produce butyrate, which can provide energy for intestinal epithelial cells (LeBlanc et al. 2017). In our study, compared with the NC group, the abundance of *Ruminococcaceae* in the MDG group increased significantly. Wang et al. (2018) found that the abundance of *Ruminococcaceae* showed a decreasing trend in *L. plantarum* ZDY2013 group, which is different from our result. It may be due to the different strains used in the experiment. Biagioli et al. (2019) mentioned that some functional activities are

strain-specific. Our study showed that compared with the NC group, the abundance of *Bacteroides* in the HDG group increased significantly. Li et al. (2017) found that *L. casei* CCFM419 increased the abundance of *Bacteroides*, which is consistent with our result. *Bacteroides* are producers of short-chain fatty acids (SCFAs) (Du et al. 2020). SCFAs are produced by the fermentation of microorganisms in the gut and help regulate host energy homeostasis and physiological processes (Horiuchi et al. 2020). This correlation means that the presence of *L. plantarum* BW2013 can provide a positive impact on host health. In our study, *Desulfovibrio* was enriched in the NC group in the heat map, while *Parabacteroides*, *Alloprevotella*, *Ruminococcaceae*, *Lachnospira*, and *Bacteroides* were concentrated in the treatment groups. Our results collectively suggested that *L. plantarum* BW2013 the effect of ameliorating gut microbiota composition, but its effects vary with the dose.

Conclusion

In this study, our results showed that treatment with *L. plantarum* BW2013 exerted an effect on the gut microbiota composition in mice. At the phylum level, the abundance of Bacteroidetes increased in the LDG group compared with the NC group, while the abundance of Firmicutes increased in the MDG group. At the genus level, the abundance of *Alloprevotella* was higher in the LDG group compared with the NC group. By contrast, the abundance of *Ruminococcaceae* increased in the MDG group, but *Candidatus_Saccharimonas* decreased. In addition, *Bacteroides* abundance increased in the HDG group, but *Alistipes* and *Candidatus_Saccharimonas* decreased. These results indicated that *L. plantarum* BW2013 had the effect of ameliorating the composition of gut mice, but its effect varies with dosing.

Authors' contributions
Zuming Li, Jia Liu and Zhihui Bai conceived and designed the experiments; Tong Tong, Qian Li and Yuxi Ling performed the experiments; Tong Tong, Qian Li, Xiaohui Niu and Michael Zhang analyzed the data; Tong Tong and Xiaohui Niu wrote the paper; Ran Xia, Zhichao Wu and Xiu Liu gave important suggestions; Zuming Li, Michael Zhang,Tong Tong and Xiaohui Niu revised the manuscript.

Conflict of interest

Literature

Bai C, Liu T, Xu J, Ma X, Huang L, Liu S, Yu H, Chen J, Gu X. Effect of high calorie diet on intestinal flora in LPS-induced pneumonia rats. Sci Rep. 2020 Feb 3;10(1):1701. https://doi.org/10.1038/s41598-020-58632-0

Bi R, Gao J, Pan L, Lai X. Progress in the treatment of diabetes mellitus based on intestinal flora homeostasis and the advancement of holistic analysis methods. Nat Prod Commun. 2020;15(4):1–11. https://doi.org/10.1177/1934578X20918418

Biagioli M, Capobianco D, Carino A, Marchianò S, Fiorucci C, Ricci P, Distrutti E, Fiorucci S. Divergent effectiveness of multispecies probiotic preparations on intestinal microbiota structure depends on metabolic properties. Nutrients. 2019 Feb 2;11(2):325.

Cruz BCDS, Conceição LLD, Mendes TAO, Ferreira CLLF, Gonçalves RV, Peluzio MDCG. Use of the synbiotic VSL#3 and yacon-based concentrate attenuates intestinal damage and reduces the abundance of *Candidatus Saccharimonas* in a colitis-associated carcinogenesis model. Food Res Int. 2020 Nov;137:109721. https://doi.org/10.1016/j.foodres.2020.109721

Deng X, Tian H, Yang R, Han Y, Wei K, Zheng C, Liu Z, Chen T. Oral probiotics alleviate intestinal dysbacteriosis for people receiving bowel preparation. Front Med (Lausanne). 2020 Feb 28;7:73. https://doi.org/10.3389/fmed.2020.00073

Du X, Xiang Y, Lou F, Tu P, Zhang X, Hu X, Lyu W, Xiao Y. Microbial community and short-chain fatty acid mapping in the intestinal tract of quail. Animals (Basel). 2020 Jun 9;10(6):1006. https://doi.org/10.3390/ani10061006

Edgar RC. UPARSE: highly accurate OTU sequences from microbial amplicon reads. Nat Methods. 2013 Oct;10(10):996–998. https://doi.org/10.1038/nmeth.2604

Evariste L, Barret M, Mottier A, Mouchet F, Gauthier L, Pinelli E. Gut microbiota of aquatic organisms: A key endpoint for ecotoxicological studies. Environ Pollut. 2019 May;248:989–999. https://doi.org/10.1016/j.envpol.2019.02.101

Fonseca HC, de Sousa Melo D, Ramos CL, Dias DR, Schwan RF. Probiotic properties of lactobacilli and their ability to inhibit the adhesion of enteropathogenic bacteria to Caco-2 and HT-29 cells. Probiotics Antimicrob Proteins. 2021 Feb;13(1):102–112. https://doi.org/10.1007/s12602-020-09659-2

Goldfeder RL, Wall DP, Khoury MJ, Ioannidis JPA, Ashley EA. Human genome sequencing at the population scale: a primer on high-throughput dna sequencing and analysis. Am J Epidemiol. 2017 Oct 15;186(8):1000–1009. https://doi.org/10.1093/aje/kww224

Hasan N, Yang H. Factors affecting the composition of the gut microbiota, and its modulation. PeerJ. 2019 Aug 16;7:e7502. https://doi.org/10.7717/peerj.7502

He LH, Ren LF, Li JF, Wu YN, Li X, Zhang L. Intestinal flora as a potential strategy to fight SARS-CoV-2 infection. Front Microbiol. 2020a Jun 9;11:1388. https://doi.org/10.3389/fmicb.2020.01388

He Y, Xu R, Wang W, Zhang J, Hu X. Probiotics, prebiotics, antibiotic, Chinese herbal medicine, and fecal microbiota transplantation in irritable bowel syndrome: Protocol for a systematic review and network meta-analysis. Medicine (Baltimore). 2020b Aug 7; 99(32):e21502. https://doi.org/10.1097/MD.0000000000021502

Horiuchi H, Kamikado K, Aoki R, Suganuma N, Nishijima T, Nakatani A, Kimura I. *Bifidobacterium animalis* subsp. *lactis* GCL2505 modulates host energy metabolism via the short-chain fatty acid receptor GPR43. Sci Rep. 2020 Mar 5;10(1):4158. https://doi.org/10.1038/s41598-020-60984-6

Hsu CN, Hou CY, Chan JYH, Lee CT, Tain YL. Hypertension programmed by perinatal high-fat diet: effect of maternal gut microbiota-targeted therapy. Nutrients. 2019 Dec 2;11(12):2908. https://doi.org/10.3390/nu11122908

Jia Q, Wang L, Zhang X, Ding Y, Li H, Yang Y, Zhang A, Li Y, Lv S, Zhang J. Prevention and treatment of chronic heart failure through traditional Chinese medicine: Role of the gut microbiota. Pharmacol Res. 2020 Jan;151:104552. https://doi.org/10.1016/j.phrs.2019.104552

Kim HB, Isaacson RE. The pig gut microbial diversity: Understanding the pig gut microbial ecology through the next generation high throughput sequencing. Vet Microbiol. 2015 Jun 12;177(3–4):242–251. https://doi.org/10.1016/j.vetmic.2015.03.014

Koh A, De Vadder F, Kovatcheva-Datchary P, Bäckhed F. From dietary fiber to host physiology: short-chain fatty acids as key bacterial metabolites. Cell. 2016 Jun 2;165(6):1332–1345. https://doi.org/10.1016/j.cell.2016.05.041

Kong C, Gao R, Yan X, Huang L, Qin H. Probiotics improve gut microbiota dysbiosis in obese mice fed a high-fat or high-sucrose diet. Nutrition. 2019 Apr;60:175–184. https://doi.org/10.1016/j.nut.2018.10.002

LeBlanc JG, Chain F, Martín R, Bermúdez-Humarán LG, Courau S, Langella P. Beneficial effects on host energy metabolism of short-chain fatty acids and vitamins produced by commensal and probiotic bacteria. Microb Cell Fact. 2017 May 8;16(1):79. https://doi.org/10.1186/s12934-017-0691-z

Li X, Wang E, Yin B, Fang D, Chen P, Wang G, Zhao J, Zhang H, Chen W. Effects of *Lactobacillus casei* CCFM419 on insulin resistance and gut microbiota in type 2 diabetic mice. Benef Microbes. 2017 May 30;8(3):421–432. https://doi.org/10.3920/BM2016.0167

Li Y, Liu T, Zhang X, Zhao M, Zhang H, Feng F. *Lactobacillus plantarum* helps to suppress body weight gain, improve serum lipid profile and ameliorate low-grade inflammation in mice administered with glycerol monolaurate. J Funct Food. 2019;53: 54–61. https://doi.org/10.1016/j.jff.2018.12.015

Ling Y, Li W, Tong T, Li Z, Li Q, Bai Z, Wang G, Chen J, Wang Y. Assessing the microbial communities in four different daqus by using PCR-DGGE, PLFA, and Biolog analyses. Pol J Microbiol. 2020;69(1):27–37. https://doi.org/10.33073/pjm-2020-004

Liu WH, Yang CH, Lin CT, Li SW, Cheng WS, Jiang YP, Wu CC, Chang CH, Tsai YC. Genome architecture of *Lactobacillus plantarum* PS128, a probiotic strain with potential immunomodulatory activity. Gut Pathog. 2015 Aug 15;7:22. https://doi.org/10.1186/s13099-015-0068-y

Liu Z, Luo G, Du R, Sun W, Li J, Lan H, Chen P, Yuan X, Cao D, Li Y, et al. Effects of spaceflight on the composition and function of the human gut microbiota. Gut Microbes. 2020 Jul 3;11(4):807–819. https://doi.org/10.1080/19490976.2019.1710091

Ma Q, Li Y, Li P, Wang M, Wang J, Tang Z, Wang T, Luo L, Wang C, Wang T, et al. Research progress in the relationship between type 2 diabetes mellitus and intestinal flora. Biomed Pharmacother. 2019 Sep;117:109138. https://doi.org/10.1016/j.biopha.2019.109138

Margiotta E, Miragoli F, Callegari ML, Vettoretti S, Caldiroli L, Meneghini M, Zanoni F, Messa P. Gut microbiota composition and frailty in elderly patients with Chronic Kidney Disease. PLoS One. 2020 Apr 1;15(4):e0228530.

https://doi.org/10.1371/journal.pone.0228530

Martin M. Cutadapt removes adapter sequences from high-throughput sequencing reads. EMBnet J. 2011 May;7(1):10–12. https://doi.org/10.14806/ej.17.1.200

Parker BJ, Wearsch PA, Veloo ACM, Rodriguez-Palacios A. The genus *Alistipes*: Gut bacteria with emerging implications to inflammation, cancer, and mental health. Front Immunol. 2020 Jun 9;11:906. https://doi.org/10.3389/fimmu.2020.00906

Peng H, Zhang J. Commercial high-throughput sequencing and its applications in DNA analysis. Biologia. 2009;64(1): 20–26. https://doi.org/10.2478/s11756-009-0028-4

Qi H, Liu Y, Qi X, Liang H, Chen H, Jiang P, Wang D. Dietary recombinant phycoerythrin modulates the gut microbiota of H22 tumor-bearing mice. Mar Drugs. 2019 Nov 26;17(12):665. https://doi.org/10.3390/md17120665

Qiu L , Tao X , Xiong H , Yu J , Wei H . *Lactobacillus plantarum* ZDY04 exhibits a strain-specific property of lowering TMAO via the modulation of gut microbiota in mice. Food Funct. 2018 Aug 15; 9(8):4299–4309. https://doi.org/10.1039/c8fo00349a

Quast C, Pruesse E, Yilmaz P, Gerken J, Schweer T, Yarza P, Peplies J, Glöckner FO. The SILVA ribosomal RNA gene database project: improved data processing and web-based tools. Nucleic Acids Res. 2013 Jan 1;41(D1):D590–D596. https://doi.org/10.1093/nar/gks1219

Ranasinghe PD, Satoh H, Oshiki M, Oshima K, Suda W, Hattori M, Mino T. Revealing microbial community structures in large- and small-scale activated sludge systems by barcoded pyrosequencing of 16S rRNA gene. Water Sci Technol. 2012;66(10):2155–2161. https://doi.org/10.2166/wst.2012.428

Ren D, Gong S, Shu J, Zhu J, Liu H, Chen P. Effects of mixed lactic acid bacteria on intestinal microbiota of mice infected with *Staphylococcus aureus*. BMC Microbiol. 2018 Sep 6;18(1):109. https://doi.org/10.1186/s12866-018-1245-1

Schwalm ND 3rd, Groisman EA. Navigating the gut buffet: control of polysaccharide utilization in *Bacteroides* spp. Trends Microbiol. 2017 Dec;25(12):1005–1015. https://doi.org/10.1016/j.tim.2017.06.009

Seddik HA, Bendali F, Gancel F, Fliss I, Spano G, Drider D. *Lactobacillus plantarum* and its probiotic and food potentialities. Probiotics Antimicrob Proteins. 2017 Jun;9(2):111–122. https://doi.org/10.1007/s12602-017-9264-z

Shinde T, Vemuri R, Shastri MD, Perera AP, Tristram S, Stanley R, Eri R. Probiotic *Bacillu*s coagulans MTCC 5856 spores exhibit excellent *in vitro* functional efficacy in simulated gastric survival, mucosal adhesion and immunomodulation. J Funct Food. 2019;52:100–108. https://doi.org/10.1016/j.jff.2018.10.031

Song JJ, Tian WJ, Kwok LY, Wang YL, Shang YN, Menghe B, Wang JG. Effects of microencapsulated *Lactobacillus plantarum* LIP-1 on the gut microbiota of hyperlipidaemic rats. Br J Nutr. 2017 Oct; 118(7):481–492. https://doi.org/10.1017/S0007114517002380

Sun M, Liu Y, Song Y, Gao Y, Zhao F, Luo Y, Qian F, Mu G, Tuo Y. The ameliorative effect of *Lactobacillus plantarum*-12 on DSS-induced murine colitis. Food Funct. 2020 Jun 24;11(6):5205–5222. https://doi.org/10.1039/d0fo00007h

Wang C, Zhao J, Zhang H, Lee YK, Zhai Q, Chen W. Roles of intestinal *bacteroides* in human health and diseases. Crit Rev Food Sci Nutr. 2020a Aug 6:1–19. https://doi.org/10.1080/10408398.2020.1802695

Wang X, Zhang M, Wang W, Lv H, Zhang H, Liu Y, Tan Z. The *in vitro* effects of the probiotic strain, *Lactobacillus casei* ZX633 on gut microbiota composition in infants with diarrhea. Front Cell Infect Microbiol. 2020b Sep 10;10:576185. https://doi.org/10.3389/fcimb.2020.576185

Wang Y, Guo Y, Chen H, Wei H, Wan C. Potential of *Lactobacillus plantarum* ZDY2013 and *Bifidobacterium bifidum* WBIN03 in relieving colitis by gut microbiota, immune, and anti-oxidative stress. Can J Microbiol. 2018 May;64(5):327–337. https://doi.org/10.1139/cjm-2017-0716

Zhang F, Li Y, Wang X, Wang S, Bi D. The impact of *Lactobacillus plantarum* on the gut microbiota of mice with DSS-induced colitis. Biomed Res Int. 2019 Feb 20;2019:3921315. https://doi.org/10.1155/2019/3921315

Zhao LL, Yin HC, Lu TF, Niu YJ, Zhang YY, Li SQ, Wang YP, Chen HY. Application of high-throughput sequencing for microbial diversity detection in feces of specific-pathogen-free ducks. Poult Sci. 2018 Jul 1;97(7):2278–2286. https://doi.org/10.3382/ps/pex348

Zhu Y, Luo J, Yang Z, Miao Y. High-throughput sequencing analysis of differences in intestinal microflora between ulcerative colitis patients with different glucocorticoid response types. Genes Genomics. 2020 Oct;42(10):1197–1206. https://doi.org/10.1007/s13258-020-00986-w

Isolation, Identification, Biocontrol Activity, and Plant Growth Promoting Capability of a Superior *Streptomyces tricolor* Strain HM10

MEDHAT REHAN[1,2]*, ABDULLAH S. ALSOHIM[1], HUSSAM ABIDOU[3], ZAFAR RASHEED[4]
and WALEED AL ABDULMONEM[5]

[1] Department of Plant Production and Protection, College of Agriculture and Veterinary Medicine,
Qassim University, Buraydah, Saudi Arabia
[2] Department of Genetics, College of Agriculture, Kafrelsheikh University, Kafr El-Sheikh, Egypt
[3] Department of Basic Science, Second Faculty of Agriculture, University of Aleppo, Aleppo, Syria
[4] Department of Medical Biochemistry, College of Medicine, Qassim University, Buraydah, Saudi Arabia
[5] Department of Pathology, College of Medicine, Qassim University, Buraydah, Saudi Arabia

A b s t r a c t

Streptomyces is a genus with known biocontrol activity, producing a broad range of biologically active substances. Our goal was to isolate local *Streptomyces* species, evaluate their capacity to biocontrol the selected phytopathogens, and promote the plant growth via siderophore and indole acetic acid (IAA) production and phosphate solubilization. Eleven isolates were obtained from local soil samples in Saudi Arabia via the standard serial dilution method and identified morphologically by scanning electron microscope (SEM) and 16S rRNA amplicon sequencing. The biocontrol of phytopathogens was screened against known soil-borne fungi and bacteria. Plant growth promotion capacity was evaluated based on siderophore and IAA production and phosphate solubilization capacity. From eleven isolates obtained, one showed 99.77% homology with the type strain *Streptomyces tricolor* AS 4.1867, and was designated *S. tricolor* strain HM10. It showed aerial hyphae in SEM, growth inhibition of ten known phytopathogens in *in vitro* experiments, and the production of plant growth promoting compounds such as siderophores, IAA, and phosphate solubilization capacity. *S. tricolor* strain HM10 exhibited high antagonism against the fungi tested (i.e., *Colletotrichum gloeosporides* with an inhibition zone exceeding 18 mm), whereas the lowest antagonistic effect was against *Alternaria solani* (an inhibition zone equal to 8 mm). Furthermore, the most efficient siderophore production was recorded to strain HM8, followed by strain HM10 with 64 and 22.56 h/c (halo zone area/colony area), respectively. Concerning IAA production, *Streptomyces* strain HM10 was the most effective producer with a value of 273.02 µg/ml. An autochthonous strain *S. tricolor* HM10 should be an important biological agent to control phytopathogens and promote plant growth.

K e y w o r d s: *Streptomyces tricolor* HM10, plant growth-promoting, biocontrol, soil-borne disease

Introduction

In the search for new and active natural resources and to find friendly environmental solutions for yield increase and crop protection, Actinobacteria (especially *Streptomyces*) are gaining great interest in agriculture concerning plant growth-promoting and/or biological control (Kunova et al. 2016; Vurukonda et al. 2018).

From all known antibiotics that are produced by microorganisms, Actinobacteria produces two-thirds of them. *Streptomyces* produce 80% of the secondary metabolites with biological activities from the total production of Actinobacteria (Waksman et al. 2010; Barka et al. 2016; Takahashi and Nakashima 2018). At least in 5,000 publications, the scientists listed Actinobacteria's bioactive compounds produced by the *Streptomyces* genus. Actinobacteria that have been isolated from the soil are able to inhibit phytopathogen growth, among the others *Ralstonia solanacearum, Pantoae dispersa,* and *Fusarium palmivora* (Anderson

and Wellington 2001; Bérdy 2005; El-Naggar et al. 2006; Kaur et al. 2019).

The *Streptomyces* genus is ubiquitous and can live in symbiosis with eukaryotic organisms, ranging from marine animals, insects, and plants to fungi, or be free-living in soil (Seipke et al. 2012).

Streptomyces species can promote plant growth and suppress plant pathogens. By inhibiting fungal pathogens, *Streptomyces* can protect the roots of plant via antifungal compounds and lytic enzyme production (Doumbou et al. 2001; Palaniyandi et al. 2013; Bonaldi et al. 2014). Moreover, through the siderophore or auxin production, plant growth promotion has been observed. The combination of a wide variety of substances and the bacteria abundance in soil suggest that *Streptomyces* can play a significant role in microbe-microbe and plant-microbe interactions. It makes this microorganism a promising agent as biofertilizers and plant protection products (Sadeghi et al. 2012; Law et al. 2017; Jung et al. 2018; Vurukonda et al. 2018).

The selection of biological control agents usually starts with an *in vitro* screening using a dual culture assay within a selected group of strains against a group of pathogens. Actinobacteria secretes a wide variety of extracellular antibiotics and enzymes (Doumbou et al. 2001; Yekkour et al. 2012; Singh et al. 2018), which can be quantified as the clear zone of growth inhibition of the pathogen's mycelium.

Upon the beginning of sporulation and development of aerial hyphae, the production of *Streptomyces* secondary metabolites is induced. Furthermore, the *Streptomyces* inoculation time of the strains varied from the co-inoculation on the same day to seven days before the pathogen. As a biological agent, *Streptomyces* ma.FS-4 is an important agent to control the plant pathogenic fungi in banana (Trejo-Estrada et al. 1998; Boukaew et al. 2011; Pliego et al. 2011; Schrey et al. 2012; Ji et al. 2014; Duan et al. 2020).

On the other hand, some fungal pathogens require iron (Fe) for their pathogenicity. The beneficial rhizobacteria that produce siderophores are chelating ferric iron from the surrounding environment and subsequently could inhibit the growth of pathogen via iron competition (Expert et al. 2012). At the same time, these bacteria provide the iron available for plant growth and work as plant inducers.

Otherwise, the environment is highly contaminated due to agrochemical usage like pesticides and/or fertilizers. Some opponents expressed concern about the heavy use of pesticides, which has led to a significant shift in people's attitudes to pesticide use in both the surrounding environment and agriculture (Yoon et al. 2013; Nicolopoulou-Stamati et al. 2016; Brauer et al. 2019).

Experimental

Materials and Methods

***Streptomyces* isolation and media composition.** A total of five soil samples from around healthy plants were collected from 10–20 cm depth of agricultural soil, Qassim University Campus, Buraydah, Qassim, KSA. By the standard serial dilution method, these soil samples were prepared for bacterial strains isolation (Valan Arasu et al. 2009). Soil samples (3–4 g) of each sample were suspended in distilled water (9 ml) and vortexed. Furthermore, a serial dilution up to 10^{-3} dilution of each sample was performed. *Streptomyces* were subsequently isolated by spread plate technique on PDA (Potato Dextrose Agar) medium and incubated for a week at 28°C. Selected *Streptomyces* colonies were isolated and characterized by their colony morphology and pigments. These colonies were further purified and sub-cultured on tryptone soyagar (15 g/l pancreatic digest of casein, 5 g/l enzymatic digest of Soybean, 5 g/l sodium chloride, 15 g/l agar, final pH 7.3). For secondary metabolites production, glucose soybean meal broth (GSB) consisted of 10 g/l glucose, 10 g/l soybean meal, 10 g/l NaCl, 1 g/l $CaCO_3$, and pH adjusted to 7.0 was used as the production medium.

Isolated strains classification and identification. *Morphological characteristics.* The morphological properties of isolated *Streptomyces* strains were characterized with colony characteristics, pigment color, areal hyphae, the opacity of colony, colony consistency, fragmentation pattern, and growth under the surface of liquid media. Otherwise, for visualization of aerial hyphae, hypha, and spore characteristics under the scanning electron microscope (SEM), *S. tricolor* strain HM10 was grown for 48 h in a growth medium. The bacteria were harvested at 6,000 rpm by centrifugation for 10 min and subjected to the method of a critical drying point (Dhanjal and Cameotra 2010). The cells were washed with phosphate-buffered saline (PBS, pH 7.4) three times and fixed by incubation in a modified Karnovsky's fixative solution (2.5 ml of 50% glutaraldehyde, 2 g paraformaldehyde) for four hours. Cells were washed with PBS and distilled water and dehydrated by the increasing ethanol concentrations (30%, 50%, 70%, 90% and 100%) for critical point drying. *t*-Butyl alcohol was used to layer the dehydrated samples for freeze-drying, subsequently, and the samples were coated with titanium and viewed at 1,000 to 5,000-fold magnification with SEM (AMRAY 3300FE).

Morphological characteristics. The isolated *Streptomyces* were grown at 28°C for 7 days in Tryptone Soy Agar medium. The soluble pigments color, the hyphae color and airborne hyphae were detected.

PCR amplification of 16S rRNA and phylogenetic characteristics. DNA was extracted according to the simple method of DNA extraction with little modifications (Cook and Meyers 2003). Briefly, isolated *Streptomyces* strains were cultured in TSB (tryptone Soybroth) at 30°C for 24–48 h. Cells were centrifugated for 3 min at 12,000 rpm, washed once with TE buffer (pH 7.7). Cells were resuspended again in TE buffer (500 μl), heated at 95°C for 10 min in boiling water bath, and kept on ice to cool, followed by centrifugation at 12,000 rpm for 5 min. The extracted DNA was transferred to a clean tube and stored at 4°C for PCR amplification. PCR amplification was conducted using GoTaq® Green Master Mix (Promega, USA) for 16S rDNA in 50 μl volumes by universal primers 27 F 5'-AGAGTTT-GATCATGGCTCAG-3' and 1492 R 5'-TACGGTTAC-CTTGTTACGACTT-3'. PCR products were electrophoresed in 1% agarose gel to ensure the amplification of the fragment of correct size. Products were purified and sequenced (Capillary Electrophoresis Sequencing (CES), ABI 3730xl System, Macrogen company, South Korea). A phylogenetic tree was inferred with a maximum likelihood method using with the following parameters: Tamura-Nei model, Neighbor-Joining method to a matrix of pairwise distances estimated using the Maximum Composite Likelihood (MCL) approach, Uniform Rates. Evolutionary analyses were conducted in MEGA X (Kumar et al. 2018).

Antimicrobial activity assays. The isolated *Streptomyces* strains were grown for three days in GSB liquid media. Their antifungal activity against ten fungal plant pathogens was measured according to Kanini et al. (2013). The fungal strains were grown on Potato Dextrose Agar (PDA) plates for 3 days at 30°C, then a 6-mm mycelium disk from each selected fungus was then placed in the center of a new PDA plate. The bacterial suspensions (50 μl from a 5-day culture of each *Streptomyces* strain tested) were put into the opposite sides of each PDA plate. The inoculated plates with fungi and *Streptomyces* were kept in the incubator for five days at 28°C. The antagonistic activity of the strains tested was observed via measuring the inhibition zone distance. The antibacterial assay was also measured with five-day cultures filtrate from *Streptomyces* tested strains against the bacterial strains selected using the agar well diffusion method with modifications (CLSI 2011). Briefly, each tested strain was grown in LB media overnight, and an inoculum of each tested strain (about 2 ml) was added to 25 ml of new LB media before solidification (at nearly 50°C). In the agar medium, wells of six mm in diameter were perforated, and 50 μl of each five-day *Streptomyces* cultures were placed into the wells, followed by incubation at 30 or 37°C (depended on the bacteria favorite temperature). After 24 h of incubation, the inhibition zones were recorded.

Plant growth promotion (PGP) assessment *in vitro*. Three parameters related to plant growth promotion were evaluated in *Streptomyces* strains.

Siderophores production. The CAS (Chrome Azurol S) assay to detect siderophore production, according to (Schwyn and Neilands 1987) was applied. Briefly, iron (III) solution was prepared by mixing 1 mM $FeCl_3$ in 10 ml of 10 mM HCl. In another conical flask, 60.5 mg of CAS was dissolved in distilled water (50 ml). The orange color mixture was then added to the previously prepared solution of the iron (10 ml), which turned the solution color to purple. Whereas stirring, the previous purple solution was slowly poured into HDTMA (hexadecyltrimethylammonium) (72.9 mg), dissolved in 40 ml of distilled water, which turned into dark blue color after mixing. *Streptomyces* strains on PDB of approximately the same OD_{600} were put into a succinate medium mixed with CAS dye and incubated for 72–96 h. A clear to orange halo around the growing bacterial cells were detected. The molecules' color intensity and diffusion potential were directly related to the chelating strength and the concentration of produced siderophore.

Production of extracellular indole-3-acetic acid (IAA). *Streptomyces* strains were grown in nutrient broth medium for one day at 28°C. Cells were diluted up to (10^8 CFU/ml) in NB medium supplemented with L-tryptophane (500 μg/ml), and grown with shaking for five days at 28°C. Cells were pelleted for 10 min at 12,000 rpm, while the supernatant was collected. Using Salkowski reagent, which consisted of 0.5 M $FeCl_3$ (1 ml) in 35% $HCLO_4$ (50 ml), IAA concentration was measured with a colorimetric assay (Bano and Musarrat 2003) after 25–30 min using a spectrophotometer at the wavelength 530 nm. The standard curve was made to evaluate the IAA concentration.

Phosphate solubilization. Pikovskaya agar (PKV) medium was prepared, and $Ca_3(PO_4)_2$ was added separately after autoclaving to agar plates. A 50 μl of each strain containing approximately (10^8 CFU/ml) was added to agar plates and incubated for five days at 28°C. Bacterial colonies with clarification halos around were considered phosphate solubilizers (Donate-Correa et al. 2005).

Fermentation, extraction, and cancer cell culture. *S. tricolor* HM10 and *Streptomyces thinghirensis* strain HM3 were grown in GSB medium for six days. The fermented broth was extracted with equal volume from ethyl acetate, and vacuum evaporated. The resulted extract was dissolved in phosphate buffer saline (PBS, pH 7) and used to assay of cytotoxic activity. The A549 lung cancer cell-lines were purchased from ATCC (VA, USA) and were grown in DMEM according to manufacturer's instruction. Briefly, A549 cells were grown in DMEM medium with 10% heat-inactivated fetal bovine

serum (FBS) at 37°C in 5% CO_2 as described previously (Al Abdulmonem et al. 2020).

Treatment of lung cancer cells with the two *Streptomyces* extracts and cytotoxicity assay. The cultured cancer cells were serum-starved overnight and were treated with *S. tricolor* HM10 and *S. thinghirensis* HM3 extracts (10–200 μg/ml) for 12 hours, and the cytotoxicity was determined by the CytoTox-Glo™, Cytotoxicity Assay Kit (Promega, Madison, WI, USA).

DNA sequencing and NCBI Accession Numbers. The 16S rRNA nucleotide sequences for eight *Streptomyces* strains were deposited in GenBank under the accession numbers MN527229–MN527236.

Results

***Streptomyces* isolation and cultural characteristics.** Cultural characteristics for isolated strains (i.e., pigmentation, the opacity of colony, colony consistency, and growth under the liquid media surface) were recorded. The various pigments for the strains ranging from cream, yellow to brown with sediment of balls in liquid culture were observed (Table I). Aerial hyphae and spores (SEM) were detected in *S. tricolor* strain HM10 (Fig. 1). Based on the pigment production, morphological, physiological, and 16S rRNA amplicon sequences, the isolated strains were identified. Out of eleven isolated strains, eight strains were identified with a sequence of the 16S rRNA gene. These strains and their similarity to the already published *Streptomyces* strains at the NCBI website (https://www.ncbi.nlm.nih.gov/) were listed in Table II.

Screening *Streptomyces* isolates for their biocontrol activity. *Fungal pathogens.* The eleven isolated
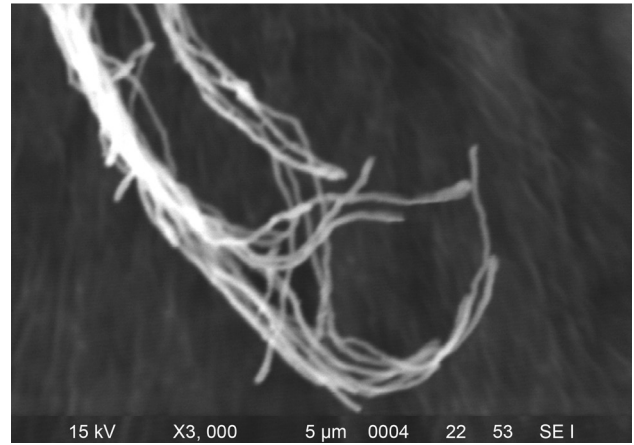

Fig. 1. Scanning electron microscopy of *Streptomyces tricolor* strain HM10 hyphae grown on GSA medium.

Streptomyces strains were tested against ten soil-borne fungal phytopathogens with a dual plate assay. *S. tricolor* strain HM10 and *S. thinghirensis* strain HM3 exerted inhibitory effects on all tested pathogenic fungal species, i.e., *Fusarium oxysporum*, *Fusarium graminearum*, *Fusarium solani*, *Fusarium moniliforme*, *Colletotrichum gloeosporides*, *Alternaria solani*, *Thielaviopsis basicola*, *Botrytis cinerea*, *Myrothecium roridum*, and *Rhizoctonia solani* (Table III). The highest antagonistic effect was shown from *S. tricolor* strain HM10. The inhibition zone for *C. gloeosporides* exceeded 18 mm, whereas much smaller was against *A. solani* (8 mm) (Fig. 2). The second superior strain was *S. thinghirensis* strain HM3, which showed antagonistic activity for all tested fungal species with the inhibition zone ranged from 3 to 15 mm. On the other hand, four identified strains, including *Streptomyces* sp. strain HM2, *Streptomyces* sp. strain HM6, *Streptomyces panayensis*

Table I
Characteristics of eleven Actinomycetes strains.

Symbol of isolate	Pigmentation	Opacity of colony	Colony consistency	Growth under the surface of liquid media
Streptomyces griseorubens strain HM1 (Actino1)	Brown	Opaque	Rough	Sediment of balls
Streptomyces sp. strain HM2 (Actino2)	White	Opaque	Rough	Sediment of balls
Streptomyces thinghirensis strain HM3 (Actino4)	Yellow*	Opaque	Rough	Sediment of balls
Streptomyces sp. strain HM4 (Actino5)	Yellow	Opaque	Rough	Sediment of balls
Actino7	Red	Opaque	Rough	Sediment of balls
Streptomyces sp. strain HM6 (Actino8)	Cream	Opaque	Rough	Sediment of balls
Streptomyces panayensis strain HM7 (Actino9)	Cream	Opaque	Rough	Sediment of balls
Streptomyces sp. strain HM8 (Actino MS9)	Dark brown	Opaque	Rough	Sediment of balls
Actino10	Cream light pink	Opaque	Rough	Sediment of balls
Actino11	Cream	Opaque	Rough	Sediment of balls
Streptomyces tricolor strain HM10 (Actino12)	Yellow**	Opaque	Rough	Sediment of balls

* – Yellow pigment colored the surrounding media
** – Dark green pigment colored the surrounding media

Table II
Identified Streptomyces strains via 16S rRNA amplicon sequencing and their similarity
with identified strains at the NCBI website.

No.	The isolated strain	*Streptomyces* similar strain	Similarity (%)
1	*Streptomyces griseorubens* strain HM1 (Actino1)	*Streptomyces griseorubens* strain SELJFHG3	99.46
2	*Streptomyces* sp. strain HM2 (Actino2)	*Streptomyces* sp. SYP-A7193	99.85
3	*Streptomyces thinghirensis* strain HM3 (Actino4)	*Streptomyces thinghirensis* strain TG26	99.62
4	*Streptomyces* sp. strain HM4 (Actino5)	*Streptomyces* sp. E4N275g	99.46
5	*Streptomyces* sp. strain HM6 (Actino8)	*Streptomyces* sp. SYP-A7193	99.23
6	*Streptomyces panayensis* strain HM7 (Actino9)	*Streptomyces panayensis*	99.54
7	*Streptomyces* sp. strain HM8 (ActinoMS9)	*Streptomyces* sp. strain 16K303	99.46
8	*Streptomyces tricolor* strain HM10 (Actino12)	*Streptomyces tricolor* strain AS 4.1867	99.77

Table III
Antagonism of eight identified *Streptomyces* strains against ten different plant pathogenic fungi.

Isolates	Tested Fungi*										
	F. mon	F. so	F. ox	F. gra	Collet	Bot	Alt	Rhiz	Myro	Thiel	Total
Streptomyces griseorubens strain HM1	–	–	+++ 3 mm	–	–	–	–	–	–	–	1
Streptomyces sp. strain HM2	–	–	–	–	–	–	–	–	–	–	0
Streptomyces thinghirensis strain HM3	+++ 5 mm	+++ 9 mm	+++ 8 mm	+++ 8 mm	+++ 8 mm	+++ 15 mm	+++ 12 mm	+++ 11 mm	+++ 3 mm	+++ 7.5 mm	10
Streptomyces sp. strain HM4	–	–	–	–	+++ 7 mm	+++ 5 mm	+++ 4 mm	+++ 2 mm	–	–	4
Actino7	+	+++ 3 mm	+	+++ 5 mm	–	+++ 9 mm	+++ 1 mm	+++ 2 mm	+++ 10 mm	+++ 3 mm	5
Streptomyces sp. strain HM6	–	–	–	–	–	–	–	–	–	–	0
Streptomyces panayensis strain HM7	–	–	–	–	–	–	–	–	–	–	0
Streptomyces sp. strain HM8	–	–	–	–	–	–	–	–	–	–	0
Actino10	–	–	–	+++ 11 mm	+++ 1 mm	–	+++ 3 mm	–	–	–	3
Actino11	–	–	–	–	–	–	–	–	–	–	0
Streptomyces tricolor strain HM10	+++ 11 mm	+++ 12 mm	+++ 13 mm	+++ 11 mm	+++ 18 mm	+++ 16 mm	+++ 8 mm	+++ 1 mm	+++ 13 mm	+++ 16 m	10
Total	3	3	4	3	4	3	5	3	2	3	

+ – The *Actinomyces* could suppress fungal mycelium growth for a distinct period at first only

F. ox – *Fusarium oxysporum*, F. gra – *Fusarium graminearum*, F. so – *Fusarium solani*, F. mon – *Fusarium moniliforme*, Collet – *Colletotrichum gloeosporides*, Alt – *Alternaria solani*, Thiel – *Thielaviopsis basicola*, Bot – *Botrytis cinerea*, Myro – *Myrothecium roridum*, and Rhiz – *Rhizoctonia solani*

strain HM7, and *Streptomyces* sp. strain HM8 produced no secondary metabolites or the antagonistic effect against the fungi tested.

Bacterial strains. The inhibitory effect of the spent medium after the growth of identified *Streptomyces* strains against three species of bacteria was presented in Table IV. The spent medium of *S. thinghirensis* strain HM3 displayed a more significant inhibitory effect on *Escherichia coli* (Gram-negative) than *Bacillus subtilis* (Gram-positive), but no inhibitory effect was observed on *Pseudomonas putida* (Fig. 3). The spent medium of *Streptomyces griseorubens* strain HM1

medium exhibited an inhibitory effect on *P. putida*. Six other *Streptomyces* strains showed no inhibitory effect on these bacteria.

Screening of *Streptomyces* strains with plant growth promoting. *Siderophore production.* All identified *Streptomyces* strains can produce siderophores and chelate the iron ions from the CAS medium (Table V, Fig. 4). The largest clear zone was recorded for *Streptomyces* sp. strain HM8 followed by *S. tricolor* strain HM10 with 64 and 22.56 h/c (halo zone area/colony area). Otherwise, *S. thinghirensis* strain HM3 showed the lowest value with 1.67 h/c.
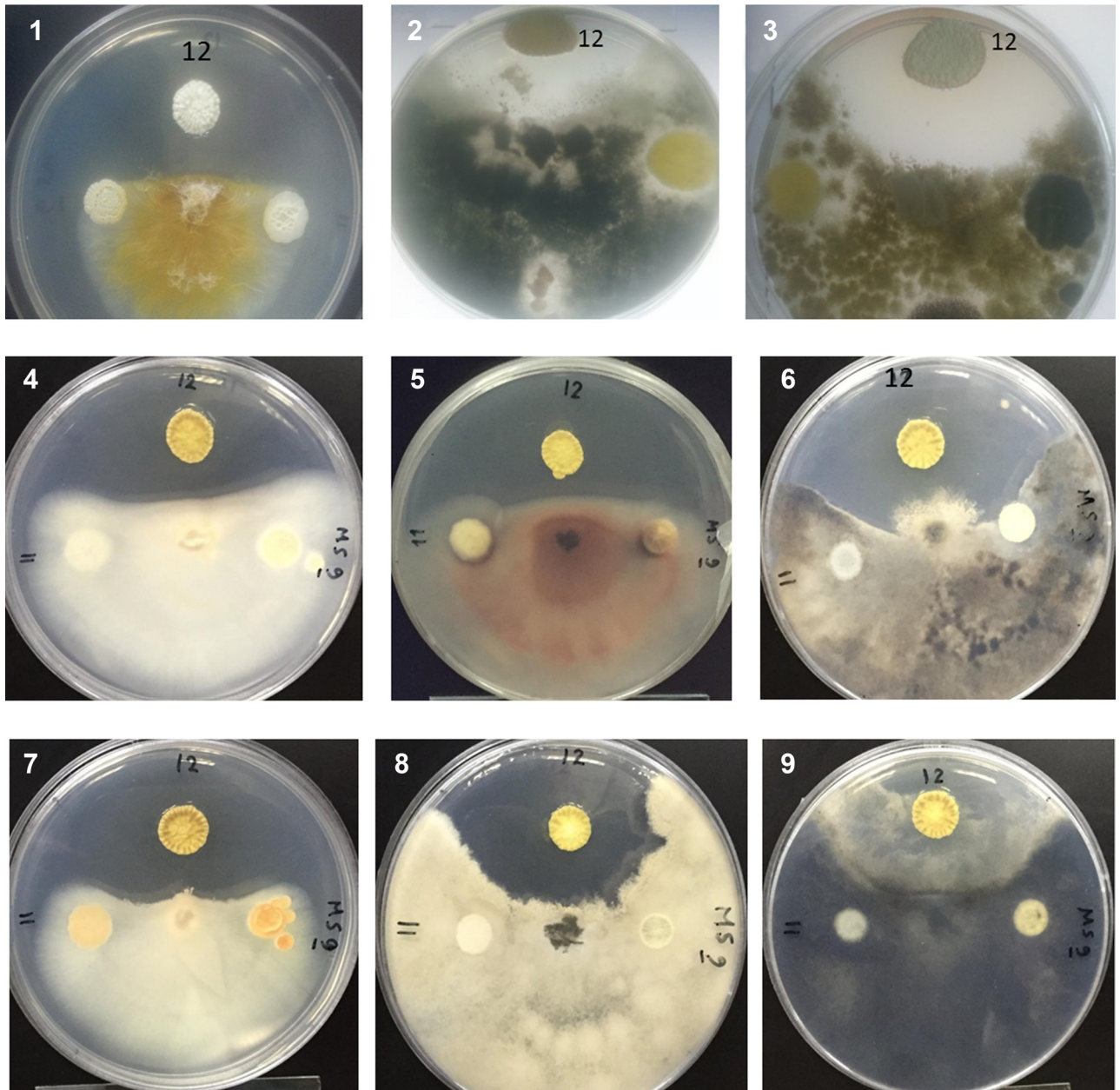
Fig. 2. Antagonistic activity of *Streptomyces tricolor* HM10 against nine fungi including: 1 – *Fusarium graminearum,* 2 – *Thielaviopsis basicola,* 3 – *Colletotrichum gloeosporides,* 4 – *Fusarium oxysporum,* 5 – *Fusarium moniliforme,* 6 – *Botrytis cinerea,* 7 – *Fusarium solani,* 8 – *Rhizoctonia solani,* 9 – *Alternaria solani.*
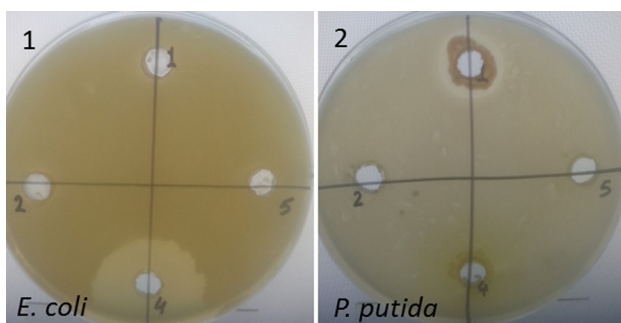

Fig. 3. Antibacterial activity of some selected isolated *Streptomyces* against two Gram-negative bacteria, *Escherichia coli* and *Pseudomonas putida*.
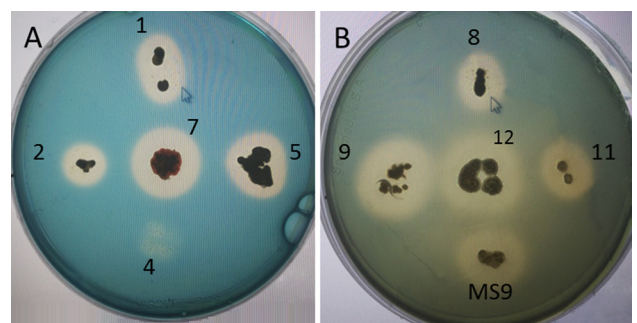
Fig. 4. Iron cheating of isolated eleven *Streptomyces* strains in the CAS general assay to detect siderophore production according to (Schwyn and Neilands 1987).

Table IV
The antagonism effect of eight identified *Streptomyces* strains against three bacterial strains.

Isolates	*Pseudomonas putida*	*Escherichia coli*	*Bacillus subtilis*	Total
Streptomyces griseorubens strain HM1	+ 3 mm	–	–	1
Streptomyces sp. strain HM2	–	–	–	1
Streptomyces thinghirensis strain HM3	–	+ 12 mm	Trace 3 mm	2
Streptomyces sp. strain HM4	–	–	–	0
Streptomyces sp. strain HM6	–	–	–	0
Streptomyces panayensis strain HM7	–	–	–	0
Streptomyces sp. strain HM8	–	–	–	0
Streptomyces tricolor strain HM10	–	–	–	0

Table V
The production of siderophores, extracellular indole-3-acetic acid (IAA) and phosphor fixing
of eleven isolated *Streptomyces* strains.

Isolate	Iron[1]				Phosphor[2]	IAA[3] µg/ml
	Reaction	Width	D/D colony	h/c		
Streptomyces griseorubens strain HM1	++	2 mm	9.5/5.5	1.98	+	77.19
Streptomyces sp. strain HM2	++	1.5 mm	10.1/7.5	2.15	+	89.36
Streptomyces thinghirensis strain HM3	+	1 mm	11/8	1.67	Trace	86.66
Streptomyces sp. strain HM4	++	2.5 mm	11/5.5	3.36	–	72.26
Actino7	+++	5 mm	16.5/8	4.25	–	112.96
Streptomyces sp. strain HM6	++	2 mm	11.5/7.5	2.35	–	43.65
Streptomyces panayensis strain HM7	+++	5 mm	14/4	12.25	+	99.3
Streptomyces sp. strain HM8	+++	11 mm	24/3	64	Trace	75.6
Actino10	+++	10 mm	25.5/4.5	32.1	+	172.13
Actino11	+++	9 mm	20/3.5	32.65	–	270.33
Streptomyces tricolor strain HM10	+++	11.5 mm	28.5/6	22.56	+	273.02

[1] – + A thin yellow area surrounding the colony (about 1 mm width), ++ less than 5 mm width of the yellow area surrounding the colony, +++ more than 5 mm width of the yellow area surrounding the colony, D = diameter, h/c = halo zone area/colony area

[2] – + A thin transparent area surrounding the colony (about 1 mm width), ++ less than 5 mm width of the transparent area surrounding the colony, +++ more than 5 mm width of the transparent area surrounding the colony

[3] – Quantitative estimation of IAA as microgram per ml according the equation: $y = 185.8x + 41.05$

Phosphate solubilization. Four of eight (50%) *Streptomyces* strains have clear ability to solubilize phosphate with nearly the same capability (Table V). For other two strains (25%) the traces of soluble phosphate were visible, whereas two more strains had no ability to solubilize phosphate (*Streptomyces* sp. strain HM4 and *Streptomyces* sp. strain HM6).

IAA production. *S. tricolor* strain HM10 was the most efficient indole acetic acid (IAA) producer with a 2.75-fold higher production (273.02 µg/ml) than *S. panayensis* strain HM7 (99.3 µg/ml). The lowest activity was observed for *Streptomyces* sp. strain HM6 with value 43.65 µg/ml (Table V).

Cytotoxic activity. Treatment of cancer cells with crude extracts of *S. tricolor* HM10 and *S. thinghirensis* strain HM3 with varying concentrations up to 200 µg/ml for 12 hours showed no effects on the cell's viability ($p > 0.05$). The complete data on cell viability have been summarized in Table VI.

Phylogenetic analysis. For the phylogenetic classification of bacteria, sequencing of gene encoding 16S rRNA is the most promising technique. In this work, the sequences of 16S rRNA amplicons of identified *Streptomyces* strains were aligned using ClustalW in MEGA X software. The phylogenetic analysis of identified eight strains was conducted based on the sequences of related species and their accession numbers, as Kaur et al. (2019) (Fig. 5). This analysis involved 38 nucleotide sequences and confirmed that these eight isolates belonged to genus *Streptomyces*. Two groups were constructed in the tree; group 1 contained seven identified *Streptomyces* strains while the strain *Streptomyces* sp. strain HM8 belongs to group 2. Moreover, the closest relatives to the superior strain
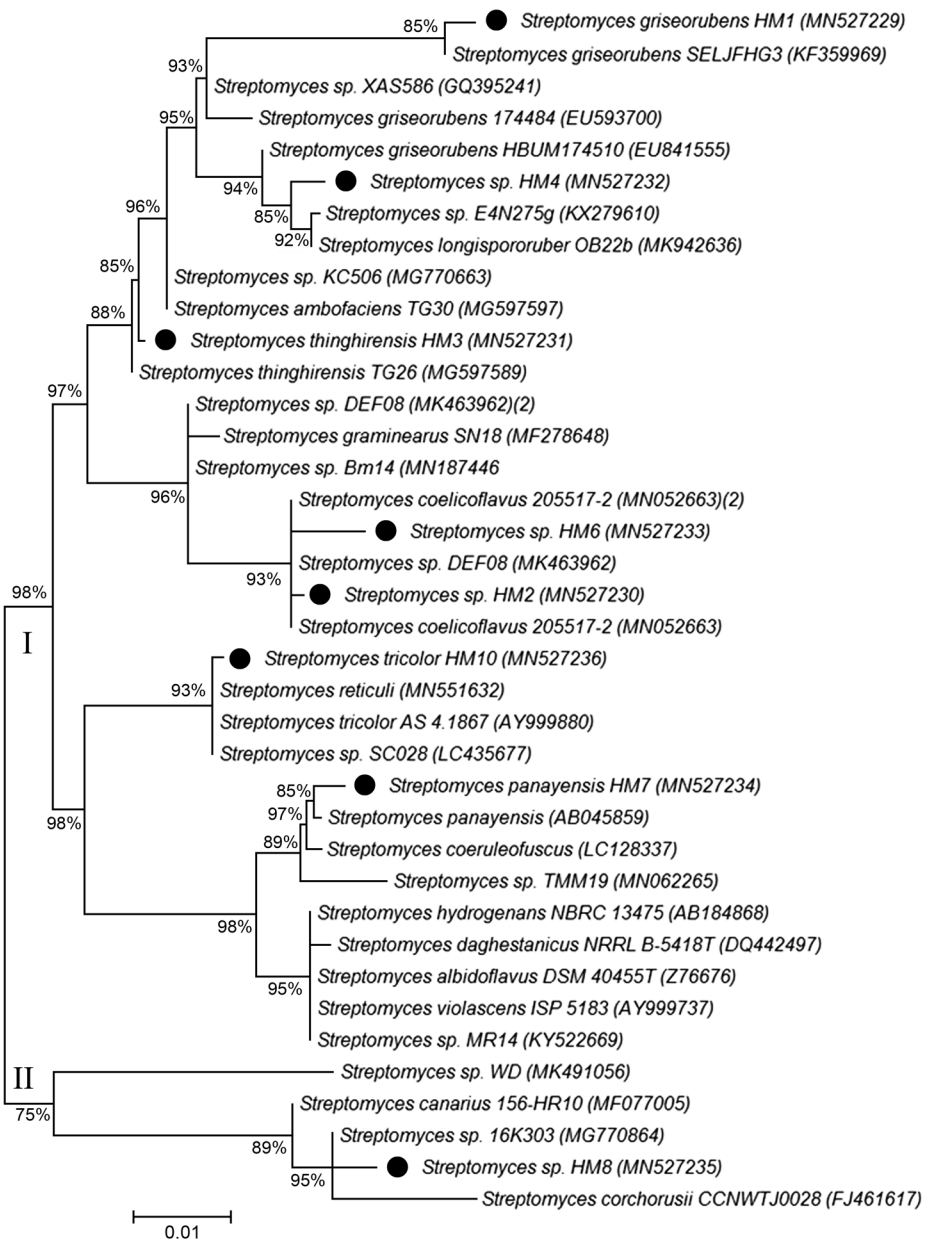
Fig. 5. Phylogenetic tree based on 16S rRNA sequences. The evolutionary history was inferred by using the Maximum Likelihood method and Tamura-Nei model. The tree with the highest log likelihood (−4351.16) is shown. Initial tree for the heuristic search were obtained automatically by applying the Maximum Parsimony method. This analysis involved 38 nucleotide sequences. Evolutionary analyses were conducted in MEGA X.

S. tricolor HM10 (MN527236) were *S. tricolor* AS 4.1867 (AY999880), *Streptomyces reticuli* (MN551632), and *Streptomyces* sp. SC028 (LC435677), respectively. Meanwhile, the second superior strain *S. thinghirensis* HM3 (MN527231) showed high similarity to *S. thinghirensis* TG26 (MG597589).

Discussion

Streptomyces are familiar with biocontrol activity against plant and animal pathogens. For a wide variety of plant pathogens, Actinomycete-fungus antagonism

has been demonstrated. *S. tricolor* HM10 (MN527236) and *S. thinghirensis* strain HM3 (MN527231) exerted a significant effect against ten soil-borne fungi with a broad spectrum of antifungal activity. Moreover, *Streptomyces* sp. 9p displayed a broad-spectrum antifungal activity against four phytopathogens including *C. gleosporioides* OGC1, *Alternaria brassiceae* OCA3, *Phytophthora capsici*, and *R. solani* MTCC 4633 (Shivakumar et al. 2012). *Streptomyces hygroscopicus* strain SRA14 exhibited *in vitro* antagonism and inhibition growth of *Sclerotium rolfsii* and *C. gloeosporioides* due to extracellular antifungal metabolites, whereas *Streptomyces* sp. VV/R4 strains reduced the fungal

Table VI
Effects of *Streptomyces tricolor* HM10 and *Streptomyces thinghirensis* strain HM3 crude extracts on the viability of A549 cancer cells. Treated versus untreated cells ($p > 0.05$).

Streptomyces thinghirensis HM3 (µg/ml)	% Cells Viability (Mean + SD)	*Streptomyces tricolor* strain HM10 (µg/ml)	Cells Viability (%) (Mean ± SD)
Untreated cells	98.3 ± 8.2	Untreated cells	99.1 ± 6.1
20	98.2 ± 9.2	20	99.2 ± 5.5
40	97.4 ± 6.8	40	98.3 ± 6.6
60	98.5 ± 7.3	60	97.1 ± 4.6
80	97.3 ± 9.6	80	98.2 ± 7.3
100	96.2 ± 9.1	100	98.3 ± 8.8
120	98.4 ± 7.2	120	97.7 ± 9.5
140	98.8 ± 9.5	140	99.1 ± 6.4
160	96.2 ± 9.1	160	98.2 ± 7.2
180	98.2 ± 8.2	180	97.1 ± 7.3
200	97.1 ± 8.5	200	98.3 ± 9.5

pathogens infection rate. Moreover, *Streptomyces albireticuli* MDJK11 and MDJK44 showed robust inhibition on the *F. solani* growth and *Streptomyces alboflavus* MDJK44 showed higher biocontrol activity than *S. albireticuli* MDJK11 (Prapagdee et al. 2008; Evangelista-Martínez 2014; Vurukonda et al. 2018; Wang et al. 2018; González-García, et al. 2019). Several mechanisms of antagonistic phenomena against fungi, including antibiosis and parasitism, have been proposed. In some cases, chitinases as hydrolytic enzymes and other enzymes such as glucanases or proteases play an important role in the biocontrol of *Fusarium* diseases and may act against the fungal cell wall (Shivakumar et al. 2012; Bubici 2018; Vurukonda et al. 2018; Newitt et al. 2019).

S. thinghirensis strain HM3 showed activity against *B. subtilis* and *P. putida* in this study. Liu et al. (1996) isolated 93 *Streptomyces* strains from potato tubers lenticels. Antagonistic activity against the virulent *Streptomyces scabies* RB3II were shown for twenty-two strains. The *in vitro* studies of either *Streptomyces pulcher* or *Streptomyces canescens* demonstrated that culture filtrates from 80% of strains significantly inhibited *Pseudomonas solanacearum* and *Clavibacter michiganensis* subsp. *michiganensis* in tomato (El-Abyad et al. 1993). Meanwhile, *Streptomyces* sp. WD5 isolate from Fayoum in Egypt, had a broad-spectrum antagonistic activity against Gram-positive bacterium, *Staphylococcus aureus* MTCC 96 (23 mm), and Gram-negative bacterium *Pseudomonas aeruginosa* MTCC 2453 (11 mm), whereas *Streptomyces rubrogriseus* HDZ-9-47 with biofumigation improved its efficacy against *Meloidogyne incognita*, and reduced root galls by 41% (Jin et al. 2019; Salah El-Din Mohamed and Zaki 2019).

Plant growth-promoting activities like siderophore and auxin production or phosphate dissolving, helps plants to grow up. *Streptomyces* has positive effects on root and shoot growth and seed germination. About 98 rhizospheric Actinobacteria isolates were positive in the production of siderophore, hydrogen cyanide, and ammonia (Anwar et al. 2016). *Streptomyces djakartensis* TB-4 and *Streptomyces* sp. WA-1 solubilized phosphate conconcentrations reached 72.13 mg/100 ml and 70.36 mg/100 ml, respectively (Anwar et al. 2016). About 18 isolates from Actinobacteria were able to solubilize phosphate, which was demonstrated as a clear zone formation in a medium containing tricalcium-phosphate, and this concentration ranged from 2.05 ± 0.06 to 2.72 ± 0.08 (Wahyudi et al. 2019). *Streptomyces enissocaesilis* TA-3, *Streptomyces nobilis* WA-3, and *Streptomyces kunmingenesis* WC-3 produced 79.5, 79.23, and 69.26 µg/ml of IAA, respectively. (Anwar et al. 2016). Furthermore, *Streptomyces fradiae* NKZ-259 produced IAA at the highest concentration (82.363 µg/ml) using 2 g/l tryptophan after six days (Myo et al. 2019). Bioinformatic analysis of *Streptomyces avermitilis* strain SA51 presented metabolic pathways promoting plant growth in addition to the genes involved in the pathway of iron transport and metabolism and indole alkaloid biosynthesis (Vurukonda et al. 2020).

In this work, based on the 16S rRNA amplicon sequences, eight *Streptomyces* strains were identified and phylogenetically analyzed. *Streptomyces* sp. strain HM8 was located in group II, while the remaining seven strains consisted group I. In Pakistan, Anwar et al. (2016) isolated 98 rhizospheric actinomycetes. About 30% of the isolates exhibited maximum genetic similarity with *Streptomyces* (98–99%) via sequencing

of the 16S rRNA gene. *Streptomyces* strain 5.1 had 98.9% similarity to *Streptomyces kashimirensis* and *Streptomyces salmonis* (Suárez-Moreno et al. 2019). *Streptomyces* sp. NEAU-S7GS2 formed a subclade with the nearest neighbor *Streptomyces angustmyceticus* NRRL B-2347T, *Streptomyces tubercidicus* DSM40261T, *Streptomyces nigrescens* NBRC 12894T, and *Streptomyces libani* subsp. *libani* NBRC 13452T with 99.72, 99.79, 99.86 and 99.86% similarities in the 16S rRNA amplicon sequences (Liu et al. 2019).

Conclusions

S. tricolor strain HM10 (MN527236) and *S. thinghirensis* strain HM3 (MN527231) exerted a significant effect against ten soil-borne fungi with a broad-spectrum antifungal activity. Strain HM10 showed highly efficient siderophore and IAA production and the ability to solubilize phosphate. These activities can help to promote plant growth. These new isolates should be a valuable tool for reducing the heavy usage of chemical fertilizers and fungicides.

Availability of data and materials

All data generated or analyzed in this study are presented within this manuscript. All materials used in this study, including raw data, shall be available upon reasonable request. The 16S rRNA nucleotide sequences for selected eight *Streptomyces* strains were deposited in GenBank (NCBI) under the accession numbers MN527229–MN527236.

Conflict of interest

The authors do not report any financial or personal connections with other persons or organizations, which might negatively affect the contents of this publication and/or claim authorship rights to this publication.

Literature

Al Abdulmonem W, Rasheed Z, Aljohani ASM, Omran OM, Rasheed N, Alkhamiss A, A M Al Salloom A, Alhumaydhi F, Alblihed MA, Al Ssadh Het al. Absence of CD74 isoform at 41kDa prevents the heterotypic associations between CD74 and CD44 in human lung adenocarcinoma-derived cells. Immunol Invest. 2020 Jul 9:1–15. https://doi.org/10.1080/08820139.2020.1790594

Anderson AS, Wellington EM. The taxonomy of *Streptomyces* and related genera. Int J Syst Evol Microbiol. 2001 May 01;51(3):797–814. https://doi.org/10.1099/00207713-51-3-797

Anwar S, Ali B, Sajid I. Screening of rhizospheric actinomycetes for various *in-vitro* and *in-vivo* plant growth promoting (PGP) traits and for agroactive compounds. Front Microbiol. 2016 Aug 29;7:1334–1334. https://doi.org/10.3389/fmicb.2016.01334

Bano N, Musarrat J. Characterization of a new *Pseudomonas aeruginosa* strain NJ-15 as a potential biocontrol agent. Curr Microbiol. 2003 May 1;46(5):324–328. https://doi.org/10.1007/s00284-002-3857-8

Barka EA, Vatsa P, Sanchez L, Gaveau-Vaillant N, Jacquard C, Klenk H-P, Clément C, Ouhdouch Y, van Wezel GP. Taxonomy, physiology, and natural products of *Actinobacteria*. Microbiol Mol Biol Rev. 2016 Mar;80(1):1–43. https://doi.org/10.1128/MMBR.00019-15

Bérdy J. Bioactive microbial metabolites. J Antibiot (Tokyo). 2005 Jan;58(1):1–26. https://doi.org/10.1038/ja.2005.1

Bonaldi M, Kunova A, Saracchi M, Sardi P, Cortesi P. Streptomycetes as biological control agents against basal drop. Acta Hortic. 2014;1044:313–318. https://doi.org/10.17660/ActaHortic.2014.1044.40

Boukaew S, Chuenchit S, Petcharat V. Evaluation of *Streptomyces* spp. for biological control of *Sclerotium* root and stem rot and *Ralstonia* wilt of chili pepper. BioControl. 2011 Jun;56(3):365–374. https://doi.org/10.1007/s10526-010-9336-4

Brauer VS, Rezende CP, Pessoni AM, De Paula RG, Rangappa KS, Nayaka SC, Gupta VK, Almeida F. Antifungal agents in agriculture: friends and foes of public health. Biomolecules. 2019 Sep 23; 9(10):521. https://doi.org/10.3390/biom9100521

Bubici G. *Streptomyces* spp. as biocontrol agents against *Fusarium* species. CAB Rev. 2018;18(50):1–15. https://doi.org/10.1079/PAVSNNR201813050

CLSI. M100-S21 performance standards for antimicrobial susceptibility testing; twenty-first informational supplement. Wayne (USA): The Clinical Laboratory and Standards Institute; 2011.

Cook AE, Meyers PR. Rapid identification of filamentous actinomycetes to the genus level using genus-specific 16S rRNA gene restriction fragment patterns. Int J Syst Evol Microbiol. 2003 Nov 01;53(6):1907–1915. https://doi.org/10.1099/ijs.0.02680-0

Dhanjal S, Cameotra S. Aerobic biogenesis of selenium nanospheres by *Bacillus cereus* isolated from coalmine soil. Microb Cell Fact. 2010Jul 05;9(1):52. https://doi.org/10.1186/1475-2859-9-52

Donate-Correa J, León-Barrios M, Pérez-Galdona R. Screening for plant growth-promoting rhizobacteria in *Chamaecytisus proliferus* (tagasaste), a forage tree-shrub legume endemic to the Canary Islands. Plant Soil. 2005 Jan;266(1–2):261–272. https://doi.org/10.1007/s11104-005-0754-5

Doumbou CL, Hamby Salove MK, Crawford DL, Beaulieu C. Actinomycetes, promising tools to control plant diseases and to promote plant growth. Phytoprotection. 2001;82(3):85–102. https://doi.org/10.7202/706219ar

Duan Y, Chen J, He W, Chen J, Pang Z, Hu H, Xie J. Fermentation optimization and disease suppression ability of a *Streptomyces* ma. *FS-4* from banana rhizosphere soil. BMC Microbiol. 2020 Dec; 20(1):24. https://doi.org/10.1186/s12866-019-1688-z

El-Abyad MS, El-Sayed MA, El-Shanshoury AR, El-Sabbagh SM. Towards the biological control of fungal and bacterial diseases of tomato using antagonistic *Streptomyces* spp. Plant Soil. 1993 Feb; 149(2):185–195. https://doi.org/10.1007/BF00016608

El-Naggar MY, El-Assar SA, Abdul-Gawad SM. Meroparamycin production by newly isolated *Streptomyces* sp. strain MAR01: taxonomy, fermentation, purification and structural elucidation. J Microbiol. 2006 Aug;44(4):432–438.

Evangelista-Martínez Z. Isolation and characterization of soil *Streptomyces* species as potential biological control agents against fungal plant pathogens. World J Microbiol Biotechnol. 2014 May; 30(5):1639–1647. https://doi.org/10.1007/s11274-013-1568-x

Expert D, Franza T, Dellagi A. Iron in plant-pathogen interactions. In: Expert D, O'Brian M, editors. Molecular aspects of

iron metabolism in pathogenic and symbiotic plant-microbe associations. Dordrecht (Netherlands): Springer; 2012. p. 7–39. https://doi.org/10.1007/978-94-007-5267-22

González-García S, Álvarez-Pérez JM, Sáenz de Miera LE, Cobos R, Ibañez A, Díez-Galán A, Garzón-Jimeno E, Coque JJR. Developing tools for evaluating inoculation methods of biocontrol *Streptomyces* sp. strains into grapevine plants. PLoS One. 2019 Jan 24; 14(1):e0211225. https://doi.org/10.1371/journal.pone.0211225

Ji SH, Gururani MA, Chun SC. Isolation and characterization of plant growth promoting endophytic diazotrophic bacteria from Korean rice cultivars. Microbiol Res. 2014 Jan 20;169(1):83–98. https://doi.org/10.1016/j.micres.2013.06.003

Jin N, Lu X, Wang X, Liu Q, Peng D, Jian H. The effect of combined application of *Streptomyces rubrogriseus* HDZ-9-47 with soil biofumigation on soil microbial and nematode communities. Sci Rep. 2019 Dec;9(1):16886. https://doi.org/10.1038/s41598-019-52941-9

Jung SJ, Kim NK, Lee DH, Hong SI, Lee JK. Screening and evaluation of *Streptomyces* species as a potential biocontrol agent against a wood, decay fungus, *Gloeophyllum trabeum*. Mycobiology. 2018 Apr 03;46(2):138–146. https://doi.org/10.1080/12298093.2018.1468056

Kanini GS, Katsifas EA, Savvides AL, Hatzinikolaou DG, Karagouni AD. Greek indigenous Streptomycetes as biocontrol agents against the soil-borne fungal plant pathogen *Rhizoctonia solani*. J Appl Microbiol. 2013 May;114(5):1468–1479. https://doi.org/10.1111/jam.12138

Kaur T, Rani R, Manhas RK. Biocontrol and plant growth promoting potential of phylogenetically new *Streptomyces* sp. MR14 of rhizospheric origin. AMB Express. 2019 Dec;9(1):125. https://doi.org/10.1186/s13568-019-0849-7

Kumar S, Stecher G, Li M, Knyaz C, Tamura K. MEGA X: Molecular Evolutionary Genetics Analysis across computing platforms. Mol Biol Evol. 2018 Jun 01;35(6):1547–1549. https://doi.org/10.1093/molbev/msy096

Kunova A, Bonaldi M, Saracchi M, Pizzatti C, Chen X, Cortesi P. Selection of *Streptomyces* against soil borne fungal pathogens by a standardized dual culture assay and evaluation of their effects on seed germination and plant growth. BMC Microbiol. 2016 Dec; 16(1):272. https://doi.org/10.1186/s12866-016-0886-1

Law JWF, Ser HL, Khan TM, Chuah LH, Pusparajah P, Chan KG, Goh BH, Lee LH. The potential of *Streptomyces* as biocontrol agents against the rice blast fungus, *Magnaporthe oryzae* (*Pyricularia oryzae*). Front Microbiol. 2017 Jan 17;8:3. https://doi.org/10.3389/fmicb.2017.00003

Liu D, Anderson NA, Kinkel LL. Selection and characterization of strains of *Streptomyces* suppressive to the potato scab pathogen. Can J Microbiol. 1996 May 01;42(5):487–502. https://doi.org/10.1139/m96-066

Liu D, Yan R, Fu Y, Wang X, Zhang J, Xiang W. Antifungal, plant growth-promoting, and genomic properties of an endophytic Actinobacterium *Streptomyces* sp. NEAU-S7GS2. Front Microbiol. 2019 Sep 10;10:2077. https://doi.org/10.3389/fmicb.2019.02077

Myo EM, Ge B, Ma J, Cui H, Liu B, Shi L, Jiang M, Zhang K. Indole-3-acetic acid production by *Streptomyces fradiae* NKZ-259 and its formulation to enhance plant growth. BMC Microbiol. 2019 Dec;19(1):155. https://doi.org/10.1186/s12866-019-1528-1

Newitt J, Prudence S, Hutchings M, Worsley S. Biocontrol of cereal crop diseases using *Streptomycetes*. Pathogens. 2019 Jun 13;8(2):78. https://doi.org/10.3390/pathogens8020078

Nicolopoulou-Stamati P, Maipas S, Kotampasi C, Stamatis P, Hens L. Chemical pesticides and human health: the urgent need for a new concept in agriculture. Front Public Health. 2016 Jul 18;4:148. https://doi.org/10.3389/fpubh.2016.00148

Palaniyandi SA, Yang SH, Zhang L, Suh JW. Effects of Actinobacteria on plant disease suppression and growth promotion. Appl Microbiol Biotechnol. 2013 Nov;97(22):9621–9636. https://doi.org/10.1007/s00253-013-5206-1

Pliego C, Ramos C, de Vicente A, Cazorla FM. Screening for candidate bacterial biocontrol agents against soilborne fungal plant pathogens. Plant Soil. 2011 Mar;340(1–2):505–520. https://doi.org/10.1007/s11104-010-0615-8

Prapagdee B, Kuekulvong C, Mongkolsuk S. Antifungal potential of extracellular metabolites produced by *Streptomyces hygroscopicus* against phytopathogenic fungi. Int J Biol Sci. 2008;4(5):330–337. https://doi.org/10.7150/ijbs.4.330

Sadeghi A, Karimi E, Dahaji PA, Javid MG, Dalvand Y, Askari H. Plant growth promoting activity of an auxin and siderophore producing isolate of *Streptomyces* under saline soil conditions. World J Microbiol Biotechnol. 2012 Apr;28(4):1503–1509. https://doi.org/10.1007/s11274-011-0952-7

Salah El-Din Mohamed W, Zaki DFA. Evaluation of antagonistic actinomycetes isolates as biocontrol agents against wastewater-associated bacteria. Water Sci Technol. 2019 Jun 15;79(12):2310–2317. https://doi.org/10.2166/wst.2019.231

Schrey SD, Erkenbrack E, Früh E, Fengler S, Hommel K, Horlacher N, Schulz D, Ecke M, Kulik A, Fiedler HP, et al. Production of fungal and bacterial growth modulating secondary metabolites is widespread among mycorrhiza-associated Streptomycetes. BMC Microbiol. 2012;12(1):164. https://doi.org/10.1186/1471-2180-12-164

Schwyn B, Neilands JB. Universal chemical assay for the detection and determination of siderophores. Anal Biochem. 1987 Jan; 160(1):47–56. https://doi.org/10.1016/0003-2697(87)90612-9

Seipke RF, Kaltenpoth M, Hutchings MI. *Streptomyces* as symbionts: an emerging and widespread theme? FEMS Microbiol Rev. 2012 Jul;36(4):862–876. https://doi.org/10.1111/j.1574-6976.2011.00313.x

Shivakumar S, Thapa A, Bhat D, Golmei K, Dey N. *Streptomyces* sp. 9p as effective biocontrol against chilli soilborne fungal phytopathogens. Eur J Exp Biol. 2012;2(1):163–173.

Singh DP, Patil HJ, Prabha R, Yandigeri MS, Prasad SR. Actinomycetes as potential plant growth-promoting microbial communities. In: Prasad R, Gill SS, Tuteja N, editors. New and future developments in microbial biotechnology and bioengineering: crop improvement through microbial biotechnology. Amsterdam (Netherlands): Elsevier; 2018. p. 27–38. https://doi.org/10.1016/B978-0-444-63987-5.00002-5

Suárez-Moreno ZR, Vinchira-Villarraga DM, Vergara-Morales DI, Castellanos L, Ramos FA, Guarnaccia C, Degrassi G, Venturi V, Moreno-Sarmiento N. Plant-growth promotion and biocontrol properties of three *Streptomyces* spp. isolates to control bacterial rice pathogens. Front Microbiol. 2019 Feb 25;10:290. https://doi.org/10.1016/10.3389/fmicb.2019.00290

Takahashi Y, Nakashima T. Actinomycetes, an inexhaustible source of naturally occurring antibiotics. Antibiotics (Basel). 2018 May 24;7(2):45. https://doi.org/10.3390/antibiotics7020045

Trejo-Estrada SR, Sepulveda IR, Crawford DL. *In vitro* and *in vivo* antagonism of *Streptomyces violaceusniger* YCED9 against fungal pathogens of turfgrass. World J Microbiol Biotechnol. 1998; 14(6):865–872. https://doi.org/10.1023/A:1008877224089

Valan Arasu M, Duraipandiyan V, Agastian P, Ignacimuthu S. *In vitro* antimicrobial activity of *Streptomyces* spp. ERI-3 isolated from Western Ghats rock soil (India). J Mycol Med. 2009 Mar;19(1):22–28. https://doi.org/10.1016/j.mycmed.2008.12.002

Vurukonda SSKP, Giovanardi D, Stefani E. Plant growth promoting and biocontrol activity of *Streptomyces* spp. as endophytes. Int J Mol Sci. 2018 Mar 22;19(4):952. https://doi.org/10.3390/ijms19040952

Vurukonda SSKP, Mandrioli M, D'Apice G, Stefani E. Draft genome sequence of plant growth-promoting *Streptomyces* sp. strain SA51, isolated from olive trees. Microbiol Resour Announc. 2020 Jan 02;9(1):e00768-19. https://doi.org/10.1128/MRA.00768-19

Wahyudi AT, Priyanto JA, Afrista R, Kurniati D, Astuti RI, Akhdiya A. Plant growth promoting activity of Actinomycetes isolated from soybean rhizosphere. Online J Biol Sci. 2019 Jan 01;19(1):1–8. https://doi.org/10.3844/ojbsci.2019.1.8

Waksman SA, Schatz A, Reynolds DM. Production of antibiotic substances by Actinomycetes. Ann N Y Acad Sci. 2010 Dec;1213(1):112–124. https://doi.org/10.1111/j.1749-6632.2010.05861.x

Wang C, Wang Y, Ma J, Hou Q, Liu K, Ding Y, Du B. Screening and whole-genome sequencing of two *Streptomyces* species from the rhizosphere soil of peony reveal their characteristics as plant growth-promoting Rhizobacteria. BioMed Res Int. 2018 Sep 05;2018:1–11. https://doi.org/10.1155/2018/2419686

Yekkour A, Sabaou N, Zitouni A, Errakhi R, Mathieu F, Lebrihi A. Characterization and antagonistic properties of *Streptomyces* strains isolated from Saharan soils, and evaluation of their ability to control seedling blight of barley caused by *Fusarium culmorum*. Lett Appl Microbiol. 2012 Dec;55(6):427–435. https://doi.org/10.1111/j.1472-765x.2012.03312.x

Yoon MY, Cha B, Kim JC. Recent trends in studies on botanical fungicides in agriculture. Plant Pathol J. 2013 Mar 01;29(1):1–9. https://doi.org/10.5423/PPJ.RW.05.2012.0072

Supplementary materials are available on the journal's website.

Enhancing the Efficiency of Soybean Inoculant
for Nodulation under Multi-Environmental Stress Conditions

JENJIRA WONGDEE, WATCHARIN YUTTAVANICHAKUL, APHAKORN LONGTHONGLANG,
KAMONLUCK TEAMTISONG, NANTAKORN BOONKERD, NEUNG TEAUMROONG
and PANLADA TITTABUTR*

School of Biotechnology, Institute of Agricultural Technology, Suranaree University of Technology,
Nakhon Ratchasima, Thailand

A b s t r a c t

The development of rhizobial inoculants with increased resistance to abiotic stress is critical to mitigating the challenges related to climate change. This study aims at developing a soybean stress-tolerant *Bradyrhizobium* inoculant to be used under the mixed stress conditions of acidity, high temperature, and drought. Six isolates of *Bradyrhizobium* with high symbiotic performance on soybean were tested to determine their growth or survival abilities under *in vitro* conditions. The representative stress-tolerant *Bradyrhizobium* isolates 184, 188, and 194 were selected to test their ability to promote soybean growth under stress conditions compared to the type strain *Bradyrhizobium diazoefficiens* USDA110. The plant experiment indicated that isolate 194 performed better in symbiosis with soybean than other *Bradyrhizobium* strains under stress conditions. Based on the stress tolerance index, soybeans inoculated with isolate 194 showed a high growth performance and significantly better nodulation competition ability than USDA110 under several stress conditions. Interestingly, supplementation of sucrose in the culture medium significantly enhances the survival of the isolate and leads to improved plant biomass under various stress conditions. Analysis of the intra-cellular sugars of isolate 194 supplemented with sucrose showed the accumulation of compatible solutes, such as trehalose and glycerol, that may act as osmoprotectants. This study indicates that inoculation of stress-tolerant *Bradyrhizobium* together with sucrose supplementation in a medium could enhance bacterial survival and symbiosis efficiency under stress conditions. Although it can be applied for inoculant production, this strategy requires validation of its performance in field conditions before adopting this technology.

K e y w o r d s : *Bradyrhizobium*, nodulation competition, stress conditions, compatible solutes, osmoprotectant

Introduction

Bradyrhizobium is used as a soybean inoculant, because it reduces atmospheric nitrogen gas (N_2) into a nitrogenous compound that can be utilized directly by the plant. Application of a *Bradyrhizobium* inoculant, an environment-friendly biofertilizer, is, therefore, an essential factor that can increase the soybean yield and reduce the utilization of chemical N fertilizer (Suyal et al. 2016; Ntambo et al. 2017; Jalloh 2020). Although the effective nitrogen-fixing *Bradyrhizobium* is used as an inoculant, several abiotic factors have been reported to interfere with successful nodulation. Abiotic factors, as defined here, such as salinity, unfavorable soil pH,

nutrient deficiency, mineral toxicity, extreme temperature, and soil moisture, are environmental stress factors that can affect the efficiency of symbiosis. For example, in severe drought stress, the total dry weight of soybean inoculated with a commercial liquid inoculant of *Bradyrhizobium* (Simbiose Nod Soja®) was decreased; even co-inoculation with *Azospirillum brasilens* had this effect when compared to the normal condition (Silva et al. 2019). Wang et al. (2016) also showed that salt stress negatively affects alfalfa (*Medicago sativa* L.) production and biological nitrogen fixation. However, inoculation with an effective rhizobial inoculant had a positive effect on alfalfa's salt tolerance by improving antioxidant enzymes and osmotic adjustment capacity.

* Corresponding author: P. Tittabutr, School of Biotechnology, Institute of Agricultural Technology, Suranaree University of Technology, Nakhon Ratchasima, Thailand; **e-mail: panlada@sut.ac.th**

Thus, it is necessary to develop an inoculant that can support plant growth under abiotic conditions.

In the field, stress conditions cause rapid death of the *Bradyrhizobium* inoculum and reduce its capability to compete for nodulation and fix nitrogen (Sindhu et al. 2010; Gopalakrishnan et al. 2015). The most critical factors, potentially limiting the rhizobium-legume symbiosis, are pH, drought, and high temperature (Dimkpa et al. 2009; Zhang et al. 2020), and several times these stress factors were found in combination as a multi-environmental stress condition. However, the ability of the legume hosts to grow and survive in stress conditions is improved when they are inoculated with stress-tolerant strains of rhizobia (Wei et al. 2008; Kajić et al. 2019). Therefore, inoculation with multi-stress-tolerant *Bradyrhizobium* strains may enhance the field performance of soybean production.

Moreover, efforts to develop a rhizobial inoculant could be made by increasing nodule occupancy under stress conditions. Iturralde et al. (2019) suggested that improving nodule occupation should also focus on optimizing the inoculant formulation and inoculation technology. Amendment of some sugars in the inoculant formulation is one strategy to improve bacterial survival under stress conditions (Singh et al. 2014). The ability of rhizobia to tolerate stress could be increased by maintaining the osmotic equilibrium across membranes by accumulating compatible solutes, mainly organic osmolytes (Saxena et al. 2013; Maryani et al. 2018). Many of the best-characterized osmoregulatory mechanisms are designed to adjust compatible solute levels by modulating their biosynthesis, catabolism, uptake, and efflux (Kajić et al. 2019). However, the composition of endogenous compatible solutes accumulated by rhizobia varies at the species level. Therefore, the accumulation of compatible solutes would be another mechanism to improve the stress tolerance and survival of rhizobia, finally supporting the nodulation and nitrogen fixation ability of inoculated *Bradyrhizobium* under stress conditions.

Thus, the objectives of the present work were to select stress-tolerant strains of *Bradyrhizobium* and search for an appropriate sugar that contributes to the accumulation of compatible solutes in their cells to improve stress tolerance of *Bradyrhizobium* inoculant under several environmental stress conditions. The plant growth experiments were performed in both single and mixed stress conditions. The effect of supplemented sugar on the accumulation of compatible solutes in *Bradyrhizobium* cells and its effect on cell survival and soybean growth under stress conditions were also investigated. Then, the symbiosis efficiency of the developed *Bradyrhizobium* inoculant on soybean was determined by testing in the soil collected from different locations in Thailand.

Experimental

Materials and Methods

***Bradyrhizobium* strains and culture conditions.** The six isolates of soybean *Bradyrhizobium*, including isolates 184, 188, 193, 194, 197, and 199, were obtained from the Department of Agriculture (DOA), Ministry of Agriculture and Cooperatives, Thailand, and used in this study based on their symbiotic performance in soybean under normal conditions. Box-PCR (Schneider and De Bruijn 1996) and dendrogram analysis (Quantity One® Version 4.6.3 for Windows and Macintosh) were performed to investigate the bacterial DNA fingerprint profiles in order to avoid repetitive isolates. *Bradyrhizobium* strains were grown at 28°C on yeast extract-mannitol (YM) broth or agar containing congo red (pH 6.8) (Somasegaran and Hoben 1994) as basal growth condition. The soybean *Bradyrhizobium* strain used in this experiment was *B. diazoefficiens* USDA110 as type strain, while *Bradyrhizobium* sp. strain CB1809 was used as the stress-tolerant strain under *in vitro* conditions (Botha et al. 2004).

Determination of growth and survival of *Bradyrhizobium* strains under *in vitro* stress conditions. To observe the stress tolerance of *Bradyrhizobium* strains under *in vitro* conditions, the cell cultures were washed with normal saline twice before adjusting to 10^8 CFU/ml. Then, 10 μl of bacterial cells were dropped on a YM agar medium prepared to determine their ability to grow in different stress conditions. For acid stress, YM agar media were prepared at pH 4, 5, 6, and 6.8 using acetic acid (CH_3COOH; as a representative organic acid found in the natural soil), and 0.5 ml/l of 8 mM bromothymol blue was added as a pH-indicating colorant. Then, plates were incubated at 28°C. For high-temperature stress, YM agar media were prepared at pH 6.8 and incubated in the adjusted incubator at 28, 35, 40, and 45°C. Seven days after incubation, the ability of *Bradyrhizobium* strains to grow on acid-formulated medium and at high-temperature conditions was determined using the growth score as indicated in Table SI. For drought stress, 1 ml of the same bacterial cell concentration was overlaid on 0.2 μm filter membrane and incubated in the adjusted desiccator chamber containing silica gel, saturated $CH_3COOK \cdot 1.5\,H_2O$, and KI solutions to give relative humidity (RH) values of 3, 22, and 67.8%, respectively (Boumahdi et al. 1999). After seven days of incubation, the percentage of cell survival in the drought condition in comparison with the initial cell number was determined using the dilution plate count technique.

Soybean growth and planting conditions. Seeds of surface-sterilized soybean (*Glycine max* (L.) Merr.) variety "Chiang mai 60" were germinated and transferred

to Leonard jars containing 0.35 kg of the sterilized sand (autoclaved at 121°C for 90 min). The *Bradyrhizobium* cells washed with normal saline were inoculated at 10^8 cells per soybean seedling grown under normal and stress conditions. Plants were watered with N-free plant nutrient solution (Somasegaran and Hoben 1994) and grown at 25°C at a 12/12 day/night cycle with a light intensity of 639 $\mu E/m^2/s$ as a normal condition, while other stress conditions were adjusted as follows: (i) acid condition – N-free solution was adjusted to pH 4.5; (ii) high-temperature condition – plants were incubated in growth chambers (Contherm's Biosyn Series of Tissue and Plant Growth Chambers-620RHS P6 Models, Wellington, New Zealand) at 40°C; and (iii) drought condition – the sand was desiccated at −3.20 bars using polyethylene glycol (PEG) 8000 solution (Michel 1983). For the mixed stress conditions, two stress factors as indicated were combined (the stress condition of three factors was not performed here due to the drastic effect on plant growth). Data on nitrogen fixation, number of nodules, plant biomass, and nodule dry weight were collected at 30 DAI (days after inoculation) as an appropriate time for determining the symbiotic efficiency.

Determination of stress tolerance index (STI). The stress tolerance index (STI) was determined according to Shetty et al. (1995) following equations (1) and (2):

$$STI = DWS/DWC \qquad (1)$$
$$STI = DWH/DWC \qquad (2)$$

where, DWS – dry weight of plants grown under stress, DWH – dry weight of plants grown under stress with inoculation of bacteria, and DWC – dry weight of plants grown in the control condition (without stress and inoculation of bacteria).

Nodulation competition test. The plasmid pCAM120 containing Tn5 fusion with the β-glucuronidase (GUS) gene (Wilson et al. 1995) was transformed into USDA110 as a reporter gene for monitoring the nodule occupancy compared with the selected stress-tolerant strain under stress conditions. This GUS-tagged USDA110 was obtained from the Applied Soil Microbiology Laboratory, School of Biotechnology, the Suranaree University of Technology, Thailand, and cultured in a YM medium with an appropriate antibiotic. In Leonard's jar experiment, surface-sterilized soybean seeds were co-inoculated with stress-tolerant *Bradyrhizobium* and GUS-tagged USDA110 in normal saline using a ratio of 1:1 at 10^8 cells/seed. Plant growth conditions were adjusted in single stress and mixed stress conditions as described above. After one month, soybean nodules were collected, cut in half, and stained with 5-bromo-4-chloro-3-indolyl glucuronide (X-Gluc) as a substrate according to the method of Krause et al. (2002). The blue and white-colored nodules were observed, and the percentage of nodule occupancy was

determined using a method described by Payakapong et al. (2004) and Talbi et al. (2013).

Characterization of plant growth-promoting (PGP) properties of *Bradyrhizobium*. Some PGP properties of the selected *Bradyrhizobium* were characterized in comparison with that of *Bradyrhizobium* sp. USDA110. The PGP traits were determined as described below.

P-solubilization. The 10 μl of bacterial culture (10^8 CFU/ml) was dropped on Pikovskaya's (PVK) medium plates containing 5 g/l of $Ca_3(PO_4)_2$ as a sole source of phosphorus. The plates were incubated at 30°C for 7 days. The ability of bacteria to solubilize the insoluble P was observed based on the clearing zone in the PVK agar plates (Nautiyal 1999).

Exopolysaccharide (EPS) production. The 100 ml of 7 day-olds bacterial culture in 100 ml YM broth was centrifuged at 4,000 rpm for 20 min to remove bacterial cells. Then, the supernatant was transferred to a new centrifuge tube and mixed with final 35% (v/v) ethanol, and incubated overnight at 4°C. The EPS pellet was precipitated by centrifugation and dried at 30°C for a day. The EPS was measured as dry weight (mg) per 100 ml culture (Castellane et al. 2017).

Indole acetic acid (IAA) production. The ability of rhizobial strains to produce IAA was determined in YM broth medium added with tryptophan (0.1 g/l). This broth medium was inoculated with standard inoculum 1.0×10^8 CFU/ml. The broth cultures were incubated in dark at 30°C for 7 days and then centrifuged at 4,000 rpm for 15 min. The supernatant was collected for 1 ml to mix with 2 ml of Salkowski's reagent (1 ml of 0.5 M $FeCl_3$ in 50 ml of 35% of $HCLO_4$ solution) and kept in the dark. The optical density (OD) was recorded at 530 nm after 15 min (Sarwar et al. 1992). The IAA production of tested bacterial strains was also determined when they grew under stress conditions as described above.

1-aminocyclopropane-1-carboxylic acid (ACC) deaminase activity. The cells from the early stationary phase were washed twice with minimal medium and induced for the ACC deaminase production by inoculation in 15 ml of YM-supplemented minimal medium containing 1 mM ACC, then shaking at 200 rpm for 40 hr. The α-ketobutyrate released from ACC during the culture supernatant incubation with ACC was measured for the ACC deaminase activity as described previously by Mayak et al. (2004).

Bacterial growth assay using sugar as an osmoprotectant under stress conditions. *Bradyrhizobium* strains were aerobically grown at 28°C in YM broth for seven days as a starter. Then, 1% (v/v) (containing 10^8 CFU/ml) of starter was inoculated into minimal broth medium (MSM) (Miller 1996) containing sucrose at different concentrations ranging from 0 to

500 mM (Gouffi et al. 1999; Le Rudulier 2005). Then, the stress conditions were applied by adjusting the conditions as described for the determination of cell survival and adaptation under stress. The number of surviving cells was determined at 10 DAI (like during the stationary phase). The selected sugar was used for further experiments to determine the appropriate concentrations that support the specific growth rate in each stress condition.

Determination of cell survival in the sand under stress conditions. Ten grams of sterilized sand were added into a test tube (50 ml); then, the pH was adjusted to 7.0 with 2 N NaOH and the sand was incubated at 28°C as a normal condition, while other stress conditions were adjusted explicitly as follows. For the acidic condition, the sand pH was adjusted to 4.5 with acetic acid. For the high temperature, the sand was incubated at 40°C. For drought, the sand was desiccated to −3.02 bars using PEG8000. The mixed stress conditions were also arranged as described above. To determine the bacterial cells' response to stress conditions, 10^8 *Bradyrhizobium* cells were inoculated into the prepared sand tubes in each condition and incubated for two days (as an approximate time for soybean germination after sowing). The survival of cells under the stress conditions was investigated by serial dilution and total plate count. The number of living bacteria was determined as CFU/g of the sand (Idris et al. 2007) and the percentage survival of cells in stress conditions was calculated in relation to the initial cell number.

Analysis of the accumulation of sugars in bacterial cells by HPLC. The cell pellets were precipitated from 20 ml of the cultured medium at 10^8 CFU/ml and washed twice with sterilized 0.85% NaCl solution. The intracellular compatible solutes were extracted twice by incubating at 65°C for 5 min in 1 ml of 70% (v/v) ethanol. Crude extracts were centrifuged at 5,000 g for 5 min (Lai et al. 1991), and ethanol was evaporated using a rotary evaporator (Buechi R-142, Nordrhein-Westfalen, Germany) at 45°C. The cell extracts were dissolved in 1 ml deionized water and filtered through a 0.2 μm hydrophobic membrane, and immediately injected into the chromatograph. The sugars were determined using HPLC with an ion-exchange column (Aminex HPX-87H, 7.8×300 mm, Bio-Rad) at 45°C and a refractive index detector (RI-150, Thermo Spectra System, USA). The mobile phase was 4 mM sulfuric acid at a flow rate of 0.4 ml/min (Sangproo et al. 2012). A flow rate of 0.3 ml/min and a column temperature of 60°C were used for sugar analyses.

Testing the symbiosis efficiency of *Bradyrhizobium* inoculant supplemented with the selected sugar. The symbiosis efficiency tests were performed both in an experiment with the sterilized sand and in the soils collected from Suphan Buri Province (14°24′8″ N,

100°9′16″ E), Phetchaburi Province (12°47′59″ N, 99°58′1″ E), and Yasothon Province (15°47′41″ N, 104°8′26″ E). These representative soils had been used in a crop rotation system of legume and rice (Table SII). All *Bradyrhizobium* strains were grown in YM medium with and without supplementation of an appropriate concentration of the selected sugar. The bacterial inoculant was prepared as previously described. The plant experiment was performed under normal and different stress conditions using the same strategy as described above. The symbiosis efficiency of *Bradyrhizobium* inoculant supplemented with the selected sugar was also tested in soil samples collected from different locations. In this case, plants were watered with sterilized water and grown at 25°C on a 12/12 day/night cycle with a light intensity 639 μE/m²/s. At 30 DAI, data on nodule number, plant biomass, and nodule dry weight were collected.

Statistical analysis. Mean values and standard deviations of the data in all experiments were determined with SPSS software (SPSS versions 19.0 Windows; SPSS Inc., Chicago, IL, USA) and the significance of the values determined by Tukey's HSD (Honestly Significant Difference) test (Tukey 1949). Student's *t*-test was also used to determine the significant difference of the means between two sets of data.

Results

Growth, properties, and survival ability of *Bradyrhizobium* isolates *in vitro* under stress conditions. Six *Bradyrhizobium* isolates and the type strains were tested on an agar medium adjusted to different stress conditions. The strain CB1809 and isolates 188, 194, and 197 grew very well in the acid condition of pH 5, while a poor growth of most strains was observed in strong acid of pH 4. Every strain, except isolate 199 and USDA110, could grow on the medium plate at high temperatures, even at 45°C, while CB1809 and 188 showed a better growth ability than other strains. Under drought conditions, isolate 194 exhibited the highest percentage of survival (Table SI). Thus, several *Bradyrhizobium* isolates can resist various stress conditions, while it seems that isolate 194 was able to grow under several stress conditions. Since these *Bradyrhizobium* isolates will be inoculated on plant grown under stress conditions, it is interesting to investigate their plant growth-promoting (PGP) properties. Thus, isolate 194 was selected to preliminary determine its PGP properties compared to the reference strain of USDA110 (Table I). The EPS production by isolate 194 and USDA110 was 9 and 6 mg/100 ml culture, respectively. Likewise, the ACC deaminase activity of isolate 194 was higher than that of USDA110 (1.100 and 0.736 μmol α-ketobutyrate/mg

Table I
Characterization of the plant growth-promoting (PGP) properties of USDA110 and isolate 194.

PGP properties	USDA110	Isolate 194
EPS production (mg/100 ml)	$6^b \pm 1.25$	$9^a \pm 1.45$
ACC deaminase (μmol α-ketobutyrate/mg protein/h)	$0.74^b \pm 0.05$	$1.10^a \pm 0.05$
P-solubilization	no	no
IAA production (μg/ml)		
Normal condition	$0.015^b \pm 0.002$	$0.030^a \pm 0.004$
Acidity	$0.007^b \pm 0.000$	$0.010^a \pm 0.001$
Drought	$0.009^b \pm 0.001$	$0.020^a \pm 0.002$
High temperature	$0.006^b \pm 0.000$	$0.013^a \pm 0.000$

Means (n = 3) in the same PGP activity followed by different letters in the same row are significantly different at $p \leq 0.05$, ± standard deviation

protein/h, respectively). Unfortunately, the P-solubilization ability of both isolate 194 and USDA110 could not be detected. Furthermore, the ability of IAA production by isolate 194 and USDA110, which might be involved in supporting plant growth under stress conditions, was determined exclusively under normal and stress conditions. It was found that although isolate 194 was able to produce IAA higher than that of USDA110 under all tested conditions, the level of IAA production tended to reduce when encountering stresses (Table I).

To further investigating these *Bradyrhizobium* isolates on plant growth promotion under stress conditions, DNA polymorphism using Box-PCR and dendrogram analyses were used to select the representative *Bradyrhizobium* strains to avoid the repetitive isolate selection. The result indicated that there are two clades of *Bradyrhizobium*. The first large clade contained the closely related strains CB1809, USDA110, DASA1014, and isolates 184 and 197, while isolates 193, 188, 194, and 199 were separated to form the second clade (Fig. S1). Based on these data, isolates 184, 188, and 194 were selected for further experiments.

Plant growth promotion by selected *Bradyrhizobium* isolates under single and mixed stress conditions. All *Bradyrhizobium* strains promoted soybean growth well under normal conditions when compared with non-inoculated plants. However, the symbiotic efficiency of these bacteria in soybean was reduced when plants were grown under stress conditions, especially under mixed stresses (Fig. 1). Among the isolated strains, isolate 194 provided the highest plant biomass when tested under all single stress conditions, and the plant biomass was significantly different from that of USDA110 under the single stress of drought and in high-temperature conditions. However, the nodule dry weight and nodule number of soybean inoculated with isolate 194 were not significantly different from those of plants inoculated with USDA110. Isolate 194 displayed the highest nitrogenase activity on

soybean grown under every stress condition except in the drought condition, where isolate 184 exhibited the highest nitrogenase activity. However, isolate 184 had the lowest level of nitrogenase activity when plants were grown under other single stress conditions, while isolate 188 was in the middle range. Therefore, symbiosis with soybean was improved for isolate 194 compared to other isolated strains under both single and mixed stress conditions. However, the performance was not significantly different from that of USDA110 (Fig. 1). The STI value indicated that isolate 194 was the strain that best-facilitated plant growth under single and mixed stress conditions, while isolate 188 could also promote soybean growth under drought and mixed acid-drought conditions (Table SIII). Thus, isolate 194 was selected for comparison with USDA110.

Soybean nodulation competitiveness of isolate 194 and the type strain USDA110 under stress conditions. To investigate the competitive ability of isolate 194 with USDA110, which is usually used as the soybean inoculant, both single and dual nodule occupancies were observed in soybean co-inoculated with isolate 194 and the GUS tagged strain of USDA110 under normal and stress conditions. The nodulation occupancy of isolate 194 under normal, drought, and high-temperature stress conditions was significantly higher than that of USDA110, while there was no significant difference in nodule occupancy of these two strains under acid stress conditions (Fig. 2). Similarly, the nodulation competitiveness of isolate 194 was significantly better than that of USDA110 under mixed stress conditions. Some nodules were occupied by both bacteria and called dual occupied nodules. However, the percentage of dual occupied nodules was low in all conditions. This result indicated that isolate 194 has the potential to compete for nodulation under several stress conditions.

Improved growth rate of *Bradyrhizobium* under stress conditions by supplementation of the culture medium with sugar. Optimization of the inoculant
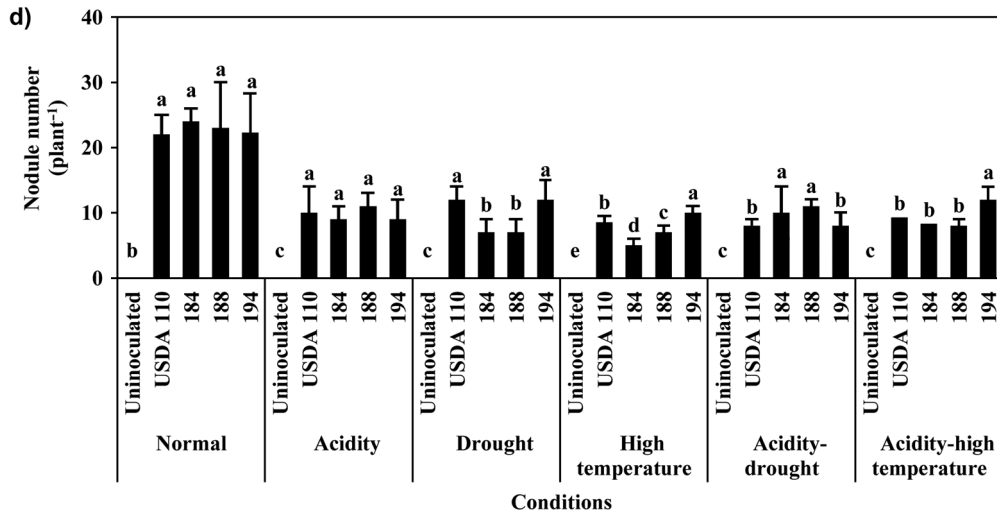
a)

b)

c)
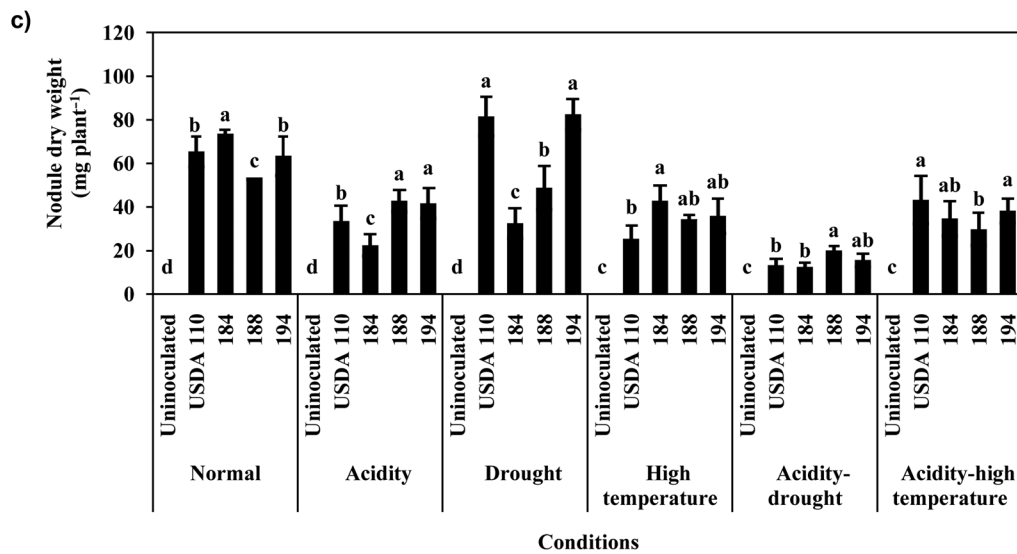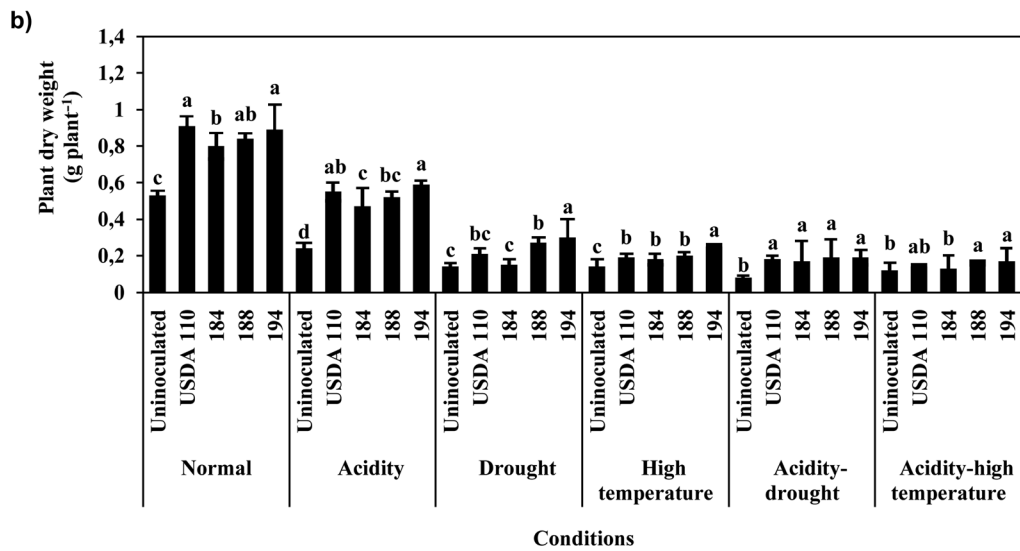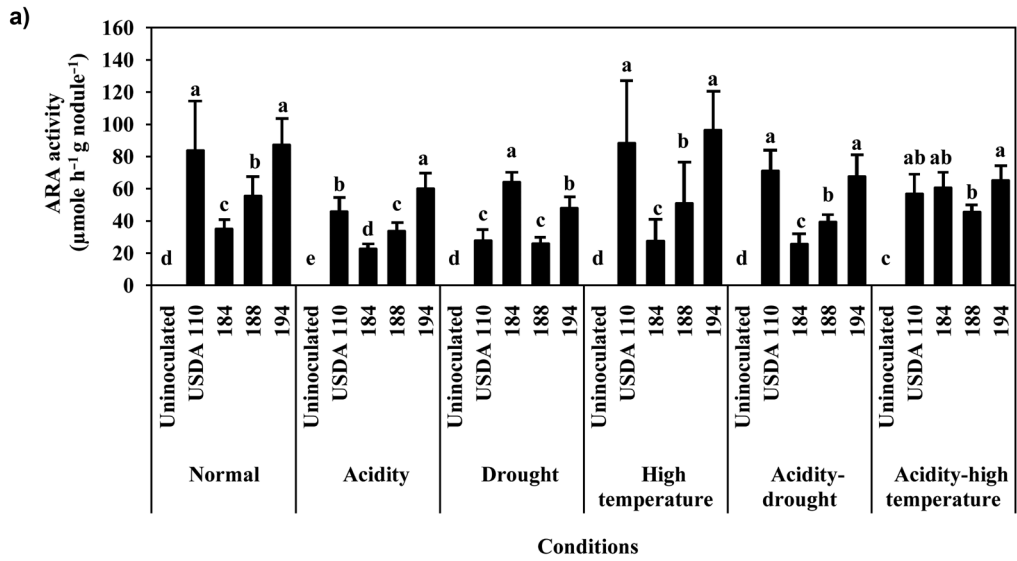
Fig. 1. Symbiotic efficiency of stress-tolerant *Bradyrhizobium* strains grown in soybean in Leonard's jars containing the sand under stress conditions. The Acetylene Reduction Assay (ARA activity) was applied to determine the nitrogenase activity of plants inoculated with different bacterial strains under normal and stress conditions (a). The plant dry weight of non-inoculated and inoculated plants (b) and nodule dry weight per plant (c) were measured, and the nodule numbers were counted per plant (d). Means and standard deviations were calculated from three replicates; for each parameter under the same condition, values with different letters were significantly different at $p \leq 0.05$.
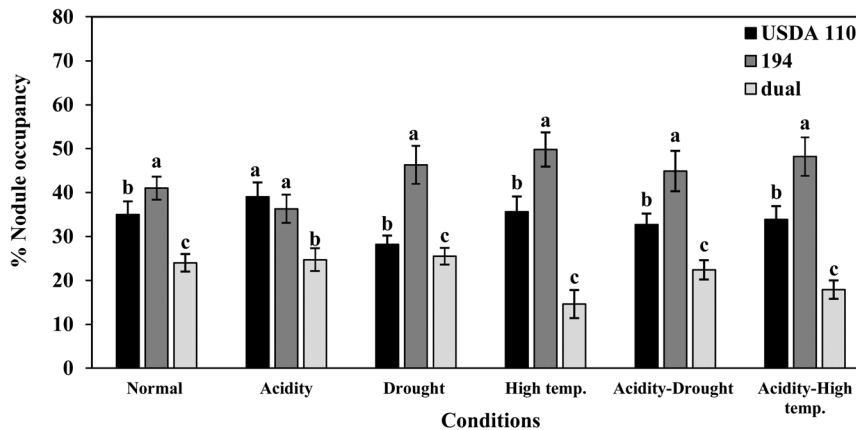

Fig. 2. Nodulation competition of *Bradyrhizobium* strains USDA 110 and isolate 194 in soybean grown in Leonard jars containing the sterilized sand under different stress conditions. Means and standard deviations were calculated from three replicates, and values in each condition with different letters were significantly different at $p \leq 0.05$.

formulation is one of the strategies to improve *Bradyrhizobium* inoculant efficiency. Our preliminary result of sugar supplementation in culture medium implied that of the six supplemented sugars (mannitol, glucose, trehalose, sucrose, glycerol, and polyvinyl alcohol), sucrose was the most effective sugar for improving the growth of isolate 194 under stress conditions (data not shown). Although a low concentration of sucrose (1 mM sucrose) was added in the culture medium, it could enhance the growth rate of isolate 194 better than other tested sugars. Therefore, sucrose was selected as a supplement to the medium, and the suitable concentration was further determined for improving the growth rate of isolate 194 in different stress conditions. Under normal conditions, compared with non-

sugar supplementation, there was no significant difference in specific growth rate per day (μ, in the range 0.40–0.42) when sucrose was supplemented in the range 5–300 mM. At concentrations of 400 and 500 mM, sucrose significantly reduced the growth of isolate 194 under normal conditions (Fig. S2a). The growth rate of isolate 194 in the medium without sucrose supplementation was obviously reduced when cultured under stress conditions. However, it was found that sucrose supplementation in the range of 50–300 mM could improve μ of the isolate 194 under acid (μ 0.31–0.34), drought (μ 0.38–0.42), and high-temperature stress (μ 0.32–0.34) conditions (Fig. S2b, S2c, and S2d). Since the best μ was obtained under several stress conditions when sucrose was supplemented at 300 mM, this

concentration level was selected to study further how sucrose could maintain the growth of isolate 194 under stress conditions based on the generation of other sugars that may act as compatible solutes inside the cell.

Sugars accumulation inside the bacterial cell may contribute to its stress tolerance ability. Since the supplementation of sucrose in culture medium leads to an increased bacterial ability to tolerate stress, it was hypothesized that after being taken up by bacterial cells, sucrose could be transformed to other sugars that might act as compatible solutes inside the cells and resulted in supporting cell growth under several stress conditions. Therefore, the number of viable cells and the concentration of sugars (including trehalose, glycerol, sucrose, glucose, and mannitol) accumulated inside the cell were determined in sucrose and non-sucrose-supplemented cultures under normal and stress conditions. Under normal and stress conditions of acid and high temperature, the number of viable cells at 10 DAI in the culture supplemented with sucrose remained higher than that in the non-sucrose-supplemented medium. With sucrose supplementation, the numbers of viable cells were (in log10 CFU/ml) 10.07, 7.93, and 9.55, while without sucrose supplementation, the numbers of viable cells were 8.68, 7.24, and 7.70 under normal, acid, and high-temperature stress conditions, respectively. However, the numbers of viable cells of isolate 194 supplemented with and without sucrose were similar when tested under drought stress: the cell numbers were (in log10 CFU/ml) 9.39 and 9.64, respectively. It was clearly shown that supplementation of the medium with sucrose tended to promote higher levels of sugar accumulation inside the cell than in non-sucrose-supplemented cells. Mannitol and glucose were the main sugars accumulated in the cells when cultured for 0–10 days under normal and stress conditions of acid and high temperature. However, mannitol, sucrose, trehalose, and glycerol, which are classified as compatible solutes, could also be detected inside the cell when cultured with sucrose supplementation (Fig. 3). The concentration and the type of sugar accumulation fluctuated per day depending on culture conditions. However, it was noticed that high accumulation of these compatible solutes at 8–10 DAI could reduce the loss of viable cells as shown under drought and high-temperature stress conditions (Fig. 3c and 3d). This result suggested that these compatible solutes may functionally interchange and protect the cells from stress. Therefore, supplementing the culture medium with sucrose could be used as a strategy to prepare a *Bradyrhizobium* inoculum for further application in the field under stress conditions.

Sucrose-supplemented inoculum could improve cell survival under stress conditions. To investigate whether *Bradyrhizobium* inoculum prepared from sucrose-supplemented culture could improve its ability to tolerate stress, the survival of cells after inoculation into the sand at 2 DAI was determined under different stress conditions. The survival of isolate 194 was improved under normal conditions when cells were derived from the sucrose-supplemented inoculum. However, the percentage of cells surviving was obviously decreased when tested under single stress and mixed stress conditions (Fig. 4). Acidity stress adversely affected the cell survival of isolate 194 to remain only 1.5%, which was equal to 10^4–10^5 cells/g of the sand at 2 DAI when sucrose was not supplied in the inoculum. The survival of isolate 194 was significantly improved to 21% when the inoculum was supplemented with sucrose.

Interestingly, the cell survival of the sucrose-supplemented inoculum of isolate 194 was significantly increased to more than 80% under drought and high-temperature stress conditions. In addition, under the mixed stress of acid-drought conditions, the survival of isolate 194 increased up to 54% when supplemented with sucrose. However, the survival of this strain under the mixed stress of acid-high-temperature condition was less than 1% even when sucrose was supplemented into medium (Fig. 4).

Plant growth promotion by sucrose-supplemented *Bradyrhizobium* inoculum under single and mixed stress conditions. The experiment was performed in a Leonard jar containing the sterilized sand under normal and stress conditions. The plant biomass was highest when inoculated with a sucrose-supplemented inoculum of the isolate 194 under normal and all stress conditions, and the biomass was significantly different from that of other treatments in all conditions, except under mixed acid-drought stress (Fig. 5). In terms of nodule number and nodule dry weight, the stress conditions affected the symbiosis efficiency by reducing the nodule formation on soybean. In most cases, although the sucrose-supplemented inocula of isolate 194 tended to increase nodule number, this treatment was not significantly different from that with non-sucrose-supplemented inoculum. However, the dry nodule weight produced from soybean inoculated with a sucrose-supplemented inoculum of isolate 194 was significantly increased in all single stress and the mixed acid-drought conditions (Fig. 5c). From these results, it could be concluded that supplementing the medium with sucrose would be suitable for improving plant growth under stress conditions with isolate 194. Therefore, soil pot experiments were performed with inocula of isolate 194 with and without sucrose supplemented to test the performance.

Performance of the developed *Bradyrhizobium* inoculum on soybean symbiosis. The performance of isolate 194 inoculums supplemented with and without sucrose on plant symbiosis was determined in pots

a) Normal conditon

b) Acid condition

c) Drought condition
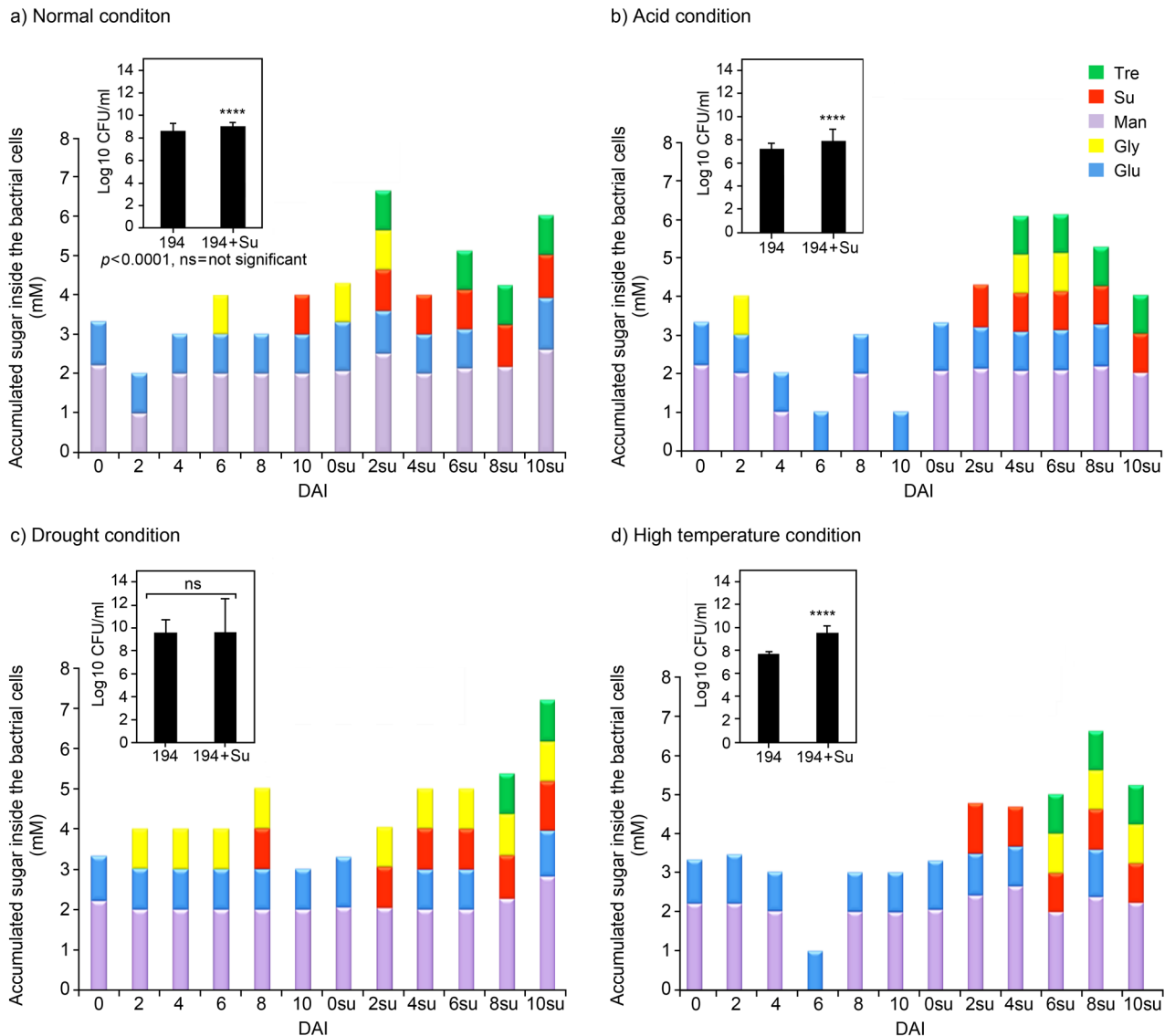

d) High temperature condition

Fig. 3. Accumulation of intracellular sugars in isolate 194 cultured in minimal broth medium (MSM) supplemented with and without 300 mM sucrose under different conditions and the number of viable cells at 10 DAI (days after inoculation). Student's t-test was used to determine the significance of the difference in the means between the two data sets of viable cells in each condition.
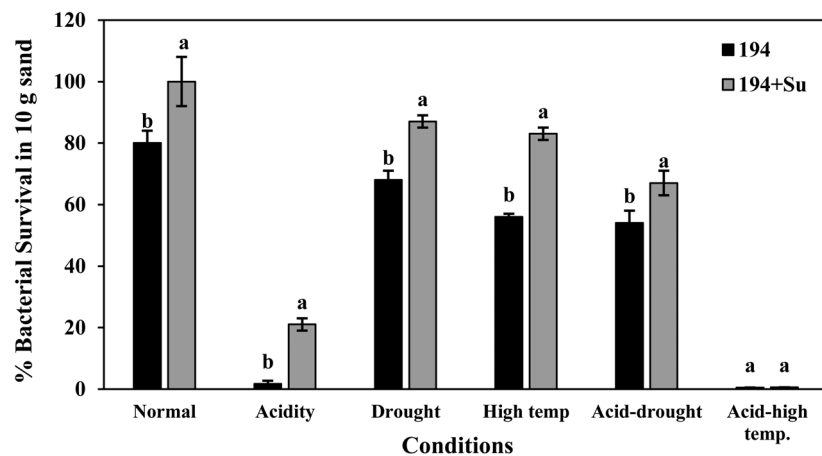

Fig. 4. Survival of isolate 194 supplemented with and without 300 mM sucrose in the sand under different stress conditions at 2 DAI (days after inoculation). Means and standard deviations were calculated from three replicates, and in each condition, values with different letters were significantly different at $p \leq 0.05$.
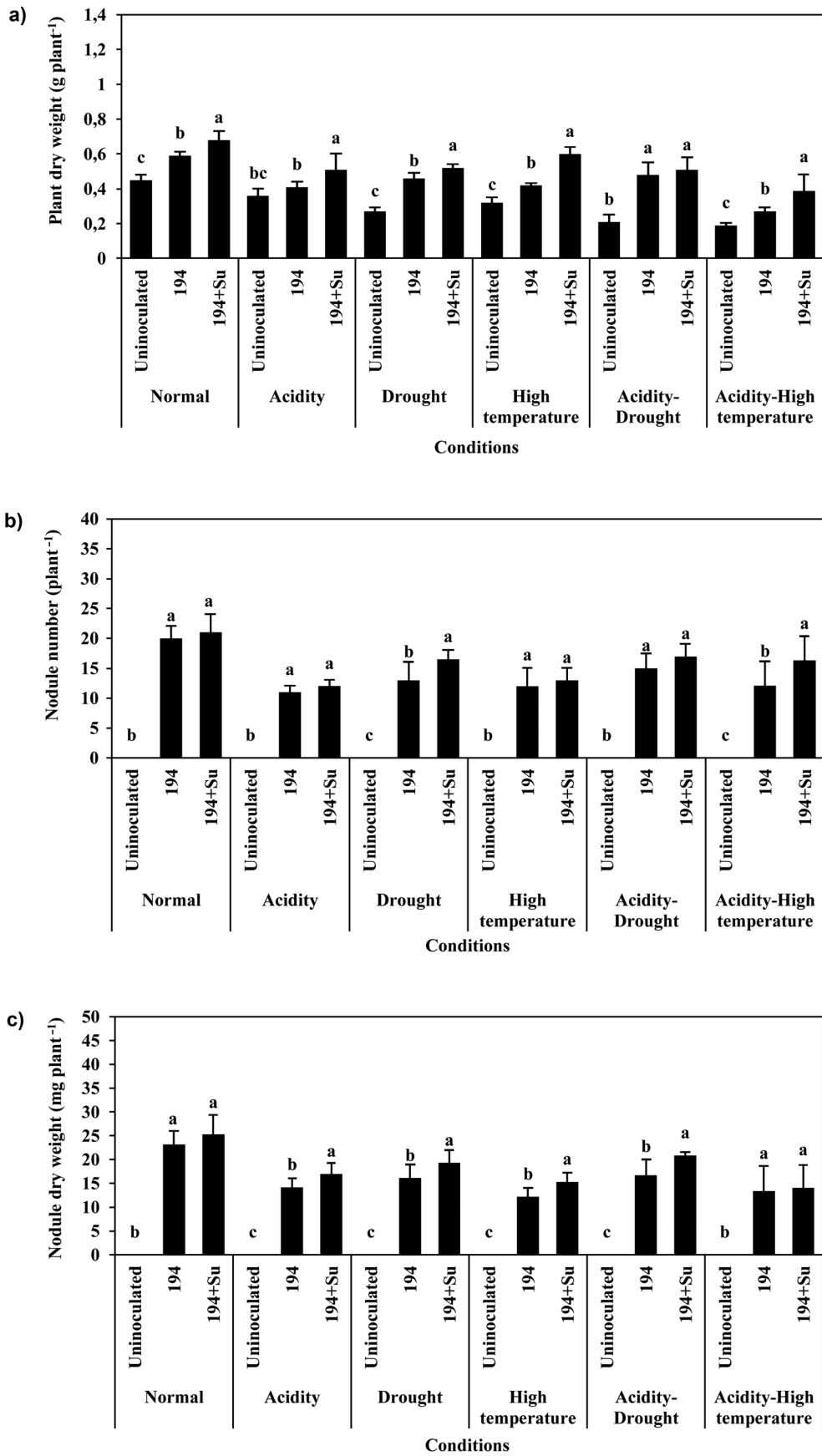
Fig. 5. Symbiotic efficiency of stress-tolerant *Bradyrhizobium* inoculants supplemented with and without 300 mM sucrose on soybean grown in Leonard jars containing the sterilized sand under different stress conditions. Means and standard deviations were calculated from three replicates, and in each condition, values with different letters were significantly different at $p \leq 0.05$.
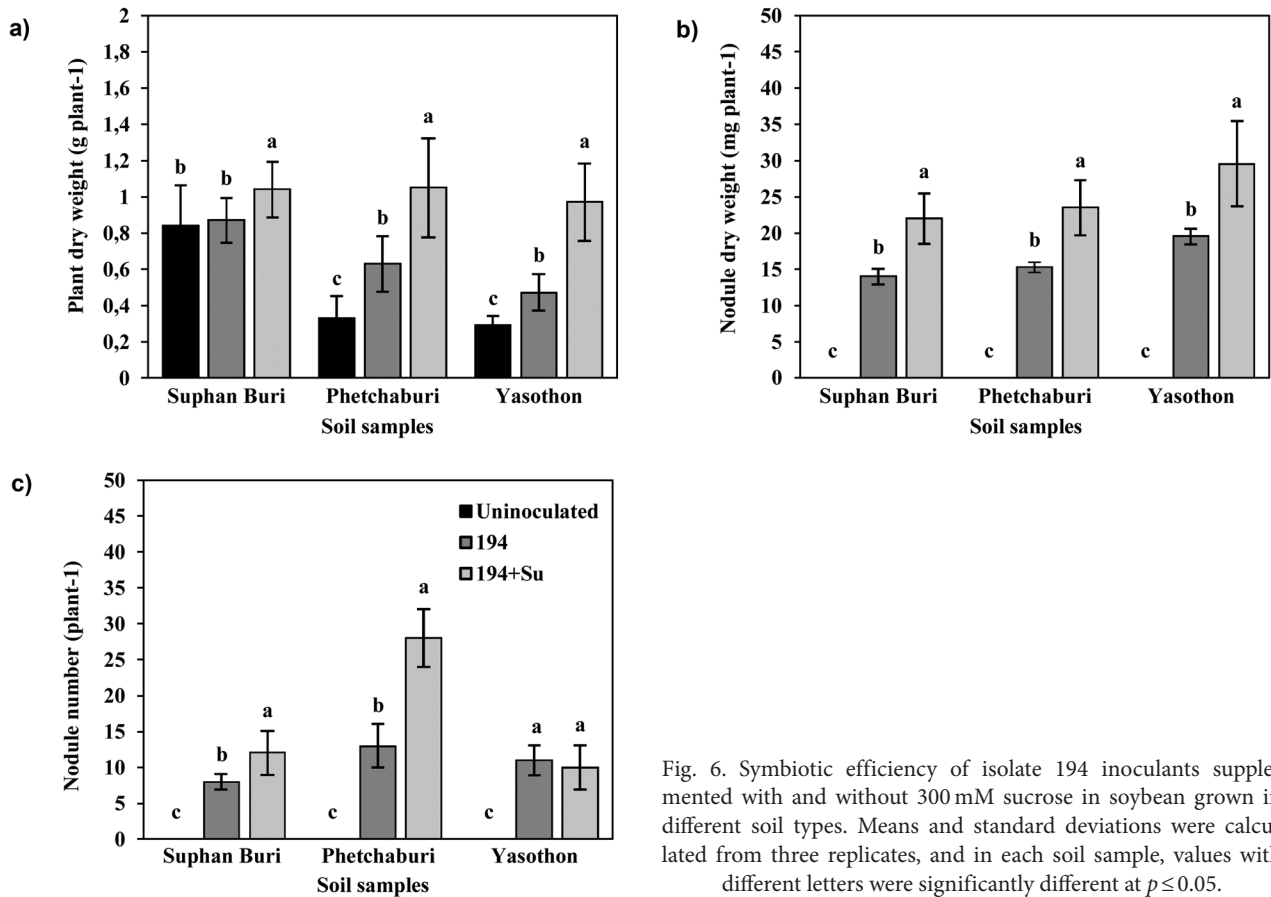
Fig. 6. Symbiotic efficiency of isolate 194 inoculants supplemented with and without 300 mM sucrose in soybean grown in different soil types. Means and standard deviations were calculated from three replicates, and in each soil sample, values with different letters were significantly different at $p \leq 0.05$.

containing soil collected from three different locations in Thailand where soybean had been planted (Table SII). The results of plant growth and symbiosis are shown in Fig. 6. Soybean inoculated with sucrose-supplemented inoculum had a significantly higher biomass and nodule dry weight than non-inoculated plants or plants inoculated with non-sucrose-supplemented inoculum when tested in all soil samples. The nodule number obtained on plants using sucrose-supplemented inoculum was significantly increased when compared with non-sucrose-supplemented inoculum when grown in soil collected from Suphan Buri and Petchaburi provinces. These preliminary data revealed the good performance of inoculum supplemented with sucrose under soil conditions. However, further field experiments are needed to ensure the efficiency of the developed inoculum.

Discussion

In this study, the abiotic stress-tolerant ability of isolated *Bradyrhizobium* strains was compared with that of type strains of *Bradyrhizobium,* including USDA110 and CB1809. USDA110 is normally used as soybean inoculum in Thailand, while the strain CB1809 has been reported as a stress-tolerant *Bradyrhizobium* in several conditions, such as acid soil and alkaline soil

(Botha et al. 2004; Indrasumunar et al. 2011). However, it has been reported that USDA110 is sensitive to acid stress, and it grew slowly in acid agar medium at pH 4.5 (Indrasumunar et al. 2011; Manassila et al. 2012). Our results indicate that although soybean inocula perform well with soybean under normal conditions, their performance could be reduced if the *Bradyrhizobium* strains cannot tolerate conditions of stress (Fig. 1 and Table SI). Soil environmental condition is one of the critical factors that affect the persistence and survival of rhizobial inocula; thus, changes in the rhizosphere environment could influence the competitiveness and persistence of rhizobia (Abd-Alla et al. 2014). Environmental stress conditions, such as acid soil, drought, or high temperature in the field, can occur in terms of mixed stresses. Therefore, mixed stress conditions might have an extreme effect on symbiosis and plant growth. Stress in the environment additionally affects soybean development by impairing the function of active nodules (Dimkpa et al. 2009; Wielbo et al. 2012). This study also found that plant growth was reduced under stress conditions, especially under mixed stress conditions. It has also been reported that the drought stress generated by PEG, in the range from −1.0 to −7.0 bars, decreases root elongation and plant development (Amooaghaie 2011; Uma et al. 2013). Marsh et al. (2006) also reported the effect of high

temperature, who indicated that the yields of soybean, pigeon pea, and cowpea inoculated with *Bradyrhizobium* were decreased when plants were grown at 38°C. These data are similar to our results in that plant growth and symbiotic performance were significantly reduced at high temperatures. High temperatures may affect bacterial cell survival and damage some biological pathways in plant development. These data agree with many studies that suggest the efficiency of tolerant *Bradyrhizobium* strains under adverse conditions could promote plant growth, but that plant growth may not be similar to that of plants cultivated under normal conditions (Wielbo et al. 2012; Atieno and Lesueur 2019).

We identified isolate 194 as a *Bradyrhizobium* strain using the 16S ribosomal RNA gene and recorded it under accession number KF913342.1 in the GenBank. In this present study, this isolate was selected as a tolerant strain that can be developed as a soybean inoculant to be used under multi-stress conditions based on its performance in promoting plant growth in the sand-involving experiments. Although isolate 194 did not provide significantly higher nitrogen fixation ability than USDA110, this strain overall promoted soybean growth under stress conditions better than USDA110. Mubarik et al. (2012) reported that the nitrogenase activity of stress-tolerant *Bradyrhizobium* strains might not significantly differ from that of USDA110. However, their ability to tolerate stress was the important criterion to select the best strain as soybean inoculum for further application under conditions of stress. The stress tolerance in many bacteria is linked to the appropriate composition and membrane structure of the cell. For example, the efficiency in exopolysaccharide (EPS) production of bean rhizobia and *Bradyrhizobium* sp. strains are related to their pH tolerance, leading to increased symbiotic nitrogen fixation in legumes (Donot et al. 2012; Razika et al. 2012).

Similarly, stressed bacterial cells have a high lipopolysaccharide production (LPS) and accumulate compound products from secondary metabolites such as polyols, polyamines, proline, trehalose, etc. (Saxena et al. 2013). These compounds could act as osmolytes, which protect the cell from osmotic stresses. Likewise, isolate 194 has a higher EPS production than USDA110 when grown on medium (Table I), which might be one reason why isolate 194 facilitates stress tolerance. Besides, its ability to grow better than USDA110 under various stress conditions may also be caused by the cellular accumulation of appropriate compatible solute compounds, as shown in Fig. 3. Furthermore, isolate 194 was found to contain some plant growth-promoting (PGP) traits. The ACC deaminase activity of isolate 194 was higher than that of USDA110 (Table I), suggesting that isolate 194 also has the potential to alleviate plant stress by reducing the production in the plant of

ethylene, which regulates many processes in response to biotic and abiotic stresses (Gamalero and Glick 2015). Another PGP trait is the production of indole-3-acetic acid (IAA). IAA is also involved in supporting plant growth under stress conditions. It has been reported that a high level of IAA promotes the formation of lateral roots (Gupta and Pandey 2019) and increases root length and surface area (Olanrewaju et al. 2017), which might be essential for plant growth under drought conditions. Isolate 194 and USDA110 also produce IAA. However, the level of IAA production was reduced when bacteria encounter conditions of stress. As shown in Table I, the levels of IAA production by isolate 194 and USDA110 tended to reduce by more than 50% under stress conditions. Sijilmassi et al. (2020) also showed a significant reduction in IAA production by rhizobia when grown under abiotic stress conditions such as drought at −2 to −7.5 bar and concentrated salt at 0.5 to 3% NaCl. Based on this result, other PGP traits of isolate 194 and USDA110 may also be reduced under stress conditions, and this might adversely affect or could not fully facilitate plant growth under stress conditions. Although the level of IAA produced by isolate 194 was significantly higher than that of USDA110 in all stress conditions, the question remains whether this level of IAA is appropriate to promote plant growth under conditions of stress and whether other PGP traits might be involved in this promotion of plant growth under different stress conditions. Therefore, it is interesting to investigate further the mechanisms of this *Bradyrhizobium*, which not only performs nitrogen fixation but also has other PGP abilities that alleviate plant stress and promote plant growth under single- and multi-stress conditions.

The results of nodulation competition between isolate 194 and USDA110 under multi-stress conditions (Fig. 2) indicates that isolate 194 can overcome the stress and competes with USDA110 to nodulate soybean under several stress conditions. Stress-sensitive *Bradyrhizobium* inoculants are directly affected by environmental stress conditions and may lose their nodulation competitiveness. Thus, the indigenous rhizobia, which generally have a low nitrogenase activity can compete with soybean inoculant, resulting in the reduction of the yield when most nodules are occupied by ineffective indigenous rhizobia (Shamseldin and Werner 2004). Therefore, the improved nodulation competition of isolate 194 under multi-stress conditions compared to USDA110 revealed the potential of developing this stress-tolerant *Bradyrhizobium* strain as a soybean inoculant for application in the field.

To improve the stress tolerance efficiency of soybean *Bradyrhizobium* inocula, using compatible solutes to protect the cell from stress was applied in this study. Several compatible solutes (sugars, polymers,

polyols, protein, and derivatives) have been studied for their function as osmotic balancers with *Rhizobium, Sinorhizobium*, and *Bradyrhizobium* (Deaker et al. 2007; Fernandez-Aunión et al. 2010; Ghalamboran and Ramsden 2010). In this experiment, sucrose was supplemented in the medium during the cultivation of *Bradyrhizobium*. Sucrose has been reported to act as an osmoprotection against several environmental osmotic stresses in rhizobia by maintaining the membrane's integrity (Le Rudulier 2005). The presence of sucrose in the culture medium is involved in the high EPS production in *Rhizobium* strains and extends the shelf life of *Rhizobium* biofertilizers (Razika et al. 2012; Singh et al. 2014). Supplementation of 0.5 mM sucrose was reported to increase cell survival of *Sinorhizobium meliloti* and *Rhizobium leguminosarum* strains during the stationary phase under salt stress (Gouffi et al. 1999). In addition, it has been most popular to use varying concentrations of sucrose as a compatible solute to induce stress tolerance in lactic acid bacteria (LABs) such as *Lactococcus lactis* (Kilimann et al. 2006) and *Lactobacillus delbrueckii* (Silva et al. 2004) and both strains could increase their survival under heat and drying conditions by supplementing with 0.06 and 1.5 M of sucrose, respectively. Interestingly, analysis of sugar accumulation inside the *Bradyrhizobium* cell after supplementation with sucrose found many more compatible solutes, such as mannitol, trehalose, and glycerol, inside the cell than in non-sucrose-supplemented cells (Fig. 3). In Gram-negative bacteria, the extracellular sucrose can enter through the inner membrane (Reid and Abratt 2005) and enter to glycolysis as a translocated sugar, which can be transformed to other sugars by several pathway links (Lee et al. 2010). This explains why different sugars could be detected inside cells of isolate 194 after being supplemented with sucrose in the culture.

Moreover, the stressed bacterial cells could synthesize compounds alleviating the stress from the supplied molecules by a biosynthetic *de novo* pathway (Blanco et al. 2010). Thus, the accumulation of soluble sugar inside the bacterial cell may be derived from self-production and uptake. High accumulation of compatible solutes such as glycerol and trehalose during 8–10 DAI could reduce the loss of viable cells, especially under drought and high-temperature stress conditions (Fig. 3c and 3d). The accumulation of trehalose in the cytoplasm is critical to the survival of *Bradyrhizobium japonicum* during desiccation (Streeter 2003). Trehalose and glycerol have been reported to stabilize proteins at high temperatures (Empadinhas and da Costa 2008) and preserve the present form of proteins, resulting in a favored hydration of protein surfaces (Thomas et al. 2013). These sugars may maintain the ability of the cell to cope with stress conditions. The survival of sucrose-supplemented *Bradyrhizobium* isolate 194 was signifi-

cantly increased under most stress conditions (Fig. 4) and may lead to improvements in the biomass of soybean grown under several stress conditions as well as on different soils (Fig. 5 and 6). The good performance of sucrose-supplemented *Bradyrhizobium* inoculant when tested with soybean in soil samples indicates that cell survival was improved successfully, promoting the symbiosis efficiency compared with non-sucrose-supplemented inoculum. The application of trehalose could increase the survival of cells of *R. leguminosarum* bv. *trifolii* strain NZP561 when compared to treatment with lactose and water (McIntyre et al. 2007). Mannitol has also been used as an osmoprotectant and found to enhance the survival of *L. lactis* (Efiuvwevwere et al. 1999), *Rhizobium tropici* CIAT 899, and *Rhizobium gallicum* bv. *phaseoli* 8a3 (Fernandez-Aunión et al. 2010). Moreover, the application of 120 mM sucrose in a liquid medium for *Azotobacter* and *Rhizobium* inoculant production could also increase the seed germination and development of *Trigonella foenum-graecum* L. under *in vitro* condition (Nagananda et al. 2010).

This study suggests that the application of abiotic-stress-tolerant *Bradyrhizobium* strain and supplementing an appropriate sugar in the medium could be a promising strategy for developing a soybean *Bradyrhizobium* inoculant for application under multi-environmental stress conditions. Overcoming the challenges of climate change is very important for soybean inoculant developers. However, further testing of the soybean inoculant developed here under various field conditions is needed to validate its symbiotic efficiency and promote plant growth and soybean yield before adopting this technology.

Conflict of interest

The authors do not report any financial or personal connections with other persons or organizations, which might negatively affect the contents of this publication and/or claim authorship rights to this publication.

Literature

Abd-Alla MH, Issa AA, Ohyama T. Impact of harsh environmental conditions on nodule formation and dinitrogen fixation of legumes. In: Ohyama T, editor. Advances in biology and ecology of nitrogen fixation. Rejeka (Croatia): IntechOpen; 2014.
https://doi.org/10.5772/56997

Amooaghaie R. Role of polyamines in the tolerance of soybean to water deficit stress. World Acad Sci Eng Technol. 2011;56:498–502.

Atieno M, Lesueur D. Opportunities for improved legume inoculants: enhanced stress tolerance of rhizobia and benefits to agroecosystems. Symbiosis. 2019 Mar;77(3):191–205.
https://doi.org/10.1007/s13199-018-0585-9

Blanco AR, Sicardi M, Frioni L. Competition for nodule occupancy between introduced and native strains of *Rhizobium leguminosarum* biovar *trifolii*. Biol Fertil Soils. 2010 Apr;46(4):419–425. https://doi.org/10.1007/s00374-010-0439-y

Botha WJ, Jaftha JB, Bloem JF, Habig JH, Law IJ. Effect of soil bradyrhizobia on the success of soybean inoculant strain CB 1809. Microbiol Res. 2004 Sep;159(3):219–231. https://doi.org/10.1016/j.micres.2004.04.004

Boumahdi M, Mary P, Hornez JP. Influence of growth phases and desiccation on the degrees of unsaturation of fatty acids and the survival rates of rhizobia. J Appl Microbiol. 1999 Oct;87(4):611–619. https://doi.org/10.1046/j.1365-2672.1999.00860.x

Castellane TCL, Campanharo JC, Colnago LA, Coutinho ID, Lopes ÉM, Lemos MVF, de Macedo Lemos EG. Characterization of new exopolysaccharide production by *Rhizobium tropici* during growth on hydrocarbon substrate. Int J Biol Macromol. 2017 Mar; 96:361–369. https://doi.org/10.1016/j.ijbiomac.2016.11.123

Deaker R, Roughley RJ, Kennedy IR. Desiccation tolerance of rhizobia when protected by synthetic polymers. Soil Biol Biochem. 2007 Feb;39(2):573–580. https://doi.org/10.1016/j.soilbio.2006.09.005

Dimkpa C, Weinand T, Asch F. Plant-rhizobacteria interactions alleviate abiotic stress conditions. Plant Cell Environ. 2009 Sep; 32(12):1682–1694. https://doi.org/10.1111/j.1365-3040.2009.02028.x

Donati AJ, Lee HI, Leveau JH, Chang WS. Effects of indole-3-acetic acid on the transcriptional activities and stress tolerance of *Bradyrhizobium japonicum*. PLoS one. 2013 Oct;8(10):e76559. https://doi.org/10.1371/journal.pone.0076559

Donot F, Fontana A, Baccou J, Schorr-Galindo S. Microbial exopolysaccharides: main examples of synthesis, excretion, genetics and extraction. Carbohydr Polym. 2012 Jan;87(2):951–962. https://doi.org/10.1016/j.carbpol.2011.08.083

Efiuvwevwere B, Gorris L, Smid E, Kets E. Mannitol-enhanced survival of *Lactococcus lactis* subjected to drying. Appl Microbiol Biotechnol. 1999 Jan;51(1):100–104. https://doi.org/10.1007/s002530051369

Empadinhas N, da Costa MS. Osmoadaptation mechanisms in prokaryotes: distribution of compatible solutes. Int Microbiol. 2008 Sep;11(3):151–161.

Fernandez-Aunión C, Hamouda T, Iglesias-Guerra F, Argandoña M, Reina-Bueno M, Nieto J, Aouani ME, Vargas C. Biosynthesis of compatible solutes in rhizobial strains isolated from *Phaseolus vulgaris* nodules in Tunisian fields. BMC Microbiol. 2010 Jul;10(1):192. https://doi.org/10.1186/1471-2180-10-192

Gamalero E, Glick BR. Bacterial modulation of plant ethylene levels. Plant Physiol. 2015 Sep;169(1):13–22. https://doi.org/10.1104/pp.15.00284

Ghalamboran M, Ramsden JJ. Viability of *Bradyrhizobium japonicum* on soybean seeds enhanced by magnetite nanoparticles during desiccation. World Acad Sci Eng Technol. 2010 Mar;63:198–203. https://doi.org/10.5281/zenodo.1073008

Gopalakrishnan S, Sathya A, Vijayabharathi R, Varshney RK, Gowda CL, Krishnamurthy L. Plant growth promoting rhizobia: challenges and opportunities. Biotech. 2015 Aug;5(4):355–377. https://doi.org/10.1007/s13205-014-0241-x

Gouffi K, Pica N, Pichereau V, Blanco C. Disaccharides as a new class of nonaccumulated osmoprotectants for *Sinorhizobium meliloti*. Appl Environ Microbiol. 1999 Apr;65(4):1491–1500. https://doi.org/10.1128/AEM.65.4.1491-1500.1999

Gupta S, Pandey S. Unravelling the biochemistry and genetics of ACC deaminase – An enzyme alleviating the biotic and abiotic stress in plants. Plant gene. 2019 Jun;18:100175. https://doi.org/10.1016/j.plgene.2019.100175

Idris HA, Labuschagne N, Korsten L. Screening rhizobacteria for biological control of *Fusarium* root and crown rot of sorghum in Ethiopia. Biol Control. 2007 Jan;40(1):97–106. https://doi.org/10.1016/j.biocontrol.2006.07.017

Indrasumunar A, Dart PJ, Menzies NW. Symbiotic effectiveness of *Bradyrhizobium japonicum* in acid soils can be predicted from their sensitivity to acid soil stress factors in acidic agar media. Soil Biol Biochem. 2011 Oct;43(10):2046–2052. https://doi.org/10.1016/j.soilbio.2011.05.022

Iturralde ET, Covelli JM, Alvarez F, Pérez-Giménez J, Arrese-Igor C, Lodeiro AR. Soybean-nodulating strains with low intrinsic competitiveness for nodulation, good symbiotic performance, and stress-tolerance isolated from soybean-cropped soils in Argentina. Front Microbiol. 2019 May;10:1061. https://doi.org/10.3389/fmicb.2019.01061

Jalloh AA. Potential of native rhizobia isolates to improve production of legume crops in small holder farms. Biosci Res. 2020 Aug; 8(2):681–692.

Kajić S, Komes A, Rajnović I, Sikora S. Selection of stress tolerant indigenous rhizobia nodulating alfalfa (*Medicago sativa* L.). Agric Conspec Sci. 2019 Sep;84(4):365–370.

Kilimann KV, Doster W, Vogel RF, Hartmann C, Gänzle MG. Protection by sucrose against heat-induced lethal and sublethal injury of *Lactococcus lactis*: An FT-IR study. Biochim Biophys Acta Proteins Proteom. 2006 Jul;1764(7):1188–1197. https://doi.org/10.1016/j.bbapap.2006.04.016

Krause A, Doerfel A, Gottfert M. Mutational and transcriptional analysis of the type III secretion system of *Bradyrhizobium japonicum*. Mol Plant Microbe Interact. 2002 Dec;15(12):1228–1235. https://doi.org/10.1094/MPMI.2002.15.12.1228

Lai MC, Sowers KR, Robertson DE, Roberts MF, Gunsalus RP. Distribution of compatible solutes in the halophilic methanogenic archaebacteria. J Bacteriol. 1991 Sep;173(17):5352–5358. https://doi.org/10.1128/jb.173.17.5352-5358.1991

Le Rudulier D. Osmoregulation in rhizobia: The key role of compatible solutes. Grain Legume. 2005; 42:18–19.

Lee JW, Choi S, Kim JM, Lee SY. *Mannheimia succiniciproducens* phosphotransferase system for sucrose utilization. Appl Environ Microbiol. 2010 Mar;76(5):1699–1703. https://doi.org/10.1128/AEM.02468-09

Manassila M, Nuntagij A, Tittabutr P, Boonkerd N, Teaumroong N. Growth, symbiotic, and proteomics studies of soybean *Bradyrhizobium* in response to adaptive acid tolerance. Afr J Biotechnol. 2012 Oct;11(83):14899–14910. https://doi.org/10.4314/AJB.V11I83

Marsh LE, Baptiste R, Marsh DB, Trinklein D, Kremer RJ. Temperature effects on *Bradyrhizobium* spp. growth and symbiotic effectiveness with pigeon pea and cowpea. J Plant Nutr. 2006 Feb;29(2):331–346. https://doi.org/10.1080/01904160500476921

Maryani Y, Dewi W, Yunus A. Study on rhizobium interaction with osmoprotectant rhizobacteria for improving mung bean yield. Conf Ser Earth Environ Sci. 2018 Mar;129(1):012011. https://doi.org/10.1088/1755-1315/129/1/012011

Mayak S, Tirosh T, Glick BR. Plant growth-promoting bacteria that confer resistance to water stress in tomatoes and peppers. Plant Sci. 2004 Feb;166:525–530. https://doi.org/10.1016/j.plantsci.2003.10.025

Mcintyre HJ, Hore TA, Miller SH, Dufour JP, Ronson CW. Trehalose biosynthesis in *Rhizobium leguminosarum* bv. *trifolii* and its role in desiccation tolerance. Appl Environ Microbiol. 2007 Jun; 73(12):3984–3992. https://doi.org/10.1128/AEM.00412-07

Michel BE. Evaluation of the water potentials of solutions of polyethylene glycol 8000 both in the absence and presence of other solutes. Plant Physiol. 1983 May;72(1):66–70. https://doi.org/10.1104/pp.72.1.66

Mubarik NR, Habibah H, Wahyudi AT. Greenhouse experiments of symbiotic effectiveness of acid-aluminium tolerance *Bradyrhizobium japonicum* strains on soybean plant. In: Nejadkoorki F, editor. International Conference on Applied Life Sciences. Rejeka (Croatia): Intech Open; 2012. p. 337–342. https://doi.org/10.5772/intechopen.84101

Nagananda G, Das A, Bhattacharya S, Kalpana T. *In vitro* studies on the effects of biofertilizers (*Azotobacter* and *Rhizobium*) on seed germination and development of *Trigonella foenum-graecum* L. using a novel glass marble containing liquid medium. Int J Botany. 2010 Sep;6(4):394–403. https://doi.org/10.3923/ijb.2010.394.403

Nautiyal CS. An efficient microbiological growth medium for screening phosphate solubilizing microorganisms. FEMS Microbiol Lett. 1999 Jan;170(1):265–270. https://doi.org/10.1111/j.1574-6968.1999.tb13383.x

Ntambo M, Chilinda IS, Taruvinga A, Hafeez S, Anwar T, Sharif R, Kies L. The effect of rhizobium inoculation with nitrogen fertilizer on growth and yield of soybeans (*Glycine max* L.). Int J Biosci. 2017 Mar;10(3):163–172. https://doi.org/10.12692/ijb/10.3.163-172

Olanrewaju OS, Glick BR, Babalola OO. Mechanisms of action of plant growth promoting bacteria. World J Microb Biot 2017 Oct; 33(11):1–16. https://doi.org/10.1007/s11274-017-2364-9

Payakapong W, Tittabutr P, Teaumroong N, Boonkerd N. Soybean cultivars affect nodulation competition of *Bradyrhizobium japonicum* strains. World J Microbiol Biotechnol. 2004 Apr;20(3):311–315. https://doi.org/10.1023/B:WIBI.0000023838.06663.c5

Razika G, Amira B, Yacine B, Ammar B. Influence of carbon source on the production of exopolysacharides by *Rhizobium sullae* and on the nodulation of *Hedysarum coronarium* L. Legume. Afr J Microbiol Res. 2012 Jan;6(30):5940–5946. https://doi.org/10.5897/AJMR12.393

Reid SJ, Abratt VR. Sucrose utilisation in bacteria: genetic organisation and regulation. Appl Microbiol Biotechnol. 2005 Jan;67(3):312–321. https://doi.org/10.1007/s00253-004-1885-y

Sangproo M, Polyiam P, Jantama SS, Kanchanatawee S, Jantama K. Metabolic engineering of *Klebsiella oxytoca* M5a1 to produce optically pure d-lactate in mineral salts medium. Bioresour Technol. 2012 Sep;119(0):191–198. https://doi.org/10.1016/j.biortech.2012.05.114

Sarwar M, Arshad M, Martens DA, Frankenberger WT. Tryptophan-dependent biosynthesis of auxins in soil. Plant and Soil, 1992 Jan;147(2):207–215. https://doi.org/10.1007/BF00029072

Saxena S C, Kaur H, Verma P, Petla BP, Andugula VR, Majee M. Osmoprotectants: potential for crop improvement under adverse conditions. In: Tuteja N, Singh Gill S, editors. Plant acclimation to environmental stress. New York (USA): Springer; 2013. p. 197–232. https://doi.org/10.1007/978-1-4614-5001-6_9

Schneider M, De Bruijn F. Rep-PCR mediated genomic fingerprinting of rhizobia and computer-assisted phylogenetic pattern analysis. World J Microbiol Biotechnol. 1996 Mar;12(2):163–174. https://doi.org/10.1007/BF00364681

Shamseldin A, Werner D. Selection of competitive strains of *Rhizobium* nodulating *Phaseolus vulgaris* and adapted to environmental conditions in Egypt, using the *gus*-reporter gene technique. World J Microbiol Biotechnol. 2004 Jun;20(4):377–382. https://doi.org/10.1023/B:WIBI.0000033060.27180.8c

Shetty KG, Hetrick BAD, Schwab AP. Effects of mycorrhizae and fertilizer amendments on zinc tolerance of plants. Environ Pollut. 1995 Apr;88(3):307–314. https://doi.org/10.1016/0269-7491(95)93444-5

Sijilmassi B, Filali-Maltouf A, Fahde S, Ennahli Y, Boughribil S, Kumar S, Amri A. *In vitro* plant growth promotion of rhizobium strains isolated from lentil root nodules under abiotic stresses. Agronomy. 2020 Jul;10(7):1006. https://doi.org/10.3390/agronomy10071006

Silva ER, Zoz J, Oliveira CES, Zuffo AM, Steiner F, Zoz T, Vendruscolo EP. Can co-inoculation of *Bradyrhizobium* and *Azospirillum* alleviate adverse effects of drought stress on soybean (*Glycine max* L. Merrill.)? Arch Microbiol. 2019 Apr;201(3):325–335. https://doi.org/10.1007/s00203-018-01617-5

Silva J, Carvalho AS, Pereira H, Teixeira P, Gibbs PA. Induction of stress tolerance in *Lactobacillus delbrueckii* ssp. *bulgaricus* by the addition of sucrose to the growth medium. J Dairy Res. 2004 Mar; 71(1):121–125. https://doi.org/10.1017/S0022029903006411

Sindhu SS, Dua S, Verma M, Khandelwal A. Growth promotion of legumes by inoculation of rhizosphere bacteria. In: Khan MS, Musarrat J, Zaidi A, editors. Microbes for legume improvement. Vienna (Austria): Springer; 2010. p. 195–235. https://doi.org/10.1007/978-3-211-99753-6_9

Singh A, Dipuraj MH, Kumar Y, Peter J, Mishra S, Saxena L. Optimization of production parameters and evaluation of shelf life of *Rhizobium* biofertilizers. Elixir Bio Tech. 2014 Feb;67:21787–21795.

Somasegaran P, Hoben HJ. Handbook for rhizobia. Methods in legume-rhizobium technology. New York (USA): Springer-Verlag; 1994. https://doi.org/10.1007/978-1-4613-8375-8

Streeter JG. Effect of trehalose on survival of *Bradyrhizobium japonicum* during desiccation. J Appl Microbiol. 2003 Feb;95(3):484–491. https://doi.org/10.1046/j.1365-2672.2003.02017.x

Suyal DC, Soni R, Sai S, Goel R. Microbial inoculants as biofertilizer. In: Singh D, Singh H, Prabha R, editors. Microbial inoculants in sustainable agricultural productivity. New Delhi (India): Springer; 2016. p. 311–318. https://doi.org/10.1007/978-81-322-2647-5_18

Talbi C, Argandoña M, Salvador M, Alché JD, Vargas C, Bedmar EJ, Delgado MJ. *Burkholderia phymatum* improves salt tolerance of symbiotic nitrogen fixation in *Phaseolus vulgaris*. Plant Soil. 2013 Jun;367(1):673–685. https://doi.org/10.1007/s11104-012-1499-6

Thomas CS, Xu L, Olsen BD. Effect of small molecule osmolytes on the self-assembly and functionality of globular protein-polymer diblock copolymers. Biomacromolecules. 2013 Aug;14(9):3064–3072. https://doi.org/10.1021/bm400664t

Tukey JW. Comparing individual means in the analysis of variance. Biometrics. 1949 Jun;5(2):99–114.

Uma C, Sivagurunathan P, Sangeetha D. Performance of bradyrhizobial isolates under drought conditions. Int J Curr Microbiol App Sci. 2013 May; 2(5):228–232.

Wang, Y, Zhang Z, Zhang P, Cao Y, Hu T, & Yang P. Rhizobium symbiosis contribution to short-term salt stress tolerance in alfalfa (*Medicago sativa* L.) Plant soil. 2016 Jan; 402(1–2):247–261. https://doi.org/10.1007/s11104-016-2792-6

Wei GH, Yang XY, Zhang ZX, Yang YZ, Lindsröm K. Strain *Mesorhizobium* sp. CCNWGX035: A stress-tolerant isolate from *Glycyrrhiza glabra* displaying a wide host range of nodulation. Pedosphere. 2008 Feb; 18(1):102–112. https://doi.org/10.1016/S1002-0160(07)60108-8

Wielbo J, Kidaj D, Koper P, Kubik-Komar A, Skorupska A. The effect of biotic and physical factors on the competitive ability of *Rhizobium leguminosarum*. Cent Eur J Biol. 2012; 7(1):13–24. https://doi.org/10.2478/s11535-011-0085-x

Wilson K J, Sessitsch A, Corbo JC, Giller KE, Akkermans AD, Jefferson RA. β-Glucuronidase (GUS) transposons for ecological and genetic studies of rhizobia and other Gram-negative bacteria. Microbiology. 1995 Jul; 141(7):1691–1705. https://doi.org/10.1099/13500872-141-7-1691

Zhang J, Singh D, Guo C, Shang Y, Peng S. Rhizobia at extremes of acidity, alkalinity, salinity, and temperature. In: Singh R, Manchanda G, Maurya I, Wei Y, editors. Microbial versatility in varied environments. Singapore (Singapore): Springer; 2020. p. 51–65. https://doi.org/10.1007/978-981-15-3028-9_4

Supplementary materials are available on the journal's website.

ORIGINAL PAPER

Diversity of Endophytic Fungal Community in Leaves of *Artemisia argyi* Based on High-throughput Amplicon Sequencing

QIU-FANG WU, LING-MIN HE, XIN-QIANG GAO, MEI-LING ZHANG,
JING-SHUN WANG and LI-JIANG HOU*

College of Biology and Food Engineering, Anyang Institute of Technology, Anyang, China

Abstract

To investigate the community structure and diversity of endophytic fungi in the leaves of *Artemisia argyi*, leaf samples were collected from five *A. argyi* varieties grown in different cultivation areas in China, namely, Tangyin Beiai in Henan (BA), Qichun Qiai in Hubei (QA), Wanai in Nanyang in Henan (WA), Haiai in Ningbo in Zhejiang (HA), and Anguo Qiai in Anguo in Hebei (AQA), and analyzed using Illumina high-throughput sequencing technology. A total of 365,919 pairs of reads were obtained, and the number of operational taxonomic units for each sample was between 165 and 285. The alpha diversity of the QA and BA samples was higher, and a total of two phyla, eight classes, 12 orders, 15 families, and 16 genera were detected. At the genus level, significant differences were noted in the dominant genera among the samples, with three genera being shared in all the samples. The dominant genus in QA was *Erythrobasidium*, while that in AQA, HA, and BA was *Sporobolomyces*, and that in WA was *Alternaria*, reaching a proportion of 16.50%. These results showed that the fungal community structure and diversity in QA and BA were high. The endophytes are of great importance to the plants, especially for protection, phytohormone and other phytochemical production, and nutrition. Therefore, this study may be significant with the industrial perspective of *Artemisia* species.

Introduction

Mugwort (*Artemisia argyi*) is found in Europe (Artemisia vulgaris), Africa (Artemisia vulgaris), India (Artemisia vulgaris), Asia (Artemisia argyi), and America (Artemisia douglasiana). Early humans may have transported this plant throughout the world for its medicinal and food value (Adams et al. 2012). Its leaves are rich in essential oils, flavonoids, sugars, and other major components with pharmacological properties, such as bacteriostatic, insect-resistant, anti-inflammatory, antitussive, expectorant, soothing, antiallergic, antioxidant, and antitumor compounds, etc. Jiang et al. 2019a, 2019b). They are widely used in traditional Chinese medicine as well as in pharmaceutical products, animal feed, disinfectants, and other everyday products. With the increasing use of mugwort products, research on the quality and yield of mugwort cultivation to meet the growing global demand has increased.

Recent studies have shown that endophytic fungi, as a natural constituent of the plant micro-ecosystem, live in the tissues of healthy plants without causing any disease symptoms. These fungi have the functions of promoting plant growth, increasing plant disease resistance, inhibiting pathogenic bacteria, and even affecting the yield and quality of plants (Chu et al. 2020). Furthermore, endophytic fungi in plant leaves can not only directly or indirectly affect the synthesis of major therapeutic constituents of medicinal plants (Jiang et al. 2008). However, they can also have a significant influence on the internal microenvironment of roots, stems, and leaves, as well as affect the quality of these plants (Zhang 2017).

In a previous study, Zhang et al. (2011) isolated 19 strains of endophytic Actinomycetes from the leaves of *A. argyi* using plate culture screening method combined with crude extract of fermentation broth. Among these isolates, 11 strains presented extracellular

amylase activity and exhibited protease activity, and eight strains showed cellulase activity. Besides, two strains had antagonistic activity against pathogenic bacteria, and three strains presented antagonistic activity against penicillin-resistant *Staphylococcus aureus*. Furthermore, Shi et al. (2014) isolated and screened ten strains of Actinomycetes from the collective site of *A. argyi* rhizome by combining the primary screening method of confrontation culture with the rescreening method of fermentation broth, and noted that 70% of the isolates presented different degrees of antibacterial activity. Liu et al. (2019) used the plate culture method to isolate 13 strains of endophytic fungi belonging to three genera from the stems and leaves of North *A. argyi* grown in Tangyin, China and detected six species and three genera of endophytic fungi in the leaves. However, all these studies had employed traditional culture techniques, which cannot support the growth of unculturable microorganisms in the stems and leaves of *A. argyi*. To date, studies on the diversity of the endophytic fungal community in *A. argyi* based on high-throughput sequencing have not yet been reported. Therefore, to evaluate the influence of endophytic fungi on the growth and quality of *A. argyi*, the present study employed high-throughput amplicon sequencing technology to compare and analyze the diversity and composition of endophytic fungal community structure in the leaves of *A. argyi* cultivated in different regions in China. Besides, the degree of health and biocontrol application potential of *A. argyi* was also examined. The results obtained can provide a scientific basis and guidance for large-scale cultivation of *A. argyi* and its application for the biocontrol of plant diseases and pests.

Experimental

Materials and Methods

Overview of the test site. The experimental site was located in the *A. argyi* cultivation base of Anyang Institute of Technology in Henan Province, China (N36°0′, E114°35′). The region has a warm, temperate, continental monsoon climate with mild weather conditions and four distinct seasons. The annual average temperature is 14.9°C, the annual sunshine duration is 2,500 h, and the annual average precipitation is 538.4 mm, with 206 days of frost-free period and sandy loam soil.

Sample collection. *A. argyi*, commonly known as Chinese mugwort, is widely distributed in Henan, Hebei, Hubei, Anhui, and Zhejiang in China. Different ecological species have different biological flora. The leaves of 2-year-old *A. argyi* without diseases and pests on its surface were collected in June 2020 at the *A. argyi* cultivation base in Anyang Institute of Techno-

logy. Five kinds of *A. argyi* leaves were collected from Tangy in Beiai in Henan (BA), Qichun Qiai in Hubei (QA), Wanai in Nanyang in Henan (WA), Haiai in Ningbo in Zhejiang (HA), and Anguo Qiai in Anguo in Hebei (AQA). The experimental field was weeded manually without the use of herbicides. Fertilizers were not applied, and two crops were cultivated in a year.

During sampling, the third leaf of *A. argyi* was selected, and 15 samples (three biological replicates per *A. argyi* variety and five *A. argyi* varieties in total) were put into sterile plastic bags with labels (indicating the sample number, name, place, date, and collector), transported to the laboratory, and stored in a −80°C refrigerator for the subsequent isolation of DNA.

Extraction and electrophoresis of endophytic fungi total DNA from *A. argyi* leaves. Firstly, the samples were surface-washed with 70% ethanol solution three times, then washed with $1 \times PBS$ solution three times, dried, and then extracte with liquid nitrogen grinding or tissue disrupter. Then, the endophytic fungi total DNA was extracted with the OMEGA kit, qualitatively detected using agarose gel electrophoresis, quantified by nucleic acid quantitative spectrophotometer (Nanodrop, USA), and stored in a refrigerator at −20°C for the subsequent analysis.

PCR amplification and sequencing of ITS1-ITS2 region of 18S rRNA. The extracted total DNA was used as a template, and the internal transcribed spacer (ITS) region of fungi (ITS1-ITS2 region) was amplified using specific PCR primers (ITS1F: 5'-CTTGGTCATT-TAGAGGAAGTAA-3'; ITS2: 5'-GCTGCGTTCATC-GATGC-3'). The reaction system for PCR comprised the following: Phusion Master Mix (2×), 15 μl; primer (2 μmol/l), 3 μl; DNA (1 ng/μl), 10 μl; and ddH2O, 2 μl. The PCR conditions were as follows: pre-denaturation at 95°C for 3 min, followed by 25 cycles of denaturation at 94°C for 30 s, annealing at 55°C for 30 s, and extension at 72°C for 30 s, and a final extension at 72°C for 7 min. The PCR products were qualitatively detected by electrophoresis using 2% agarose gel in $1 \times TAE$ solution, purified, quantified, and a test library was constructed using Qubit 3.0. Subsequently, the test DNA library was subjected to high-throughput amplicon sequencing performed by Sangon Bioengineering Co., Ltd. (Shanghai) using the Illumina MiSeq sequencing platform (Liao et al. 2020). The raw data of high-throughput amplicon sequencing was uploaded to the NCBI SRA database, and could be downloaded from website (https://www.ncbi.nlm.nih.gov/bioproject/PRJNA714493) and the clean data was obtained by quality control and filtering from the raw data.

Bioinformatics analysis. UPARSE was used for operational taxonomic unit (OTU) classification of the representative sequences at 97% similarity level, and the fungal community composition in each sample was

determined at different classification levels. Mothur software was used to analyze the dilution curves, and Shannon index, Simpson index, species richness index (ACE), and Chao1 index were employed to determine the microbial ecological diversity. The sequences were compared with the functional genes in the NCBI NT database using BLAST. The optimized sequences were identified at the phylum, class order, family, and genus levels according to the reference sequences in the database, and the community composition, abundance, and diversity were compared and analyzed. Ramette's method was used for principal component analysis (PCA), Excel (2007) was utilized to construct a histogram, and SPSS (19.0) software was employed to statistically analyze the class group test data of endophytic fungi in *A. argyi*.

FUNGuild functional analysis. The fungi classification and functional analysis was completed by FUNGuild (Fungi Functional Guild) software. It is a tool for classification and analysis of fungal communities through microecological guild depending on the currently published literature or authoritative website data.

Fig. 1. Venn graph of OTUs distribution in the samples.

Results

Qualitative analysis of endophytic fungi in *A. argyi* leaves. The optimal sequence and information about the genus or species number (OTUs) of the endophytic fungal community in *A. argyi* leaves were obtained using high-throughput amplicon sequencing (Table I). After merging and filtering of double-ended reads, the clean tags for endophytic fungi in WA, AQA, HA, BA, and QA samples were 53,504.0, 69,364.0, 71,661.0, 81,561.0, and 89,829.0, respectively. Species classification based on similarity level ≥97% revealed 709.0 OTUs , and the number of OTUs in WA, AQA, HA, BA, and QA samples was 165.0, 205.0, 230.0, 224.0, and 285.0, respectively (Fig. 1). QA presented the highest sequence number and species classification, which was mostly consistent with the values of alpha-diversity index. The dilution curve for the endophytic fungi in the five samples is shown in Fig. 2. When the sequencing data reached 50,000, the number of OTUs in the
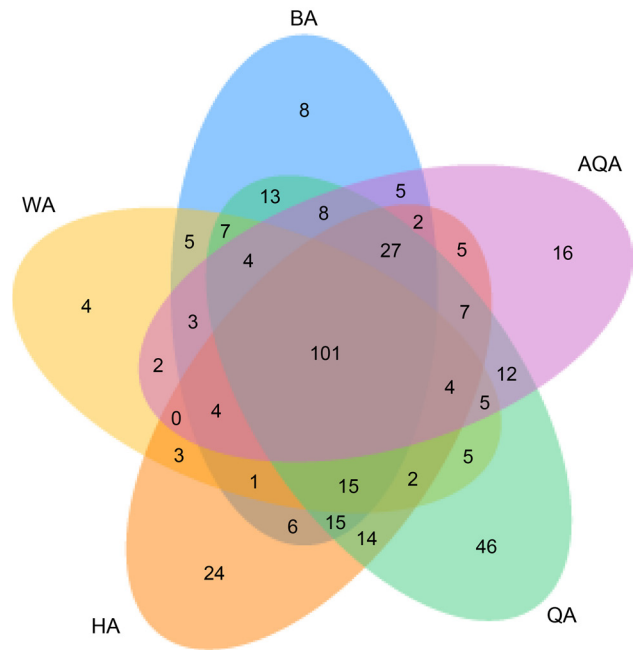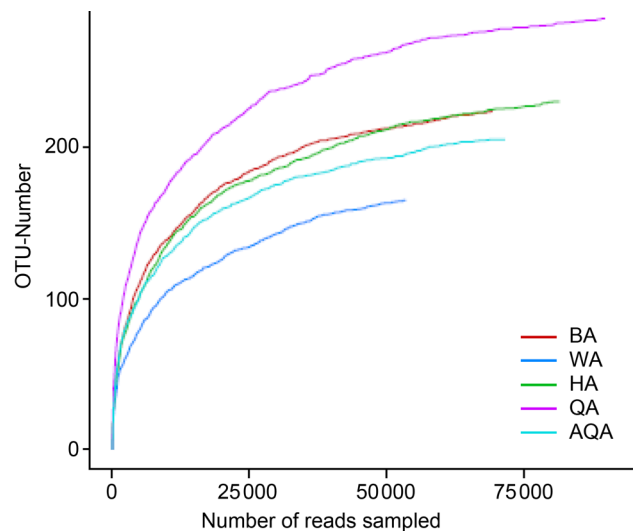

Fig. 2. Rarefaction curve of the samples.

five samples remained flat, indicating that the sequencing depth of the samples was essentially reasonable and that the obtained data could reflect the composition of

Table I
Richness and diversity of endophytic fungi in *A. argyi* leaves.

Treatments	No. of reads	Shannon index	Chao1 index	ACE index	Simpson index
WA	53504.0	2.09±0.01a	180.53±15.03a	193.54±8.34a	0.25±0.000a
AQA	69364.0	2.19±0.01a	223.91±9.32a	226.58±11.53a	0.24±0.000a
HA	71661.0	2.57±0.02a	239.38±10.02a	242.84±10.02a	0.14±0.000a
BA	81561.0	2.62±0.04a	255.54±8.39a	253.33±9.14a	0.08±0.000a
QA	89829.0	2.99±0.03a	291.73±15.12a	297.24±12.02a	0.12±0.001a

Note: Same lowercase letters indicate no significant difference among the samples ($p > 0.05$).

the fungal community structure in the samples under natural conditions more tangibly and comprehensively.

Analysis of endophytic fungal diversity in *A. argyi* leaves. The values of soil microbial alpha-diversity were all > 100% based on the Coverage values (Table I). The microbial community diversity increased with the increasing values of Shannon, Chao1, and ACE indices and decreasing values of Simpson index. The Shannon, Chao1, and ACE indices for the samples exhibited the following trend: WA < AQA < HA < BA < QA, which indicated that the diversity of endophytic fungi in QA was the highest. The Simpson index presented the following trend: BA < QA < HA < AQA < WA, suggesting that BA showed the highest fungal diversity. The alpha-diversity index revealed that the microbial diversity of BA and QA was the highest.

Composition of endophytic fungi in *A. argyi* leaves. High-throughput amplicon sequencing detected two phyla, Ascomycota and Basidiomycota, in the five samples (WA, AQA, HA, BA, and QA) (Fig. 2). In WA, Ascomycota was predominant, accounting for 28.34%, followed by Basidiomycota with a relative abundance of 17.85% (Fig. 3). In AQA, HA, BA, and QA samples, Basidiomycota was dominant with a relative abundance of 33.45%, 41.41%, 40.64%, and 64.72%, respectively (Fig. 3), followed by Ascomycota with a relative abundance of 10.10%, 17.12%, 24.48%, and 16.27%, respectively (Fig. 3). In addition, unclassified fungal group with the relative abundance of 52.83%, 50.98%, 41.33%, 34.40%, and 18.27% was also detected in WA, AQA, HA, BA, and QA, respectively (Fig. 3), accounting for a large proportion of endophytic fungi in *A. argyi* leaves.

Furthermore, differences in the community composition and abundance of endophytic fungi at the class,
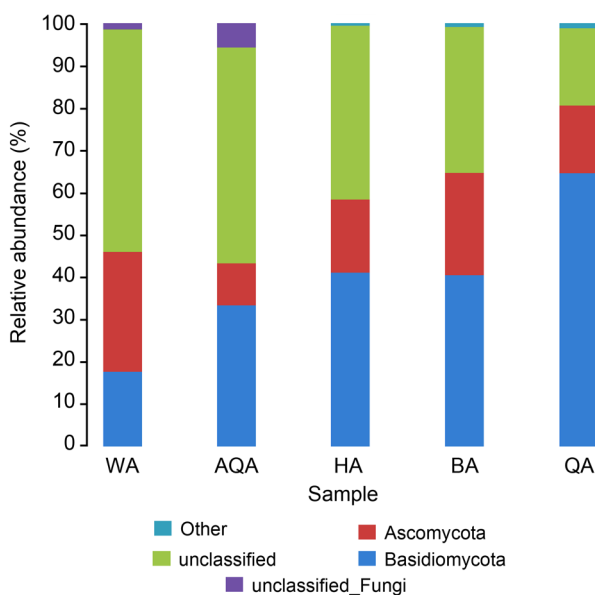
order, family, and genus levels were noted in the five *A. argyi* samples. In WA and BA, Dothideomycetes belonging to Ascomycota was predominant, accounting for 20.96% and 22.33%, respectively, followed by Microbotryomycetes belonging to Basidiomycota, accounting for 8.36% and 17.25%, respectively. In AQA, Microbotryomycetes was dominant (15.52%), followed by Cystobasidiomycetes belonging to Basidiomycota (12.90%). In HA, Cystobasidiomycetes was dominant (19.10%), followed by Microbotryomycetes (15.92%). In QA, Cystobasidiomycetes was predominant (41.96%), followed by Dothideomycetes (12.68%). The dominant order in WA was Pleosporales, accounting for 17.73%, whereas that in AQA, HA, and BA was Sporidiobolales, with the relative abundance of 15.40%, 15.52%, and 15.25%, respectively. In QA, Erythrobasidiales was predominant with a relative abundance of 31.57%. The dominant family in WA was Pleosporaceae, accounting for 16.50%, while that in AQA, HA, and BA was Spordiobolaceae with a relative abundance of 15.39%, 15.52%, and 15.26%, respectively. In QA, Erythrobasidiaceae was predominant, with a relative abundance of 31.57%.

A total of 16 genera, including *Erythrobasidium*, *Sporobolomyces*, *Alternaria*, *Symmetrospora*, *Aureobasidium*, *Cryptococcus*, *Filobasidium*, *Papiliotrema*, *Coniothyrium*, *Dioszegia*, *Kondoa*, *Sphaerulina*, *Leucosporidium*, unclassified_*Phaeosphaeriaceae*, and unclassified_*Ascomycota*, were found in the samples (Fig. 4). Besides, other unclassified fungi were also detected. The common genera detected in all five samples were *Sporobolomyces*, *Erythrobasidium*, and *Alternaria*. While both AQA and QA contained *Cryptococcus*, which was not detected in the other samples, *Sphaerulina*, *Aureobasidium*, *Symmetrospora*, and unclassified_*Ascomycota* were found in WA, HA, and BA. Furthermore, *Papiliotrema* and unclassified_*Phaeosphaeriaceae* were detected in HA, but not in WA. Ten genera, including *Symmetrospora*, *Aureobasidium*, *Filobasidium*, *Papiliotrema*, *Sphaerulina*, unclassified_*Ascomycota*, and three genera found in all the five samples, were common in BA and QA. However, *Leucosporidium* was detected only in BA, whereas *Coniothyrium*, *Dioszegia*, *Kondoa*, *Cryptococcus*, unclassified_*Phaeosphaeriaceae* were found only in QA. According to the sequencing results, the richness of the endophytic fungal community structure in the five samples presented the following trend: QA > BA > HA > WA > AQA.

Analysis of phylogenetic relationship of the endophytic fungi in *A. argyi* leaves. The phylogenetic relationship of the endophytic fungi among the five *A. argyi* leaves samples was investigated based on the heat map of the genetic distance between the samples (Fig. 5). The color block represents the distance value, with the distance between the samples decreasing with the increasing grayness. Three branches can be observed in

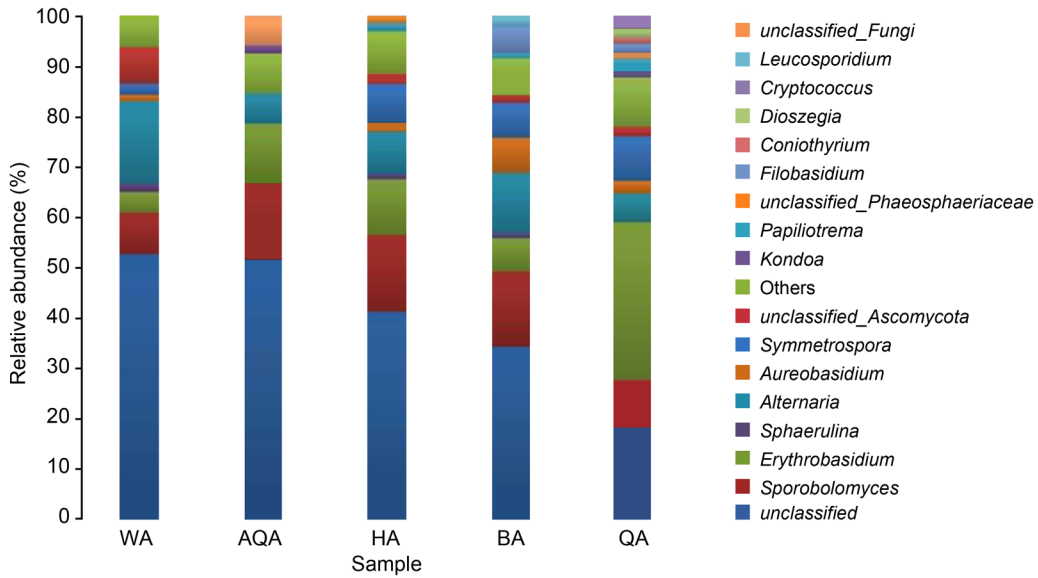Fig. 3. Fungal community composition in the samples at the phylum level.

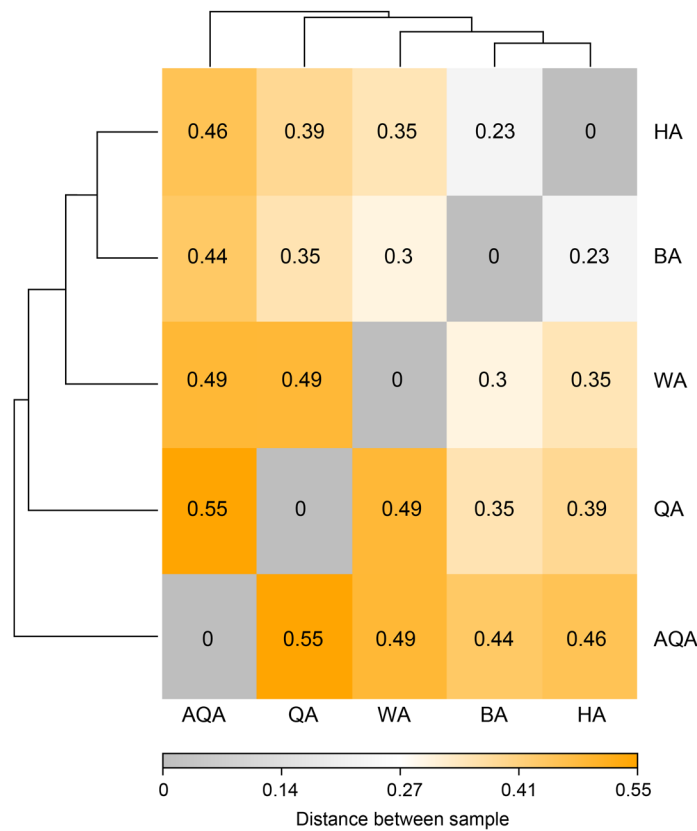Fig. 4. Fungal community composition in the samples at the genus level.

Fig. 5. Heatmap of genetic distance between the samples.

the figure, with HA and BA, which presented a closer genetic relationship, merging into one branch, WA forming another branch, and AQA forming another branch. In addition, QA exhibited a systematic branch, indicating the distant genetic relationship between QA and the other samples.

PCA analysis. PCA can reduce the dimension of data based on linear algebra. The original high-dimen-sional data are transformed and projected into the spatial coordinate system with lower dimensions (i.e., principal components) to show the natural distribu-tion of samples. Each point represents a sample, and the shorter the distance is between the two points, the higher is the similarity in the microbial community structure between the two samples, and the smaller is the difference. The percentages on the axis parentheses
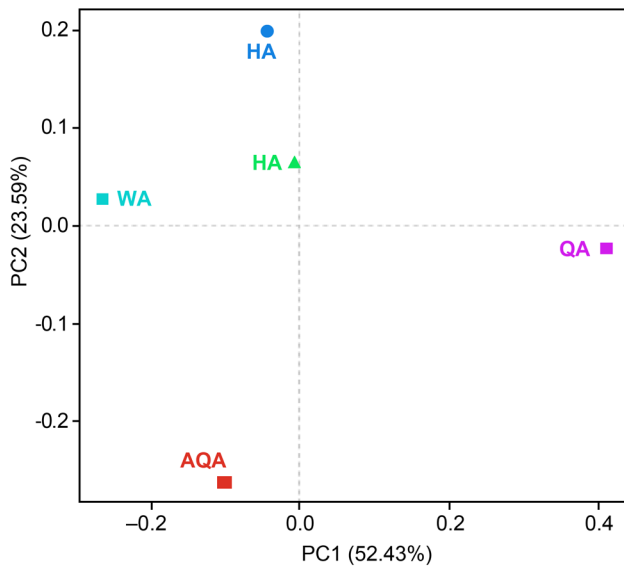
Fig. 6. PCA of the samples.

represent the percentage of variance in the original data that the corresponding principal component can explain. If PCA is 50%, then the variance of the X-axis can explain 50% of the overall analysis results. As shown in Fig. 6, the distance between QA and the other four samples was long, indicating that the similarity in the fungal communities between these samples was very low, whereas the difference was considerable.

Similarly, the distance between AQA and the other four samples was very long, implying that the difference in the fungal communities between the samples was very large. In contrast, the distance between HA and BA was relatively short, followed by that between HA and WA, which suggested that the similarity in the fungal communities between these samples was relatively higher, whereas the difference was more negligible when compared to former ones. Furthermore, the distance between BA and QA and AQA was long, indicating that the similarity in the fungal communities between these samples was low, but the difference was large, and consistent with the results of the heat map analysis. Thus, it can be concluded that the endophytic fungal community structure in the five *A. argyi* leaves samples was significantly different.

Discussion

In this study, 18 S rRNA amplicon sequencing of endophytic fungi in the leaves of *A. argyi* was conducted using a high-throughput sequencing platform based on fungal ITS1-ITS2 sequences. The variation in the sequencing reads was 53,504.0–89,829.0, with QA presenting the highest number of sequencing reads. The variation in the number of OTUs was between 165 and 205, with QA exhibiting the maximum number of OTUs. Furthermore, OTUs analysis showed the presence of common fungal populations, variations in the fungal populations, as well as unique OTUs among the five samples. Moreover, the diversity of the endophytic fungal community in the leaves of *A. argyi* was lower than that of *A. argyi* roots. The alpha-diversity, Shannon, Chao1, and ACE indices showed that the diversity of endophytic fungi in QA leaves was the highest, whereas the Simpson index revealed that the diversity of endophytic fungi in BA leaves was the highest.

Furthermore, QA and BA presented the highest alpha-diversity index. These results revealed that the diversity of the endophytic fungal community in *A. argyi* leaves was low, consistent with the findings of Liu et al. (2019). High-throughput amplicon results detected two phyla, five classes, nine orders, nine families, and nine genera in WA; two phyla, six classes, eight orders, eight families, and eight genera in AQA; two phyla, six classes, 10 orders, 11 families, and 11 genera in HA; two phyla, eight classes, 13 families, and 13 genera in BA; and two phyla, 10 classes, 13 orders, 16 families, and 15 genera in QA, indicating that the diversity of endophytic fungi was the highest in QA, followed by that in BA.

The finding that Basidiomycota was the dominant phylum in BA is not in agreement with that reported by Liu Miao et al. (2019). At the genus level, significant differences were noted with respect to the dominant genus of endophytic fungi among the five samples. The predominant genus of endophytic fungi in WA, AQA, HA, and BA was unclassified, with a relative abundance of 52.83%, 50.98%, 41.33%, and 34.40%, respectively, whereas *Erythrobasidium,* with the relative abundance of 31.35%, was dominant in QA. In contrast, Liu Miao et al. (2019) isolated three genera and six species of endophytic fungi from the leaves of *Artemisia* sp. by using traditional culture, isolation, and molecular identification methods and found that *Alternaria* sp. was the dominant genus. These inconsistent results could be owing to the different sampling times, cultivation climates, and soil types. *Erythrobasidium* has been noted to infect the leaf veins of sugar orange, causing citrus yellow shoot and has been detected in a significantly higher proportion in the diseased plants. In the present study, the abundance of *Erythrobasidium* was the highest in QA, and its ecological function needs to be further investigated.

Analysis of the fungal genera and species detected in the present study showed 33 pathogenic fungi, three symbiotic fungi, 34 saprophytic fungi, eight major plant pathogenic fungi, four biological control fungi, 39 environmental fungi, and 19 other fungi in the leaves of *A. argyi* (Table II). While the overall proportion of the detected beneficial biological control fungi, including

Table II
FUNGuild Functional analysis.

Generic	Type	Generic	Type
Aspergillus_intermedius	biocontrol fungi- saprotroph	*Phanerochaete*	pathotroph
Aspergillus_sydowii	biocontrol fungi-saprotroph	*Phlebia*	pathotroph-saprotroph-symbiotroph
Penicillium_catenatum	biocontrol fungi-saprotroph	*Phoma*	saprotroph-symbiotroph
Penicillium_oxalicum	biocontrol fungi-saprotroph	*Podosphaera*	pathotroph-saprotroph-symbiotroph
Botryosphaeria	pathotroph-saprotroph-symbiotroph	*Ramichloridium*	pathotroph-saprotroph
Botrytis	pathotroph-saprotroph	*Rhodotorula*	saprotroph
Cladosporium	pathotroph-saprotroph-symbiotroph	*Sarocladium*	pathotroph-saprotroph
Clonostachys	pathotroph-saprotroph	*Schizophyllum*	pathotroph-symbiotroph
Curvularia	saprotroph	*Sphaerulina*	saprotroph
Cyphellophora	pathotroph-saprotroph-symbiotroph	*Sporisorium*	saprotroph
Cystobasidium	saprotroph	*Sporobolomyces*	pathotroph-symbiotroph
Diaporthe	pathotroph-saprotroph-symbiotroph	*Stagonospora*	saprotroph
Dothidea	saprotroph	*Stemphylium*	saprotroph
Edenia	pathotroph	*Tilletiopsis*	saprotroph
Entocybe	pathotroph	*Trametes*	pathotroph-saprotroph
Entodesmium	pathotroph	*Tricharina*	pathotroph-saprotroph-symbiotroph
Erythrobasidium	pathotroph	*Trichomeriaceae*	pathotroph
Filobasidium	pathotroph-saprotroph-symbiotroph	*Trichosporon*	pathotroph-saprotroph-symbiotroph
Fusarium	pathotroph-saprotroph	*Verticillium*	pathotroph
Gibellulopsis	pathotroph-saprotroph	*Alternaria*	pathotroph-saprotroph
Herpotrichiellaceae	pathotroph-saprotroph-symbiotroph	*Amphisphaeriaceae*	pathotroph-saprotroph-symbiotroph
Knufia	pathotroph	*Amphobotrys*	pathotroph-saprotroph-symbiotroph
Leptosphaeria	pathotroph	*Anthracocystis*	pathotroph
Limonomyces	saprotroph	*Apiotrichum*	pathotroph
Microdochium	pathotroph-saprotroph-symbiotroph	*Articulospora*	pathotroph
Mycosphaerella	pathotroph-symbiotroph	*Ascochyta*	pathotroph
Myrmecridium	saprotroph	*Aurantiporus*	pathotroph
Myrothecium	symbiotroph	*Aureobasidium*	pathotroph
Neosetophoma	pathotroph-saprotroph-symbiotroph	*unclassified*	other
Occultifur	saprotroph	*unclassified_Ascomycota*	other
Paraconiothyrium	pathotroph-saprotroph	*unclassified_Fungi*	other
Paraphoma	pathotroph-saprotroph	*unclassified_Phaeosphaeriaceae*	other
Phaeosphaeria	pathotroph-saprotroph	Others	other

Penicillium catenatum, Penicillium oxalicum, Aspergillus intermedius, Aspergillus sydowii, was not high, environmental fungi formed a large proportion of the fungal population detected in this study. These environmental fungi could develop the symbiotic association with plants and transform the inorganic materials that plants cannot utilize into organic matter, degrade toxins such as phenol, decompose lignin, provide nutrients to plants, and promote plants' growth and development, and improve the contents of medicinal components in plants. Nevertheless, further studies are needed to determine whether the detected beneficial biocontrol fungi and environmental fungi are directly related to the incidences of *A. argyi* diseases. Besides, research on

the ecological functions of many other fungi detected in the present study, whose effects on plants are still unclear, could be crucial for healthy plant growth and development and the biocontrol of pathogens.

Sporobolomyces usually exist on the surface of leaves and accumulate useful metabolites, such as essential oil, a carotenoid pigment, fungal polysaccharide, and extracellular enzymes, which have wide applications in food and medicine, cosmetics, and breeding industries. Besides, *Sporobolomyces* can also remove chromium in sludge and degrade cellulose and lignin (Wei et al. 2014). *Alternaria*, which is widely distributed in soil and plants, is a biocontrol agent with potential applications (Chu et al. 2020). Some species of this genus

isolated from *Artemisia annua* have been noted to present antitumor and antioxidant effects (Li et al. 2020), while some *Alternaria* spp. could control tobacco red root disease (Wang et al. 2001). Ma et al. (2017) found that the endophytic fungus *Cryptococcus* J22 in the leaves of Nuoli contains high content of total phenols and total flavonoids and ABTS, a strong scavenger of free radicals. Moreover, the total flavonoid contents in the leaves of *A. argyi* cultivated in Hubei Province have been reported to be relatively high, possibly owing to the relatively high proportion of *Cryptococcus* (Dong et al. 2016; Gong et al. 2019). *Filobasidium* is mainly found in the body and surface of plants (Ma et al. 2018; Liu et al. 2019), and could produce a variety of extracellular enzymes, such as α-amylase, which help in disease control and have a broad application prospect in the field of medicine (Wang et al. 2015). Thus, the antitumor, antimicrobial, and antioxidant properties of *A. argyi* might possibly be attributed to the presence of *Sporobolomyces*, *Alternaria*, *Cryptococcus,* and *Filobasidium,* and requires further investigation. Besides, the characteristics and functions of unclassified and other fungi found within the leaves of *A. argyi* should also be studied.

Endophytic fungi live in healthy plant tissues but do not infect or damage the host plants. Strobel et al. (2003, 2004) showed that the growth of endophytic fungi in medicinal plants produced natural medicinal products with therapeutic effects (Wang et al. 2016). In the present study, a minor proportion of the endophytic fungi in the leaves of *A. argyi* was found to have potential antitumor and antioxidant properties, which could have significant application prospects in medicine and health.

The present study is the first to use high-throughput amplicon sequencing to investigate the fungal community structure in the leaves of *A. argyi* grown in five different regions in China. The results showed that QA and BA had rich fungal community structure and diversity, presenting differences, although not significant, in the fungal species and distribution. The PCA results revealed that the phylogenetic relationship of the five *A. argyi* leaves samples was distant. Moreover, the majority of the fungal species were detected in the leaves of *A. argyi*, with few major pathogenic fungi and very few beneficial biocontrol fungi. These results can provide a theoretical basis for accomplishing the healthy growth and quality of perennial root plants.

Conflict of interest

The authors do not report any financial or personal connections with other persons or organizations, which might negatively affect the contents of this publication and/or claim authorship rights to this publication.

Literature

Adams JD, Garcia C, Garg G. Mugwort (*Artemisia vulgaris*, *Artemisia douglasiana*, *Artemisia argyi*) in the treatment of menopause, premenstrual syndrome, dysmenorrhea and attention deficit hyperactivity disorder. Chin Med. 2012;03(03):116–123.
https://doi.org/10.4236/cm.2012.33019

Dong P, Mei Q, Dai W. [Comparison study on contents of total flavonoids and heavy metals and Se in folium *Artemisiae argyi* from different producing areas] (in Chinese). Lishizhen Med Mater Med Res. 2016;27(1):74–76.
https://doi.org/10.3969/j.issn.1008-0805.2016.01.027

Gong M, Lu J, Xiao Y. [Determination of total flavonoids and three main aglycones in folium *Artemisiae argyi* from different origins] (in Chinese). China Pharm. 2019;22(05):966–968.
https://doi.org/10.3969/j.issn.1008-049X.2019.05.049

Jiang S, Qian D, Duan J, Yan H, Yu G. [Research on correlation between plant endophytes and geoherbalism] (in Chinese). Chin Tradit Herb Drugs. 2008;39(08):1268–1272.

Jiang Z, Chang X, Zhang Z, Qu Y, Tian C, Gu L, Zhang S. [Advances in the phytochemistry and pharmacology of *Artemisia argyi*] (in Chinese). Chin J Vet Drug. 2019b;53(02):79–88.
https://doi.org/10.11751/ISSN.1002-1280.2019.02.10

Jiang Z, Zhang J, Qu Y, Zhang S, Chang X, Guo X. [Effect of essential oil from *Artemisia vulgaris* on CYP450 isoforms activity and expression] (in Chinese). China Anim Husb Vet Med. 2019a; (2): 79–88. https://doi.org/10.16431/j.cnki.1671-7236.2019.11.035

Li Z, Zhang Z, Qiu T, Liu Z, Zhang Z, Gao S, Xu L. [Culturable fungi from permafrost of Greater Khingan Mountains and biological activities of their fermented products] (in Chinese). Nat Prod Res Dev. 2020;32(3):453–463.
https://doi.org/10.16333/j.1001-6880.2020.3.015

Liao Y, Huang Y, Zou C,Huang Q, Wang Z. [Analysis of fungi diversity in root zone soil of banana plants] (in Chinese). Guihaia Jan. 2020;40(1): 99–107.
https://doi.org/10.1193/guihaia.gxzw201811032

Liu H, Yao Z, Chong W, Sun Y, Lei Y. [Community structure analysis of yeast attached to flat peach leaves in Xinjiang] (in Chinese). Ecol Sci. 2019;38(4):29–34.
https://doi.org/10.14108/j.cnki.1008-8873.2019.04.005

Liu m, Li W, Liu Y, Zhang S, Wen C, Wang B, Liu M, Ma B. [Isolation, identification and phylogenetic analysis of endophytic fungi from Tangyin *Artemisia argyi*] (in Chinese). J Zhejiang Agric Sci. 2019;60(6):1011–1014.
https://doi.org/10.16178/j.issn.0528-9017.20190650

Luo X, Xu S, Chen L, Wang D, Zhang L, Fei X, Zhao Z. [Isolation and identification of endophytic fungi in roots, stems and leaves of *Dendrobium officinale*] (in Chinese). Chin J Inf Tradit Chin Med. 2020;27(3):57–60.
https://doi.org/10.3969/j.issn.1005-5304.201810125

Ma W, Wu Y, Hu Z, Zhang J, Yu J. [Antioxidant activity of secondary metabolites from the endophytic fungus isolated and identified from Noni (*Morinda Citrifolia* Linn.)] (in Chinese). J Trop Biol. 2017;8(4):424–430.
https://doi.org/10.15886/j.cnki.rdswxb.2017.04.09

Max, Sun S, Li Y, Sun Y, Lei Y. [Diversity analysis of the epiphytic yeasts in the flowers of *Rosa chinensis* Jacq. from Shihezi, Xinjiang. Guangdong] (in Chinese). Guangdong Agric Sci. 2018; 45(8):43–49.
https://doi.org/10.16768/j.issn.1004-874X.2018.08.007

Shi X, Su J, Hao B, Guo Q, Han J. [Isolation and screening antifungal activity of endophytic actinomycetes from *Artemisia argyi*] (in Chinese). J Yunnan Agric Univ. 2014.
https://doi.org/10.3969/j.issn.1004-390X(n).2014.04.007

Strobel G, Daisy B, Castillo U, Harper J. Natural products from endophytic microorganisms. J Nat Prod. 2004 Feb;67(2):257–268. https://doi.org/10.1021/np030397v

Strobel G, Daisy B. Bioprospecting for microbial endophytes and their natural products. Microbiol Mol Biol Rev. 2003 Dec;67(4):491–502. https://doi.org/10.1128/MMBR.67.4.491-502.2003

Wang H, Zhang T, Zhang M. [Advances on taxonomic studies of the genus Alternaria] (in Chinese). J Shandong Agric Univ (Nat Sci Ed). 2001;32(3):406–410. https://doi.org/10.3969/j.issn.1000-2324.2001.03.033

Wang J, Cui L, Lan L, Jiang L. Diversity of culturable extracellular proteases producing marine fungi isolated from the intertidal zone of Naozhou Island in South China Sea. Microbiology. 2015; 042(002): 238–253. https://doi.org/10.13344/j.microbiol.china.140900

Wang L, Jiao J, Chen L, Zhang Y, Li J, He B. [Isolation of endophytic fungi from *Ligustrum vicaryi* and screening of their anti-bacterial activity] (in Chinese). J Kunming Med Univ. 2016; 37(3): 18–21. https://doi.org/10.3969/j.issn.1003-4706.2016.03.005

Wei N, Xu Q, Zhang N, Li B. [Ballistosporous yeasts: a review on systematics, cell differentiation, and their applications] (in Chinese). Microbiol China. 2014;41(6):1211–1218. https://doi.org/10.13344/j.microbiol.china.130492

Zhang B, Ma Y, Guo H, Zhu H, Li W. [Absolute configuration determination of two drimane sesquiterpenoids from the endophytic fungi *Talaromyces purpureogenus* of *Panax notoginseng*] (in Chinese). Chem J Chin Univ. 2017;38(6):1046–1051. https://doi.org/10.7503/cjcu20170006

Zhang X, Zhang L, Li J. [Isolation, phylogenetic analysis and relative characteristics of endophytic actinomycete isolated from *Artemisiae argyi*] (in Chinese). J Agric Univ Hebei. 2011; 34(6): 60–64. https://doi.org/10.3969/j.issn.1000-1573.2011.06.012

Occurrence of Beta-Lactamases in Colistin-Resistant Enterobacterales Strains in Poland – a Pilot Study

ELŻBIETA M. STEFANIUK[1], ALEKSANDRA KOZIŃSKA[2], IZABELA WAŚKO[2],
ANNA BARANIAK[3], STEFAN TYSKI[1, 4]*

[1] Department of Antibiotics and Microbiology, National Medicines Institute, Warsaw, Poland
[2] Department of Medicines Biotechnology and Bioinformatics, National Medicines Institute, Warsaw, Poland
[3] Department of Molecular Microbiology, National Medicines Institute, Warsaw, Poland
[4] Department of Pharmaceutical Microbiology, Medical University of Warsaw, Warsaw, Poland

Abstract

Sixty-five colistin-resistant Enterobacterales isolates recovered from different clinical specimens were analyzed. The strains were collected in 12 hospitals all over Poland within a period of nine months. Strains were analyzed for eight genes from the *mcr* family. The presence of *mcr*-1 gene was detected in three *Escherichia coli* strains. The 45/65 isolates were identified as ESBL producers. CTX-M-1-like enzymes were the most common ESBLs (n = 40). One *E. coli* and seven *Klebsiella pneumoniae* strains produced carbapenemases, with the NDM being produced by five isolates. Among all the strains tested, four and five were resistant to new drugs meropenem/vaborbactam and ceftazidime/avibactam, respectively.

K e y w o r d s: Enterobacterales, colistin-resistance, ESBLs, carbapenemases

The number of bacterial isolates extremely resistant to previously effective drugs is growing dynamically. Infections are increasingly being caused by pathogens that are not susceptible to all available antibiotics. This issue is particularly acute for Gram-negative bacilli, both the Enterobacterales strains and non-fermenting rods. Colistin is used as one of the last available treatment options for patients with severe infections caused by carbapenem-resistant Gram-negative rods. Due to the increasing role of colistin in the treatment of human infections caused by multidrug-resistant (MDR) bacteria, the resistance to this antibiotic ought to be monitored (Prim et al. 2017; Petrosillo et al. 2019; Stefaniuk and Tyski 2019).

Until recently, colistin resistance was thought to be dependent only on mutations in the genes regulating LPS synthesis. In 2015, the plasmid-coded colistin resistance associated with the presence of *mcr* genes was first described (Liu et al. 2016). Since then, there have been many reports about plasmid resistance to colistin among strains isolated from human infections (Kluytmans 2017; Elbediwi et al. 2019). In Poland, the first *Escherichia coli* strain with the *mcr*-1 gene was described in 2016 (Izdebski et al. 2016). However, we do not have more information about the presence of *mcr* genes in Poland. As β-lactam antibiotics are "first-line" drugs in the treatment of infections caused by Enterobacterales, the susceptibility of strains to this group of antimicrobial agents was tested; the most important resistance mechanism to this group of drugs is the production of β-lactamases. This study aimed to determine the occurrence of β-lactamases, including carbapenemases, in colistin-resistant Enterobacterales strains in Poland. Such strains are extremely dangerous because of treatment difficulties. Recently, new β-lactam/β-lactamase inhibitor combinations have been introduced into therapy, especially for ESBLs and carbapenemase-producing strains. We have also tested all collected strains against these new drugs as a possible alternative treatment.

The twelve hospitals located all over Poland, in the following voivodeships: Lesser Poland (n = 2), Lublin

---

(n = 1), Masovian (n = 2), Pomeranian (n = 1), Silesian (n = 2), Warmia-Masurian (n = 2), and West Pomeranian (n = 2), involved in this study were of similar sizes and had similar profiles, as regional, secondary-care medical centers, with all major types of wards. A total of 65 non-duplicate clinical isolates of Enterobacterales were recovered from inpatients with various infections between April 2019 and December 2019 and were included in this study. The strains were of the following species: *Klebsiella pneumoniae* (n = 45; 69.2%), *E. coli* (n = 15; 23.1%), *Enterobacter cloacae* (n = 3; 4.0%), and *Klebsiella oxytoca* (n = 2; 3.1%). All bacterial strains were identified to the species level in local hospital laboratories, and their susceptibility to antibiotics was determined using available methods. The strains were sent to the Department of Microbiology and Antibiotics of the National Medicines Institute (NMI) in Warsaw, Poland, together with basic clinical information (the date of isolation, the species, the specimen type, the patient's age and sex, and the hospitalization ward). The detailed analysis of patient's demographic data and local antibiotics susceptibility data was performed in the NMI. The strains used in the study were stored at −80°C. Before the investigation, strains were transferred onto the non-selective blood-containing agar (BAP; Columbia Agar with 5% Sheep Blood; Becton Dickinson, USA). All strains were re-identified by using ID GN cards in VITEK 2 Compact (bioMérieux, Marcy l'Etoile, France).

Based on the information provided by the laboratories, the results of antibiotic susceptibility of the studied bacterial strains were pre-analyzed. In the NMI, the colistin MIC value (mg/l) was determined by a reference broth microdilution method according to ISO 20776 (ISO 2019). Susceptibility to colistin was performed in triplicate for each strain, using the same culture to establish a pool of strains with MIC > 2 mg/l of colistin. E-tests with concentration gradients of ceftazidime, ceftazidime/avibactam, imipenem, meropenem, and meropenem/vaborbactam (MIC Strep; Liofilchem, Italy) were used for determination of their MICs (mg/l) in colistin-resistant Enterobacterales strains. Susceptibility results were interpreted according to the guidelines of the EUCAST (EUCAST 2020a). The following strains: *E. coli* ATCC 25922, *E. coli* ATCC 35218, *E. coli* NCTC 13846 (*mcr*-1), and *K. pneumoniae* ATCC 700603 were used as controls (EUCAST 2020b).

All Enterobacterales isolates were tested for ESBLs and carbapenemases production by phenotypic and genotypic methods. ESBLs were detected by the double-disk synergy (DDS) test with disks containing amoxicillin with clavulanate (20 µg and 10 µg, respectively), cefotaxime (30 µg), and ceftazidime (30 µg) (EUCAST 2017). The detection of carbapenemases were assessed by the disk test with phenylboronic acid for KPCs,

the synergy test with EDTA for MBLs, and disc with temocillin for OXA-48-like carbapenemases (Żabicka et al. 2015).

Total bacterial DNA was purified with a Genomic DNA Prep Plus kit (A&A Biotechnology, Gdańsk, Poland).

The $bla_{CTX-M-1}$-, $bla_{CTX-M-2}$-, $bla_{CTX-M-8}$- $bla_{CTX-M-9}$-, $bla_{CTX-M-25}$-, bla_{SHV}-, bla_{TEM}- bla_{KPC}-, bla_{NDM}-, bla_{IMP}-, bla_{VIM}-, $bla_{OXA48-like}$ genes were identified by PCR as described previously (Woodford et al. 2006; Empel et al. 2008).

All isolates were screened by PCR for the presence of plasmid-mediated *mcr* genes, including *mcr*-1 (Liu et al. 2016), *mcr*-2 (Xavier et al. 2016), *mcr*-3 (Yin et al. 2017), *mcr*-4 (Rebelo et al. 2018), *mcr*-5 (Borowiak et al. 2017), *mcr*-7 (Wang et al. 2018), *mcr*-8 (Yuan et al. 2019) and *mcr*-9 (Carroll et al. 2019), as previously described.

The isolates came from patients of various ages from 1 to 89 years; the most numerous group comprised of patients aged 61–80 (n = 32; 49.2%) and 31–60 years of age (n = 16; 24.6%). The remaining patients were 16–30 years of age (n = 4), ≥ 81 years of age (n = 11), and < 3.1 years (n = 2). The most frequently represented hospital wards were: Intensive Care Unit (n = 20, 30.8%), internal medicine (n = 14, 21.5%), pulmonary (n = 12; 18.5%), and burn wards (n = 8; 12.3%). The remaining patients were hospitalized in the following order: surgery (n = 3), rehabilitation (n = 3), urology (n = 1), and oncology (n = 1). Three patients from whom the tested strains were isolated were patients of the surgical outpatient clinics (n = 2) and one resident of the Long Term Care Facility with documented hospital history.

Just over 40% of all patients' clinical specimens (n = 28; 43.1%) for microbiological testing came from the lower respiratory tract, including: bronchial lavage (n = 16; 24.6%), and sputum (n = 11; 16%), pleural fluid (n = 1), specimens from skin and soft tissue infections (n = 8, 12.3%), and urine (n = 13, 20%). Only 16.9% (n = 11) of the Enterobacterales isolates tested were collected from blood; single isolates came from peritoneal fluid (n = 1), bile (n = 1), and rectal swabs (n = 3). *K. pneumoniae* was the dominant organism in lower respiratory tract infections, followed by *E. coli*. *K. pneumoniae* caused nearly half of the cases of urinary tract infections (UTIs). In seven cases, *K. pneumoniae* (10.8%) was the pathogen isolated from blood.

Resistance to colistin was demonstrated in all 65 isolates. The MIC values of colistin in resistant strains ranged from 4 mg/l to > 64 mg/l. For PCR, positive results were achieved only with primers specific to the *mcr*-1 gene variant in three *E. coli* strains. One was simultaneously resistant to imipenem (MIC = 12 mg/l) and intermediate to meropenem (MIC = 4 mg/l). It was also resistant to ceftazidime/avibactam with an MIC of 32 mg/l, but sensitive to meropenem/avibactam

Table I
Susceptibility of colistin-resistant Enterobacterales strains (n = 65) to ceftazidime, ceftazidime/avibactam, imipenem, meropenem, and meropenem/vaborbactam.

Strains (n; %)	Colistin MIC (mg/l) Value	Colistin	mcr-1	CAZ S	CAZ R	CAZ/AVB S	CAZ/AVB R	IPM S	IPM I	IPM R	MEM S	MEM I	MEM R	MEM/VB S	MEM/VB R
		Number of isolates													
K. pneumoniae (n = 45; 69.2%)	4	11	0	0	11	9	2	9	0	2	9	1	1	10	1
	8	4	0	4	0	4	0	4	0	0	4	0	0	4	0
	16	2	0	0	2	1	0	2	0	0	2	0	0	2	0
	32	1	0	1	0	1	1	1	0	0	1	0	0	1	0
	64	1	0	1	0	1	0	1	0	0	1	0	0	1	0
	> 64	26	0	14	12	24	2	19	1	6	19	2	5	23	3
E. coli (n = 15; 23.1%)	4	4	0	2	2	4	0	4	0	0	4	0	0	4	0
	8	5	0	3	2	5	0	5	0	0	5	0	0	5	0
	16	3	1	0	3	3	0	3	0	0	3	0	0	3	0
	32	1	1	0	1	0	1	0	0	1	0	1	0	1	0
	64	1	1	0	1	1	0	1	0	0	1	0	0	1	0
	> 64	1	0	0	1	1	0	0	1	0	0	1	0	1	0
E. cloacae complex (n = 3; 4.6%)	4	0	0	0	0	0	0	0	0	0	0	0	0	0	0
	8	1	0	0	1	1	0	1	0	0	1	0	0	1	0
	16	0	0	0	0	0	0	0	0	0	0	0	0	0	0
	32	0	0	0	0	0	0	0	0	0	0	0	0	0	0
	64	0	0	0	0	0	0	0	0	0	0	0	0	0	0
	> 64	2	0	1	1	2	0	0	1	1	1	1	1	2	0
K. oxytoca (n = 2; 3.1%)	4	0	0	0	0	0	0	0	0	0	0	0	0	0	0
	8	0	0	0	0	0	0	0	0	0	0	0	0	0	0
	16	1	0	1	0	1	0	1	0	0	1	0	0	1	0
	32	0	0	0	0	0	0	0	0	0	0	0	0	0	0
	64	0	0	0	0	0	0	0	0	0	0	0	0	0	0
	> 64	1	0	1	0	1	0	1	0	0	1	0	0	1	0
Total		65	3	28	37	59	6	52	3	10	53	5	7	61	4

CAZ – ceftazidime, CAZ/AVB – ceftazidime/avibactam, IPM – imipenem, MEM – meropenem, MEM/VB – meropenem/vaborbactam, S – sensitive, I – intermediate, R –resistant

(MIC = 2 mg/l). Twelve isolates from all 65 strains showed elevated MIC values of imipenem and/or meropenem from 2 mg/l to ≥ 256 mg/l: *E. coli* (n = 2), *E. cloacae* (n = 1), and *K. pneumoniae* (n = 9). Four of these strains were resistant to meropenem/vaborbactam, and five to ceftazidime/avibactam. Detailed results of susceptibility testing are presented in Table I.

In Kazmierczak and co-researcher's study (2018) the most common ESBL genes in Polish isolates was CTX-M-15 (80% of 185 ESBL-positive isolates). Authors also observed high percentages of MDR Polish strains (21%); 29.2% of them were ceftazidime-resistant and 0.8% meropenem non-susceptible, but only one isolate produced carbapenemase and it belonged to carbapenemase subtype VIM-1. A higher percentage of Enterobacterales strains resistant to ceftazidime (56.9%) and non-susceptible to meropenem (16.9%) was observed in our study.

Forty-five of the colistin-resistant isolates (69.2%) were identified as ESBL producers by the DDS test. The ESBL-positive strains belonged to three species including *E. cloacae* complex (n = 2, 4.4%), *E. coli* (n = 6, 13.3%), and *K. pneumoniae* (n = 37, 82.2%). Thirty-eight ESBL-positive isolates (84.4%) carried only one β-lactamase gene. The remaining seven strains possessed 2–4 *bla* genes. Forty-one ESBL-positive isolates (91.1% from 45 isolates) carried $bla_{\text{CTX-M-1-like}}$ genes; the most frequent organism was *K. pneumoniae* (n = 34), from which 64.7% of isolates demonstrated a colistin MIC > 64 mg/l. The $bla_{\text{CTX-M-9-like}}$ genes were detected only in two *K. pneumoniae*. Five isolates carried $bla_{\text{SHV-like}}$, and 10 carried $bla_{\text{TEM-like}}$ genes.

One *E. coli* and seven *K. pneumoniae* colistin-resistant isolates produced carbapenemases. Carbapenemase-encoding genes were detected as follows: bla_{KPC} in one *K. pneumoniae*, bla_{NDM} in five *K. pneumoniae*,

Table II
Presence of selected ESBLs and carbapenemases among colistin-resistant Enterobacterales strains (n = 65*).

Strains (n; %)	Colistin				Types of ESBLs			Types of carbapenemases		
	MIC (mg/l)		mcr-1	CTX-M-1	CTX-M-9	TEM	SHV	KPC	NDM	OXA-48
	Value	Number of isolates								
K. pneumoniae (n = 45; 69.2%)	4	11	0	6	1	2	0	0	2	0
	8	4	0	4	0	0	0	0	0	0
	16	2	0	0	0	1	0	0	0	0
	32	1	0	1	0	0	0	0	0	0
	64	1	0	1	0	0	0	0	0	0
	>64	26	0	22	1	3	4	1	3	1
E. coli (n = 15; 23.1%)	4	4	0	1	0	1	0	0	0	0
	8	5	0	3	0	0	0	0	0	0
	16	3	1	1	0	1	1	0	0	1
	64	1	1	0	0	1	0	0	0	0
E. cloacae complex (n = 3; 4.6%)	8	1	0	1	0	0	0	0	0	0
	>64	2	0	1	0	1	0	0	0	0
Total		61	3	41	2	10	5	1	5	2

* – in two *E. coli* and two *K. oxytoca* strains (3.1%) resistant to colistin, the β-lactamases were not detected

and $bla_{OXA-48-like}$ in one *E. coli* (the carbapenem-resistant isolate with *mcr*-1 gene) and one *K. pneumoniae.* Five strains carrying *bla* genes and producing carbapenemases showed MIC > 64 mg/l of colistin, which indicated their clinical significance.

The results of the detection of selected β-lactamases are shown in Table II.

The growing resistance of bacteria to antibiotics is a challenge for 21st-century medicine. Carbapenems were considered so-called "last resort" agents in the treatment of serious infections, especially in hospitalized patients. The spread of carbapenem-resistant Gram-negative rods isolated from outpatients turned out to be a challenge for treating infections (Grundmann et al. 2010; Parisi et al. 2015). The expansion of strains producing carbapenemases has been observed for several years worldwide, including in Poland (Baraniak et al. 2016). Numerous reports have indicated the disturbing phenomenon of large-scale spreading of Enterobacterales strains producing New Delhi metallo-β-carbapenemase, and to a lesser extent producing *Klebsiella pneumoniae* carbapenemase, or OXA-48-carbapenemases and VIM-carbapenemases. Most of the carbapenemases producing strains are multi-drug-resistant (MDR) strains, which significantly limit the therapeutic possibilities of life-threatening infections. Due to the frequent lack of therapeutic options for carbapenem-resistant strains infections, colistin is considered one of the few or sometimes only therapeutic options (Li et al. 2006; Nation and Li 2009; Lim et al. 2010; Sandri et al. 2013; Vicari et al. 2013). The coexistence of colistin resistance along with the production of carbapenemases in multi-drug resistant isolates poses a real threat in the use of carbapenems and colistin to fight infections (Lomonaco et al. 2018; Lee et al. 2019).

Colistin is characterized by high activity against Gram-negative rods, despite numerous reports of increasing bacterial resistance to this drug (Petrosillo et al. 2019), most of which are chromosomally coded. The spread of plasmid-encoded resistance to colistin, related to the presence of *mcr* genes, is alarming, especially since it concerns to a large extent strains with "a low level of resistance to colistin" (with a colistin minimum inhibitory concentration (MIC) range of 2–8 mg/l). The repeatedly described diagnostic problems encountered in determining the MIC values of colistin are largely responsible for the lack of knowledge about the presence of such isolates (Stefaniuk and Tyski 2019). However, numerous reports indicate the universality of such strains (Bardet and Rolain 2018; Jayol et al. 2018), including in Poland, where for the first time *E. coli* strain was identified as possessing the *mcr*-1 gene in 2016 (Izdebski et al. 2016). In Poland, little is known about the scale of the resistance of Gram-negative rods to colistin. Thus, an attempt was made to assess the degree of resistance to other antimicrobial agents of colistin-resistant strains isolated from serious life-threatening infections in patients treated in hospitals throughout Poland.

The project achieved the collection of colistin-resistant Enterobacterales rods over three quarters of 2019. Within the total number of collected strains, isolates with the *mcr*-1 gene constituted only 4.2%. Prim and co-researchers (2017) showed that the *mcr*-1 gene in clinical isolates is still rare in Europe. Our study may indicate that the colistin resistance of Polish Enterobacterales isolates is mainly chromosomally encoded.

Further research is required to confirm this assumption. It is noteworthy that the colistin-resistant *Klebsiella* strains constitute as much as 47/65 (69.2%) of isolates studied in this project, while *E. coli* represented only 15/65 (23.1%). In our study the *mcr*-1 genes were detected only in three *E. coli* strains; two of these strains produced ESBL and were susceptible to the new drugs meropenem/vaborbactam and ceftazidime/avibactam, while the third was resistant to carbapenems (produced OXA-48-like carbapenemase) and resistant to ceftazidime with avibactam. Kazmierczak and co-researchers (2018) showed the activity of ceftazidime/avibactam and other agents against Enterobacteriaceae collected in 18 European countries from 2012 to 2015. The tested isolates also came from Poland; colistin-resistant Enterobacterales isolates accounted for 1.8% of all Polish isolates (Kazmierczak et al. 2018). Ceftazidime/avibactam was the most active agent from all tested antimicrobial agents. From all colistin-resistant isolates in this study, 98.2% were susceptible to ceftazidime with avibactam.

Globally, the *mcr*-gene family is widely disseminated among Enterobacterales, mainly in *E. coli* and *K. pneumoniae* isolated from human infections (Jeannot et al. 2017). Our study suggests that *mcr*-1 is currently more common in *E. coli* strains than in *K. pneumoniae* in Poland. Some authors also report that the MICs of colistin for *E. coli* carrying the *mcr*-1 gene are lower than the MICs of colistin for *K. pneumoniae* (MICs 4–16 mg/l vs. 4–64 mg/l) (Walkty et al. 2016). In our study, MICs of colistin for *E. coli* with the *mcr*-1 gene were higher than indicated by Walkty et al. (2016), ranging from 16 to > 64 mg/l.

This is the first report on the occurrence of β-lactamases in colistin-resistant Enterobacterales strains in Poland. These data broaden the knowledge of the mechanism of resistance to colistin among Enterobacterales causing human infections in Poland. Demographic data of patients, from whom the strains resistant to colistin were isolated, indicate that the problem of this resistance cannot be limited to a selected group of patients. The small number of colistin-resistant isolates (n = 65) obtained from hospitals that participated in the pilot study may indicate that the problem of colistin resistance among Enterobacterales strains is low. However, due to the described issues of the infection therapy, this problem requires further research and analysis. In the future, the authors plan to compare the antibiotics susceptibility of Enterobacterales isolates resistant to colistin and other multidrug-resistant Enterobacterales species susceptible to colistin.

ORCID

Stefan Tyski https://orcid.org/0000-0003-3352-038X
Elżbieta M. Stefaniuk https://orcid.org/0000-0002-8169-6964
Aleksandra Kozińska https://orcid.org/0000-0001-6949-4860
Izabela Waśko https://orcid.org/0000-0001-5494-3635
Anna Baraniak https://orcid.org/0000-0001-9996-8553

Conflict of interest

The authors do not report any financial or personal connections with other persons or organizations, which might negatively affect the contents of this publication and/or claim authorship rights to this publication.

Literature

Baraniak A, Izdebski R, Fiett J, Gawryszewska I, Bojarska K, Herda M, Literacka E, Żabicka D, Tomczak H, Pewińska N, et al. NDM-producing Enterobacteriaceae in Poland, 2012-14: interregional outbreak of *Klebsiella pneumoniae* ST11 and sporadic cases. J Antimicrob Chemother. 2016 Jan;71(1):85–91.
https://doi.org/10.1093/jac/dkv282

Bardet L, Rolain JM. Development of new tools to detect colistin-resistance among *Enterobacteriaceae* strains. Can J Infect Dis Med Microbiol. 2018 Dec 5;2018:3095249.
https://doi.org/10.1155/2018/3095249

Borowiak M, Fischer J, Hammerl JA, Hendriksen RS, Szabo I, Malorny B. Identification of a novel transposon-associated phosphoethanolamine transferase gene, *mcr-5*, conferring colistin in d-tartrate fermenting *Salmonella enterica* subsp. *enterica* serovar Paratyphi B. J Antimicrob Chemother. 2017 Dec 1;72(12):3317–3324.
https://doi.org/10.1093/jac/dkx327

Carroll LM, Gaballa A, Guldimann C, Sullivan G, Henderson LO, Wiedmann M. 2019. Identification of novel mobilized colistin resistance gene *mcr-9* in a multidrug-resistant, colistin-susceptible *Salmonella enterica* serotype Typhimurium isolate. mBio. 2019 May 7;10(3):e00853-19. https://doi.org/10.1128/mBio.00853-19

Elbediwi M, Li Y, Paudyal N, Pan H, Li X, Xie S, Rajkovic A, Feng Y, Fang W, Rankin SC, et al. Global burden of colistin-resistant bacteria: Mobilized Colistin Resistance Genes Study (1980–2018) Microorganisms. 2019 Oct 16;7(10):461.
https://doi.org/10.3390/microorganisms7100461

Empel J, Baraniak A, Literacka E, Mrówka A, Fiett J, Sadowy E, Hryniewicz W, Gniadkowski M; Beta-PL Study Group. Molecular survey of beta-lactamases conferring resistance to newer beta-lactams in *Enterobacteriaceae* isolates from Polish hospitals. Antimicrob Agents Chemother. 2008 Jul;52(7):2449–2454.
https://doi.org/10.1128/AAC.00043-08

EUCAST. EUCAST guideline for the detection of resistance mechanisms and specific resistances of clinical and/or epidemiological importance. Version 2.0. Basel (Switzerland): The European Committee on Antimicrobial Susceptibility Testing; 2017 [cited 2021 Jan 29]. Available from https://www.eucast.org/resistance_mechanisms/

EUCAST. The European Committee on Antimicrobial Susceptibility Testing. Breakpoint tables for interpretation of MICs and zone diameters. Version 10.0. Basel (Switzerland): The European Committee on Antimicrobial Susceptibility Testing; 2020a.

EUCAST. The European Committee on Antimicrobial Susceptibility Testing. Routine and extended internal quality control for MIC determination and disk diffusion as recommended by EUCAST. Version 10.0. Basel (Switzerland): The European Committee on Antimicrobial Susceptibility Testing; 2020b.

Grundmann H, Livermore DM, Giske CG, Canton R, Rossolini GM, Campos J, Vatopoulos A, Gniadkowski M, Toth A, Pfeifer Y, et al; CNSE Working Group. Carbapenem-non-susceptible *Enterobacteriaceae* in Europe: conclusions from a meeting of national experts. Euro Surveill. 2010 Nov 18;15(46):19711. https://doi.org/10.2807/ese.15.46.19711-en

ISO. ISO 20776-1:2019(en) Susceptibility testing of infectious agents and evaluation of performance of antimicrobial susceptibility test devices – Part 1: Broth micro-dilution reference method for testing the in vitro activity of antimicrobial agents against rapidly growing aerobic bacteria involved in infectious diseases. Geneva (Switzerland): International Organization for Standardization; 2019.

Izdebski R, Baraniak A, Bojarska K, Urbanowicz P, Fiett J, Pomorska-Wesołowska M, Hryniewicz W, Gniadkowski M, Żabicka D. Mobile *mcr*-1-associated resistance to colistin in Poland. J Antimicrob Chemother. 2016 Aug;71(8):2331–2333. https://doi.org/10.1093/jac/dkw261

Jayol A, Nordmann P, Lehours P, Poirel L, Dubois V. Comparison of methods for detection of plasmid-mediated and chromosomally encoded colistin resistance in *Enterobacteriaceae*. Clin Microbiol Infect. 2018 Feb;24(2):175–179. https://doi.org/10.1016/j.cmi.2017.06.002

Jeannot K, Bolard A, Plesiat P. Resistance to polymyxins in Gram-negative organisms. Int J Antimicrob Agents. 2017 May;49(5):526–535. https://doi.org/10.1016/j.ijantimicag.2016.11.029

Kazmierczak KM, de Jonge BLM, Stone GG, Sahm DF. *In vitro* activity of ceftazidime/avibactam against isolates of *Enterobacteriaceae* collected in European countries: INFORM global surveillance 2012–15. J Antimicrob Chemother. 2018 Oct 1;73(10):2782–2788. https://doi.org/10.1093/jac/dky266

Kluytmans J. Plasmid-encoded colistin resistance: *mcr*-one, two, three and counting. Euro Surveill. 2017 Aug 3;22(31):30588. https://doi.org/10.2807/1560-7917.ES.2017.22.31.30588

Lee YL, Lu MC, Shao PL, Lu PL, Chen YH, Cheng SH, Ko WC, Lin CY, Wu TS, Yen MY, et al. Nationwide surveillance of antimicrobial resistance among clinically important Gram-negative bacteria, with an emphasis on carbapenems and colistin: Results from the Surveillance of Multicenter Antimicrobial Resistance in Taiwan (SMART) in 2018. Int J Antimicrob Agents. 2019 Sep;54(3):318–328. https://doi.org/10.1016/j.ijantimicag.2019.06.009

Li J, Nation RL, Tumidge JD, Milne RW, Coulthard K, Rayner CR, Paterson DL. Colistin: the re-emerging antibiotic for multidrug-resistant Gram-negative bacterial infections. Lancet Infect Dis. 2006 Sep;6(9):589–601. https://doi.org/10.1016/S1473-3099(06)70580-1

Lim LM, Ly N, Anderson D, Yang JC, Macander L, Jarkowski A, Forrest A, Bulitta JB, Tsuji BT. Resurgence of colistin: a review of resistance, toxicity, pharmacodynamics, and dosing. Pharmacother J Human Pharmacol Drug Ther. 2010 Dec;30(12):1279–1291. https://doi.org/10.1592/phco.30.12.1279

Liu YY, Wang Y, Walsh TR, Yi LX, Zhang R, Spencer J, Doi Y, Tian G, DongB, Huang X, et al. Emergence of plasmid mediated colistin resistance mechanism MCR-1 in animal and human beings in China: a microbiological and molecular biological study. Lancet Infect Dis. 2016 Feb;16(2):161–168. https://doi.org/10.1016/S1473-3099(15)00424-7

Lomonaco S, Crawford MA, Lascols C, Timme RE, Anderson K, Hodge DR, Fisher DJ, Pillai SP, Morse SA, Khan E, et al. Resistome of carbapenem- and colistin-resistant *Klebsiella pneumoniae* clinical isolates. PLoS One. 2018 Jun 8;13(6):e0198526. https://doi.org/10.1371/journal.pone.0198526

Nation TL, Li J. Colistin in the 21st century. Curr Opin Infect Dis. 2009 Dec;22(6):535–543. https://doi.org/10.1097/QCO.0b013e328332e672

Parisi SG, Bartolini A, Santacatterina E, Castellani E, Ghirardo R, Berto A, Franchin E, Menegotto N, De Canale E, Tommasini T, et al. Prevalence of *Klebsiella pneumoniae* strains producing carbap-

enemases and increase of resistance to colistin in a Italian teaching hospital from January 2012 to December 2014. BMC Infect Dis. 2015 Jun 27;15:244. https://doi.org/10.1186/s12879-015-0996-7

Petrosillo N, Taglietti F, Granata G. Treatment options for colistin resistant *Klebsiella pneumoniae*: present and future. J Clin Med. 2019 Jun 28;8(7):934. https://doi.org/10.3390/jcm8070934

Prim N, Turbau M, Rivera A, Rodríguez-Navarro J, Coll P, Mirelis B. Prevalence of colistin resistance in clinical isolates of *Enterobacteriaceae*: a four-year cross-sectional study. J Infect. 2017 Dec;75(6):493–498. https://doi.org/10.1016/j.jinf.2017.09.008

Rebelo AR, Bortolaia V, Kjeldgaard JS, Pedersen SK, Leekitcharoenphon P, Hansen IM, Guerra B, Malorny B, Borowiak M, Hammerl JA, et al. Multiplex PCR for detection of plasmid-mediated colistin resistance determinants, *mcr-1, mcr-2, mcr-3, mcr-4* and *mcr-5* for surveillance purposes. Euro Surveill. 2018 Feb;23(6):17-00672. https://doi.org/10.2807/1560-7917.ES.2018.23.6.17-00672

Sandri AM, Landersdorfer CB, Jacob J, Boniatti MM, Dalarosa MG, Falci DR, Behle TF, Bordinhao RC, Wang J, Forrest A, et al. Population pharmacokinetics of intravenous polymyxin B in critically ill patients: implications for selection of dosage regimens. Clin Infect Dis. 2013 Aug;57(4):524–531. https://doi.org/10.1093/cid/cit334

Stefaniuk E, Tyski S. Colistin resistance in Enterobacterales strains – a current view. Pol J Microbiol. 2019 Dec;68(4):417–427. https://doi.org/10.33073/pjm-2019-055

Vicari G, Bauer SR, Neuner EA, Lam SW. Association between colistin dose and microbiologic outcomes in patients with multidrug-resistant Gram-negative bacteremia. Clin Infect Dis. 2013 Feb;56(3):398–404. https://doi.org/10.1093/cid/cis909

Walkty A, Karlowsky JA, Adam HJ, Lagacé-Wiens P, Baxter M, Mulvey MR, McCracken M, Poutanen SM, Roscoe D, Zhanel GG. Frequency of MCR-1-mediated colistin resistance among *Escherichia coli* clinical isolates obtained from patients in Canadian hospitals (CANWARD 2008–2015). CMAJ Open. 2016 Oct 26;4(4):E641–E645. https://doi.org/10.9778/cmajo.20160080

Wang X, Wang Y, Zhou Y, Li J, Yin W, Wang S, Zhang S, Shen J, Shen Z, Wang Y. Emergence of a novel mobile colistin resistance gene, *mcr-8*, in NDM-producing *Klebsiella pneumoniae*. Emerg Microbes Infect. 2018 Jul 4;7(1):122. https://doi.org/10.1038/s41426-018-0124-z

Woodford N, Fagan EJ, Ellington MJ. Multiplex PCR for rapid detection of genes encoding CTX-M extended-spectrum β-lactamases. J Antimicrob Chemother. 2006 Jan;57(1):154–155. https://doi.org/10.1093/jac/dki412

Xavier BB, Lammens C, Ruhal R, Kumar-Singh S, Butaye P, Goossens H, Malhotra-Kumar S. Identification of a novel plasmid-mediated colistin-resistance gene, *mcr-2*, in *Escherichia coli*. Euro Surveill. 2016 Jul 7;21(27):pii=30280. https://doi.org/10.2807/1560-7917.ES.2016.21.27.30280

Yin W, Li H, Shen Y, Liu Z, Wang S, Shen Z, Zhang R, Walsh RT, Shen J, Wang Y. Novel plasmid-mediated colistin resistance gene *mcr-3* in *Escherichia coli*. mBio. 2017 Jun 27;8(3):e00543-17. https://doi.org/10.1128/mBio.00543-17

Yuan Y, Li Y, Wang G, Li C, Xiang L, She J, Yang Y, Zhong F, Zhang L. Coproduction of MCR-9 and NDM-1 by colistin-resistant *Enterobacter hormaechei* isolated from bloodstream infection. Infect Drug Resist. 2019 Sep 19;12:2979–2985. https://doi.org/10.2147/IDR.S217168

Żabicka D, Baraniak A, Literacka E, Gniadkowski M, Hryniewicz W. [Polish Reference Center for Antimicrobial Susceptibility: Detection of carbapenemases – recommendations] (in Polish). 2015. Warsaw (Poland): National Medicines Institute; 2015 [cited 2021 Jan 29]. Available from http://antybiotyki.edu.pl/wp-content/uploads/dokumenty/Wykrywanie-karbapenemaz_Zalecenia-KORLD_2015.pdf

INFORMACJE Z POLSKIEGO TOWARZYSTWA MIKROBIOLOGÓW

Od ostatniej informacji o działalności Zarządu Głównego Polskiego Towarzystwa Mikrobiologów, zamieszczonej w zeszytach nr 1 z 2021 r. kwartalników *Advancements of Microbiology – Postępy Mikrobiologii* i *Polish Journal of Microbiology*, ZG PTM zajmował się następującymi sprawami:

I. Zgodnie ze Statutem PTM raz w roku odbywa się zebranie członków ZG PTM. Przeprowadzono je 22.03.2021 r. w formie on-line, korzystając z pomocy informatycznej Narodowego Instytutu Leków. Materiały związane z zebraniem wcześniej rozesłano e-mailowo do członków ZG PTM i zaproszonych osób.

W zebraniu udział wzięli Prezydium ZG PTM, Przewodniczący Oddziałów Terenowych PTM lub ich przedstawiciele, z wyjątkiem reprezentacji Oddziału PTM w Rzeszowie, Przewodnicząca Głównej Komisji Rewizyjnej PTM oraz Redaktorzy naczelni czasopism PTM.

Podczas Zebrania ZG PTM poruszano następujące zagadnienia:

1. Przedstawiono informację o działalności Prezydium PTM od 30.03.2020 r. – poprzedniego zebrania ZG PTM. W załączeniu przesłano informacje o PTM zamieszczone w numerach czasopism PM i PJM: 2 – 2020, 3 – 2020, 4 – 2020, 1 – 2021.

   Podjęto **Uchwałę 4-2021** w sprawie akceptacji działalności Prezydium ZG PTM za miniony okres roczny.

2. Podjęto **Uchwałę 5-2021** w sprawie uporządkowania listy członków zwyczajnych oraz członków wspierających PTM i usunięcia z niej osób i firm niepłacących składki członkowskiej za 2020 r. w statutowo przewidzianym terminie. W porównaniu z ubiegłym rokiem podobna jest liczba osób nieopłacających składki członkowskiej za rok 2020 r., pomimo przypominania o tym podstawowym obowiązku członka PTM przez OT PTM w styczniu 2021 r. i następnie dwukrotnie przez sekretariat ZG PTM w lutym i marcu b.r. Imienne listy osób usuwanych z poszczególnych Oddziałów zestawiono w **załączniku 1 do Uchwały 5-2021.**

3. Podjęto **Uchwałę 6-2021** w sprawie przyjęcia pięciu nowych członków zwyczajnych PTM (**Załącznik 1 do Uchwały 6-2021**).

4. Spotykamy się z sytuacją, że osoby zaakceptowane Uchwałami PTM jako członkowie zwyczajni nie opłacają pierwszej składki członkowskiej, pomimo wyraźnej informacji, że trzeba spełnić oba warunki, aby być przyjętym do PTM. Na podstawie **Uchwały 12-2020**, usunięto ponad 40 deklaracji członka zwyczajnego, zaakceptowanych Uchwałami ZG PTM, którym nie towarzyszyła pierwsza opłata składki członkowskiej wniesiona w ciągu 6 miesięcy od daty Uchwał.

5. Zgodnie z **Uchwałą 33-2017** i **Uchwałą 2-2019** oraz **„Regulaminem wydatkowania i rozliczania środków pieniężnych przez Oddziały Terenowe Polskiego Towarzystwa Mikrobiologów"** każdy Oddział otrzymuje co roku fundusz złożony z 10% kwoty uzyskanej z tytułu składek członkowskich, 50% kwoty uzyskanej z tytułu pozyskania sponsora ogólnego, Członka Wspierającego PTM, darowizny, lub innej dodatkowej kwoty na rzecz PTM oraz 100% kwoty od sponsora konkretnego wydarzenia organizowanego przez dany Oddział. Przedstawiono Tabelę dotyczącą liczby członków w Oddziałach oraz Tabelę przyznanych Oddziałom środków finansowych na przestrzeni kolejnych ostatnich 3 lat.

   Dyskutowano nad rozwiązaniem problemu kumulacji środków niewykorzystywanych przez Oddziały, ponieważ za kilka lat mógłby pojawić się problem, że w jednym roku kilka Oddziałów chciałoby wykorzystać swoje nagromadzone fundusze, a wtedy budżet PTM może tego nie udźwignąć. Prezydium ZG PTM zaproponowało, aby Oddziały wydatkowały fundusze w okresie 3-letnim, jednakże po dyskusji zdecydowano, że będzie to okres czterech lat, od dnia przyznania środków, w którym należy wydatkować fundusze z danego roku. Tym samym Oddział dysponuje daną kwotą przez okres 4 lat i nie wpływa to na otrzymywanie funduszy w kolejnych latach. Po upłynięciu 4 lat niewykorzystana kwota z danego roku wraca do ogólnej puli środków PTM. Nie wpływa to na dostępność dla OT PTM sum funduszy z ostatnich 3 lat. Podjęto w tej sprawie **Uchwałę 7-2021.** Schemat zdefiniowania okresu wydatkowania funduszy przez OT PTM przedstawiono w **Załączniku 1 do Uchwały 7-2021**.

   Sekretariat ZG PTM co roku zobowiązany jest do przedstawienia danych dotyczących liczby członków w Oddziałach oraz przyznanych Oddziałom środków finansowych w kolejnych latach. Zwrócono uwagę na fakt koniecznego udziału Komisji Rewizyjnych Oddziałów w kontrolowaniu zgodności ze Statutem PTM wydatkowania środków finansowych przez Oddziały.
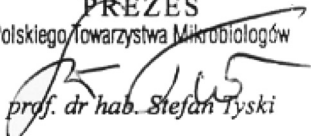
6. Przewodnicząca Oddziału Łódzkiego PTM zwróciła się z prośba o objęcie patronatem przez PTM „IV Sesji Młodych Mikrobiologów Środowiska Łódzkiego", które odbędzie się 23.06.2021 r. w formie on-line na Wydziale Biotechnologii i Nauk o Żywności Politechniki Łódzkiej. Podjęto pozytywną **Uchwałę 8-2021** w tej sprawie.

7. Przedstawiono informację o stanie finansowym PTM oraz Uchwałę Głównej Komisji Rewizyjnej PTM z 19.03.2021 r. w sprawie zatwierdzenia Sprawozdania Finansowego PTM za rok 2020. Z uznaniem podkreślono zakończenie roku 2020 zyskiem w wysokości ponad 28 tysięcy zł, co związane jest przede wszystkim z działalnością redakcji Polish Journal of Microbiology.

8. Przewodniczący Oddziałów Terenowych przedstawili sprawozdania z działalności Oddziałów w okresie od 30.03.2020 r. do 22.03.2021 r. oraz plany Oddziałów na 2021 r. Okres pandemii znacznie przyhamował działalność Towarzystwa. Niektóre Oddziały przeprowadzały spotkania on-line. Postanowiono, że adresy elektroniczne linków z dostępem do wykładów odbywających się w Oddziałach zostaną przesyłane do Sekretariatu ZG PTM, a następnie udostępnione na stronie PTM do wykorzystania przez zainteresowane osoby z innych Oddziałów.

9. Przewodniczący Oddziałów oraz członkowie Prezydium PTM przedstawili opinie i stanowiska w sprawie organizacji Ogólnopolskiego XXIX Zjazdu PTM oraz Walnego Zgromadzenia Delegatów, podczas którego wybierani są członkowie Prezydium PTM i Głównej Komisji Rewizyjnej PTM. Zdecydowanie przeważała opinia, aby w obecnej sytuacji epidemicznej nie organizować Zjazdu PTM w 2021 roku, lecz przenieść Zjazd na 2022 rok.
Wiele osób jest zmęczonych zarówno walką z pandemią COVID-19 jak i koniecznością prowadzenia zajęć i nauczania on-line. Ograniczone są możliwości i okres prowadzenia badań naukowych. Bardzo odczuwalny jest brak kontaktów międzyludzkich i możliwości bezpośrednich dyskusji. Spodziewamy się, że za półtora roku sytuacja epidemiczna będzie na tyle opanowana, przy realizacji masowych szczepień, że możliwe będzie przeprowadzenie Zjazdu w tradycyjnej formie, uwzględniającej wykłady i dyskusje na sali oraz prezentacje plakatów i dyskusje przy nich. Możliwe będzie również bezpośrednie spotkanie mikrobiologów. Biorąc pod uwagę wypowiedzi Przewodniczących Oddziałów przygotowano i następnie podjęto **Uchwałę 9-2021** dotyczącą przesunięcia Zjazdu PTM i Walnego Zgromadzenia Delegatów PTM na rok 2022.

10. Przedstawiono informacje z FEMS oraz IUMS.
W dniach 16–20.11.2020 r. odbył się Międzynarodowy Kongres International Union of Microbiological Societies IUMS 2020 w Daejeon w Korei Południowej w formie hybrydowej. Planowany na 11–15.07.2021 r. w Hamburgu Kongres FEMS 2021 nie odbędzie się, natomiast w terminie 20–24.06.2021 odbędzie się on-line wspólny kongres FEMS i ASM (American Society for Microbiology): World Microbe Forum 2021. https://www.worldmicrobeforum.org/. Brak informacji z FEMS o ewentualnym przyznaniu grantów dla młodych naukowców z Polski. Wprowadzony w FEMS od zeszłego roku sposób informowania towarzystw o otrzymanych grantach nie pozwala na uzyskanie wiedzy o liczbie i tematyce aplikowanych wnioskach grantowych.
FEMS przyjął, że International Microorganisms Day będzie odbywać się 17 września każdego roku.
Pani prof. dr hab. Elżbieta Anna Trafny, Członek Prezydium PTM, Redaktor Naczelna Polish Journal of Microbiology, została włączona do grona naukowców oceniających składane projekty grantowe, FEMS Grant Committee. Jest to duży sukces Pani profesor i wyraz uznania dla naszego Towarzystwa.

11. Informacje o wydawanych przez PTM czasopismach: *Polish Journal of Microbiology* (PJM) oraz *Advancents of Microbiology – Postępy Mikrobiologii* (PM).

* Kwartalnik PJM powiększył w ostatnim roku wartości współczynnika IF oraz CiteScore, które obecnie wynoszą: Impact Factor 2019: 0,897 / 5-year 1,052; CiteScore 2019: 1,3.
Po raz pierwszy w historii czasopisma zaczęło ono przynosić zysk Towarzystwu, ponieważ przychody związane z opłatami redakcyjnymi przewyższyły koszty wydawania czasopisma. Redakcja nie ma problemów z napływem manuskryptów, głównie od autorów z krajów dalekiego wschodu. Obserwowane są trudności z pozyskiwaniem recenzentów i utrzymaniem krótkiego terminu od otrzymania manuskryptu do decyzji odnośnie publikacji.

* Kwartalnik PM powoli przekształca się w czasopismo o szerokim odbiorze międzynarodowym, powiększając liczbę artykułów w języku angielskim. Do redakcji zaczynają przychodzić manuskrypty autorów zagranicznych. Redakcja sygnalizuje małą liczbę nadsyłanych manuskryptów i trudności z pozyskaniem recenzentów. Wydaje się jednak, że przyjęty kierunek rozwoju czasopisma w oparciu o współpracę z wydawnictwem Exeley jest właściwy. Wymagany jest jednak czas aby wprowadzane zmiany w kierunku umiędzynarodowienia czasopisma zaczęły przynosić wymierne efekty w postaci wzrostu współczynników oceny czasopisma, zwłaszcza cytowalności i IF oraz dużej liczby autorów zagranicznych.

W trakcie dyskusji nad rozwojem czasopism podnoszono kwestię zwiększenia cytowalności publikacji z czasopism PTM, a także listy MNiSW dotyczącej punktowanych czasopism.
Oba czasopisma znajdują się na liście filadelfijskiej, ale mają niską punktację MNiSW: PM – 20, a PJM – 40 punktów.

12. Na dzień 31 marca 2021 r. Polskie Towarzystwo Mikrobiologów liczy 860 członków. Najliczniejsze oddziały terenowe, to OT Warszawa – 156 członków i OT Kraków – 113 członków.

  II. Prezydium ZG PTM podjęto **Uchwałę 10-2021** w sprawie organizacji przełożonego na 2022 rok Ogólnopolskiego XXIX Zjazdu PTM w nowym terminie tj. dniach **13–16.09.2022 r.** w Warszawie. Podejmujemy starania, aby zachować przyznane środki finansowe przez MNiSW na organizację Zjazdu w nowym terminie. Natomiast FEMS wyraziła już zgodę na przesunięcie przyznanych środków na organizacje Zjazdu w 2022 r.

  III. Prezydium ZG PTM podjęło **Uchwałę 11-2021** w sprawie objęcia patronatem cyklicznej konferencji: „POMOR-SKIE SPOTKANIA Z MIKROBIOLOGIĄ", w tym roku pt. „Drobnoustroje – wrogowie i sprzymierzeńcy", w dniach 24–25.06.2021 r. w formie on-line. Organizatorem Konferencji była Katedra Biotechnologii Molekularnej i Mikrobiologii Politechniki Gdańskiej, Katedra Mikrobiologii Gdańskiego Uniwersytetu Medycznego oraz **Oddział PTM w Gdańsku.**

  IV. Na stronie PTM udostępniono link do zebrania naukowo-szkoleniowego organizowanego przez **Odział PTM w Bydgoszczy** oraz firmę ARGENTA w dniu – 23.04.2021 r.

  V. Oddział PTM w Krakowie w dniu 29.04.2021 r. przeprowadził ogólnodostępne szkolenie on-line na temat: „Leptospira – powracający patogen". Na stronie PTM udostępniono link do szkolenia.

  VI. Oddział PTM we Wrocławiu współorganizował Konferencje Naukowo-Szkoleniową pt; „Nowe technologie w laboratorium okresu pandemii COVID-19", która odbyła się w formie zdalnej 18.05. 2021 r. Na stronie PTM udostępniono link do konferencji.

  VII. Oddział PTM w Krakowie zaprosił na wykład on-line pt.: „Odporność poszczepienna – w tym po szczepieniach przeciw COVID-19", który odbył się 27.05. 2021 r.

  VIII. Na stronie PTM udostępniono link do konferencji cyklicznej „HydroMikro2021", której współorganizatorem byli członkowie **Oddziału PTM w Gdańsku**, pt. „Mikroorganizmy w środowisku wodnym – zagrożenia i nadzieje". Konferencja odbyła się on-line 09–11.06.2021 r. w Instytucie Oceanologii PAN w Sopocie.

  IX. Oddział PTM w Szczecinie zapraszał na spotkanie naukowo-szkoleniowe na temat: Wirus SARS-CoV-2 a układ odpornościowy człowieka, on-line 10.06.2021 r.

  X. Prezydium ZG PTM podjęto **Uchwałę 12-2021** w sprawie przyjęcia jedenastu nowych członków zwyczajnych PTM (**Załącznik 1 do Uchwały 12-2021**).

  XI. Uchwałą 13-2021 Prezydium ZG PTM objęło patronatem konferencję „IV Mazowieckie Spotkanie Mikrobiologów i Epidemiologów" organizowaną w wersji on-line w dniu 07.06.2021 r. przez Konsultanta Wojewódzkiego w dziedzinie Mikrobiologia Lekarska Panią Prof. dr hab. Ewę Augustynowicz-Kopeć.

  XII. Uchwałą 14-2021 Prezydium ZG PTM zdecydowało o zawarciu umowy z Panią mgr Karoliną Stępień dotyczącej wprowadzania informacji na stronę PTM oraz do portalu facebook, w latach 2021–2022.

  XIII. Informowaliśmy i zapraszaliśmy członków PTM do udziału w pierwszym wspólnym Kongresie Federacji Europejskich Towarzystw Mikrobiologicznych (FEMS) i Amerykańskiego Towarzystwa Mikrobiologicznego (ASM): The 2021 World Microbe Forum, on-line 20–24 czerwca 2021 r. Siedmiu członków PTM wzięło udział w tym Kongresie uzyskując zniżki w opłacie rejestracyjnej.

  XIV. FEMS zakłada, że pandemia SARS-CoV-2 wkrótce wygaśnie i zaprasza do udziału w konferencji organizowanej w formie klasycznej – stacjonarnej „Conference on Microbiology 2022" w dniach 30 czerwca – 2 lipca 2022 r. w Belgradzie, Serbia. Informacje na stronie PTM.

Warszawa, 14.06.2021 r.

SEKRETARZ
Polskiego Towarzystwa Mikrobiologów
dr hab. n. farm. Agnieszka E. Laudy

PREZES
Polskiego Towarzystwa Mikrobiologów
prof. dr hab. Stefan Tyski
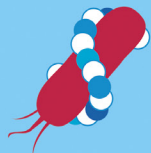
CZŁONKOWIE WSPIERAJĄCY PTM

Członek Wspierający PTM – Złoty
od 27.03.2017 r.

HCS Europe – Hygiene & Cleaning Solutions
ul. Warszawska 9a, 32-086 Węgrzce k. Krakowa
tel. (12) 414 00 60, 506 184 673, fax (12) 414 00 66
www.hcseurope.pl

Firma projektuje profesjonalne systemy utrzymania czystości i higieny dla klientów o szczególnych wymaganiach higienicznych, m.in. kompleksowe systemy mycia, dezynfekcji, osuszania rąk dla pracowników służby zdrowia, preparaty do dezynfekcji powierzchni dla służby zdrowia, systemy sterylizacji narzędzi.

Członek Wspierający PTM – Srebrny
od 12.09.2017 r.

Firma Ecolab Sp. z o.o. zapewnia: najlepszą ochronę środowiska pracy przed patogenami powodującymi zakażenia podczas leczenia pacjentów, bezpieczeństwo i wygodę personelu, funkcjonalność posiadanego sprzętu i urządzeń. Firma jest partnerem dla przemysłów farmaceutycznego, biotechnologicznego i kosmetycznego.

Członek Wspierający PTM – Zwyczajny
od 12.09.2017 r.

Merck Sp. z o.o. jest częścią międzynarodowej grupy Merck KGaA z siedzibą w Darmstadt, Niemcy i dostarcza na rynek polski od roku 1992 wysokiej jakości produkty farmaceutyczne i chemiczne, w tym podłoża mikrobiologiczne